Draft

Evaluation of Restoration Alternatives for the Northwest Fork of the Loxahatchee River Chapters 6, 7 and 8

South Florida Water Management District
Watershed Management Department
Coastal Ecosystems Division

May 9, 2005

CHAPTER 6

TABLE OF CONTENTS

LIST OF FIGURES

LIST OF TABLES

Chapter 6:

Modeling Freshwater Inflows and Salinity in the Loxahatchee River and Estuary

Estuaries are the most productive ecosystems on the earth and freshwater inflows are the single most important determinant of estuary health. Any alterations in the timing and amount of inflows will influence the overall estuary productivity and health. In the Loxahatchee River, the importance of freshwater inflows has been presented in the previous chapters. Salinity in the Northwest Fork of the Loxahatchee River and Estuary is controlled by both freshwater inflows and tidal circulation, which represent the competition between river and ocean influences. The hydroperiods of the Loxahatchee River floodplain ecosystem may also be influenced by freshwater inflows into the river. Formulation of the restoration plan for the Northwest Fork of the Loxahatchee River and Estuary depends largely on accurate predictions of long-term freshwater inflow and salinity in the Loxahatchee River and Estuary.

This chapter describes the three models used in predicting freshwater inflows and salinity conditions in the Loxahatchee River Watershed. The Watershed (WaSh) Model simulates long-term freshwater inflows from tributaries into the Northwest Fork. The 2-D Estuarine Hydrodynamic and Salinity (RMA) Model simulates the influence of the freshwater inflows on salinity conditions within the Loxahatchee River and Estuary. The Long-Term Salinity Management Model (LSMM) predicts daily salinity conditions for use in evaluating Loxahatchee River Watershed ecosystem responses to restoration scenarios.

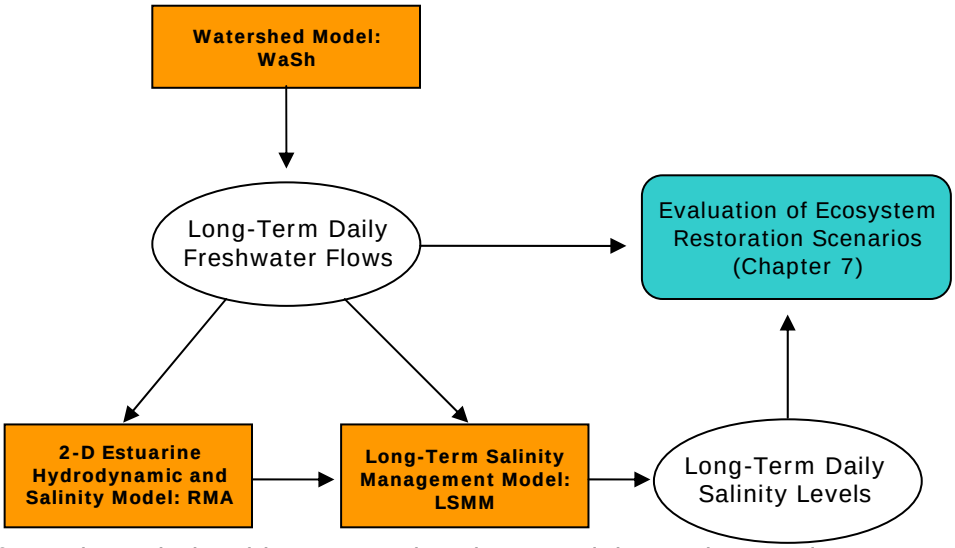

Figure 6-1. The Relationship Among the Three Models Used to Evaluate Restoration Plan Scenarios for the Ecosystems in the Loxahatchee River Watershed.

MODELING FRESHWATER INFLOWS

THE WATERSHED (WASH) MODEL DESCRIPTION

Freshwater inflows from major tributaries of the Northwest Fork of Loxahatchee River and Estuary are simulated with a watershed model called WaSh. The WaSh model was developed based on restructuring HSPF (Hydrologic Simulation Program – Fortran, Donigian et al., 1984) into a cell-based system with the addition of a groundwater model and a full dynamic channel routing model (Wan et al., 2003). The WaSh model is capable of simulating hydrology and water quantity in watersheds with high groundwater tables and dense drainage canal networks, which is typical in south Florida. The model consists of four basic components: (1) a cell-based representation of the watershed basin land surface, (2) a groundwater component that is consistent with the basin cell structure, (3) a surface water drainage system, and (4) water management practices. Key features of the model are surface water-groundwater interactions, irrigation demands and transfers between elements of the surface water drainage network. For each cell, the model uses an infiltration routine to determine the amount of rainfall that infiltrates into the groundwater, evaporates into the atmosphere, or drains to the surface water system. Currently, the HSPF (Version 12) modules PWATER and IWATER are used for this portion. The infiltrated water is routed to a groundwater model that represents the unconfined aquifer in the watershed. The groundwater model receives the infiltrated water, exchanges groundwater between cells and also exchanges water between surface water flow and groundwater flow. The surface water drainage system consists of a cell-based system and a reach-based system. The reach-based system is typically configured to follow the major canals, streams and rivers and supports branches and common flow structures. The water quality component of WaSh is built on the surface water, groundwater, and channel flow components of the model. The application of the model in Loxahatchee watershed focuses on hydrologic simulation. The WaSh model is supported by a Graphic User Interface (GUI) that is developed as an Arcview extension. The GUI handles file management (both on the local platform and on the server), model configuration, execution and post processing. The WaSh model also supports numerous water management practices such as irrigation, reservoirs, Stormwater Treatment Areas (STAs), and land use changes. Key components of the WaSh model are summarized in **Table 6-1**.

Table 6-1. The Watershed (WaSh) Model Components and Functions.

Model Component	Modeling Approach	Functions
Surface Water Flow	PWATER and IWATER of HSPF with PQUAL, SEDMNT, IQUAL, and SOLIDS for water quality	High water table algorithms of HSPF
Groundwater Flow	A new 2D unconfined groundwater flow model with a prescribed leaching function for water quality constituents	Canal drainage and recharge
Channel Flow	A new 1D fully dynamic shallow wave model with a scalar mass transport function for water quality	Structures, branching, point sources
Water Management	Reservoirs, Stormwater Treatment Areas, irrigation supply and demands, land use changes.	Executed by an Arcview graphic user interface (GUI)

Model Cell Structure and Cell-Based Routing

The WaSh model uses a uniform structured grid network. Each cell represents a discrete part of the model domain and has associated physical characteristics such as land use, soil type, ground elevation, impervious area, and a representative ground slope. Hydrological parameters relating runoff, infiltration, and evaporation are specific to these attributes, particularly land use types. If tertiary canals are present in the cell, the length and width of canals in the cell are computed and added as a cell attribute. Generally, the cell attributes are obtained by combining the cell network with Geographic Information System (GIS) coverage for each of the physical characteristics. For the purpose of routing the simulated daily runoff from each cell, a special cell attribute is assigned to indicate where runoff from that cell is directed. Each cell is labeled as one of three primary types: (1) free cell, (2) canal cell, or (3) reach cell. A free cell represents an area of the basin that does not contain canals. Canal cells are any cells with tertiary canals that are not coincident with the reaches. Reach cells are cells that contain a reach (major canals) in the primary canal system. Some secondary canals can be included in the reach system. These labels are needed to designate the types of surface and groundwater interactions that may occur for a given cell. **Table 6-2** lists the methods in which water is routed for each type of cell.

Table 6-2. WaSh Water Routing Operations for Each Cell Type.

Cell Type	Flow Routing Operations
Free	Infiltration is directed to cell groundwater Surface water is directed to a nearby cell's canals
Canal	Infiltration is directed to cell groundwater Surface water is directed to cell canals Groundwater can be exchanged with canal surface water Surface water can be exchanged between the canal and the reach
Reach	Infiltration is directed to cell groundwater Surface water is directed to the cell's reach or nearby cell's canals Groundwater can be exchanged with canal or reach surface water Reach water can be exchanged with canal water

Surface and Groundwater Interaction

The surface and ground water is modeled in the same grid network. For each cell, WaSh uses the PWATER and IWATER modules of HSPF (Version 12) to simulate surface water hydrology (**Table 6-1**). A detailed description of these modules is available in the HSPF user's manual (Donigian et al., 1984). Version 12 includes recent model enhancements that simulate irrigation demand, high water tables, and wetland conditions that are common in south Florida (Aqua Terra, 1996, 1998). The HSPF routine is implemented in one-hour time steps for 24-hour blocks. Thus for each day, the HSPF-based routine is applied for each cell and water balance, consisting of rainfall, evaporation, soil storage, surface runoff and infiltration to groundwater, are calculated. At the end of each one-day simulation period, the accumulated surface runoff and infiltration are routed to the drainage and groundwater systems, respectively. All the HSPF model parameters are calibrated and assigned to each cell based on the land use and soil type characteristics as additional cell attributes.

The groundwater module in WaSh is based on the numerical solution of the standard groundwater flow equation for an unconfined aquifer. The model operates on a daily time step, during which it receives infiltrated water, loses water to evaporation, and exchanges water with adjacent cells and with canals. The basic governing equation for the groundwater module is:

$$\rho\frac{\partial h}{\partial t}=\frac{\partial}{\partial x}K_x(h-h_c)\frac{\partial h}{\partial x}+\frac{\partial}{\partial y}K_y(h-h_c)\frac{\partial h}{\partial y}+S_i-S_e+S_c+S_r \qquad [1]$$

where h is the groundwater elevation, ρ is the porosity, K_x and K_y are the hydraulic conductivity in the x-, and y- directions, h_c is the aquifer base elevation, and S_i, S_e, S_c and S_r are source/sink terms representing infiltration, evaporation, exchanges with the canal cells and exchanges with reaches. The governing equation is solved numerically using the basin cell structure. A second-order finite difference approximation is used for the second derivatives, and an explicit backward difference approximation is used for the time derivative. During each time step the right-hand side of the equation is evaluated based on current time level conditions, and the new water elevation is found. By designating the equation parameters and water elevation h for each cell by the indexes $_{i,j}$, and the time level by the index ^{m}, the resulting finite difference equation for each cell is:

$$\frac{1}{\rho_{i,j}}\frac{h_{i,j}^{m+1}-h_{i,j}^{m}}{\Delta t}=K_x\left[\frac{(\frac{h_{i,j}^{m}+h_{i+1,j}^{m}}{2}-h_c)}{\Delta x}\left(\frac{h_{i+1,j}^{m}-h_{i,j}^{m}}{\Delta x}\right)-\frac{(\frac{h_{i,j}^{m}+h_{i-1,j}^{m}}{2}-h_c)}{\Delta x}\left(\frac{h_{i,j}^{m}-h_{i-1,j}^{m}}{\Delta x}\right)\right]+$$
$$Ky\left[\frac{(\frac{h_{i,j}^{m}+h_{i,j+1}^{m}}{2}-h_c)}{\Delta y}\left(\frac{h_{i,j+1}^{m}-h_{i,j}^{m}}{\Delta y}\right)-\frac{(\frac{h_{i,j}^{m}+h_{i,j-1}^{m}}{2}-h_c)}{\Delta y}\left(\frac{h_{i,j}^{m}-h_{i,j-1}^{m}}{\Delta y}\right)\right]+S_{i_{i,j}}^{m}-S_{e_{i,j}}^{m}+S_{c_{i,j}}^{m}+S_{r_{i,j}}^{m} \qquad [2]$$

where Δt is the time step (one day), and Δx and Δy are the grid cell dimensions in each direction. During each time step the right-hand side of the equation is evaluated based on current time level conditions, and the new water elevation is found by solving for $h_{i,j}^{m+1}$. When an active cell is adjacent to the grid boundary or to an inactive cell, a no-flow condition is imposed.

Implementation of the groundwater model has required some modification to the PWATER module, primarily to account for evaporation from groundwater and also to link to the irrigation and high water table modules. The original HSPF groundwater algorithm is based on groundwater storage, AGWS. Changes to the storage for each time step are due to infiltration (GWI), evaporation (BASET), and discharge to surface water (AGWO). Infiltration is predicted using subroutines representing the Stanford Watershed Model approach. Evaporation is modeled as a loss term, which is based on a model parameter BASETP. The discharge is based on a rating curve, specified by the model parameters AGWRC and KVARY. This groundwater discharge algorithm in HSPF has been disabled and replaced by the equivalent parameters in WaSh. For each of the cells, two of the source terms on the right hand side of the equation, $S_{i_{i,j}}^{m}$ and $S_{e_{i,j}}^{m}$ are set equal to output variables from HSPF PWATER groundwater subroutine related to infiltration (GWI) and evaporation (BASET). The groundwater elevation $h_{i,j}$, replaces the storage variable, AGWS, and when combined with the two source terms, represent essentially the same processes as AGWO in HSPF. However, this modification provides a process-based approach to represent

surface and groundwater interactions when compared with the rating curve-based groundwater discharge approach in HSPF. For example, the source/sink terms for a canal/reach cell are now defined as:

$$S^{m}_{c_{i,j}} = \frac{\Delta H \; C_c}{A} \qquad [3]$$

$$S^{m}_{r_{i,j}} = \frac{\Delta H \; C_r}{A} \qquad [4]$$

where ΔH is the difference in groundwater elevation and canal or reach surface water elevation, which are dynamically tracked in WaSh, A is the cell area, and C_c and C_r are the conductance of canal or reach, respectively. The conductance is physically related to the hydraulic conductivity of the stream bed material and the length and width of the canal. In the Loxahatchee watershed, the hydraulic conductivity of the deep canals (reaches) and shallow canals is different. The hydraulic conductivity and canal dimension are provided as input data for each cell according to the basin hydrography and land use.

Irrigation Demand and High Water Table Conditions

The WaSh groundwater module has also been developed to interact with the irrigation module and the high water table module of HSPF. WaSh simulates the irrigation demand by monitoring the moisture in the upper and lower soil zones and generating a demand for water based on the existing moisture relative to the desired moisture level that is specified by the user. After the irrigation demand is calculated, the algorithm tries to meet the demand by supplying water from a number of sources. Groundwater can serve as both an irrigation source and an irrigation sink (receptor) in the HSPF irrigation algorithm. In each case, the amount of water demanded from, or applied to, the groundwater is extracted or added to the cell's groundwater volume. At the beginning of each day, the irrigation demand is calculated and if groundwater is effected, the groundwater elevation $h_{i,j}$ is adjusted according to the following equation:

$$h_{i,\,j} = h_{i,\,j} + \Delta V / \rho \qquad [5]$$

where ΔV is the volume (expressed as depth) of groundwater irrigation demand or application for the cell calculated by the HSPF irrigation module, and ρ is the aquifer porosity as defined previously in Equation [1].

The high water table module in HSPF requires certain vertically referenced parameters and variables to allow for exchange of water between storage components when the groundwater level interferes with the upper and lower zone storage (UZS and LZS). For applications in WaSh, the vertical referencing is already completed, since the surface elevation (a cell attribute) and the groundwater elevation h are all referenced to the same datum. Thus, the only required modification is to provide these two variables to the high water table algorithms. The HSPF high water table algorithm then calculates the exchange between the storage zones and the groundwater. The groundwater elevation is updated with Equation [5], where ΔV now represents the exchange between the upper and lower storage zones.

Drainage Canal Network and Canal Routing

The surface water drainage canal network is modeled implicitly in the cell-based system and explicitly in the reach-based system. The major channels are simulated in the reach-based system which consists of a series of reaches and nodes. This drainage system is separated from the cell system, but its elements (reaches and nodes) overlay the cell network and coincide with a subset of the cells. This system is typically configured to follow the major canals, streams and rivers in the basin. The small or tertiary canals are represented in the cell-based system. These canals receive surface and subsurface runoff from the adjacent cells and exchange water with neighboring canal cells.

Flow through the reach-based systems is modeled using the continuity equation [Equation 6] and the depth- and width-averaged shallow water wave equation [Equation 7]. The governing equations are:

$$\frac{\partial wh}{\partial t} = \frac{\partial q}{\partial s} + Q_e \qquad [6]$$

$$\frac{\partial q}{\partial t} + \frac{\partial uq}{\partial s} + \frac{gw}{2}\frac{\partial h^2}{\partial s} = -w\tau_b - gwh\frac{\partial \eta}{\partial s} \qquad [7]$$

where q is the flow, u is the width- and depth-average flow velocity, g is the acceleration due to gravity, w is the canal width, h is the water depth (referenced to the canal bed), η is the bed elevation, t is time and s is distance along the canal. The bottom stress τ_b is based on a Manning's n formulation. Boundary conditions can be one of two types: a specified flow or a specified water elevation. Specified flow conditions are typically used when a flow structure controls the flow out of the system. The water elevation (or head) condition is used when the system drains unobstructed into a receiving water body. The governing equations are solved using a finite volume procedure, with the reach and node system for a single branch equivalent to a finite volume staggered grid approach.

The source term Q_e in the continuity equation [6] consists of point sources or sinks, exchange with groundwater, and exchange with canals from the cell-based system. The units for the source term are flow per unit length of channel. The general form for the source term can be expressed as:

$$Q_e = Q_{kp} + Q_{ki} + Q_{r,gw} \qquad [8]$$

where Q_{kp} are external sources or sinks (user specified time series), $Q_{r,gw}$ is the exchange with the groundwater and is equal to S_r, the exchange calculated in the groundwater model, Equation [1], and Q_{ki} is the exchange with the canal cells where the tertiary canals are connected with the reach.

When the reach-based system contains branches, the flow in each branch is determined independently. The method for estimating the flow between branches depends on whether the flow is natural at the connection or whether a structure exists. When a structure is present at the branch connections, the flow is determined using a rating curve specific to the structure. Since the flow can be bi-directional, the flow direction for the time step is first determined from the water elevations in the reaches at the branch juncture. The water elevations for headwater and tailwater

are then assigned appropriately and the rating curve is used to calculate the flow. It is noted that structures can also occur at any node along the reach node system. When a structure is present, the flow at that node is determined at the beginning of the time step using the structure flow formulas and its value replaces the momentum equation for that node. When no structures are present at the branch connections, the flow is solved using the shallow water wave equation, Equation [7], and the continuity equation, Equation [6]. The two equations are solved explicitly for the flow between branches using the two reaches that connect the branches. The calculated flow in the 'local' explicit solution is then used as a boundary condition for the implicit solution for the upstream branch and as a source to the downstream reach.

Flow in the cell-based canal system (i.e., the tertiary canals) is represented in the WaSh model using the same governing equations and numerical scheme as used for the reach-based system. To implement this approach, the cell-based canal parameters are first mapped into a 'local' branch and reach network. When this mapping is completed, the solution algorithm for the reach system can be applied to the local system with only minor modifications to the downstream boundary condition and the source terms. The source term in the cell canal would then include surface runoff simulated with HSPF routines.

The tertiary canals are characterized by the total length *LC* of these canals within the cell, the average canal width w_c, the average canal bottom elevation, and a critical or 'design' water depth. These parameters are attributes of the cell. They can be obtained by mapping GIS hydrologic data onto the basin grid and then specifying widths, bottom elevations and critical depths based on the cell land use. The surface water elevation is the dependent variable in the system. In order to map these parameters into a branched network, each cell's canals are designated as a single reach. The reach parameters for the cell are determined as follows:

If the total canal length *L* is less than the cell length *LC*, then:

$$\Delta s = L, \quad and \ w = w_c \qquad [9]$$

If the total canal length *L* is greater than the cell length *LC*, then:

$$\Delta s = LC, \quad and \ w = w_c * \frac{L}{LC} \qquad [10]$$

After the cell-based canal parameters are transformed into reach parameters, the connectivity of the branch network is determined. The connectivity of the cells is used directly to establish branches and the assignments of reaches within each branch. The canal-to-canal flow is generally towards the reaches, but the instantaneous flow is determined by the difference in relative surface water elevations between hydraulically connected canal cells. When canal cells exist in cells with reaches, the canals are assumed to be hydraulically connected to the reach via a structure. It is in these cells that water can flow between the canals and reaches. Between the reaches and tertiary canals, the flow is assumed to be controlled by pumps. The pumping capacity is derived from land use types, representing the design (or estimated) drainage capacities for the canal systems associated with each land use. The drainage capacities of the major land use types are the key parameters for calibrating the magnitude of peak flow during a high magnitude and low frequency event.

IMPLEMENTING THE WASH MODEL

Model Setup

The WaSh Model was implemented into four regions of the Loxahatchee River Watershed (**Figure 6-2**). These 4 regions include all of the major drainage basins described in **Chapter 2** except the Coastal Basin. The JDSP region (**A**) includes the North Fork, Kitch Gauge, Park River, and the Loxahatchee Estuary Basins (refer to **Chapter 2** for delineation of these basins). The Pal-Mar and Grove region (**B**) includes the Pal-Mar, Historic Cypress Creek, Grove West, and Grove East Basins. The Jupiter Farms region (**C**) includes the Jupiter Farms and the Wild & Scenic Basins. The C-18 region (**D**) represents the C-18/Corbett Basin and flow diversion from the L-8/Grassy Basin. The cells for each of the regions are show in **Figure 6-2.** The cell size was 750 ft by 750 ft for the Jupiter Farms region, 1000 ft by 1000 ft the JDSP region and Pal-Mal/Grove region, and 1500 ft by 1500 ft for the C-18 region.

Input data required to generate the model grid include primary and secondary basin coverages, polygon features with basin name attributes, hydrography including streams and canals as line or polyline features, the 2000 base land use coverage, soil coverage, and land surface elevation. The land surface contour was re-sampled (100 ft intervals) based on 5 ft by 5 ft LIDAR data to get a smooth land surface profile and to remove data artifacts. For limited areas where LIDAR data are not available, the 1-foot contour was used. Using the ArcView GUI, these coverages are over-laid to get an aerial extent of the model domain along with cell attributes of land use type, soil, canal length and width, and elevation.

When creating the primary reaches for the basins, the hydrography theme is overlaid on the grid and those grid cells intersecting with polylines of the hydrography theme are classified as canal cells. The canal length in a grid cell is calculated with all the intersecting canal segments inside a grid cell. Reach cells are created by digitizing major river segments and canals starting from the basin outlet. After digitizing, the length of a reach, which is typically the grid cell size, is specified to allow for redistribution of the nodes along the reach network. Each of the reach segments has a reach ID along with the width and bottom elevation assigned according to the cross-section of the major canal and river segment. In **Figure 6-2** the cells are colored coded to represent canal cells (turquoise), reach cells (pink), and free cells (light green). The surface elevation of cells is used to create flow paths. In general, flow in free cells is routed to the nearest canal or reach cell (**Figure 6-2, Region B**). A no flow boundary condition is imposed along the boundary cells.

Each of the cells is linked with a Master Lookup Database consisting of HSPF parameters, evapotranspiration coefficients, canal parameters, and aquifer properties. Based on the grid cell attribute, this master database is queried to populate the respective parameters for each cell in the grid. Some of the model parameters can be changed during the model calibration process.

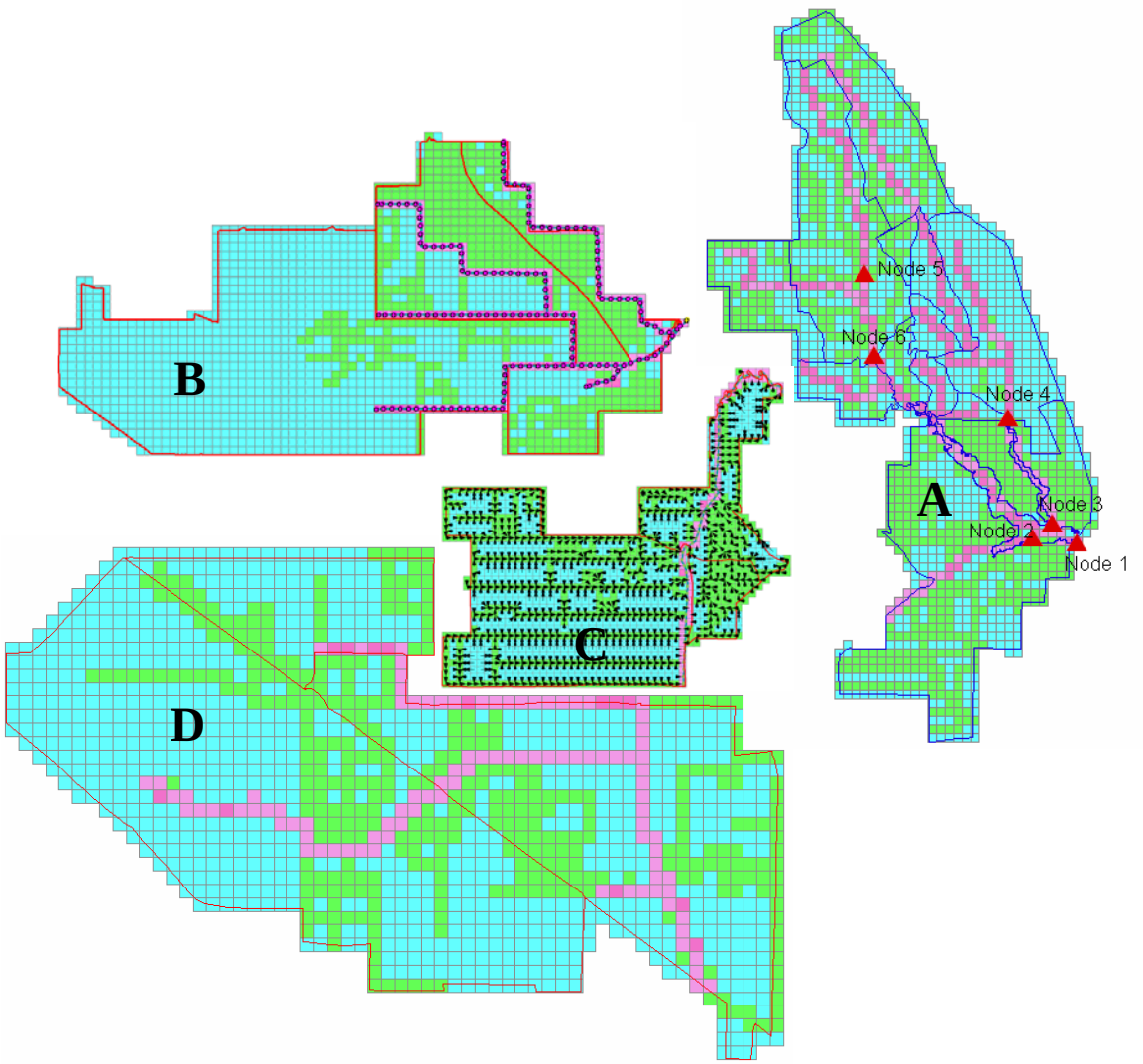

Figure 6-2. The Loxahatchee WaSh Model Grids: A. JDSP Model, B. Pal-Mar-Grove Model, C. Jupiter Farm Model, and D. C-18 Model. Free cells, Canal cells, and Reach cells are color coded turquoise, light green, and pink, respectively. In the JDSP Model, the blue line represents the model boundary, and the nodes represent examples of possible model output locations. In the Pal-Mar-Grove Model, the nodes are show in the reach system. In the Jupiter Farm model, flow routing directions are shown with arrows.

The other important input data required by the model are rainfall and evapotranspiration (ET). These data were obtained from the District's South Florida Water Management Model (SFWMM) for the period from 1965 to 2000. The data set was extended to March 2004 with available rainfall and ET data stored in District DbHydro database in the model area. Daily rainfall is disaggregated into hourly rainfall based on an analysis of available hourly rainfall distribution in south Florida.

Model Calibration and Validation

The Loxahatchee WaSh Model has been calibrated with five flow monitoring stations (**Figure 6-3)**. Flow data collected at the G-92 structure are not used since it was found that the data are likely not accurate. The Kitching Creek station started to collect data in the early 1980s.

The data are not continuous until 1990, and thus only the data collected after 1990 are used for calibration and validation of the JDSP Model. The Hobe Grove and the Cypress Creek stations have been collecting data since 1980; however, there are significant periods of time when data were not collected or are missing. Data collected from the flow stations at S-46 and Lainhart Dam have the longest record. Only the data collected after 1987 were used for WaSh model calibration and validation due to structure changes of G-92 (**Chapter 2**). All the collected flow data were evaluated for their validity before being used for model calibration and validation. In addition, water level data collected in a groundwater well (PB-689) were used. The well is located in the C-18/Corbett basin where the land use is dominated by wetland.

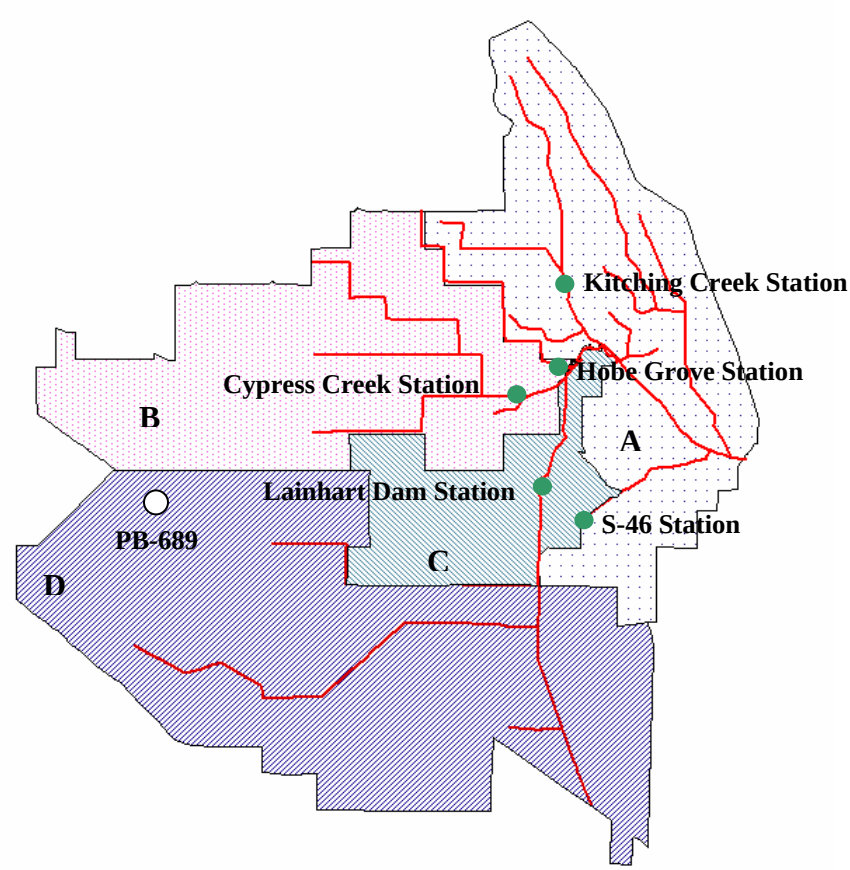

Figure 6-3. Flow (Green Dots) and Groundwater (White Dot) Monitoring Stations in the Loxahatchee River Watershed for WaSh Model Calibration.

Model calibration involves conducting a model simulation of each region for the period of record and comparing the simulated flow with the observed flow. The model parameters are then adjusted in subsequent simulations to improve the shape of simulated flow time-series until the model output meets the performance criteria. In general, the hydrological calibration is conducted in two main steps:

1. Macro Scale: Adjust hydrological parameters to obtain the long-term basin water budget.
2. Micro Scale: Fine tune model parameters to get the best match between observed and simulated flow. At this stage, the shape of the hydrograph with respect to peak and base flow is adjusted. Groundwater levels were also checked with data from observation wells.

In the first step, the long-term water budget is used to ensure that the model calibrations are not biased for one type of climatic condition. Another component of the water budget calibration is verifying that the fractions of groundwater and surface water contribution to runoff properly reflect the partitioning between surface runoff and subsurface runoff. For this component of the simulation, the average annual water budget for each of the land uses as well as for the entire watershed were used to make decisions to adjust parameters. An initial run of the model was made using model parameters that were calibrated in the St. Lucie Estuary watershed (Wan et al., 2003). The most sensitive model parameters in completing the water budget calibrations are evaporation coefficients for individual months and infiltration parameters of HSPF. An example of the water budget is given in **Table 6-3** for the Pal-Mar and Grove region. The water budget is partitioned into the Pal-Mar and historic Cypress Creek basins which consist mostly of wetland and forest, and the Grove West and Grove East basins which consist mostly of irrigated citrus groves. Citrus irrigation significantly increases the runoff from a water budget perspective.

Table 6-3. Average Annual Water Budget (in inches) for the Pal-Mar and Grove Region.

Basins	Rainfall	Irrigation	ET	Runoff		Storage
				Surface	Subsurface	
Pal-Mar & Historic Cypress Creek	61.2	--	44.9	13.6	2.6	1.7
Grove West & Grove East	61.2	8.2	40.2	16.9	11.9	0.2

All values are in inches. ET = Evapotranspiration.

Once the long-term calibration is completed, the next step is to validate the model by matching the simulated daily flow hydrograph to the measured daily flow values recorded for each of the flow stations. The more significant parameters to be calibrated during this step includes the groundwater cell conductance parameters that control the rate at which groundwater flows to the canals, the irrigation parameters, and the canal pumping parameters that control the rate at which tertiary canals flow to primary reaches. To a lesser degree, the length – scale parameter associated with surface drainage (LSUR) has an affect on the shape of the hydrographs. Reducing LSUR increases runoff and decreases infiltration. The model validation process is similar to the calibration process, except that a different period of record is used for the relevant input data. The model parameters are kept constant. Model validation is considered complete if the simulation meets the performance criteria. Otherwise, the model is re-calibrated and validated.

Model calibration and validation performance are evaluated with two of three criteria recommended by the ASCE Task Committee on Definition of Criteria for Evaluation of Watershed Models (1993): the deviation of volume, the Nash-Sutcliffe coefficient, and coefficient of daily gain. The coefficient of gain from the daily mean is not used because of its similarities with the Nash-Sutcliffe coefficient in this particular case. Instead, the coefficient of determination (R^2) is calculated as part of the hydrologic analysis.

The deviation of volume, *DV*, quantifies the difference in observed and predicted water volumes and is calculated:

$$DV = \frac{\sum_{i=1}^{n}(Vm - Vs)}{\sum_{i=1}^{n} Vm} \times 100\% \qquad [11]$$

where *DV* is the deviation of volume (%), *Vm* is the measured water yield for the period of comparison, and *Vs* is the modeled water yield for the period of comparison.

The Nash-Sutcliffe coefficient, *NS*, measures how well the daily simulated flow corresponds with the measured flow. This coefficient is calculated:

$$NS = 1 - \frac{\sum_{i=1}^{n}(Qm - Qs)^2}{\sum_{i=1}^{n}(Qm - Q)^2} \quad [12]$$

where *Qm* is the measured daily discharge, *Qs* is the simulated daily discharge, and *Q* is the average measured daily discharge. A Nash-Sutcliffe value of 1.0 indicates a perfect fit while a value of 0 indicates that the model is predicting no better than the average of the observed data.

The model calibration and validation performance results are summarized in **Table 6-4.** Note that during the period of model calibration or validation, those days with missing or problematic data were excluded, so the count of days indicates the number of days with valid flow data. In general, the model simulates daily flow reasonably well with almost all R^2 and *NS* values about 0.5 for both calibration and validation analyses. Except for the Hobe Grove station, the *DV* ranged from –0.83% to 8.5 % for calibration and –2.87% to 12.5% for validation.

Table 6-4. WaSh Model Calibration and Validation Performance Results.

Monitoring Station	S-46	Lainhart Dam	Cypress Creek Station	Hobe Grove Station	Kitching Creek Station
Calibration Results					
Period	1987-1996	1987-1996	1980-1986	1981-1985	1990-1996
Number of days	3193	3193	1680	1058	2192
DV (%)	–1.78	–0.83	–7.50	–14.67	0.21
NS	0.69	0.47	0.43	0.08	0.51
R^2	0.71	0.53	0.53	0.54	0.51
Validation Results					
Period	1997-2004	1997-2004	1987-1990	1987-1989	1997-2000
Number of days	2587	2587	990	687	1461
DV (%)	12.52	9.43	–2.87	10.66	9.09
NS	0.71	0.56	0.61	0.27	0.54
R^2	0.73	0.32	0.72	0.63	0.57

To aid in the evaluation of model calibration and validation performance, three types of plots are prepared:

1. Daily flow distribution: Plot of the distribution of the measured and modeled daily flow to visually examine the overall model performance. Particular attentions are paid to the low flow regime.
2. Double mass curve: To compare the measured and modeled daily flow in a cumulative manner along with increasing rainfall. This is a visual check of the deviation of volume (*DV*) calculated in **Table 6-4**.
3. Daily flow time series of modeled flow and observed flow for selected periods.

Figure 6-4 includes the three plots for the Lainhart Dam and S-46 stations which provide the longest period of flow data for model calibration and validation. **Figure 6-4 A** and **B** compare the

frequency distribution of the modeled versus the observed daily flows. A slight high frequency of flow in the range of about 10 cfs is predicted by the model at Lainhart Dam, possibly due to low flow leakage at the structure becoming significant but is not measured. The double mass curves for both stations (**Figure 6-4 C** and **D**) show consistent model performance when comparing the patterns of the increase of modeled and measured flow with increasing rainfall. At Lainhart Dam, the model over-predicted flow for a 3-month period during the wet season of 1999. This has been attributed partly to the 9% *DV* in **Table 6-3**. **Figure 6-4 E** and **F** are the time-series plots of measured flow and modeled flow from 2000 through 2003. Overall, the figure shows that the model simulates daily flows over Lainhart Dam and S-46 structures reasonably well.

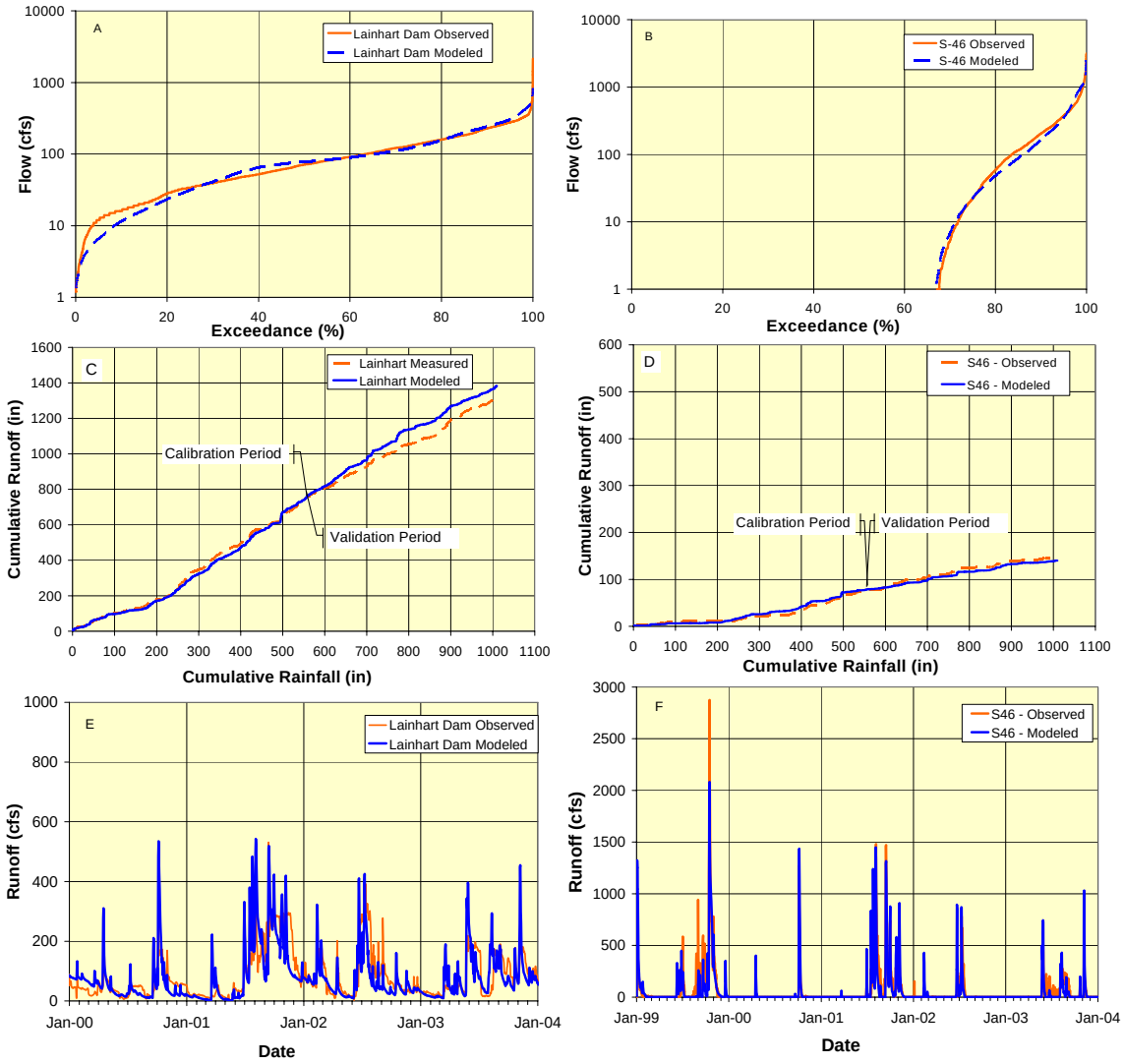

Figure 6-4. WaSh Model Calibration and Validation Plots at Lainhart and S-46 Stations (1/1/87 through 1/31/04): A. Daily flow distribution at Lainhart Dam station. B. Daily flow distribution at S-46 station. C. Double mass curve at Lainhart Dam station. D. Double mass curve at S-46 station. E. Time-series plot at Lainhart Dam station (2000-2004). F. Time-series plot at S-46 station (1999-2004).

Calibration of the C-18 and Jupiter Farms portion of the model is difficult because the Jupiter Farms Basin, the C-18/Corbett Basin, and the Grassy Water Preserve Basin are hydrologically connected. The model represented G-92 structure by using the 'special structure' option. In its

simplest form, the special structure consisted of a weir with a 12-foot elevation located in a reach consistent with its location along the C-18 canal. When the water elevation in the C-18 canal is above 12 feet, the weir structure will allow water from the C-18 canal to flow out of the basin. This discharge was subsequently used as input into the Jupiter Farms Basin as the model boundary condition. The flow rate is determined internally by the model, and is dependent on the prescribed weir configuration and the water elevation in the C-18 canal. The width of the special weir was adjusted in a series of simulations until approximately 50 cfs of water flows during normal operations and a maximum of approximately 400 cfs flows under the flood control mode.

Similarly, for the inter-basin transfer of water from the Grassy Waters Preserve (West Palm Beach Water Catchment Area) into the C-18 Canal, a special structure was imposed in a separate model set up for the L-8 Basin to allow for a time series of flow as the boundary condition for the C-18 Basin model. Water flow was based on stage in the Water Catchment Area. According to a water budget model developed for the West Palm Beach Water Catchment Area (Sculley, 1995), an annual contribution of 20,000 ac-ft of water from the Water Catchment Area to the C-18 Basin during April 1992 to March 1995 was used as a target to calibrate the special structure. The time-series plots for Lainhart Dam and S-46 station (**Figure 6-4 E** and **F**) indicate that the special structures provide a reasonable estimation of inter-basin transfers over the G-92 structure and through the existing culverts in Grassy Waters Preserve into the C-18 Basin.

The Kitching Creek station collects flow from a large area dominated by forest and wetland. **Figure 6-5** presents the performance of the model calibrated and validated at Kitching Creek. Overall, the figure shows that the model is capable of simulating flow fairly well in this area. The daily flow distribution of the modeled flow matches very well with the measured flow. The double mass curves are consistent with 0.21% of *DV* for calibration and 9.09% for validation shown in **Table 6-3**. However, the time-series plot (**Figure 6-5 C**) did show that in 1998 there were a few significant events that are not predicted by the model. Such deviations are likely related to the quality of rainfall data.

The plots for the Cypress Creek and Hobe Grove Ditch stations are shown in **Figure 6-6**. The plots for the Cypress Creek station are consistent with the model calibration and validation performance measures shown in **Table 6-3**. Model calibration and validation at the Hobe Grove Ditch station is not as good as for the Cypress Creek station. This is likely due to the quality of the data collected at the site. The Hobe Grove Ditch dataset is obtained from a stage–flow relationship downstream from several culverts that discharge from Gulf Stream Grove (owned by the District) and the structure owned by the Hobe St. Lucie Water Control District. Measuring flows under these conditions is challenging due to the complexity of the hydrologic connections and grove operations along with slight tidal influence in the downstream area. The stage-flow relationship is not as accurate as other flow gauges in the District. For example, in 1987 the Hobe Grove Ditch station failed to collect accurate data during several significant storm events; these significant events were accurately recorded by the nearby Cypress Creek station (**Figure 6-6 E** and **F).** Nevertheless, model calibration and validation at the Hobe Grove Ditch station is still considered to be acceptable in light of the poor data quality.

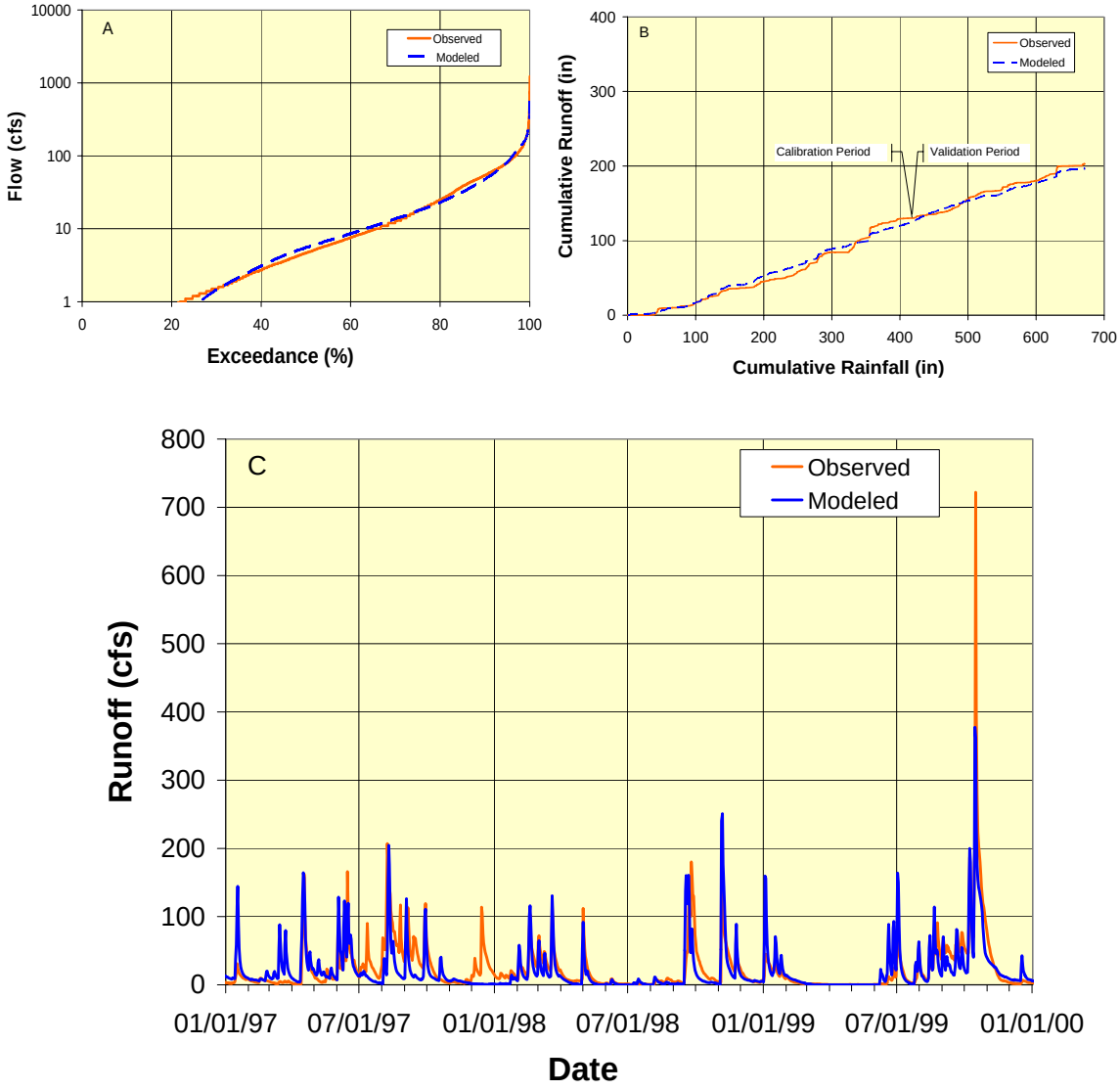

Figure 6-5. WaSh Model Calibration and Validation Plots at Kitching Creek Station (1990 through 2000): A. Daily flow distribution. B. Double mass curve. C. Time-series plot (1997-2000).

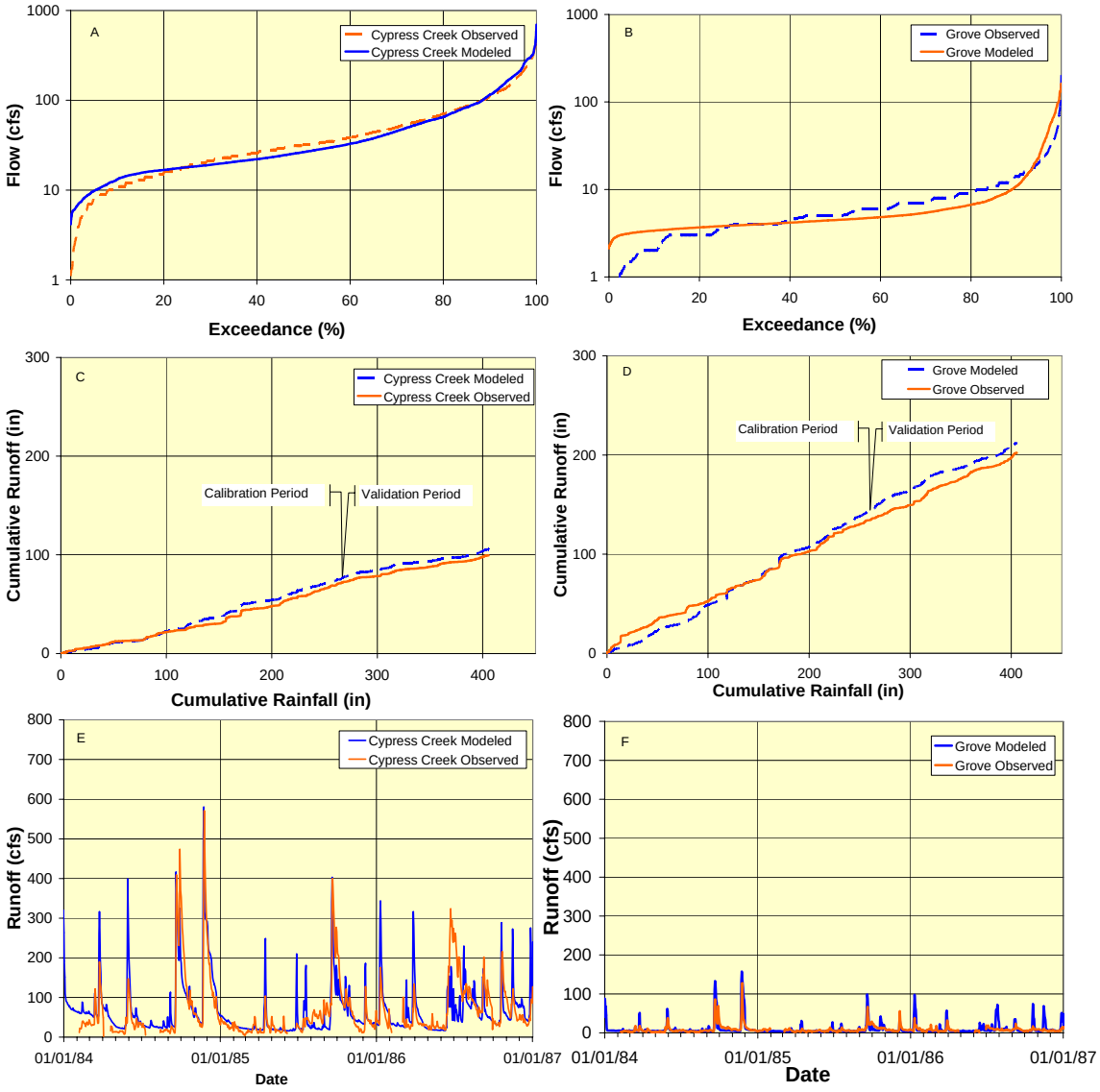

Figure 6-6. Model Calibration and Validation Plots at Cypress Creek and Hobe Grove Ditch Stations (1981 through 1990): A. Daily flow distribution at Cypress Creek station. B. Daily flow distribution at Hobe Grove Ditch station. C. Double mass curve at Cypress Creek station. D. Double mass curve at Hobe Grove Ditch station. E. Time-series plot at Cypress Creek station (1984-1987). F. Time-series plot at Hobe Grove Ditch station (1984-1987).

The calibration of groundwater level was conducted in the last step of WaSh model calibration. **Figure 6-7** shows the time series of the observed and modeled water levels at the groundwater monitoring well in the C-18 basin. Land surface elevation for the well is 24.43 feet. The cell hydrology simulated by the model is reasonable. Water level predictions could be further refined if the model is to be used for water level evaluations.

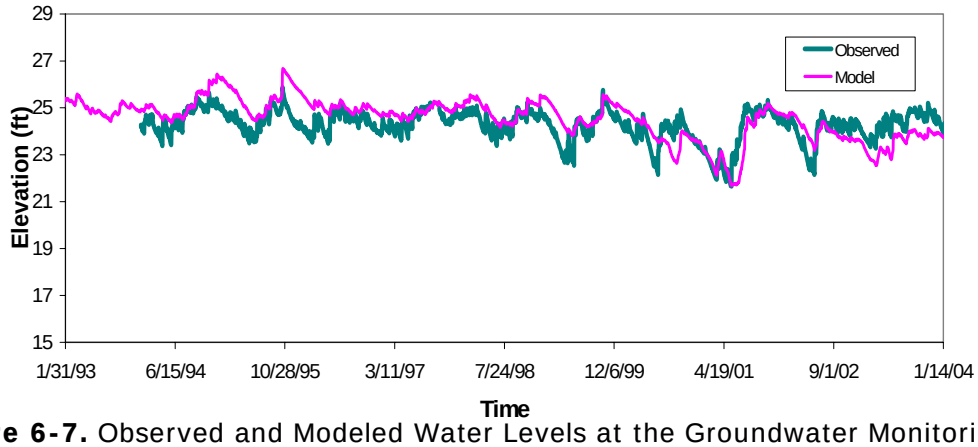

Figure 6-7. Observed and Modeled Water Levels at the Groundwater Monitoring Well (PB-689) in the C-18 Basin. Land Surface Elevation of the Well is 24.43 Feet.

WASH MODEL SIMULATION RESULTS

A final long-term simulation for the period from 1965 to 2003 was conducted after the calibration and validation of the Loxahatchee WaSh model was completed. This data set is used as the input data for the salinity simulation and alternative assessment described in **Chapter 7**. Daily flows from each of the tributaries and each of the basins described in **Chapter 2** were averaged based on the model output of the 39-year simulation. **Table 6-5** is a summary of the data expressed as daily average flows and percentage of contributions from each of the basins (tributaries) into the Loxahatchee River and Estuary and the Northwest Fork. On average, the Northwest Fork receives about 65% of total freshwater inflow into the entire Loxahatchee River and Estuary. For total freshwater inflows into Northwest Fork, flow over Lainhart Dam (C-18/Corbett G-92 plus Jupiter Farms) accounts for about 45%. The next largest contributor is Cypress Creek (32% with Pal-Mar and Grove West combined). Kitching Creek at the monitoring station contributes about 8%, and Hobe Grove Ditch contributes about 5%. The remaining 8% is contributed from the areas that are not currently covered by flow monitoring stations. However, the actual freshwater flow contribution varies on a daily basis, depending on the specific hydrologic condition and water management practices. For example, there is little freshwater flow from S-46 during the dry season whereas a disproportionately large quantity of freshwater is released from S-46 during a flood event.

Table 6-5. Flow Contributions From Each of the Basins and Major Tributaries into the Northwest Fork and Loxahatchee River and Estuary.

Basin	Average Daily Flow (cfs)	Flow Contribution	Northwest Fork Average Daily Flow (cfs)	Northwest Fork Flow Contribution
1. Kitching Gauge	17.4	5%	17.4	8%
2. North Fork	20.2	6%	--[a]	--[a]
3. Park River	5.1	2%	5.1	2%
4. Lox Estuarine	14.4	13%	--[a]	--[a]
5. C-18/Corbett G-92	69.7	22%	69.7	34%
5. C-18/Corbett S46	51.3	16%	--[a]	--[a]
6. Historic Cypress Creek	7.0	2%	7.0	3%
7. Pal-Mar	57.7	18%	57.7	28%
8. Grove West	11.1	3%	11.1	5%
9. Grove East	10.6	3%	10.6	5%
10. Jupiter Farms	21.9	7%	21.9	11%
11. Wild and Scenic	6.9	2%	6.9	3%
Totals	320.3	100%	207.4	100%

[a] This basin does not contribute flows to the Northwest Fork of the Loxahatchee River.

Tables 6-6 and **6-7** summarize the monthly mean flow for each of the years from 1965 to 2003 for flows over the Lainhart Dam and total flow into Northwest Fork covered by the four flow monitoring stations (Lainhart Dam station, Cypress Creek station, Hobe Grove station, and Kitching Creek station). For flows over Lainhart Dam (**Table 6-6**), mean monthly flows less than 35 cfs are color coded red, and those flow between 35-65 cfs are color coded light blue. These two flow ranges were selected because 35 cfs is the Minimum Flows and Levels for the Northwest Fork (SFWMD, 2002b), and 65 cfs is defined as a flow target in the model for the development of the Northern Palm Beach County Comprehensive Water Management Plan (SFWMD, 2002a). The Lainhart Dam data (**Table 6-6**) show that a low flow period occurred from 1970 through 1978. For some years, monthly mean flows were less than 35 cfs even during the wet season (June through November). Another low flow period occurred from 1987 through 1990. Extended high flow years occurred from 1991 until 1999. This pattern is consistent with the total Northwest Fork flow presented in **Table 6-7;** mean monthly flows less than 70 cfs are color coded red, and flows between 70-130 cfs are colored coded light blue. The extended low flow dry season periods in the 1960s, 1970s and 1980s probably coincide with the period during which the floodplain experienced the most significant saltwater encroachment. The high flow regime instituted in the 1990s has likely helped the floodplain hydrologic condition to recover from the preceding dry years.

Table 6-6. Monthly Mean Flows (in cfs) Over Lainhart Dam From 1965 to 2003.

	Month												
Years	Jan	Feb	Mar	Apr	May	Jun	Jul	Aug	Sep	Oct	Nov	Dec	Annual Mean
1965	39	35	14	2	1	14	29	45	10	136	71	10	34
1966	90	76	34	22	53	211	220	127	88	203	63	37	102
1967	22	40	37	18	5	52	89	114	67	193	79	26	62
1968	14	13	7	2	19	302	173	136	197	274	147	62	112
1969	71	45	116	35	154	120	79	131	135	269	173	86	119
1970	113	104	208	237	97	155	112	64	56	71	29	18	105
1971	16	18	12	3	47	19	38	46	136	79	194	73	57
1972	44	39	21	41	191	204	85	50	33	33	68	28	70
1973	28	36	14	9	13	80	66	124	134	168	41	39	63
1974	150	39	45	14	8	131	151	156	54	134	57	63	84
1975	27	30	20	7	33	104	141	31	85	108	39	15	54
1976	9	20	27	5	106	114	30	67	182	72	72	28	61
1977	60	19	10	2	25	33	11	24	271	42	24	139	55
1978	72	30	32	6	14	145	140	145	88	168	263	190	108
1979	193	79	56	47	61	51	31	19	161	146	113	66	85
1980	47	58	39	20	33	29	86	34	32	80	26	17	42
1981	7	9	3	1	2	6	6	152	176	46	53	9	39
1982	12	26	150	200	166	241	124	93	110	145	302	182	146
1983	143	200	172	108	76	141	77	135	268	342	198	157	168
1984	123	86	127	84	102	124	65	48	179	120	196	150	117
1985	72	43	28	61	21	25	65	40	144	110	53	71	61
1986	125	42	102	82	14	93	112	72	76	80	92	99	83
1987	112	36	69	25	15	24	43	30	39	137	234	34	67
1988	57	47	42	14	29	91	116	184	75	18	14	7	58
1989	4	2	17	8	7	8	30	85	25	79	14	15	25
1990	11	6	7	10	7	15	17	77	93	151	22	16	36
1991	142	118	53	141	119	160	128	86	134	192	92	83	121
1992	49	117	66	56	20	122	125	188	217	164	198	95	118
1993	231	204	200	122	92	104	87	85	164	281	149	89	150
1994	96	142	84	82	70	143	114	223	273	209	278	285	166
1995	140	96	98	85	69	101	131	288	186	352	271	153	165
1996	82	73	156	116	137	140	176	96	128	163	123	78	123
1997	81	104	84	121	93	214	109	200	222	105	83	149	130
1998	148	204	161	88	106	53	84	66	208	133	289	102	136
1999	227	89	70	39	30	172	122	109	198	335	206	109	142
2000	81	74	62	91	34	19	40	18	52	174	29	23	58
2001	16	9	46	24	8	43	197	260	254	236	145	78	110
2002	69	125	60	44	15	116	185	57	40	51	43	36	70
2003	22	14	62	46	119	137	48	149	90	73	146	75	82
Monthly Mean	78	65	67	54	57	104	94	104	130	151	120	77	92

Table 6-7. Monthly Mean Flows (in cfs) Into the Northwest Fork of the Loxahatchee River Passing the Lainhart Dam, Cypress Creek, Hobe Grove Ditch, and Kitching Creek Flow Stations From 1965 to 2003.

	Month												
Years	Jan	Feb	Mar	Apr	May	Jun	Jul	Aug	Sep	Oct	Nov	Dec	Annual Mean
1965	89	106	56	16	10	44	95	129	34	457	259	53	112
1966	281	258	115	82	184	678	682	418	271	628	206	125	328
1967	83	132	122	68	35	158	270	336	210	607	238	94	197
1968	60	54	39	23	74	952	530	420	652	848	436	181	356
1969	204	136	346	108	438	372	256	395	426	876	523	253	363
1970	337	300	671	728	268	452	328	178	167	200	93	64	315
1971	58	64	48	28	148	68	121	135	403	246	633	239	182
1972	138	133	78	137	593	639	252	155	107	110	222	95	221
1973	99	121	59	44	56	242	205	405	408	517	134	126	202
1974	483	133	145	53	39	367	428	479	175	398	181	181	257
1975	89	95	65	36	107	299	436	107	260	323	124	59	167
1976	40	77	80	29	332	354	100	208	560	227	220	99	193
1977	193	67	44	22	95	97	41	78	853	142	84	406	177
1978	234	102	106	32	50	504	449	438	244	522	840	573	343
1979	544	226	152	139	164	147	91	62	517	483	342	192	255
1980	152	173	122	66	110	95	260	107	120	285	106	70	139
1981	39	53	25	18	16	26	28	476	542	154	188	43	134
1982	55	103	504	685	566	749	417	284	356	458	983	476	470
1983	455	656	552	330	203	418	202	388	853	1,074	606	487	517
1984	367	247	382	237	300	345	166	130	563	360	615	466	348
1985	192	116	83	183	65	89	185	115	448	350	160	210	183
1986	400	122	336	232	51	272	341	259	237	255	305	334	263
1987	335	113	218	84	62	88	134	89	143	441	741	119	214
1988	176	154	138	52	92	250	348	583	254	73	58	36	185
1989	30	24	62	38	30	32	88	233	88	246	58	58	83
1990	49	41	34	42	31	46	63	243	333	435	85	68	123
1991	495	374	161	417	345	481	361	267	400	594	282	240	368
1992	147	326	179	160	64	372	415	584	645	496	632	293	359
1993	740	619	598	340	244	274	233	237	447	867	416	238	437
1994	269	438	225	216	185	465	344	670	842	675	887	874	507
1995	417	275	284	227	172	256	343	858	568	1,146	812	401	482
1996	228	186	430	304	380	389	545	270	383	543	409	225	359
1997	247	300	241	372	262	689	343	594	671	314	224	446	392
1998	431	639	485	233	279	133	228	174	661	414	908	301	404
1999	749	261	181	103	84	495	343	299	599	1,079	606	314	427
2000	216	187	161	255	100	60	114	56	150	516	85	73	165
2001	53	37	126	66	39	149	477	794	792	668	387	203	318
2002	175	343	156	151	51	288	532	164	114	138	115	102	193
2003	65	47	202	136	372	392	126	354	235	184	381	181	224
Monthly Mean	241	201	205	166	172	314	280	312	403	470	374	231	281

Because of the hydrologic variability during the past 39 years, the 39-year daily flow data at Lainhart Dam were analyzed to determine the daily flow distribution for each of the 12 months of all the 39 years. This analysis indicates that the daily flow distribution in a month during the 39 years is not normally distributed. The results are summarized in **Figure 6-8** which plots the median flow and the 75th percentile flow in the month. The 75th percentile flow represents the flow that is exceeded by only 25% of days in that month during the 39 years. Daily flow from Lainhart Dam is less than 50 cfs for 50% of time during the months of February, March, April, and May. Flows in April and May are the lowest among all the months. This again shows the importance of flow augmentation during these low flow months.

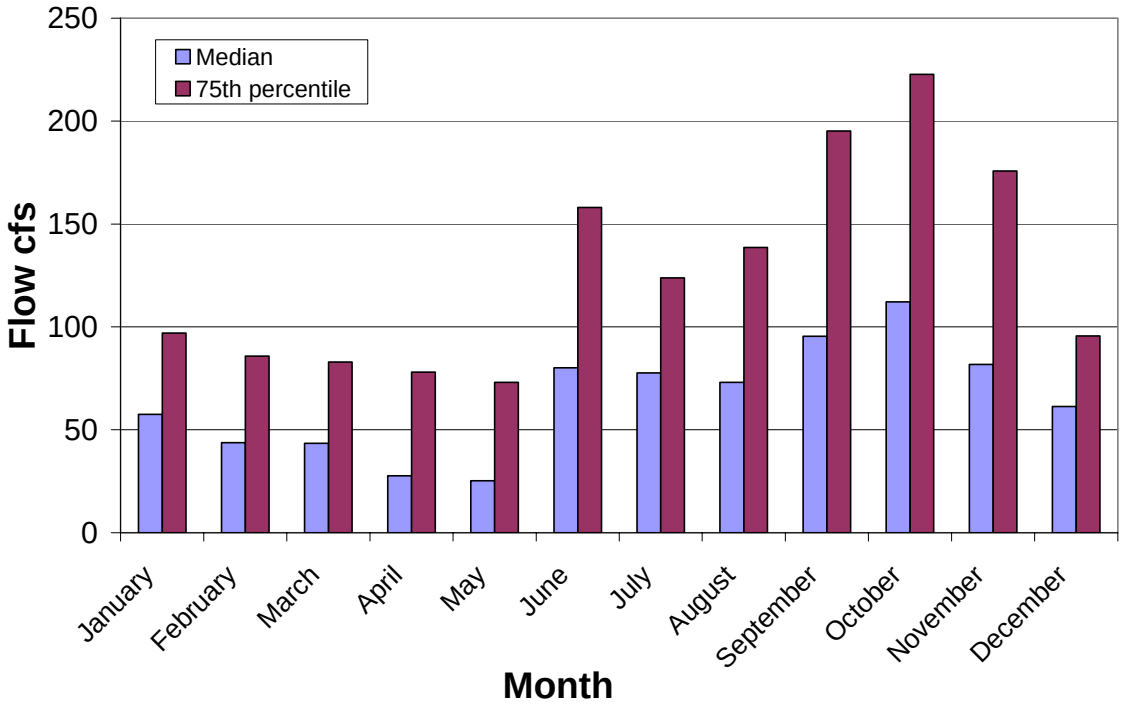

Figure 6-8. Monthly Median Flow and the 75th Percentile Flow Over Lainhart Dam for the Period 1965 to 2003.

MODELING SALINITY

THE HYDRODYNAMIC/SALINITY (RMA) MODEL DESCRIPTION

A hydrodynamic/salinity (RMA) model was developed to study the influence of freshwater flows from the tributaries of the Northwest Fork and S-46 on the salinity conditions in the Loxahatchee River and Estuary. In parallel with model development, a data collection network was established to measure tide and salinity at five sites from the embayment area near the Jupiter Inlet (RM 0.70) to River Mile 9.12. The objective of salinity data collection and model development was to establish the relationship between salinity and the amount of freshwater inflow. The main focus of the data collection and salinity modeling has been on the Northwest Fork of the Loxahatchee River.

The software programs used in the development of Loxahatchee River Hydrodynamics/Salinity Model were RMA-2 and RMA-4 (USACE, 1996). RMA-2 is a two-dimensional depth-averaged finite element hydrodynamic numerical model. It computes water surface elevations and horizontal velocity components for subcritical, free-surface flow in two dimensional flow fields. RMA-2 computes a finite element solution of the Reynolds form of the Navier-Stokes equations for turbulent flows. Friction is calculated with the Manning's n or Chezy equation, and eddy viscosity coefficients are used to define turbulence characteristics. Both steady and unsteady state (dynamic) problems can be analyzed. The program has been used to calculate water levels and flow distribution around islands; flow at bridges having one or more relief openings, in contracting and expanding reaches, into and out of off-channel hydropower plants, at river junctions, and into and out of pumping plant channels; circulation and transport in water bodies with wetlands; and general water levels and flow patterns in rivers, reservoirs, and estuaries.

The water quality model, RMA-4, is designed to simulate the depth-average advection-diffusion process in an aquatic environment. The model is used for investigating the physical processes of migration and mixing of a soluble substance in reservoirs, rivers, bays, estuaries and coastal zones. This model was used to evaluate salinity and the effectiveness of various restoration scenarios. For complex geometries, the model utilizes the depth-averaged hydrodynamics from RMA-2.

IMPLEMENTING THE RMA MODEL

Model Setup

Based on the most recent bathymetry, freshwater inflow and tide data, the RMA model was updated in early 2004. The current model mesh includes a total of 4956 nodes with elevations derived from the survey data provided by USGS. **Figure 6-9** shows the RMA model mesh construction with 1075 quadrilateral elements and 231 triangular elements. Arrows in the figure indicate the locations where freshwater inflows are applied. The four tributaries that contribute freshwater to the Northwest Fork are Lainhart Dam, Cypress Creek, Hobe Grove Ditch and Kitching Creek. The RMA model domain also includes the Southwest Fork and flows from the S-46 structure. The RMA itself does not predict the amount of freshwater entering the system from the watershed or discharge structures. The freshwater discharge amounts from these tributaries and structures are provided by the WaSh model or from recorded data from the flow gauges.

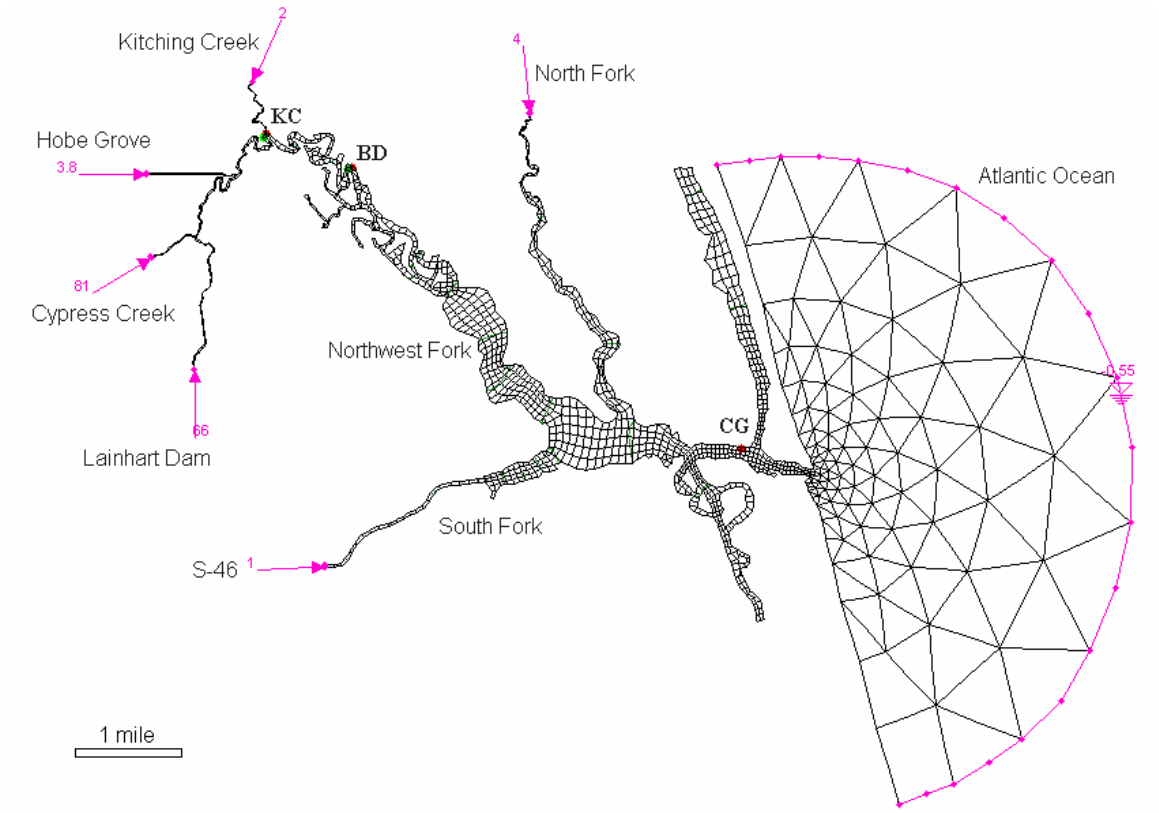

Figure 6-9. The RMA Model Domain Map. KC = Kitching Creek USGS Station; BD = Boy Scout Dock Station, CG – US Coast Guard Station.

The meandering river channel pattern is one of the fundamental characteristics of the natural system of the Northwest Fork of the Loxahatchee River. The previous studies have demonstrated that restoring the natural oxbows to the Northwest Fork can effectively reduce saltwater intrusion into the historically freshwater reaches. The meandering river channel and oxbows of the Northwest Fork are preserved in the construction of the RMA model mesh.

Several natural river channel restoration projects have been implemented in the past decade to restore oxbows to the Northwest Fork. Salinity measurements taken before and after the implementation of the projects indicate that the oxbows can reduce the extent of saltwater intrusion to the Northwest Fork. The RMA model mesh contains the geographic features of the river channel. Depending on the time period, the model simulation can be conducted with the oxbow restoration projects completed for the post-project period or without the restored oxbows for the pre-project period. The current model mesh is also detailed enough to simulate the effectiveness of potential channel restoration projects in river reaches up to the Trapper Nelson Interpretive Site. The channel above the Trapper Nelson Interpretive Site will be further refined in the mesh after an on-going GIS project is completed that will provide more detailed geometry for the river channel above the Trapper Nelson Interpretive Site. On the ocean side, the model mesh was extended three miles offshore into the Atlantic Ocean to obtain a relatively stable salinity boundary condition (Hu, 2004).

The RMA model was applied to establish the relationship between the amount of freshwater inflow and the salinity regime in the Northwest Fork Loxahatchee River. The freshwater ~ salinity relationship provided means to assess restoration plan scenarios.

Model Verification

In parallel with the preliminary RMA model setup, a data collection program was implemented. A bathymetric survey was conducted by U.S. Geological Survey (USGS) in early 2003. Water depth was recorded along survey lines in the Northwest Fork and the North Fork of the Loxahatchee River. The Northwest Fork survey covered river reaches from River Mile 4.0 to the Trapper Nelson's Interpretive Site (RM 10.50). Approximately three miles of the North Fork were also surveyed. In addition to the flow gauges located at Lainhart Dam and Kitching Creek, two additional gauges were established on Cypress Creek and Hobe Grove Ditch in November 2002. These four flow gauges monitor the majority of freshwater input to the Northwest Fork. Four tide and salinity stations have also been deployed in the estuary since November 2002 by USGS. An additional tide/salinity gauge was installed at RM 9.12 in October 2003 by the Water Supply department of the District. These five tide/salinity stations monitor the tide and salinity in the estuary continuously and record the data at 15-minute intervals. The data are retrieved at scheduled maintenance times and reported quarterly after quality assurance and quality control has been conducted. To detect temperature and salinity stratification, three of the tide/salinity stations record salinity and temperature measurements at two water depths. The three sites with double temperature/salinity sensors are located at River Mile 9.12, Boy Scout Camp dock (RM 5.92) and the U.S. Coastal Guard Station near the Jupiter Inlet (RM 0.70). All sensors were installed at water levels below lower low tides to avoid exposure to air.

In addition to tide and salinity measurements obtained from the USGS sites, the Loxahatchee River District (LRD) also has an estuarine data collection program at several additional locations that are not covered by the USGS monitoring network. The LRD uses multi-parameter datasondes to record time, dissolved oxygen, water depth, conductivity/salinity, pH and temperature. The meters are located near the bottom of the channel in order to track maximum salinity changes in the water column. The LRD data were collected at North Bay seagrass survey site (RM 1.48), Pennock Point seagrass survey site (RM 2.44), Northwest Fork near the mouth of Kitching Creek (RM 8.13), Station 66 in the Wild and Scenic Loxahatchee River and Station 69 near the Indiantown Road (RM 14.93). To measure current velocity, the LRD contracted Scientific Environmental Applications to install two bottom mount Acoustic Doppler Current Profiler (ADCP) units at various locations in the estuary in 2003.

The Loxahatchee hydrodynamic/salinity (RMA) model was verified against field data for the period from May 1 to August 12, 2003. **Figure 6-10** shows the combined freshwater inflow from four major tributaries to the Northwest Fork for the period from May 1 to August 12, 2003. Daily averaged flow rates in terms of cubic feet per second from flow gauges on upper Northwest Fork at Lainhart Dam, Cypress Creek, Hobe Grove and Kitching Creek were used for the calculation. Discharge from S-46 into the South Fork was based on measurements at the discharge structure for the model simulation period.

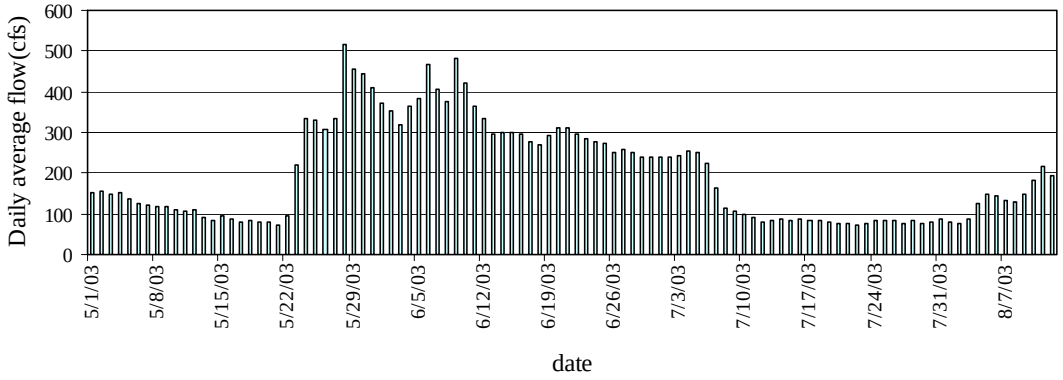

Figure 6-10. Freshwater Inflow From Major Tributaries to the Northwest Fork of the Loxahatchee River.

Figure 6-11 is a comparison of tidal data from the Coast Guard station (RM 0.70) with the RMA-2 model output for the same location. Because the two curves overlap each other when printed in the same chart, the model output and field data are plotted in separate charts using the same scale and grid lines for ease of comparison. For RMA-4 applications, a constant salinity of 35.5 ppt was applied on the ocean boundary.

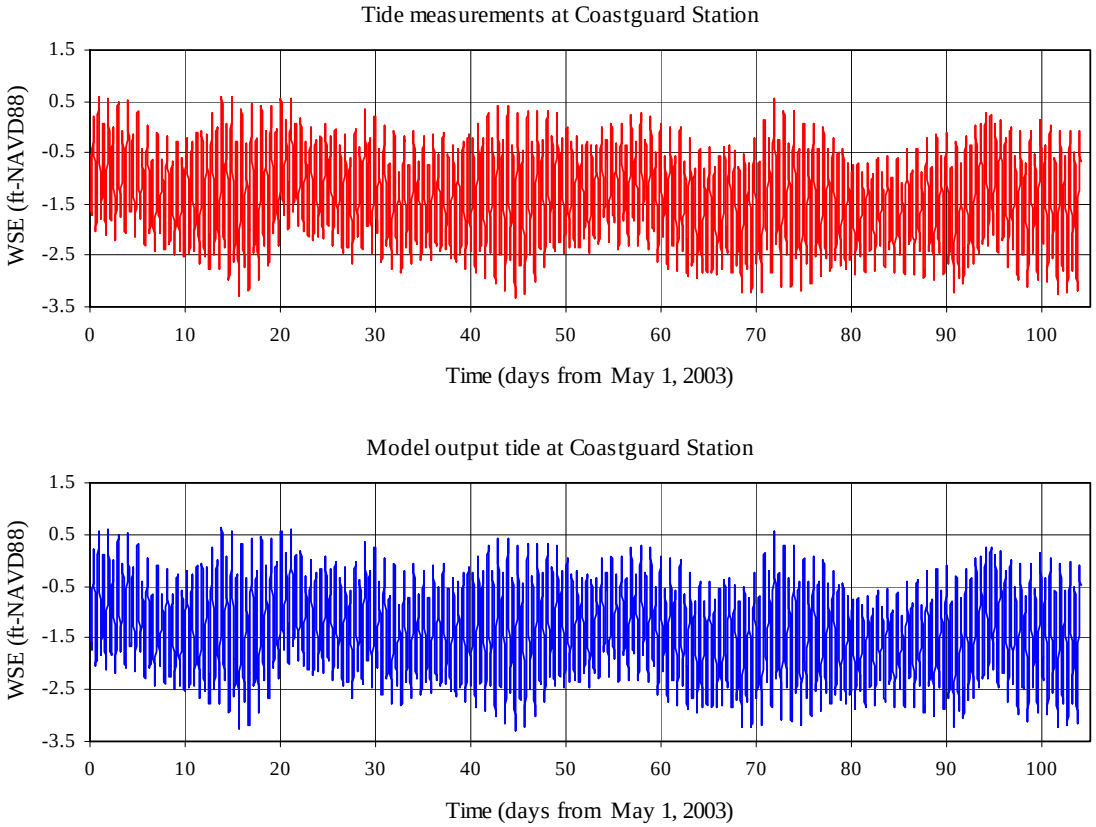

Figure 6-11. Tide Measurements at the Coast Guard Station (RM 0.70): Field Data and RMA Model Output.

Field data and model output of tides at Boy Scout Dock (RM 5.92) and Kitching Creek (RM 8.13) are plotted in **Figure 6-12** for comparison. The two stations are approximately 2 river miles apart and there is no major tributary between them. Both field data and model output indicate that the tidal regimens at these two sites are similar in terms of range.

Figure 6-13 compares model output of depth-averaged salinity with actual field salinity measurements from instruments at fixed elevations However, although these two quantities are similar, they do not represent the same physical parameters and are not directly comparable. The difference between the model output (representing depth-averaged salinity) and the actual field measurement (representing salinity at a fixed depth) could be significant when the system is stratified.

The salinity record at Boy Scout Dock increased to 10 ppt between Day 50 and Day 60. This sudden salinity increase does not seem to be related to or supported by data from other field records. A salinity of 10 ppt usually occurs at this site when freshwater inflow is below 100 cfs. The flow gauges actually recorded over 200 cfs for this period. The salinity record from the adjacent Kitching Creek station is also inconsistent with the salinity increase at the Boy Scout Dock station. Previous studies indicated that 10 ppt at Boy Scout Dock station would have raised salinity at Kitching Creek station to 2 ppt or above (Russell & McPherson, 1984); however, there was no salinity increase for Kitching Creek during this time period (see the Kitching Creek chart in **Figure 6-13**). Therefore the accuracy of the salinity field measurements at Boy Scout Dock between Day 50 and Day 60 is questionable.

Both RMA-2 and RMA-4 are two-dimensional depth-averaged models. When the system is minimally stratified, such as the condition near the Jupiter Inlet at the Coast Guard station, the modeled salinity output tracks the field salinity data rather closely. However, when the system is highly stratified, as occurs in certain areas, the modeled salinity output for that area could give a smaller salinity variation between high tide and low tide when compared to the field salinity measurements from fixed depths (see the Boy Scout Dock chart in **Figure 6-13**).

The RMA-4 output is depth-averaged salinity, which differs from salinity measured by a transducer at a fixed elevation. The conductivity transducers were installed at elevations that would remain below the water surface at low tide. Since the range between higher high and lower low water is close to 4 feet and the overall water depth is only about 6 feet to 10 feet, the conductivity transducers would be situated in the lower water column during high tide. Under these conditions, the instrument would take measurements from the surface layer at low tide and from the bottom layer at high tide. If the system is well mixed (i.e., no stratification), there should be no difference between the modeled depth-averaged salinity and field salinity measurements. However, when the system is stratified, the daily salinity variation recorded by the instruments would be wider than the daily salinity variation output from depth-averaged salinity model.

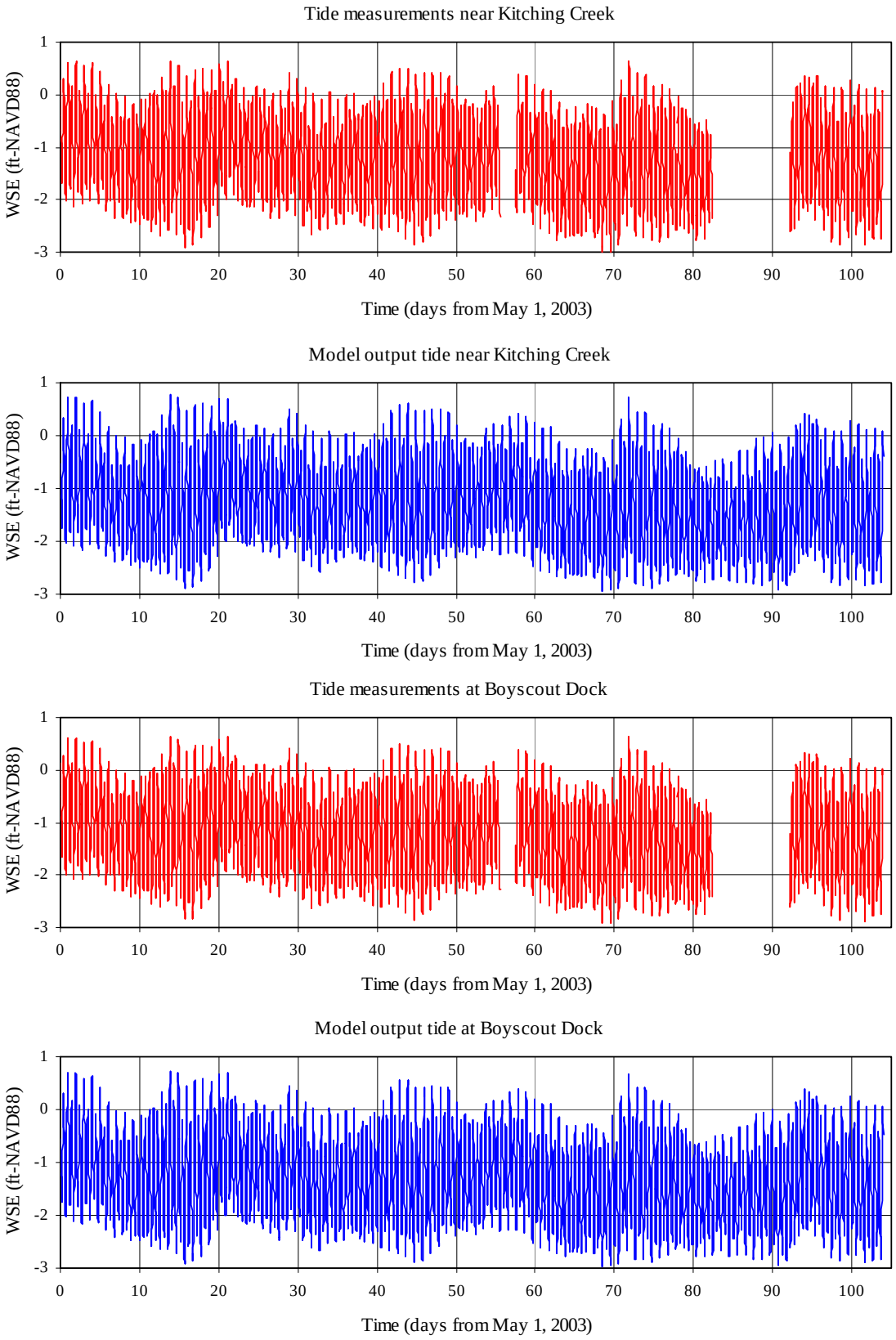

Figure 6-12. Tide at Boy Scout Dock (RM 5.92) and Kitching Creek (RM 8.13) Stations – Field Data and Model Output.

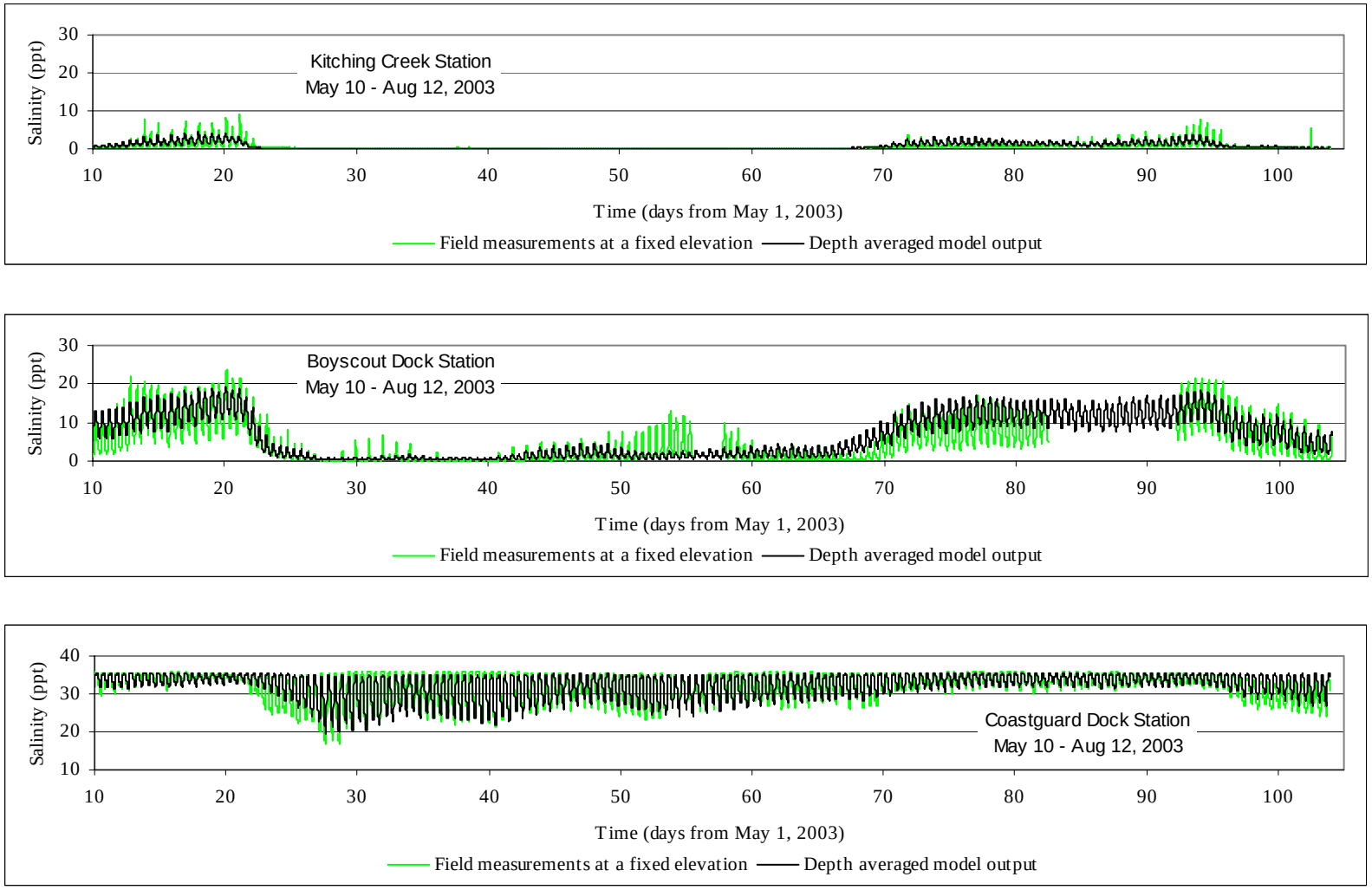

Figure 6-13. Model Output of Depth-Averaged Salinity and Field Measurements at Fixed Elevations in the Water Column.

The most likely reason for the difference between model prediction and field measurements is that there is additional freshwater inflow to the system that bypasses the four stations on the river and the major tributaries. Such additional sources of freshwater may include overland flow and groundwater seepage into the system. A groundwater monitoring network that was established in 2003 indicates active exchanges between the river and the groundwater table. The model predicted higher salinity at the beginning of dry periods when the groundwater tables are still relatively high and therefore provide additional freshwater to the system. Including groundwater input in the model will likely increase the accuracy in salinity prediction. The current model, without the input of groundwater input and overland flow, tends to be conservative (predicting higher salinity).

The current model does not include driving forces such as wind, precipitation/evaporation and the exchange between the river and the groundwater which can be significant in the upper river reaches. The model verification simulation, which was only driven by major tributary freshwater input and ocean tide, was able to predict the tide regimen rather accurately and predict the trend of salinity changes over the 3-month simulation period that included both low and high freshwater input to the estuary. This seems to indicate that the amount of freshwater inflow to the estuary and tide are the two most dominant factors that affect the salinity regimen in the estuary.

RMA MODEL SIMULATION RESULTS – FRESHWATER INFLOW AND SALINITY RELATIONSHIP

The tidal circulation and salinity structure of estuaries involves competition between freshwater river flows and ocean influences. River flow persistently adds freshwater to the estuary, however saltwater may still penetrate far inland due to gravitational and diffusive fluxes (MacCready, 2004). Although there are other factors in addition to tide and freshwater inflows that affect the salinity regime, the analysis of the field data from the Loxahatchee River suggested that tide and freshwater inflow are the two most important factors that determine the salinity conditions in the Northwest Fork (Hu, 2004). To establish the relationship between freshwater inflow and salinity in the Northwest Fork of the Loxahatchee River, the RMA model was used in 12 modeling scenarios where the amount of total freshwater flow from all three forks of the Loxahatchee River into the estuary was held constant for rates varying from 40 cfs at the low flow end to 7,000 cfs at the high flow end. These flow rates were determined based on an analysis of freshwater inflows simulated by the watershed model (WaSh). During RMA model output processing, 15 study sites were identified for ecological assessment where salinity predictions are needed. Information about study and assessment sites is provided in **Table 6-8**. Sites noted as USGS stations are locations where tide and salinity measurement data are collected by U.S. Geological Survey as discussed in the previous sections. **Figure 6-14** shows the locations of the 15 assessment sites.

Table 6-8. The 15 Salinity and Ecological Assessment Sites.

Coordinates[a]		Site		Description
X (feet)	Y (feet)	Station ID	River Mile	
955325	951200	CG	0.70	USGS Coast Guard
951456	952232	SGNB	1.48	Seagrass site - North Bay
949616	951344	SGSB	1.74	Seagrass site - Sand Bar
949538	950648	PD	1.77	USGS Pompano Drive
945680	951761	SGPP	2.44	Seagrass site - Pennock Point
945105	953335	O1	2.70	Oyster site 1
942902	954999	O2	3.26	Oyster site 2
942332	957383	O3	3.74	Oyster site 3
940923	958927	O4	4.13	Oyster site 4
938854	961625	O5	4.93	Oyster site 5
936681	963169	O6	5.45	Oyster site 6
935708	965258	BD	5.92	USGS Boy Scout Dock
934679	966363	VT9	7.06	Vegetation Transect 9
931399	966948	KC	8.13	USGS Kitching Creek
929733	964696	RM9	9.12	USGS River Mile 9.1; Vegetation Transect 7

[a] State Plane Florida East NAD83.

The objective of this RMA model application is to establish a relationship between the amount of freshwater inflow and tidally averaged salinity. The RMA model output was averaged over a lunar month that includes a full lunar tidal cycle with both spring and neap tides. Thus, these results reflect the daily averaged salinity under an average tidal condition.

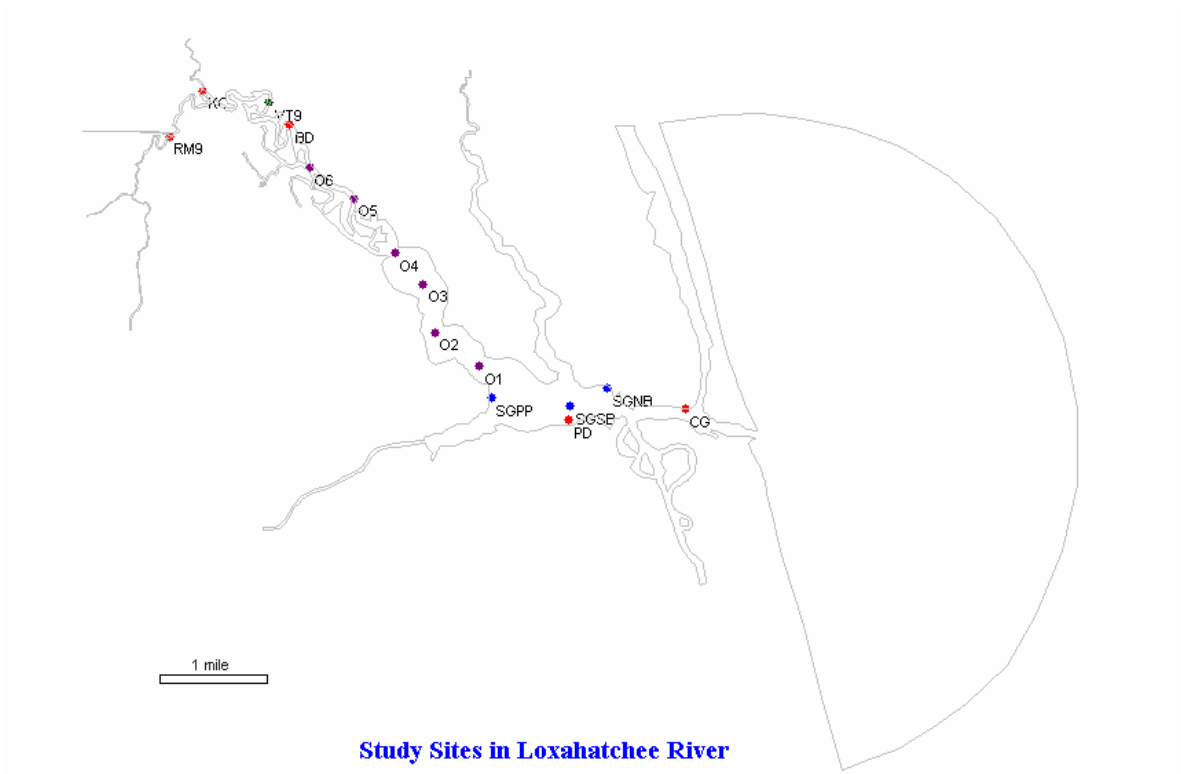

Figure 6-14. Location of Salinity and Ecological Assessment Sites. Red dots are USGS sites; Blue dots are Seagrass sites; Purple dots are Oyster sites; Green dots are Vegetation sites.

Table 6-9 is a summary of the RMA model output of average salinity for 12 flow scenarios at each of the 15 sites. Regression analysis of the results yielded regression equations with excellent curve fitting. The best fit (R^2 = 0.999 for all the 15 sites) was achieved with exponential functions in the form of

$$Y = Y_0 + a\, e^{-bX} \qquad [11]$$

Where X is freshwater inflow in cubic feet per second and Y is salinity in parts per thousand. Y_0, a, and b are regression parameters that are listed in **Table 6-9** for each of the 15 sites.

Table 6-9. Tidally Averaged Salinity (ppt) vs. Freshwater Inflow (cfs) for the 15 Study Sites in the Loxahatchee River.

Flow(cfs)	CG	SGNB	SGSB	PD	SGPP	O1	O2	O3	O4	O5	O6	BD	VT9	KC	RM9
40	34.6	34.1	33.9	33.8	33.2	32.7	32.0	31.1	30.5	27.8	25.8	23.6	16.8	9.7	4.2
70	34.4	33.6	33.3	33.2	32.3	31.7	30.5	29.2	28.3	24.4	21.6	18.8	11.0	4.9	1.4
100	34.1	33.1	32.7	32.7	31.5	30.6	29.0	27.4	26.2	21.5	18.1	15.0	7.2	2.5	0.5
150	33.7	32.4	31.8	31.7	30.1	29.0	26.8	24.7	23.1	17.3	13.5	10.3	3.6	0.9	0.2
200	33.3	31.6	30.9	30.8	28.8	27.4	24.8	22.2	20.4	13.9	10.0	7.1	1.9	0.4	0.2
300	32.5	30.1	29.1	29.0	26.4	24.5	21.1	18.0	15.9	9.1	5.6	3.4	0.6	0.2	0.2
500	31.0	27.4	26.0	25.8	22.2	19.6	15.4	11.8	9.6	3.9	1.8	0.9	0.2	0.2	0.2
800	28.8	23.8	21.8	21.6	17.1	14.0	9.6	6.3	4.6	1.2	0.5	0.3	0.2	0.2	0.2
1200	26.1	19.6	17.3	17.0	12.1	9.0	5.2	2.8	1.8	0.4	0.2	0.2	0.2	0.2	0.2
2400	19.3	10.9	8.5	8.3	4.3	2.5	0.9	0.4	0.3	0.2	0.2	0.2	0.2	0.2	0.2
4800	10.1	3.1	1.9	1.8	0.6	0.4	0.2	0.2	0.2	0.2	0.2	0.2	0.2	0.2	0.2
7000	5.0	0.6	0.3	0.3	0.2	0.2	0.2	0.2	0.2	0.2	0.2	0.2	0.2	0.2	0.2
y0	-3.074	-0.753	-0.334	-0.291	0.118	0.223	0.225	0.215	0.219	0.224	0.2	0.19	0.16	0.153	0.151
a	38.04	35.51	34.99	34.94	34.25	34.02	33.83	33.68	33.52	32.92	32.47	31.83	29.3	24.76	19.4
b	3E-04	6E-04	7E-04	7E-04	0.001	0.001	0.002	0.003	0.003	0.006	0.008	0.01	0.018	0.03	0.049

The freshwater flow versus salinity relationships tabulated in **Table 6-9** are plotted in **Figures 6-15** and **6-16**. Each curve in **Figure 6-15** represents the flow ~ salinity relationship for each of the 15 sites. For each site, salinity increases as freshwater inflow decreases.

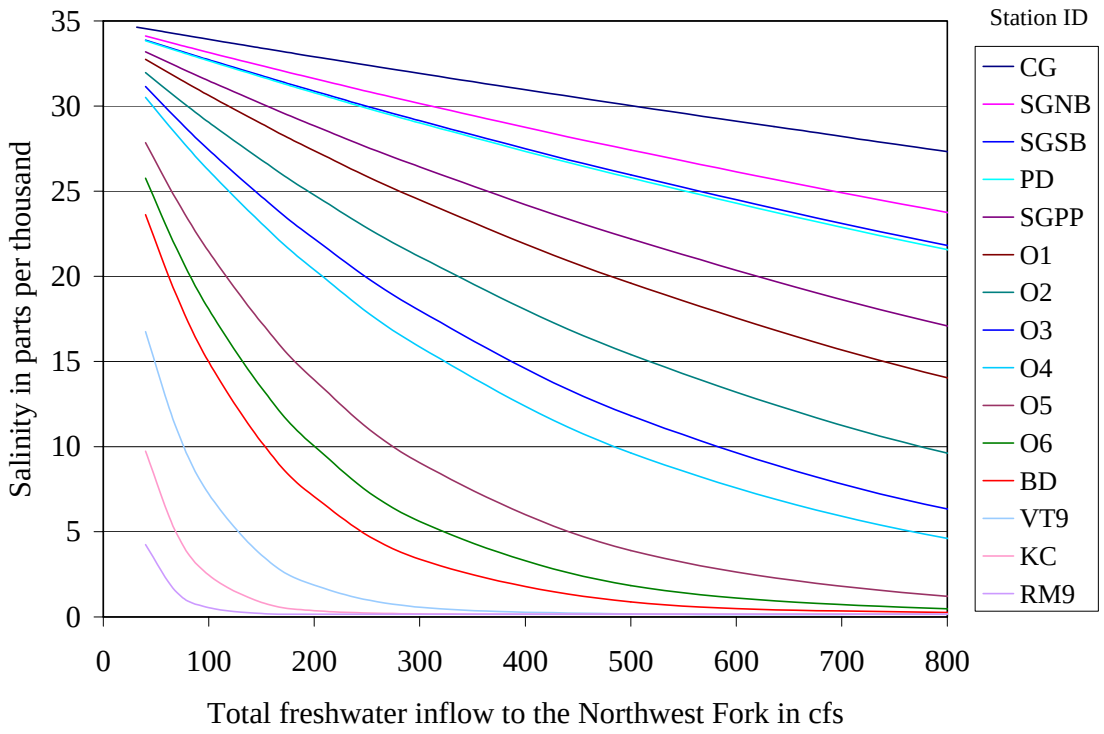

Figure 6-15. The Relationship Between Freshwater Inflow and Salinity at 15 Sites.

In order to show the details of salinity variation at low flow end, the charts were plotted only for inflows up to 800 cfs. For salinity regimens with freshwater inflows greater than 1,200 cfs,

either **Table 6-9** or Equation [11] can be used to determine the salinity value. The curves in **Figure 6-16** represent the salinity gradients at various levels of freshwater inflow. Each line represents the spatial salinity distribution for a particular inflow scenario.

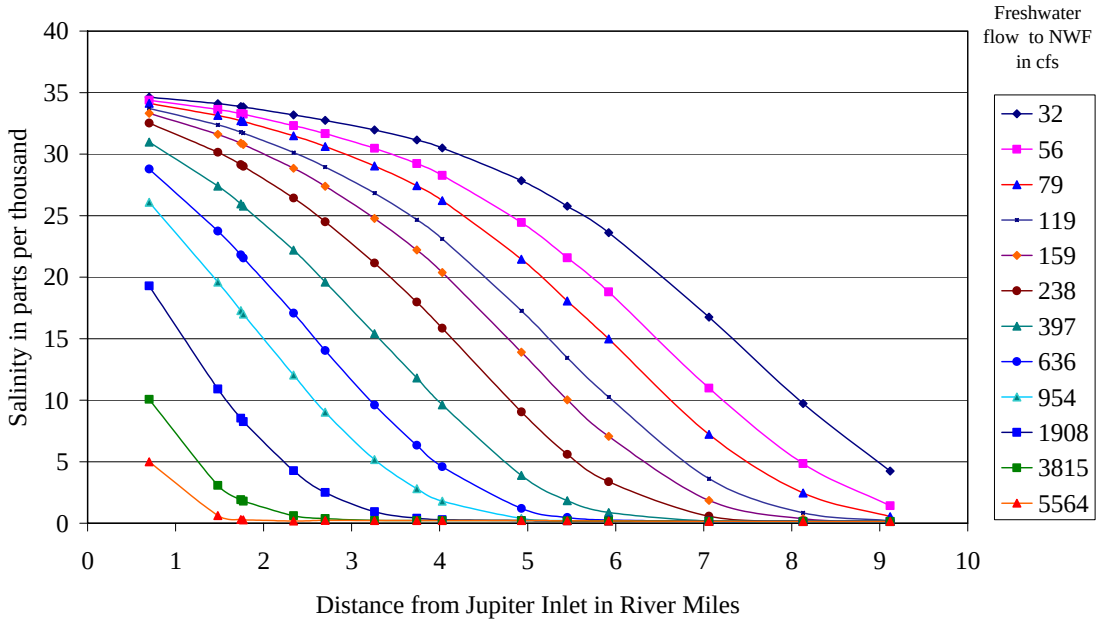

Figure 6-16. Salinity Gradients for Various Freshwater Inflow Conditions.

Although Equation [11] expresses salinity as a single dependent variable function, there are other driving forces that affect salinity including tide, wind, flux between river and groundwater, precipitation and evaporation. However, the analysis of field data indicated that freshwater inflow is the most important factor affecting salinity. When salinity is plotted against freshwater flow, the data points form a clear trend line. Comparing results from Equation [11] with actual field data provides a reality check. **Figures 6-17** through **6-20** compare the model results from Equation [11] with actual field measurements. As expected, deviations from the modeled flow ~ salinity curve indicate the existence of other driving forces that affect salinity. Nonetheless, the correlation between salinity and freshwater inflow is significant. Another factor that could cause deviations is that the system is under constant transition in response to the changes in the driving forces. Therefore it is rare for the system to reach equilibrium as the case in the constant flow simulations. The overall trend of the field measurements shows a strong correlation between the amount of freshwater inflow and salinity throughout the estuary.

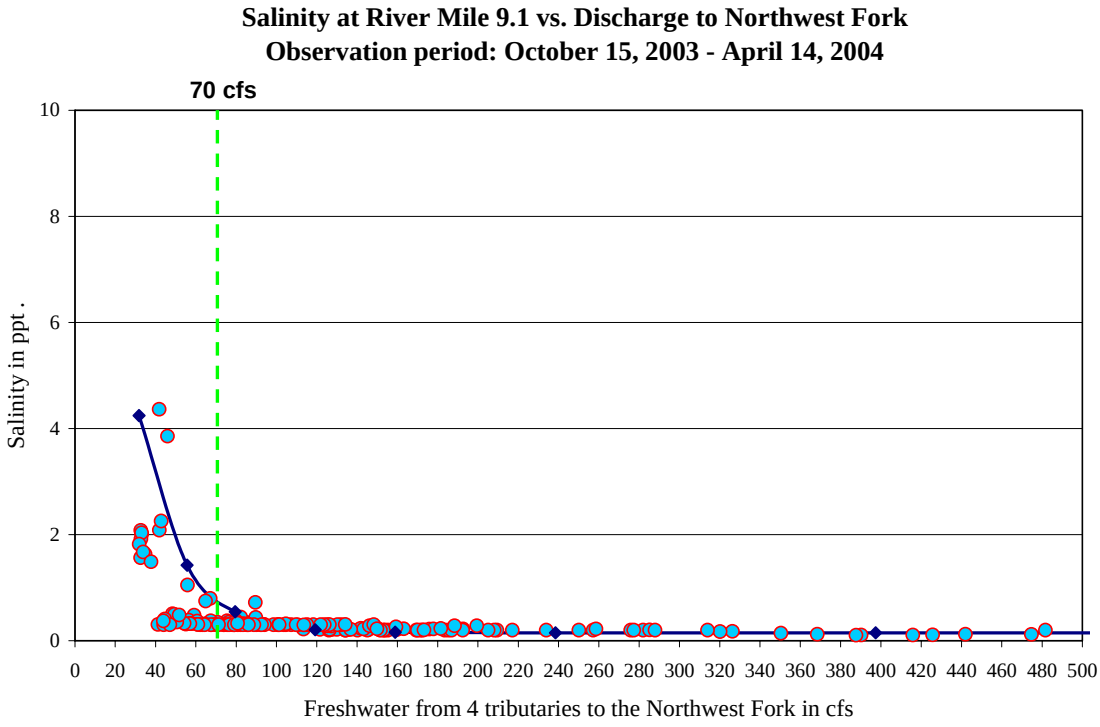

Figure 6-17. The Effects of Freshwater Inflow on Salinity at River Mile 9.1 Between October 15, 2003 and April 14, 2004.

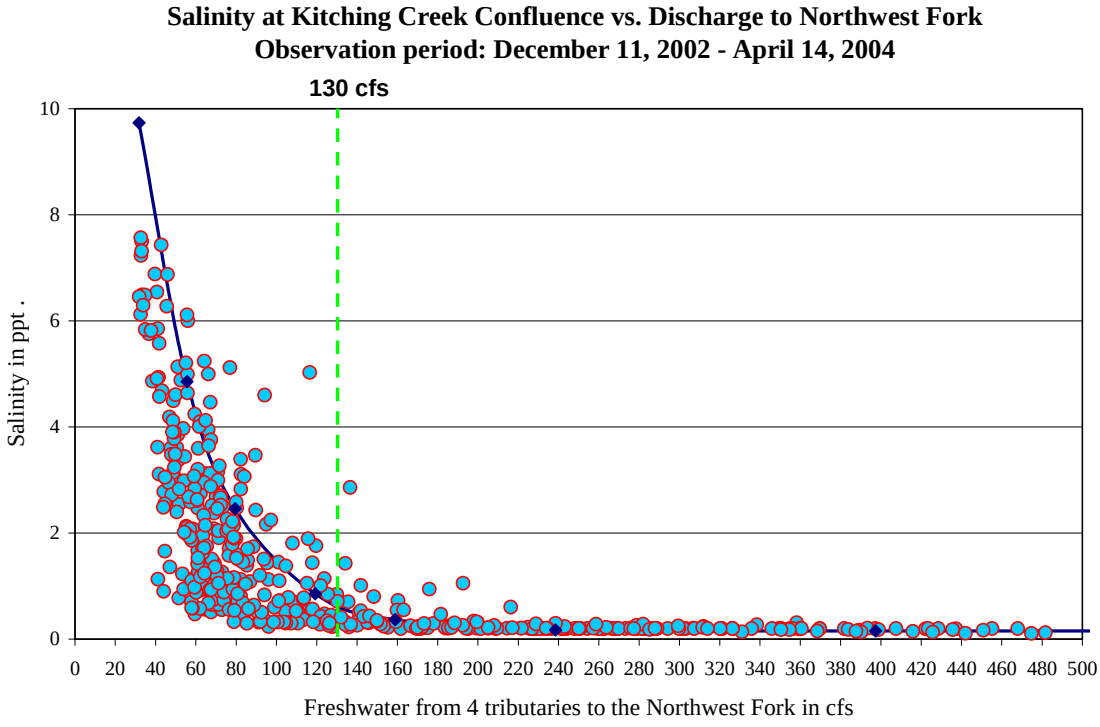

Figure 6-18. The Effects of Freshwater Inflow on Salinity at Kitching Creek Between December 11, 2002 and April 14, 2004.

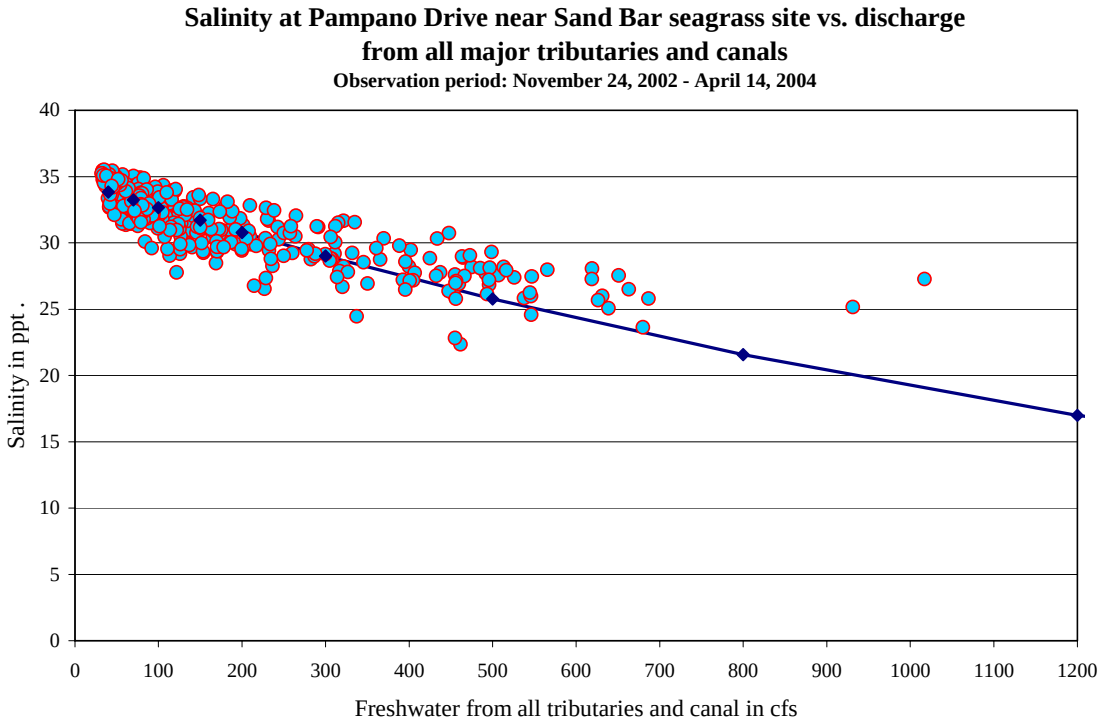

Figure 6-19. The Effects of Freshwater Inflow on Salinity at Boy Scout Dock Between December 11, 2002 and April 14, 2004.

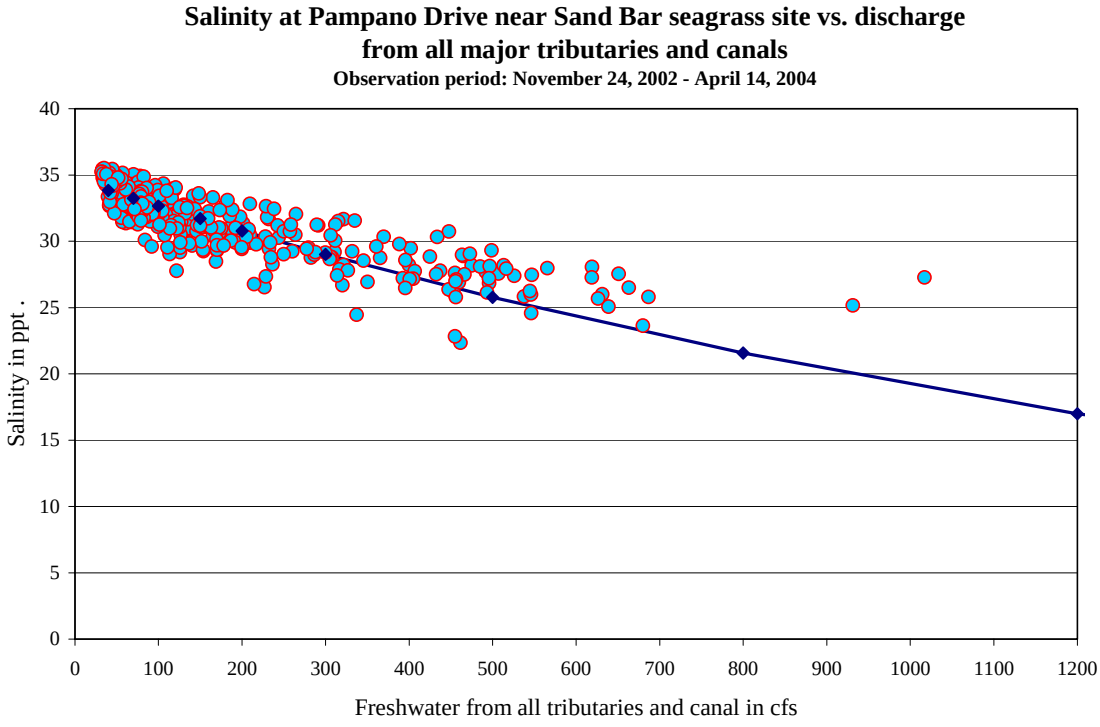

Figure 6-20. The Effects of Freshwater Inflow on Salinity in the Embayment Between November 24, 2002 and April 14, 2004.

Freshwater inflows to the Northwest Fork from the four major tributaries, several small tributaries and overland flow were modeled. If the inflows from all the tributaries were considered individually, they would form a large array of scenarios. The analysis of the field data indicates that there is a good correlation between salinity at various sites with the total freshwater flow volume to the Northwest Fork. The physical explanation for this correlation is the strong tidal mixing in the Northwest Fork. For example, when the tide rises, freshwater inflows from Kitching Creek will be pushed upstream into the river reaches above the mouth of Kitching Creek and thus influence the salinity there. It is the total volume of freshwater entering the Northwest Fork that matters the most. The origin of freshwater (whether the freshwater was from Kitching Creek or some other tributary) does not seem to be an important factor in the analysis. Such a finding has two implications:

1. Freshwater from all the tributaries affects the salinity in the Northwest Fork. Therefore, any increase of freshwater discharge from any combination of tributaries will help achieve the salinity management goal of the Northwest Fork. In addition to increasing freshwater flows from the G-92, flows from other tributaries and basins such as Cypress Creek/Pal Mar, and Kitching Creek should also be fully utilized.

2. Salinity predictions in the Northwest Fork can be based on total freshwater inflow to the Northwest Fork instead of freshwater inflow from each individual tributary. Such an approach will allow the testing of more restoration scenarios with limited resources. This capability is especially critical in the initial alternative assessment phase of the restoration plan, since numerous scenarios need to be analyzed. When the total amount of freshwater demand is determined, the analysis can then evolve into the next phase that is to consider the freshwater contribution from each tributary individually to meet the Northwest Fork freshwater demand. At that phase, a model with more refined spatial resolution such as the RMA model that was described in the previous sections can be used for scenarios where tributaries are simulated separately from each other.

The salinity value predicted by Equation [11] is tidally averaged salinity over a lunar tidal cycle. The actual salinity in the river constantly varies in response to tides. If the hourly salinity variation over each tidal cycle needs to be considered, the information is available from the original model output.

Figure 6-21 is the model output of salinity at the Pennock Point seagrass transect in a lunar month. The graphs are the output under three freshwater inflow conditions. Total freshwater inflows of the three simulations are 500 cfs, 800 cfs, and 1200 cfs. The amount of freshwater inflow affects both the overall salinity level and the range of salinity variation (the difference of salinity between high tide and low tide).

Figure 6-21 represents the salinity predictions for only one site under three flow conditions. The model simulation output included salinity for 15 sites under 12 different inflow conditions; thus 180 sets of time-series data were produced.

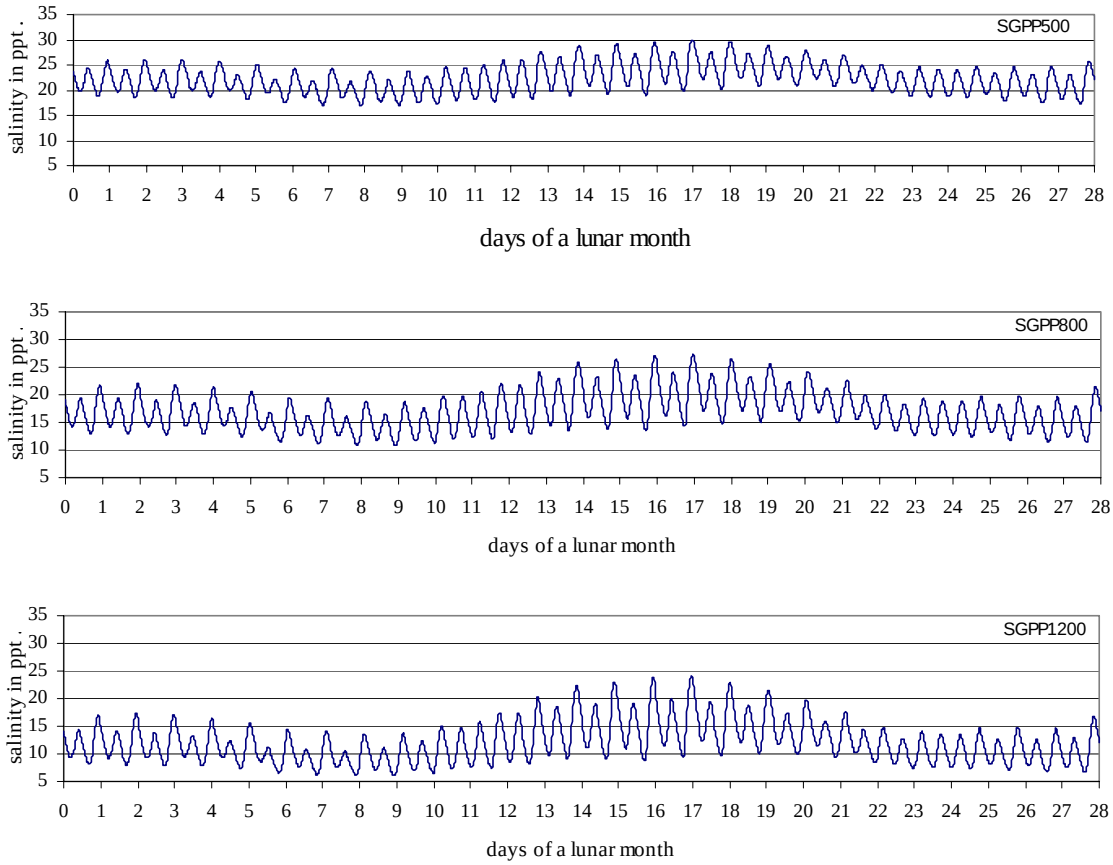

Figure 6-21. Salinity at Pennock Point Seagrass Transect in a Lunar Month - Total Freshwater Inflow to the Loxahatchee River: 500, 800, 1200 cfs.

Figure 6-21 represents one example from a large array of charts in the model output that cover a wide range of freshwater flow. The salinity conditions represented by 500, 800, and 1200 cfs are relatively high flows that begin to affect salinity conditions at the Pennock Point Seagrass site (RM 2.44).

The RMA was applied to scenarios with varying amounts of freshwater inflow. Both the field data and model simulation indicated that there is a strong correlation between freshwater inflow and the salinity regimen in the estuary. Based on model output and field data analysis, a relationship was established to predict salinity at various points in the estuary with respect to freshwater inflow rates and tidal fluctuations. The salinity ~ freshwater relationship was applied in the Loxahatchee River MFL study (SFWMD, 2002b). The RMA model was also used to provide a preliminary assessment of the impacts that inlet deepening and sea level rise have had on the salinity regime in the estuary (Hu, 2002).

LONG-TERM SALINITY MANAGEMENT MODEL

The freshwater ~ salinity relationship described in the previous section was coded into the Loxahatchee Estuary Long-Term Salinity Management Model (LSMM) to predict tidally averaged salinity in response to various restoration scenarios. This model can also simulate system operation rules and calculate the amount of freshwater demand for salinity management.

The salinity values in **Table 6-9** are based on an equilibrium state with constant freshwater inflows. In the applications of the freshwater input versus salinity relationships, the dynamic nature of the system needs to be considered. Under natural conditions, freshwater inflow is rarely constant. The salinity conditions observed in the estuary are the result of a series of transitions from one state to the next. The changes in salinity lag behind the changes in freshwater inflow. Following an increase of freshwater inflow, salinity in the estuary will decrease accordingly and gradually approach a new equilibrium state. As the amount of freshwater decreases, the salinity in the estuary will increase gradually. Depending on the direction of salinity changes, the process can be described as an exponential increase or decay. **Figure 6-22** is a graphic description of salinity transition when an increase of freshwater inflow occurs. The dotted line indicates the equilibrium salinity at the higher level of freshwater inflow.

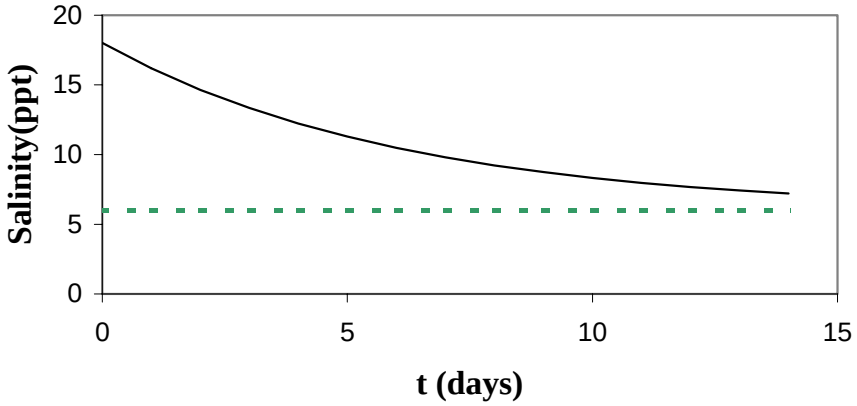

Figure 6-22. Salinity Regimen Transition Process.

The salinity condition within the estuary consists of a series of transitions from one quasi-equilibrium condition to another. This concept was reflected in the LSMM program. The program calculates the potential target (equilibrium) salinity based on the amount of freshwater inflow. Then it calculates the salinity change on daily time steps using the following equation:

$$SAL2 = SALEQ + (SAL1-SALEQ)*Exp(-cT) \quad [12]$$

Where SAL1 is the salinity at the beginning of the time step, SAL2 is the salinity at the end of the time step, SALEQ is the equilibrium salinity for certain amount of freshwater inflow after the transition has completed. T is time and c is a constant that determines the speed of transition. Apparently at the beginning of the time step (T=0), SAL2 = SAL1 and if the freshwater inflow remains the same, SAL2 will eventually reach SALEQ.

Since the freshwater inflow is provided by the watershed model (WaSh) in daily time steps, the calculation of the Long-Term Salinity Management Model is carried at fixed time steps of 24 hours. The predicted salinity depends on both target (equilibrium) salinity and the initial salinity condition at the beginning of the time step. If the amount of freshwater inflow changes before the transition is completed, then a new transition begins and the program repeats the same computational procedure under the new flow condition.

The LSMM is designed to assess daily average salinity over a long period of time. Since the program operates on daily time steps (versus minutes or seconds of a full hydrodynamic model), it allows the assessment of long term data (39 years in this model simulation) at minimum cost and computing time. In addition to using hydrologic data provided by the watershed (WaSh) model, the LSMM can also modify the hydrograph based on certain operational rules such as MFL criteria. The model also calculates the amount of freshwater demand for salinity management and nutrient loadings assuming a target concentration for inflows.

Figures 6-23 through **6-26** depict the salinity calculations of the Long-Term Salinity Management Model. The output was compared with real data from four salinity stations in the Northwest Fork and the embayment area near the Jupiter Inlet. **Table 6-10** lists the statistical characteristics of both model prediction and field data. Statistics of the entire period of 517 days shows that the mean salinity of model output is slightly higher than field data at the four stations by 0.1 to 0.6 ppt. **Tables 6-11** and **6-12** list the statistics of model prediction and field data for two relatively dry periods (March through May) and the rest of the year respectively. In general, the simulated daily salinity matches well with the observed salinities statistically.

Table 6-10. Comparison of Statistical Characteristics of Model and Field Data.

Station Name	PD		BD		KC		RM9	
Date Type	Model	Field	Model	Field	Model	Field	Model	Field
Maximum	34.7	35.5	21.8	20.2	7.6	7.6	2.9	4.4
Minimum	25.0	22.4	1.1	0.2	0.1	0.1	0.0	0.1
Mean Value	32.1	31.8	11.1	9.7	2.1	1.5	0.6	0.5
Median Value	33.1	32.4	12.5	10.1	1.8	0.7	0.4	0.3
Standard Deviation	2.40	2.50	6.22	5.49	1.94	1.71	0.62	0.58
Data Count	517	477	517	502	517	506	517	199
Number of Missing Records	0	40	0	15	0	11	0	318

Table 6-11. Comparison of Statistical Characteristics of Model and Field Data – March through May.

Station Name	PD		BD		KC		RM9	
Date Type	Model	Field	Model	Field	Model	Field	Model	Field
Maximum	34.7	35.5	21.8	20.2	7.6	7.6	2.9	4.4
Minimum	26.2	30.1	3.4	0.3	0.5	0.2	0.2	0.3
Mean Value	33.5	33.7	15.9	12.3	3.6	2.5	1.0	1.0
Median Value	33.8	33.9	15.9	13.1	3.1	1.7	0.7	0.5
Standard Deviation	1.40	1.19	3.98	4.97	2.04	2.08	0.78	0.87
Data Count	153	117	153	150	153	153	153	61
Number of Missing Records	0	36	0	3	0	0	0	92

Table 6-12. Comparison of Statistical Characteristics of Model and Field Data – June through February.

Station Name	PD		BD		KC		RM9	
Date Type	Model	Field	Model	Field	Model	Field	Model	Field
Maximum	34.5	35.1	20.3	19.6	6.0	6.9	2.0	0.8
Minimum	25.0	22.4	1.1	0.2	0.1	0.1	0.0	0.1
Mean Value	31.5	31.1	9.1	8.6	1.5	1.1	0.4	0.3
Median Value	32.2	31.7	7.9	8.6	0.7	0.3	0.2	0.3
Standard Deviation	2.48	2.48	5.90	5.34	1.52	1.32	0.41	0.10
Data Count	364	360	364	352	364	353	364	138
Number of Missing Records	0	4	0	12	0	11	0	226

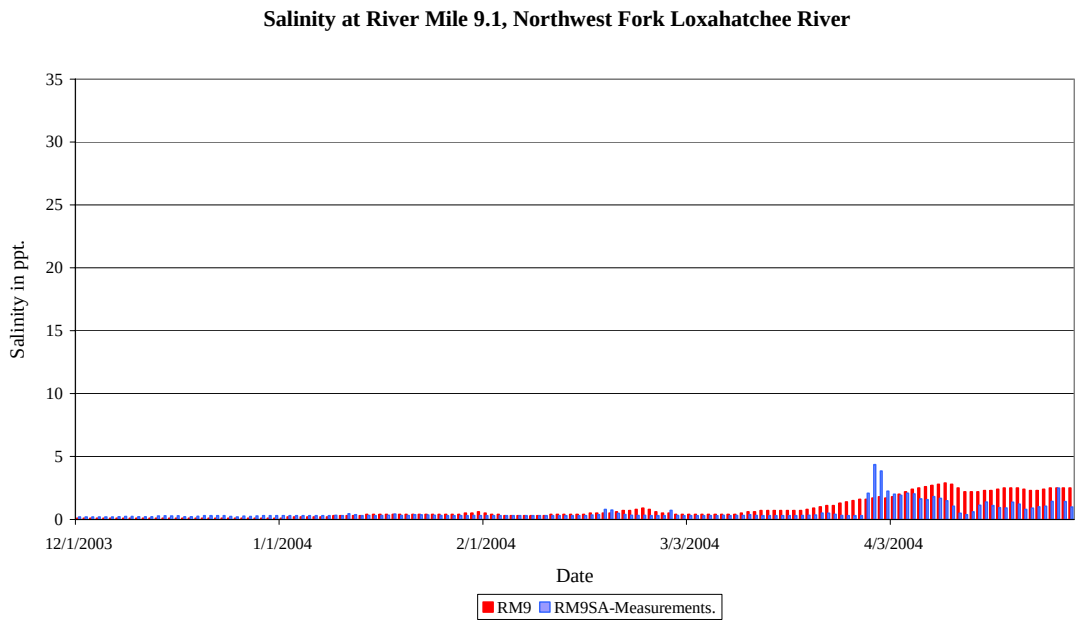

Figure 6-23. Field Measurements vs. Salinity Computation Results–River Mile 9.12

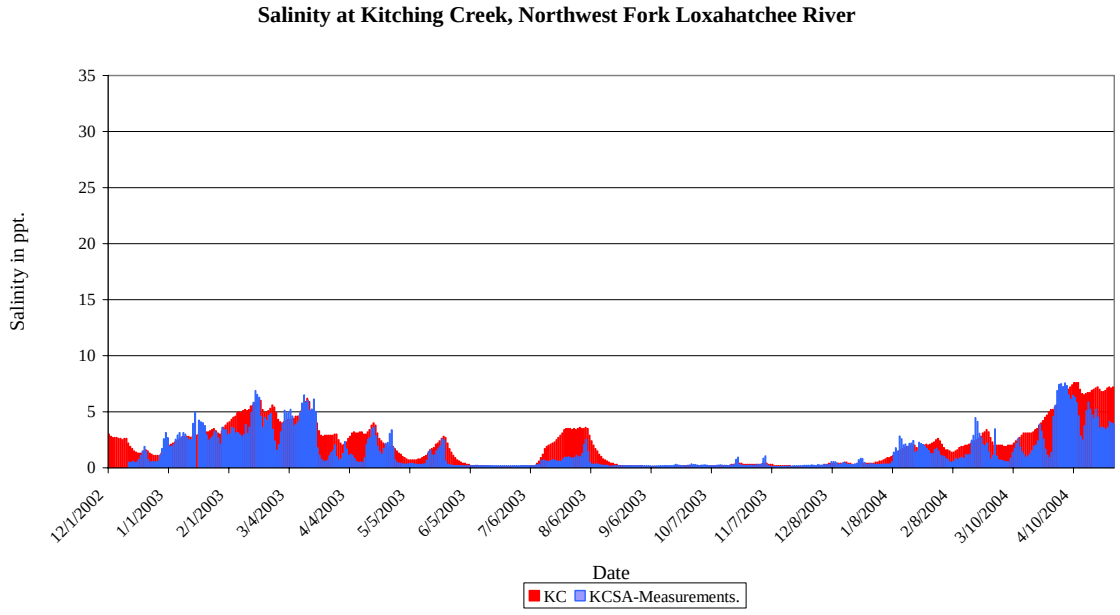

Figure 6-24. Field Measurements vs. Salinity Computation Results-Kitching Creek (RM 8.13).

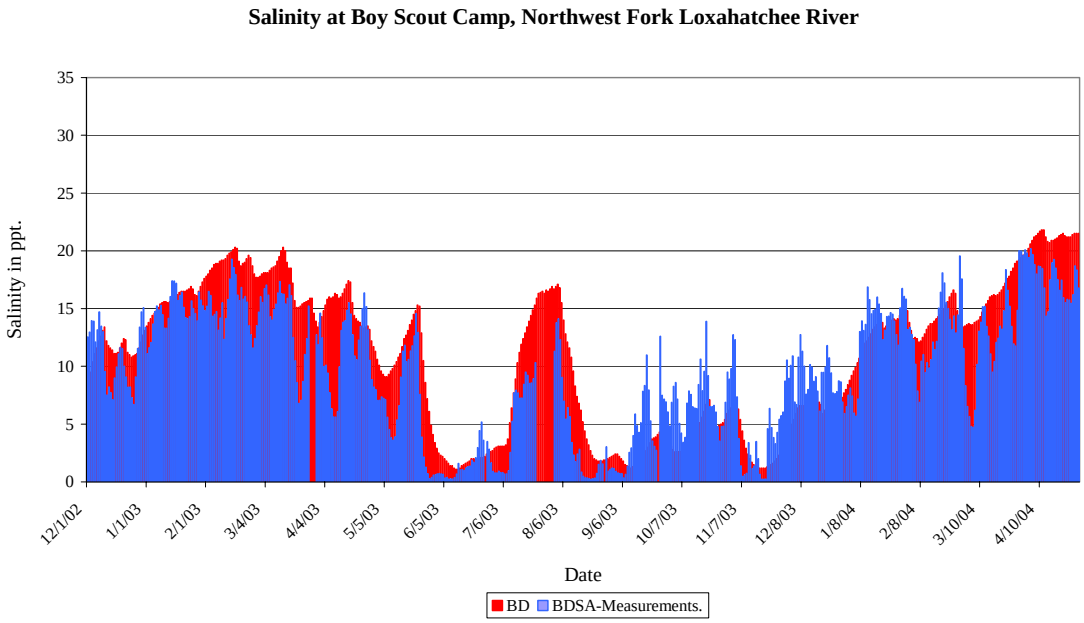

Figure 6-25. Field Measurements vs. Salinity Computation Results-Boy Scout Dock (RM 5.92).

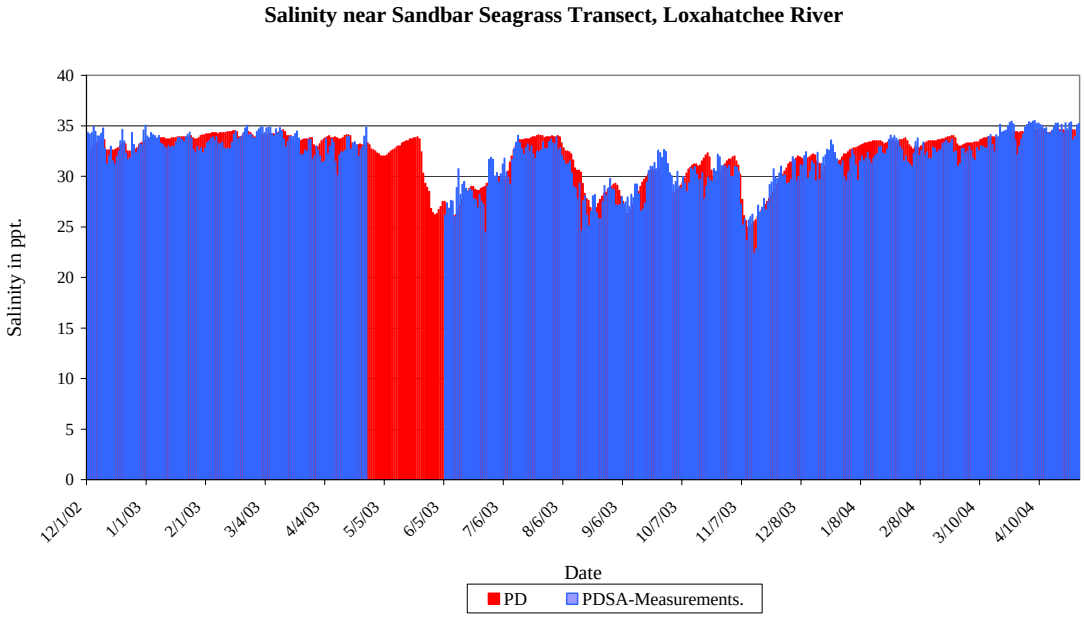

Figure 6-26. Field Measurements vs. Salinity Computation Results-Pompano Drive Embayment Area (RM 1.77).

SUMMARY

This chapter describes the hydrologic and salinity models used in the Northwest Fork of the Loxahatchee River restoration alternative evaluations. The Loxahatchee Watershed (WaSh) Model was developed to simulate freshwater flow from each of the tributaries into the Northwest Fork. The WaSh model is based on restructuring HSPF (Hydrologic Simulation Program – Fortran) into a cell-based system with the addition of a groundwater model and a full dynamic channel routing model (Wan et al., 2003). The model is capable of simulating surface and groundwater hydrology in watersheds with high groundwater tables and dense drainage canal networks. Using long-term flow data collected at S-46, Lainhart Dam, Cypress Creek, Hobe Grove Ditch, and Kitching Creek, the WaSh model was calibrated and validated. The daily flow outputs from the 39-year simulation (1965-2003) provide the basis for the base condition and flow restoration scenarios evaluated in **Chapter 7**.

The Loxahatchee River Hydrodynamics/Salinity (RMA) model was developed to simulate the influence of freshwater flows on salinity conditions in the Loxahatchee River and Estuary. The RMA model is based on the RMA-2 and RMA-4 and was calibrated against field data from five locations and provided salinity predictions for many other sites where field data are not available. Tide/salinity data collected since 2002 have provided a field database for the investigation of the impact of freshwater inflow on the salinity regime in the Northwest Fork.

To perform long-term predictions of daily salinity, a Long-Term Salinity Management Model (LSMM) was developed to predict salinity and calculate several other performance parameters under various ecosystem restoration scenarios. Field data, regression analyses and results from multi-dimensional hydrodynamic computer models were integrated into the salinity management model as a system simulation and management tool. This salinity management model contains several functions such as the calculation of additional freshwater demand for salinity management and the nutrient loading that would occur under various restoration scenarios.

Salinity prediction and other computations were conducted using the Long-Term Salinity Management Model over the 39-year period. Such long-term simulations are required to investigate ecosystem response and assess the effectiveness of proposed restoration approach. The output of the Long-Term Salinity Management Model for six simulation scenarios is described in **Chapter 7.**

CHAPTER 7

TABLE OF CONTENTS

LIST OF FIGURES

LIST OF TABLES

Chapter 7

Northwest Fork Ecosystems Restoration Scenerio Evaluation

This chapter presents the results of evaluations of Northwest Fork ecosystem restoration scenarios. The modeling tools used for the scenario evaluation are described in **Chapter 6**. The Loxahatchee Watershed Model (WaSh) simulated flow from all tributaries to the Northwest Fork. These included flows from the southern watershed areas that provide flows over Lainhart Dam, and flows from other tributary areas north of Lainhart Dam including Cypress Creek, Kitching Creek and Hobe Grove Ditch. To model realistic hydrologic conditions, the simulated flows were based on a 39-year period of record (POR) from 1965 to 2003. These data were used to establish the base project condition for scenario evaluation. The Loxahatchee Long-Term Salinity Management Model (LSMM) was then used to predict daily salinity under the five scenario conditions at 15 locations (**Figure 6-14**). The ecological benefits from the resulting flow and salinity conditions are evaluated with respect to each of the VECs described in **Chapter 4**. **Figure 7-1** provides an overview of the Northwest Fork restoration scenario evaluation process.

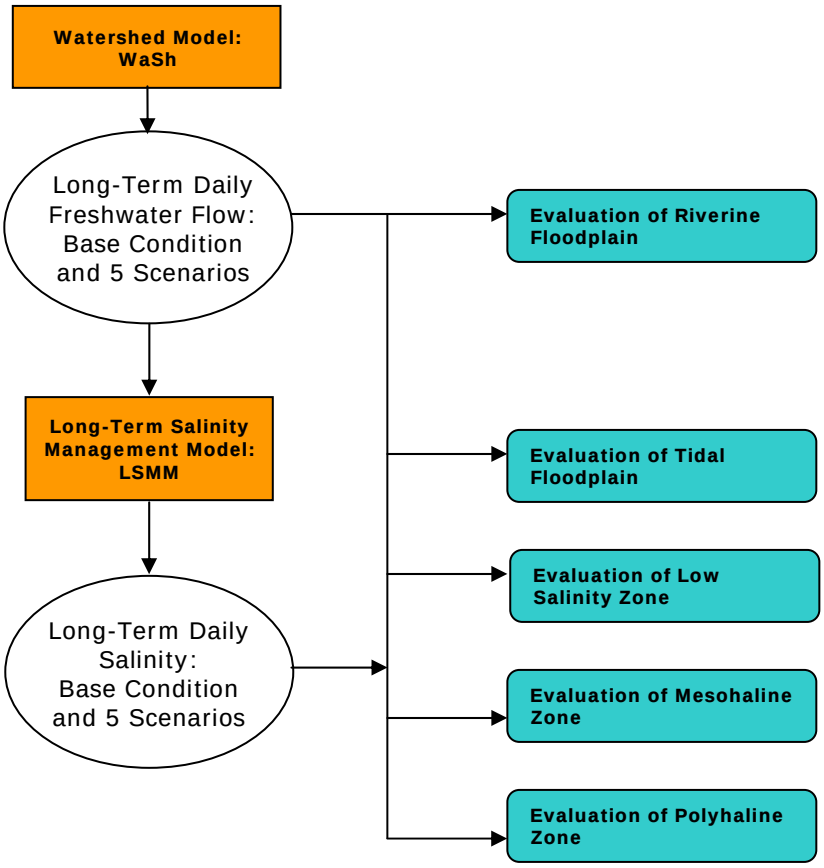

Figure 7-1. Flow Diagram of the Northwest Fork Ecosystem Restoration Scenario Evaluation.

The five restoration flow scenarios were designed to represent different levels of flows from a tributary or a combination of tributaries to the Northwest Fork. The scenarios were selected based on information provided by members of the public and agency representatives at meetings held to discuss the restoration of the Northwest Fork. For example, a flow of 65 cfs had been used as a flow target in the model for the development of the *Northern Palm Beach County Comprehensive Water Management Plan* (SFWMD, 2002). **Table 7-1** summarizes the flow component(s) of each scenario. The next section of this chapter describes and discusses the five scenarios in detail.

Table 7-1. Summary of the Northwest Fork of the Loxahatchee Flow Restoration Scenarios.

Northwest Fork Tributaries	Base condition	LD65	LD65TB65	LD90TB110	LD 200	LD200TB200
Lainhart Dam (LD)	39-year POR	65 cfs	65 cfs	90 cfs	200 cfs	200 cfs
Other tributaries (TB)[a]	39-year POR	39-year POR	65 cfs	110 cfs	39-year POR	200 cfs
Total Flow[b]	50 cfs	95 cfs	130 cfs	200 cfs	230 cfs	400 cfs

POR = Period of record.

[a] Other tributaries include Cypress Creek, Hobe Grove Ditch, and Kitching Creek.

[b] Total Flow for POR is approximated using the modeled time series data.

RESTORATION SCENARIOS

The BASE simulation represents the existing or current conditions of the Loxahatchee River Watershed and was modeled from the 39-year POR data with no modifications. Five additional simulations were conducted with certain modifications to the BASE simulation hydrographs. The modifications represent scenarios that provide additional freshwater flows to upper Northwest Fork at Lainhart Dam and tributaries (Cypress Creek, Hobe Grove, and Kitching Creek) to reduce salinity in the freshwater segments of the Northwest Fork. The results of each simulation will be presented and followed with a summary of potential impacts to the previously mentioned VEC species (riverine and tidal floodplains, larval fishes, oysters and seagrasses) in **Chapter 4**. Adult fish and other wildlife will be mentioned although their specific biological/hydrological requirements are unknown.

FRESHWATER FLOW PREDICTIONS

Scenario 1: LD65

In this scenario, the hydrograph of BASE was modified at the Lainhart Dam. Whenever flow at Lainhart Dam was below 65 cfs under the BASE condition, additional water was added to raise the Lainhart Dam flow to 65 cfs. Therefore in this simulation, freshwater flow from the Lainhart Dam was never less than 65 cfs. In this simulation, no change was made to flows from the tributaries Cypress Creek, Hobe Grove, and Kitching Creek. Flow from these three tributaries was the same as the BASE case.

With the minimum flow of 65 cfs at Lainhart Dam, this simulation located the saltwater front (>2 ppt) between RM 9.0 and the mouth of the Kitching Creek (RM 8.13).

Scenario 2: LD65TB65

In Scenario 2, the hydrograph of BASE was modified at both the Lainhart Dam and the tributaries. Whenever flow at Lainhart Dam was below 65 cfs, additional water was added to raise the Lainhart Dam flow to 65 cfs. Whenever total flow from the tributaries was below 65 cfs, additional water was added to raise the total flow from the tributaries to 65 cfs. Therefore in this simulation, freshwater flow from the Lainhart Dam was never less than 65 cfs, and total flow from the tributaries was never less than 65 cfs. The combined flow from both Lainhart Dam and the tributaries was 130 cfs in this simulation.

With the increased flows at both Lainhart Dam and the tributaries, this simulation located the saltwater front (>2 ppt) between the mouth of Kitching Creek (RM 8.13) and RM 8.0.

Scenario 3: LD90TB110

In Scenario 3, the hydrograph of BASE was modified at both Lainhart Dam and the tributaries. In this simulation, whenever flow at Lainhart Dam was below 90 cfs, additional water was added to raise the flow at Lainhart Dam to 90 cfs. Whenever total flow from the tributaries was below 110 cfs, additional water was added to raise the total flow from the tributaries to 110 cfs. Therefore, in this simulation, freshwater flow from the Lainhart Dam was never less than 90 cfs, and total flow from the tributaries was never less than 110 cfs. The combined flow from both Lainhart Dam and the tributaries was 200 cfs in this simulation.

With the increased flows at both Lainhart Dam and the tributaries, this simulation located the saltwater front (>2 ppt) between the mouth of Kitching Creek (RM 8.13) and Boy Scout Dock (RM 5.92).

Scenario 4: LD200

In Scenario 4, the hydrograph of BASE was modified at Lainhart Dam. Whenever flow at Lainhart Dam was below 200 cfs, additional water was added to raise the flow over Lainhart Dam to 200 cfs. Therefore in this simulation, freshwater flow from the Lainhart Dam was never less than 200 cfs. In this simulation, no change was made to flows from the tributaries Cypress Creek, Hobe Grove, and Kitching Creek. Flow from these three tributaries was the same as the BASE case.

With the increased flow at Lainhart Dam, this simulation located the saltwater front (>2 ppt) between the mouth of Kitching Creek (RM 8.13) and Boy Scout Dock (RM 5.92).

Scenario 5: LD200TB200

In Scenario 5, the hydrograph of BASE was modified at both the Lainhart Dam and the tributaries. Whenever flow at Lainhart Dam was below 200 cfs, additional water was added to raise the Lainhart Dam flow to 200 cfs. Whenever total flow from the tributaries was below 200 cfs, additional water was added to raise the total flow from the tributaries to 200 cfs. Therefore in this simulation, freshwater flow from the Lainhart Dam was never less than 200 cfs, and flow from the tributaries was never less than 200 cfs. The combined flow from both Lainhart Dam and the tributaries was a minimum of 400 cfs in this simulation.

With the increased flows at both Lainhart Dam and the tributaries, this simulation located the saltwater front (>2 ppt) between River Mile 6.0 and Boy Scout Dock (RM 5.92). The flows and salinity conditions of the base and the five scenarios are summarized in **Table 7-2**.

Table 7-2. Long-Term Salinity Management Model Simulation of Restoration Scenarios.

Scenario	Base Condition Hydrograph	Added Flows From Lainhart Dam	Added Flows From Tributaries	Total Added Flows	Approximate Saltwater Front Position
Base	1965-2003 base condition generated by watershed model	No additional flows	No additional flows	No additional flows from Lainhart Dam or tributaries	RM 9.5
LD65	1965-2003 base condition generated by watershed model	Water added as needed so flow is a minimum of 65 cfs at all times	No additional flows	Additional flows only from Lainhart Dam for a minimum of 65 cfs; No additional flows from tributaries	RM 8.5
LD65TB65	1965-2003 base condition generated by watershed model	Water added as needed so flow is a minimum of 65 cfs at all times	Water added as needed so flow is a minimum of 65 cfs at all times	Additional flows from Lainhart Dam and tributaries. Total flow is a minimum of 130 cfs at all times.	RM 8.0
LD90TB110	1965-2003 base condition generated by watershed model	Water added as needed so flow is a minimum of 90 cfs at all times	Water added as needed so flow is a minimum of 110 cfs at all times	Additional flows from Lainhart Dam and tributaries. Total flow is a minimum of 200 cfs at all times	RM 7.5
LD200	1965-2003 base condition generated by watershed model	Water added as needed so flow is a minimum of 200 cfs at all times	No additional flows	Additional flows only from Lainhart Dam for a minimum of 200 cfs; No additional flows from tributaries	RM 7.0
LD200TB200	1965-2003 base condition generated by watershed model	Water added as needed so flow is a minimum of 200 cfs at all times	Water added as needed so flow is a minimum of 200 cfs at all times	Additional flows from Lainhart Dam and tributaries. Total flow is a minimum of 400 cfs at all times	RM 6.0

SALINITY PREDICTIONS

The salinity prediction under each simulation scenario was averaged over the entire 39-year POR to provide an overview of differences in salinity between the scenarios. **Table 7-3** lists the average salinity for the 15 salinity study sites (**Chapter 6, Figure 6-14**).

Table 7-3. Average Salinity (in ppt) at 15 Salinity Study Sites Over the 39-Year Simulation Period.

Salinity Study Site[a]		Restoration Scenarios					
Site ID	River Mile	BASE	LD65	LD65TB65	LD90TB110	LD200	LD200TB200
CG	0.70	33.0	32.8	32.6	32.2	31.8	30.7
SGNB	1.48	32.0	31.6	31.3	30.4	29.6	27.6
SGSB	1.74	31.3	30.8	30.3	29.3	28.4	26.0
PD	1.77	31.2	30.6	30.2	29.2	28.3	25.8
SGPP	2.44	29.2	28.5	27.9	26.5	25.2	22.0
O1	2.70	26.9	26.1	25.4	23.7	22.3	18.7
O2	3.26	24.6	23.5	22.5	20.4	18.7	14.5
O3	3.74	22.5	21.0	19.9	17.4	15.5	11.0
O4	4.13	21.0	19.4	18.1	15.4	13.4	8.9
O5	4.93	16.2	13.9	12.2	9.1	7.2	3.5
O6	5.45	13.5	10.7	8.9	5.9	4.3	1.6
BD	5.92	10.9	7.9	6.2	3.7	2.5	0.7
VT9	7.06	5.8	3.0	1.8	0.7	0.4	0.2
KC	8.13	2.7	0.8	0.4	0.2	0.1	0.1
RM9	9.12	1.0	0.2	0.1	0.1	0.1	0.1

[a] Additional study site information is presented in **Chapter 6, Table 6-8.**

Table 7-3 presents the salinity gradient of each scenario for the 15 study sites. Salinity ranges from near ocean conditions at the U.S. Coast Guard Station (RM 0.70; CG) near Jupiter Inlet to freshwater conditions at River Mile 9 (RM 9.12) in the Northwest Fork of the Loxahatchee River. The five scenarios that increase freshwater flows also lower the salinity throughout the river and the estuary.

It is important to point out that the salinity condition in the Northwest Fork is extremely sensitive to the amount of freshwater inflow. A small change in freshwater flow of less than 10 cfs can cause changes in salinity as high as several ppt in the upper Northwest Fork. **Table 7-3** only provides the average salinity for each site. A complete assessment of the salinity condition under each scenario is analyzed in greater detail in the following sections.

ECOLOGICAL EVALUATION OF RESTORATION SCENARIOS

EVALUATION OF RIVERINE FLOODPLAIN

Evaluation Methods

With the establishment of river flow and stage relationships (**Chapter 5**), it is possible to evaluate predicted floodplain inundation characteristics on the riverine reach of the Northwest Fork of the Loxahatchee River. **Figures 7-2** and **7-3** illustrate the relationship between flows over Lainhart Dam and river stage levels at Transect #1 (RM 14.50) and Transect #3 (RM 12.07). The range and average ground elevations for hydric hammock and swamp forest types were determined from transect vegetation and survey data. Stage at each transect was correlated to the corresponding flow at the nearest long-term stream flow gauging station, which is Lainhart Dam. The inundation records resulting from the flow/stage relationships were then used to estimate

daily inundation. Note that in the two figures, the flow and stage relationship varies significantly when flow is about 100 cfs or less. This is due to the influence of the antecedent conditions. The lower boundary reflects a dry season condition when the stage in the river recharges the groundwater in the floodplain whereas the upper boundary reflects a wet season condition when the water stages in the floodplain are high and water flows from the floodplain into the river. Field observations of high flow conditions were conducted after heavy rainfalls. Therefore, the flow and stage relationship at one transect is much less variable during high flows than in observed low flow conditions.

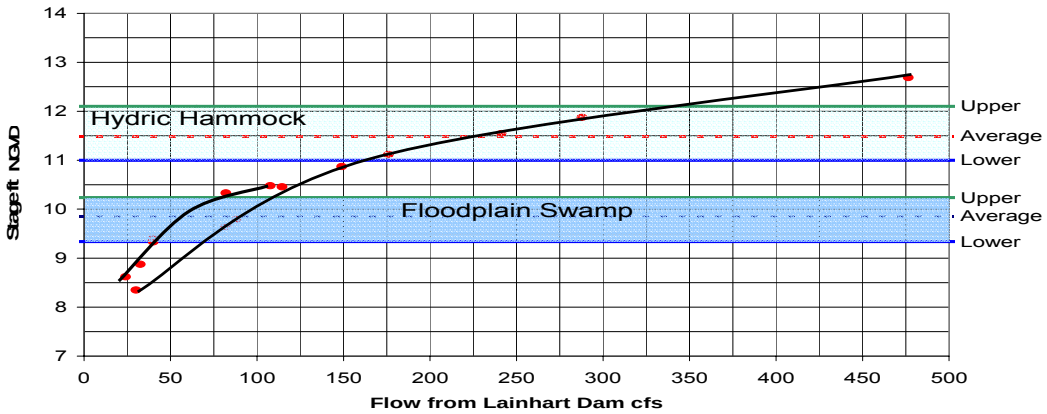

Figure 7-2. The Relationship of Forest Type Stage (Elevation in ft) and Flow (cfs) over Lainhart Dam at Transect #1.

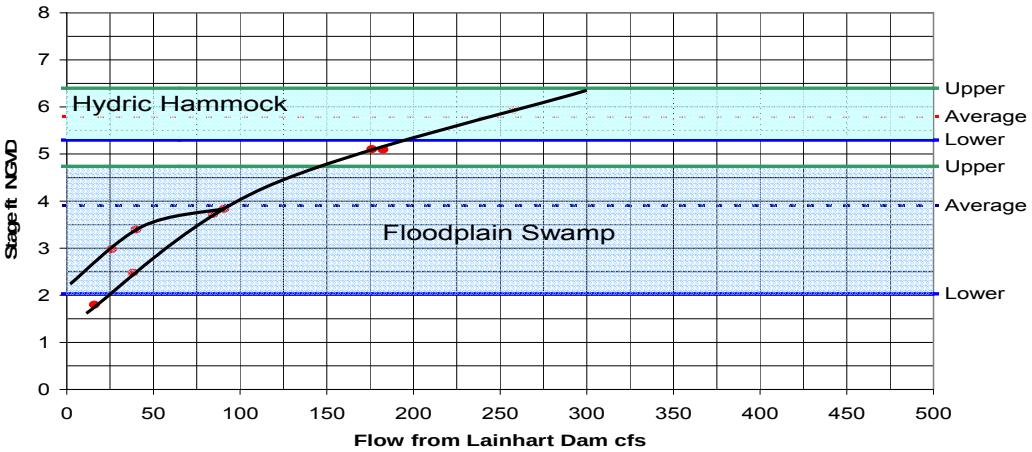

Figure 7-3. The Relationship of Forest Type Stage (Elevation in ft) and Flow (cfs) over Lainhart Dam at Transect #3.

Figures 7-4 and **7-5** show the approximate forest type stages at Transect #1 and Transect #3, respectively, for five key Lainhart Dam flows. The transect profiles are shown to illustrate the variable topography along each of the two transects and to illustrate the average ground elevation of hydric hammock and swamp communities. At 65 cfs (solid blue line), the river stage at Transect #1 corresponds to the bottom elevation of the swamp community, and at Transect #3 this

line is at the bottom of most of the swamp community, and flow is contained within the banks of the river. At 90 cfs (dashed orange line), the river stage at Transect #1 and Transect #3 is at the average elevation of the swamp community, and flow is still contained within the banks of the river. At 110 cfs (dashed blue line) the flow is out of its banks at Transect #1 and the floodplain is inundated to the upper level of the swamp community; at Transect #3 the river is in its banks with the braided channels in the swamp community flowing. At 190 cfs (dashed green line) the river stage at Transects #1 and #3 is at the bottom elevation of the hydric hammock community. At 300 cfs (dashed green line) the river stage at Transects #1 and #3 is at the upper elevation of the hydric hammock community, which indicates complete inundation of the freshwater floodplain.

The Base Case and five scenarios were evaluated with performance measures defined in **Chapter 4** to determine the impact on vegetation transects #1 through #4 from the hydroperiods associated with each scenario.

To evaluate the dry season performance in the riverine reach of the Northwest Fork, the base condition and the five alternative flow scenarios were examined for monthly average flow conditions within the 39-year modeled dataset. For the analysis, the months of December through May, inclusive, were considered the dry season, whereas the months of June through November, inclusive, were considered the wet season. To evaluate the performance in the wet season for each scenario on floodplain swamp communities, the total number of days was counted where the 20-day rolling average flow of 110 cfs was exceeded. A 20-day moving average was used to reflect the days after a storm when the flow in the river was lower than 110 cfs but the swamp remained inundated by water ponded in the low areas.

To examine the performance of wet season flows for each scenario on hydric hammock communities, the 39-year modeled dataset was used to establish days of inundation. The number of days of inundation was counted if the flow was greater than 190 cfs, 240 cfs, and 300 cfs, which correspond to the low, median and high elevation occurrences of hydric hammock at Transects #1 and #3 under **BASE** conditions.

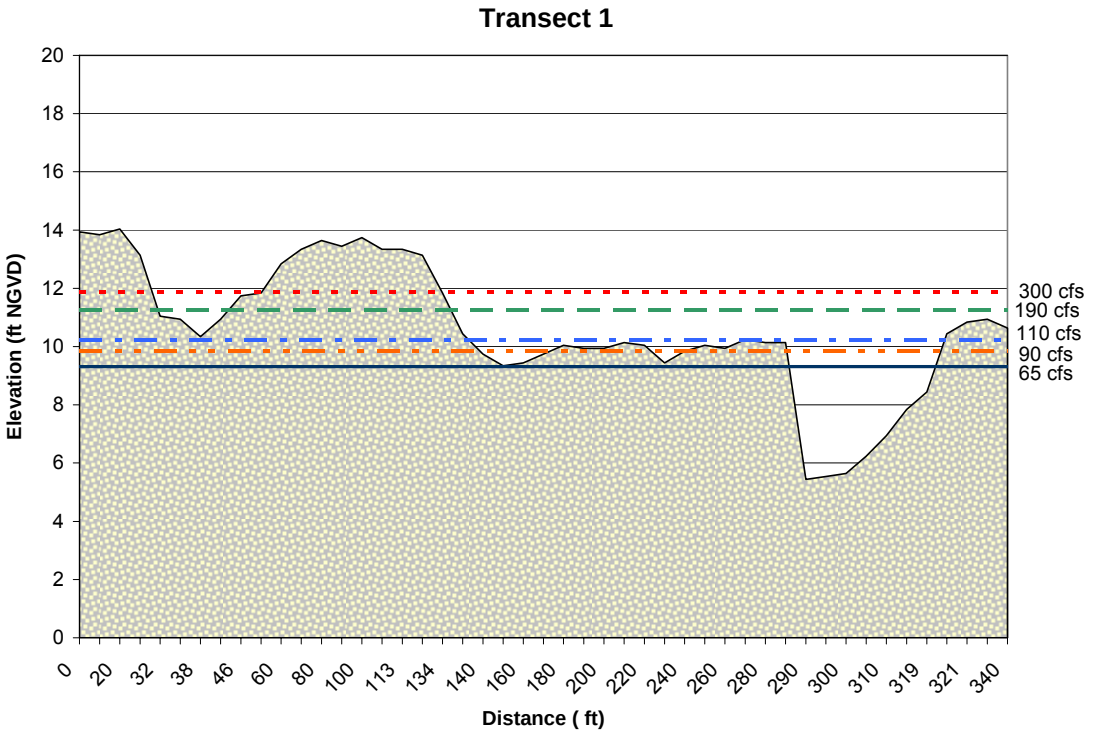

Figure 7-4. Forest Type Stage at Transect #1 and Corresponding Flows Over Lainhart Dam.

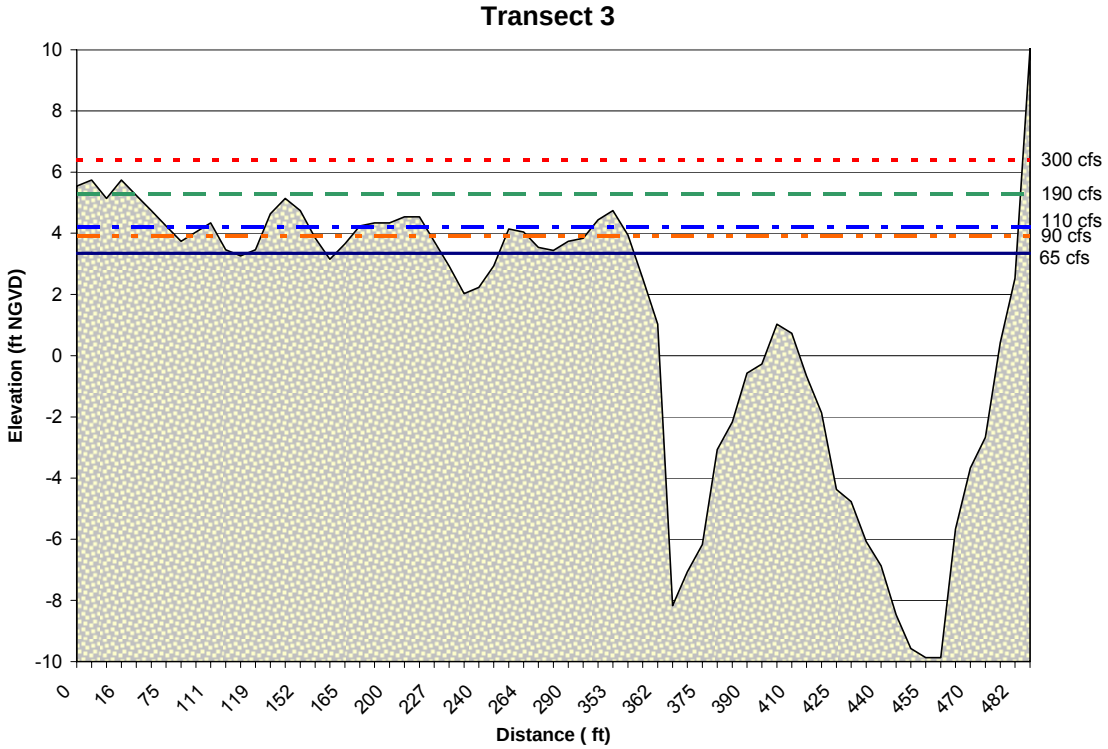

Figure 7-5. Forest Type Stage Across Transect #3 and Corresponding Flows Over Lainhart Dam.

Results and Discussion

Dry Season Evaluation

A monthly mean was determined for each month of the year and a yearly mean was determined for each year. The results are shown in **Tables 7-4** through **7-7**. Color codes were used to identify monthly average flow between 0-35 cfs (red), and 35-65 cfs (orange). Dry season flows were also evaluated for unseasonably high contributions to the Northwest Fork. The months highlighted in dark blue indicate the mean monthly flow was greater than 90 cfs during the dry season.

The **BASE** condition shows a large percentage of months when the mean monthly flows were below 35 cfs during the dry season (December to May) (**Table 7-4**). For the dry seasons of 1989 and 1990, mean monthly flows ranged from 2 to 16 cfs which may represent a stressed condition. The lowest average yearly flows occurred in 1989 (25 cfs), 1965 (34 cfs) and 1990 (36 cfs) while the highest average yearly flows occurred in 1995 (166 cfs), 1994 (165 cfs), and 1993 (150 cfs). The years 1970 and 1993 exhibited the highest dry season flows (highlighted in dark blue) with mean monthly flows ranging from 92 to 237 cfs. The average dry season flow for the 39-year period was 66 cfs. High flows during the dry season would not harm the swamp communities but may impact deciduous seed germination and seedling/sapling growth, which is needed periodically to encourage new recruits to the communities. Also, the table illustrated how a lack of rain during the wet season can add to the low flow conditions on the Northwest Fork (i.e., 1988-1989).

Table 7-4. Examination of Flow of the **BASE** Condition for the 39-Year Modeled Dataset Using Mean Monthly Flows (cfs).

Dry Season	Wet Season
< 35	< 35
< 65	< 65
>= 65 & <=90	>= 65
> 90	

LNHRT-Base

	Date												
Years	Jan	Feb	Mar	Apr	May	Jun	Jul	Aug	Sep	Oct	Nov	Dec	Average
1965	39	35	14	2	1	14	29	45	10	136	71	10	34
1966	90	76	34	22	53	211	220	127	88	203	63	37	102
1967	22	40	37	18	5	52	89	114	67	193	79	26	62
1968	14	13	7	2	19	302	173	136	197	274	147	62	112
1969	71	45	116	35	154	120	79	131	135	269	173	86	119
1970	113	104	208	237	97	155	112	64	56	71	29	18	105
1971	16	18	12	3	47	19	38	46	136	79	194	73	57
1972	44	39	21	41	191	204	85	50	33	33	68	28	70
1973	28	36	14	9	13	80	66	124	134	168	41	39	63
1974	150	39	45	14	8	131	151	156	54	134	57	63	84
1975	27	30	20	7	33	104	141	31	85	108	39	15	54
1976	9	20	27	5	106	114	30	67	182	72	72	28	61
1977	60	19	10	2	25	33	11	24	271	42	24	139	55
1978	72	30	32	6	14	145	140	145	88	168	263	190	108
1979	193	79	56	47	61	51	31	19	161	146	113	66	85
1980	47	58	39	20	33	29	86	34	32	80	26	17	42
1981	7	9	3	1	2	6	6	152	176	46	53	9	39
1982	12	26	150	200	166	241	124	93	110	145	302	182	146
1983	143	200	172	108	76	141	77	135	268	342	198	157	168
1984	123	86	127	84	102	124	65	48	179	120	196	150	117
1985	72	43	28	61	21	25	65	40	144	110	53	71	61
1986	125	42	102	82	14	93	112	72	76	80	92	99	83
1987	112	36	69	25	15	24	43	30	39	137	234	34	67
1988	57	47	42	14	29	91	116	184	75	18	14	7	58
1989	4	2	17	8	7	8	30	85	25	79	14	15	25
1990	11	6	7	10	7	15	17	77	93	151	22	16	36
1991	142	118	53	141	119	160	128	86	134	192	92	83	121
1992	49	117	66	56	20	122	125	188	217	164	198	95	118
1993	231	204	200	122	92	104	87	85	164	281	149	89	150
1994	96	142	84	82	70	143	114	223	273	209	278	285	166
1995	140	96	98	85	69	101	131	288	186	352	271	153	165
1996	82	73	156	116	137	140	176	96	128	163	123	78	123
1997	81	104	84	121	93	214	109	200	222	105	83	149	130
1998	148	204	161	88	106	53	84	66	208	133	289	102	136
1999	227	89	70	39	30	172	122	109	198	335	206	109	142
2000	81	74	62	91	34	19	40	18	52	174	29	23	58
2001	16	9	46	24	8	43	197	260	254	236	145	78	110
2002	69	125	60	44	15	116	185	57	40	51	43	36	70
2003	22	14	62	46	119	137	48	149	90	73	146	75	82
Average	78	65	67	54	57	104	94	104	130	151	120	77	92

In the **LD65** scenario, dry season monthly flows were improved (greater than 65 cfs and less than 90 cfs) (**Table 7-5**). **LD65TB65** scenario used the same Lainhart Dam flows as the **LD65** scenario (see **Table 7-2)**; therefore, the **LD65TB65** figure was not included. Similar to the base condition, 20 percent (8 of 39 years) had more than 3 months of average monthly flow greater than 90 cfs (dark blue).

Table 7-5. Examination of Flow Conditions of the **LD65** Scenario for the 39-Year Modeled Dataset Using Mean Monthly Flows (cfs).

Dry Season	
<	35
<	65
>= 65 & <=90	
>	90

Wet Season	
<	35
<	65
>=	65

LNHRT-LD65

	Date												
Years	Jan	Feb	Mar	Apr	May	Jun	Jul	Aug	Sep	Oct	Nov	Dec	Average
1965	65	70	66	65	65	66	71	79	65	160	96	65	78
1966	101	107	68	67	88	211	220	133	95	203	72	65	119
1967	65	72	71	65	65	78	109	125	81	194	92	65	90
1968	65	65	65	65	67	303	174	137	200	274	147	68	136
1969	79	67	123	65	157	121	88	134	138	269	173	86	126
1970	113	104	209	237	102	155	112	70	75	77	65	65	115
1971	65	65	65	65	87	67	69	71	143	97	196	95	90
1972	66	66	66	72	193	204	87	72	65	65	86	65	92
1973	66	68	65	65	65	97	96	125	134	170	67	66	91
1974	162	65	75	65	65	136	151	156	69	135	80	70	103
1975	65	65	65	65	70	109	141	65	106	113	65	65	83
1976	65	72	67	65	132	118	65	94	182	85	91	66	92
1977	85	65	65	65	77	68	65	69	271	72	68	142	93
1978	89	65	67	65	66	161	140	147	89	168	263	190	126
1979	193	79	67	79	74	71	65	65	170	149	116	75	100
1980	76	74	68	65	77	65	99	66	69	100	65	65	74
1981	65	65	65	65	65	65	65	177	176	70	79	65	85
1982	65	66	162	200	172	241	124	93	125	145	302	182	156
1983	143	200	172	108	76	141	77	135	268	342	198	157	168
1984	123	86	127	84	106	124	69	67	186	120	197	150	120
1985	73	65	65	85	65	71	80	70	157	112	68	85	83
1986	133	66	116	100	65	117	113	77	85	101	94	105	98
1987	114	65	87	65	65	70	77	67	75	150	234	65	95
1988	74	68	70	65	71	107	127	193	89	65	65	65	88
1989	65	65	65	65	65	65	67	100	65	99	65	65	71
1990	65	65	65	65	66	67	65	93	113	157	65	65	79
1991	161	124	77	141	125	160	128	93	134	192	93	84	126
1992	65	121	77	75	65	143	127	189	217	164	198	95	128
1993	231	204	200	122	92	104	87	86	164	281	149	89	150
1994	96	142	84	88	75	144	114	223	273	209	278	285	167
1995	140	96	98	85	70	102	131	288	186	352	271	153	165
1996	82	73	156	116	137	140	176	96	128	163	123	78	123
1997	81	104	84	123	94	214	109	200	222	105	83	149	131
1998	148	204	161	88	108	71	92	73	209	133	289	102	139
1999	227	89	71	65	65	178	123	112	198	335	206	109	148
2000	81	74	68	99	66	65	68	65	83	179	66	65	82
2001	65	65	83	66	65	86	198	260	254	236	145	78	134
2002	71	126	70	73	65	132	185	73	68	73	67	65	89
2003	65	65	85	70	140	137	68	149	93	81	147	76	98
Average	99	89	92	86	88	122	108	118	142	159	134	96	111

However, the mean monthly flows for the **LD90TB110** scenario (**Table 7-6**) have 23 of 39 years (59%) that had more than 3 months of average monthly flow greater than 90 cfs (dark blue).

Table 7-6. Examination of Flow Conditions of the **LD90TB110** Scenario for the 39-Year Modeled Dataset Using Mean Monthly Flows (cfs).

Dry Season	Wet Season
< 35	< 35
< 65	< 65
>= 65 & <=90	>= 65
> 90	

LNHRT-LD90TB110

	Date												
Years	Jan	Feb	Mar	Apr	May	Jun	Jul	Aug	Sep	Oct	Nov	Dec	Average
1965	90	92	90	90	90	90	93	99	90	171	114	90	100
1966	115	126	91	90	106	212	220	143	105	204	91	90	133
1967	90	93	94	90	90	98	126	136	101	198	107	90	110
1968	90	90	90	90	91	304	178	142	206	274	148	90	149
1969	97	91	136	90	161	126	105	144	147	269	173	93	136
1970	122	112	216	237	117	157	118	91	97	96	90	90	128
1971	90	90	90	90	107	91	91	92	151	112	200	113	110
1972	90	90	90	94	197	204	100	93	90	90	104	90	111
1973	90	91	90	90	90	113	113	131	138	177	90	90	109
1974	173	90	96	90	90	144	152	159	91	144	101	91	119
1975	90	90	90	90	92	120	145	90	120	123	90	90	103
1976	90	95	90	90	143	127	90	109	184	103	109	90	110
1977	103	90	90	90	98	90	90	91	271	92	91	149	112
1978	108	90	91	90	90	173	144	155	99	168	263	190	139
1979	193	92	90	100	94	92	90	90	176	155	126	94	116
1980	97	96	91	90	98	90	113	90	92	116	90	90	96
1981	90	90	90	90	90	90	90	189	176	91	98	90	106
1982	90	90	173	203	180	241	125	100	143	146	302	182	164
1983	143	200	172	109	92	143	93	142	268	342	198	157	171
1984	124	91	131	94	125	128	90	91	197	125	209	153	130
1985	91	90	90	104	90	93	99	92	170	120	90	104	103
1986	144	90	133	115	90	129	121	94	101	115	105	122	113
1987	123	90	106	90	90	92	96	91	96	160	234	90	113
1988	94	90	92	90	93	121	138	202	103	90	90	90	108
1989	90	90	90	90	90	90	91	114	90	115	90	90	94
1990	90	90	90	90	90	91	90	106	129	164	90	90	101
1991	173	136	97	144	138	161	131	107	136	192	103	96	135
1992	90	130	95	96	90	158	135	191	217	166	199	99	139
1993	231	204	201	124	101	107	94	102	164	281	149	94	154
1994	99	142	92	105	92	146	121	223	273	209	278	285	172
1995	140	96	101	95	90	116	133	288	186	352	271	154	169
1996	91	90	163	126	148	140	177	105	134	163	127	92	130
1997	95	111	94	133	103	214	110	200	222	108	91	149	136
1998	149	204	161	96	121	93	105	93	213	133	289	103	146
1999	227	94	90	90	90	183	130	121	198	335	206	111	157
2000	92	90	91	115	90	90	92	90	102	186	90	90	102
2001	90	90	101	90	90	108	203	260	257	236	146	92	147
2002	90	133	90	95	90	144	188	93	91	95	91	90	107
2003	90	90	102	91	156	140	90	149	106	98	154	92	113
Average	114	106	109	105	107	135	121	131	152	167	146	111	125

The **LD200** (included as **Table 7-7**) and **LD200TB200** scenarios showed 100% inundation during the dry season. Vegetation reproduction in the swamp communities may be impacted by prolonged flooding. Additionally, flooding will present a problem in the lower segments of the hydric hammock and bottomland hardwood communities, which may cause significant declines in the target species in these communities. The **LD200TB200** scenario provides a 200 cfs flow from Lainhart Dam and an additional 200 cfs in the riverine reach for a total flow of 400 cfs in the tidal reaches of the river. High flow conditions may produce higher flow velocities which in turn may increase scouring of the banks, increase the depth of the channel, and increase turbidity levels in the main river channel downstream of the tidal reaches of the Northwest Fork. Changes

in the width of the river channel were evident in historical aerial photographs that were examined for 1940 and 1995 (SFWMD, 2002b). The tidal Northwest Fork is now much wider than it appeared in 1940.

The scenarios were not analyzed for all fish and wildlife impacts. The necessity for base information on these ecological communities is addressed in **Chapter 9**. Data are needed on the general distribution, abundance, and reproductive cycles of our native amphibians and floodplain fish species to correlate to enhanced wet and dry season hydrological conditions on the Northwest Fork of the Loxahatchee River.

Table 7-7. Examination of Flow Conditions of the **LD200** Alternative for the 39-Year Modeled Dataset Using Mean Monthly Flows (cfs).

Dry Season	Wet Season
< 35	< 35
< 65	< 65
>= 65 & <=90	>= 65
> 90	

LNHRT-LD200

	Date												
Years	Jan	Feb	Mar	Apr	May	Jun	Jul	Aug	Sep	Oct	Nov	Dec	Average
1965	200	200	200	200	200	200	200	200	200	233	209	200	204
1966	205	214	200	200	200	242	248	213	200	243	200	200	214
1967	200	200	200	200	200	200	211	209	200	244	200	200	205
1968	200	200	200	200	200	309	226	215	253	274	206	200	224
1969	200	200	219	200	215	203	200	217	214	285	217	200	214
1970	209	201	274	258	204	219	207	200	201	200	200	200	214
1971	200	200	200	200	202	200	200	200	213	200	249	208	206
1972	200	200	200	200	241	237	200	200	200	200	201	200	207
1973	200	200	200	200	200	203	202	205	204	232	200	200	204
1974	244	200	200	200	200	208	201	219	200	220	200	200	208
1975	200	200	200	200	200	203	204	200	205	205	200	200	201
1976	200	200	200	200	215	202	200	201	233	200	205	200	205
1977	202	200	200	200	200	200	200	200	282	200	200	212	208
1978	203	200	200	200	200	239	204	221	200	218	276	233	216
1979	224	200	200	200	200	200	200	200	227	228	211	200	208
1980	200	200	200	200	200	200	203	200	200	206	200	200	201
1981	200	200	200	200	200	200	200	246	217	200	201	200	205
1982	200	200	244	239	236	252	204	200	223	215	307	206	227
1983	206	241	217	201	200	221	200	206	295	342	227	217	231
1984	209	200	214	200	219	207	200	200	260	204	281	218	218
1985	200	200	200	202	200	200	201	200	235	200	200	202	203
1986	223	200	220	203	200	204	202	200	200	203	200	209	205
1987	207	200	203	200	200	200	200	200	200	230	261	200	208
1988	200	200	200	200	200	204	218	247	200	200	200	200	206
1989	200	200	200	200	200	200	200	201	200	207	200	200	201
1990	200	200	200	200	200	200	200	200	216	218	200	200	203
1991	246	218	200	207	215	210	202	201	202	234	201	200	211
1992	200	204	200	200	200	241	213	242	241	220	240	200	217
1993	260	223	253	203	200	200	200	202	208	282	211	200	220
1994	200	211	200	200	200	207	204	243	300	236	307	294	233
1995	205	200	201	200	200	206	202	307	232	375	271	203	234
1996	200	200	230	207	219	204	234	200	213	218	213	200	212
1997	200	203	200	216	200	242	200	227	247	200	200	223	213
1998	223	240	217	201	212	200	201	200	262	203	306	200	222
1999	258	200	200	200	200	223	209	200	224	351	235	205	226
2000	200	200	200	208	200	200	200	200	200	249	200	200	205
2001	200	200	201	200	200	207	246	276	291	242	218	200	223
2002	200	210	200	200	200	219	233	200	200	200	200	200	205
2003	200	200	200	200	234	203	200	207	200	200	229	200	206
Average	208	204	207	204	205	213	207	213	223	231	223	206	212

Wet Season Evaluation

Simulations were examined for their impacts on several VEC species. Hydric hammock is the targeted vegetation community for the wet season (described in **Chapter 4**). With this in mind, successful achievement of these wet season conditions for a scenario must also reflect successful achievement of dry season conditions for the other targeted VEC species to achieve total biological and vegetative community health. **Tables 7-8, 7-9, 7-10**, and **7-11** show the number of days with a 20-day moving average flow over Lainhart Dam greater than 110 cfs (which represents inundation). Months with flows greater than 110 cfs for more than 20 days of flows are highlighted in green. Those years with more than 4 months (120 days) of flows greater than 110 cfs are highlighted in dark green in the Grand Total column and would be considered optimum conditions. Those years with less than 4 months of flows greater than 110 cfs are considered a dry year.

Table 7-8. Floodplain Swamp Inundation Analysis for **BASE** Condition: Number of Days in a Month With 20-Day Moving Average Flow Over Lainhart Dam Greater Than 110 cfs.

Base Flow over 110

	Date													Months with
Years	Jan	Feb	Mar	Apr	May	Jun	Jul	Aug	Sep	Oct	Nov	Dec	Grand Total	over 20 days
1965	0	0	0	0	0	0	0	0	0	12	16	0	28	0
1966	4	0	8	0	0	23	31	27	0	22	11	0	126	4
1967	0	0	0	0	0	0	18	15	0	24	18	0	75	1
1968	0	0	0	0	0	25	31	27	18	31	30	1	163	5
1969	0	0	18	0	22	21	11	16	17	31	30	5	171	4
1970	14	23	19	30	9	30	20	0	0	0	0	0	145	4
1971	0	0	0	0	0	0	0	0	18	2	29	1	50	1
1972	0	0	0	0	18	30	11	0	0	0	0	0	59	1
1973	0	0	0	0	0	2	0	26	28	29	5	0	90	3
1974	15	8	0	0	0	13	31	31	1	21	0	0	120	3
1975	0	0	0	0	0	11	24	9	1	19	0	0	64	1
1976	0	0	0	0	4	21	0	0	26	7	0	0	58	2
1977	0	0	0	0	0	0	0	0	26	13	0	16	55	1
1978	5	0	0	0	0	6	31	26	0	20	30	31	149	5
1979	31	13	0	0	0	0	0	0	14	31	22	3	114	3
1980	0	0	0	0	0	0	0	0	0	4	0	0	4	0
1981	0	0	0	0	0	0	0	11	30	14	0	0	55	1
1982	0	0	16	30	25	30	26	0	3	27	29	31	217	7
1983	31	28	31	28	1	21	1	9	30	31	30	31	272	9
1984	23	0	8	14	1	23	0	0	10	24	8	28	139	4
1985	0	0	0	0	0	0	0	0	10	19	0	0	29	0
1986	20	0	3	19	0	5	16	12	0	0	9	1	85	1
1987	23	0	0	0	0	0	0	0	0	17	30	7	77	2
1988	0	0	0	0	0	10	15	16	18	0	0	0	59	0
1989	0	0	0	0	0	0	0	5	0	2	0	0	7	0
1990	0	0	0	0	0	0	0	0	1	30	0	0	31	1
1991	13	23	0	15	15	30	31	5	21	31	5	6	195	5
1992	0	7	14	0	0	3	24	22	30	31	20	18	169	5
1993	27	28	31	25	0	0	0	0	25	31	30	16	213	7
1994	0	26	10	0	0	19	14	31	30	31	30	31	222	6
1995	31	5	0	0	0	3	26	31	30	31	30	31	218	7
1996	2	0	19	23	7	30	31	3	18	25	26	0	184	5
1997	0	5	7	14	6	29	28	29	30	21	0	17	186	5
1998	15	28	31	10	20	0	0	0	14	31	30	17	196	5
1999	29	13	0	0	0	14	22	7	30	31	30	22	198	6
2000	6	0	0	4	3	0	0	0	0	26	0	0	39	1
2001	0	0	0	0	0	0	21	31	30	31	28	0	141	5
2002	0	15	5	0	0	8	31	4	0	0	0	0	63	1
2003	0	0	0	0	4	30	0	21	18	0	23	0	96	3
Grand Total	289	222	220	212	135	437	494	414	527	750	549	313	4,562	124

Table 7-9. Floodplain Swamp Inundation Analysis for **LD65** and **LD65TB65**: Number of Day in a Month With 20-Day Moving Average Flows Over Lainhart Dam Greater Than 110 cfs.

LD65 Flow over 110

	Date													Months with
Years	Jan	Feb	Mar	Apr	May	Jun	Jul	Aug	Sep	Oct	Nov	Dec	Grand Total	over 20 days
1965	0	0	0	0	0	0	0	0	0	15	20	0	35	1
1966	11	3	15	0	0	25	31	27	0	22	11	0	145	4
1967	0	0	0	0	0	0	20	21	0	25	19	0	85	3
1968	0	0	0	0	0	26	31	28	18	31	30	1	165	5
1969	0	0	20	0	25	23	11	17	18	31	30	5	180	5
1970	14	23	19	30	11	30	20	0	0	0	0	0	147	4
1971	0	0	0	0	0	0	0	0	19	5	30	4	58	1
1972	10	0	0	0	19	30	11	0	0	0	0	0	70	1
1973	0	0	0	0	0	11	1	30	29	30	5	0	106	3
1974	16	8	0	0	0	15	31	31	2	22	0	0	125	3
1975	0	0	0	0	0	13	24	10	5	19	0	0	71	1
1976	0	0	0	0	8	25	0	0	30	10	0	0	73	2
1977	0	0	0	0	0	0	0	0	27	14	0	17	58	1
1978	6	0	0	0	0	7	31	27	0	20	30	31	152	5
1979	31	13	0	0	0	0	0	0	16	31	22	3	116	3
1980	0	0	0	0	0	0	0	0	0	15	0	0	15	0
1981	0	0	0	0	0	0	0	13	30	14	0	0	57	1
1982	0	0	22	30	27	30	26	0	4	27	29	31	226	8
1983	31	28	31	28	1	21	1	9	30	31	30	31	272	9
1984	23	0	8	14	2	23	0	0	11	24	8	28	141	4
1985	0	0	0	0	0	0	0	0	11	20	0	0	31	1
1986	21	0	3	20	0	9	16	12	0	6	9	1	97	2
1987	23	0	0	0	0	0	0	0	0	18	30	8	79	2
1988	0	0	0	0	0	16	17	19	18	0	0	0	70	0
1989	0	0	0	0	0	0	0	13	0	15	0	0	28	0
1990	0	0	0	0	0	0	0	0	2	31	0	0	33	1
1991	15	23	0	23	16	30	31	5	21	31	5	6	206	6
1992	0	7	14	0	0	4	24	23	30	31	20	18	171	5
1993	27	28	31	25	0	0	0	0	26	31	30	16	214	7
1994	0	26	10	0	0	20	14	31	30	31	30	31	223	7
1995	31	5	0	0	0	3	26	31	30	31	30	31	218	7
1996	2	0	19	23	7	30	31	3	18	25	26	0	184	5
1997	0	5	7	14	6	29	28	29	30	21	0	17	186	5
1998	15	28	31	10	20	0	0	0	14	31	30	17	196	5
1999	29	13	0	0	0	18	22	8	30	31	30	22	203	6
2000	6	0	0	11	4	0	0	0	0	26	0	0	47	1
2001	0	0	0	0	0	0	30	31	30	31	28	0	150	5
2002	0	15	5	0	0	9	31	4	0	0	0	0	64	1
2003	0	0	0	0	6	30	0	22	18	0	23	0	99	3
Grand Total	311	225	235	228	152	477	508	444	547	796	555	318	4,796	133

Table 7-10. Floodplain Swamp Inundation Analysis for **LD90TB110**: Number of Days in a Month With 20-Day Moving Average Flows Over Lainhart Dam Greater Than 110 cfs.

LD90 Flow over 110

	Date													Months with
Years	Jan	Feb	Mar	Apr	May	Jun	Jul	Aug	Sep	Oct	Nov	Dec	Grand Total	over 20 days
1965	0	0	0	0	0	0	0	0	0	17	21	0	38	1
1966	19	6	16	0	1	30	31	28	16	23	12	0	182	4
1967	0	0	0	0	0	0	23	25	3	28	20	0	99	4
1968	0	0	0	0	0	27	31	31	21	31	30	1	172	6
1969	0	0	22	0	27	27	21	18	22	31	30	5	203	7
1970	15	24	22	30	15	30	23	0	0	0	0	0	159	5
1971	0	0	0	0	13	5	0	0	22	12	30	11	93	2
1972	12	0	0	0	20	30	12	0	0	0	5	0	79	2
1973	0	0	0	0	0	19	4	31	30	31	7	0	122	3
1974	17	9	0	0	0	18	31	31	5	24	0	0	135	3
1975	0	0	0	0	0	20	26	11	11	26	0	0	94	3
1976	0	0	0	0	9	26	0	3	30	20	19	0	107	3
1977	13	3	0	0	0	0	0	0	28	16	0	20	80	2
1978	17	9	0	0	0	24	31	30	10	24	30	31	206	6
1979	31	14	0	0	0	0	0	0	17	31	24	4	121	3
1980	0	0	0	0	0	0	6	13	0	20	0	0	39	1
1981	0	0	0	0	0	0	0	14	30	16	0	0	60	1
1982	0	0	25	30	31	30	27	0	6	28	29	31	237	8
1983	31	28	31	28	4	22	2	15	30	31	30	31	283	9
1984	23	0	8	14	3	24	0	0	11	25	9	29	146	4
1985	0	0	0	13	4	0	0	0	12	23	0	17	69	1
1986	22	1	4	22	0	11	21	13	0	9	17	6	126	3
1987	24	0	18	0	0	0	0	0	0	19	30	10	101	2
1988	0	0	0	0	0	24	18	22	19	0	0	0	83	2
1989	0	0	0	0	0	0	0	19	0	19	0	0	38	0
1990	0	0	0	0	0	0	0	6	14	31	1	0	52	1
1991	16	25	0	26	20	30	31	19	25	31	5	10	238	7
1992	0	8	15	0	0	5	26	25	30	31	22	18	180	5
1993	27	28	31	25	0	14	0	0	30	31	30	17	233	7
1994	0	26	10	3	13	22	17	31	30	31	30	31	244	7
1995	31	5	0	0	0	5	28	31	30	31	30	31	222	7
1996	2	0	20	24	9	30	31	13	19	26	27	0	201	6
1997	0	11	8	16	13	30	30	30	30	21	0	18	207	5
1998	15	28	31	10	22	0	16	1	14	31	30	17	215	5
1999	29	13	0	0	0	21	24	11	30	31	30	22	211	7
2000	6	0	0	15	5	0	0	0	0	29	0	0	55	1
2001	0	0	0	0	0	1	31	31	30	31	28	0	152	5
2002	0	17	5	0	0	10	31	5	0	0	0	0	68	1
2003	0	0	0	0	7	30	1	24	22	0	25	0	109	4
Grand Total	350	255	266	256	216	565	573	531	627	859	601	360	5,459	153

Table 7-11. Floodplain Swamp Inundation Analysis for **LD200** and **LD200TB200**: Number of Days in a Month With 20-Day Moving Average Flows Over Lainhart Dam Greater Than 110 cfs.

LD200 Flow over 110

	Date													Months with
Years	Jan	Feb	Mar	Apr	May	Jun	Jul	Aug	Sep	Oct	Nov	Dec	Grand Total	over 20 days
1965	31	28	31	30	31	30	31	31	30	31	30	31	365	12
1966	31	28	31	30	31	30	31	31	30	31	30	31	365	12
1967	31	28	31	30	31	30	31	31	30	31	30	31	365	12
1968	31	29	31	30	31	30	31	31	30	31	30	31	366	12
1969	31	28	31	30	31	30	31	31	30	31	30	31	365	12
1970	31	28	31	30	31	30	31	31	30	31	30	31	365	12
1971	31	28	31	30	31	30	31	31	30	31	30	31	365	12
1972	31	29	31	30	31	30	31	31	30	31	30	31	366	12
1973	31	28	31	30	31	30	31	31	30	31	30	31	365	12
1974	31	28	31	30	31	30	31	31	30	31	30	31	365	12
1975	31	28	31	30	31	30	31	31	30	31	30	31	365	12
1976	31	29	31	30	31	30	31	31	30	31	30	31	366	12
1977	31	28	31	30	31	30	31	31	30	31	30	31	365	12
1978	31	28	31	30	31	30	31	31	30	31	30	31	365	12
1979	31	28	31	30	31	30	31	31	30	31	30	31	365	12
1980	31	29	31	30	31	30	31	31	30	31	30	31	366	12
1981	31	28	31	30	31	30	31	31	30	31	30	31	365	12
1982	31	28	31	30	31	30	31	31	30	31	30	31	365	12
1983	31	28	31	30	31	30	31	31	30	31	30	31	365	12
1984	31	29	31	30	31	30	31	31	30	31	30	31	366	12
1985	31	28	31	30	31	30	31	31	30	31	30	31	365	12
1986	31	28	31	30	31	30	31	31	30	31	30	31	365	12
1987	31	28	31	30	31	30	31	31	30	31	30	31	365	12
1988	31	29	31	30	31	30	31	31	30	31	30	31	366	12
1989	31	28	31	30	31	30	31	31	30	31	30	31	365	12
1990	31	28	31	30	31	30	31	31	30	31	30	31	365	12
1991	31	28	31	30	31	30	31	31	30	31	30	31	365	12
1992	31	29	31	30	31	30	31	31	30	31	30	31	366	12
1993	31	28	31	30	31	30	31	31	30	31	30	31	365	12
1994	31	28	31	30	31	30	31	31	30	31	30	31	365	12
1995	31	28	31	30	31	30	31	31	30	31	30	31	365	12
1996	31	29	31	30	31	30	31	31	30	31	30	31	366	12
1997	31	28	31	30	31	30	31	31	30	31	30	31	365	12
1998	31	28	31	30	31	30	31	31	30	31	30	31	365	12
1999	31	28	31	30	31	30	31	31	30	31	30	31	365	12
2000	31	29	31	30	31	30	31	31	30	31	30	31	366	12
2001	31	28	31	30	31	30	31	31	30	31	30	31	365	12
2002	31	28	31	30	31	30	31	31	30	31	30	31	365	12
2003	31	28	31	30	31	30	31	31	30	31	30	31	365	12
Grand Total	1,209	1,101	1,209	1,170	1,209	1,170	1,209	1,209	1,170	1,209	1,170	1,209	14,244	468

In the **BASE** condition scenario (**Table 7-8**), there are 18 years during the 39-year period of record that had four or more months with a 20-day moving average daily flow greater than 110 cfs. The **LD65** and **LD65TB65** scenarios improved this by just one more year as shown in **Table 7-9**. Scenario **LD90TB110** resulted in 5 more years (**Table 7-10**). The **LD200** and **LD200TB200** scenarios provided floodplain inundation year around, which is not a healthy condition for the floodplain vegetation.

To examine the performance of wet season flows for each scenario on hydric hammock communities, the number of days of inundation was counted if the flow was greater than 190 cfs, 240 cfs, and 300 cfs, which correspond to the low, median and high elevation occurrences of the hydric hammock areas at Transects #1 and #3 for the **BASE** condition. The results for the **BASE** condition**, LD65, LD65TB65,** and **LD90TB110** scenarios were the same because the added flow did not reach 190 cfs. Each scenario experienced 25 years of the 39-year POR when daily flow was over 190 cfs for more than 30 days in a year, 18 years when daily flow was over 240 cfs for more than 30 days in a year, and 6 years when daily flow was over 300 cfs in a year. Both **LD200** and **LD200TB200** scenarios produced flows that resulted in prolonged periods of inundation and therefore would be detrimental to the hydric hammock communities.

EVALUATION OF TIDAL FLOODPLAIN

Evaluation Methods

In **Chapter 4**, a salinity regimen defined by the *Ds*/*Db* ratio as a performance measure to evaluate the Northwest Fork restoration scenarios was described. District staff developed a quantitative tool based on the correlation of a measured vegetation abundance index and the *Ds*/*Db* ratio along the Northwest Fork (Zahina, 2004). Definitions for the abundance index values are provided in **Table 7-12**. Vegetation abundance index at RM 10.6 is used as a "reference" freshwater floodplain community to characterize a "healthy" community of the floodplain swamp (**Figure 7-6**). Two vertical dashed lines are shown on each graphic dividing the species into three general groups. The left-most group contains red mangrove, which is a species characteristic of saltwater communities. The middle species group contains pond apple, cabbage palm, and bald cypress, which are freshwater swamp tree species that exhibit some tolerance for saltwater (Zahina, 2004). The right-hand group contains red maple, Virginia willow, dahoon holly and pop ash, which are species that are sensitive to saltwater exposure and are expected to be the first to show stress from saltwater intrusion. The right-hand group is stressed when the abundance index for all species is below 2 and when a *Ds*/*Db* ratio nears 0.3. A *Ds*/*Db* ratio of 1 almost eliminates all the four salinity sensitive species. This tool, called Salinity-Vegetation Model for the Loxahatchee River (SAVELOX; Zahina, 2004) is used for rapid analyses of long-term salinity time-series data for sites along the near shore areas of the Northwest Fork of the Loxahatchee River.

It should be noted that as with any model, caution needs to be taken when interpreting SAVELOX modeling results. In this case, other important environmental factors that play significant roles in shaping the composition of plant communities (such as elevation and logging) are not considered. These environmental factors were considered separately and those results, with a consideration of site salinity, will provide a better indication of appropriate conditions for restoration.

Table 7-12. Abundance Index Definitions.

Description of Species Population Density	Abundance Index
1a. Species not present	0
1b. Species present.	
2a. Two or less individuals; rare	1
2b. More than two individuals.	
3a. Highly abundant or dense population (>75% cover), a dominant component of the plant community	4
3b. Species not a dominant component of the plant community.	
4a. Sparse; widespread and of low density or restricted to localized populations	2
4b. Common; widespread and of moderate density but not a dominant component of the plant community (<50% cover)	3

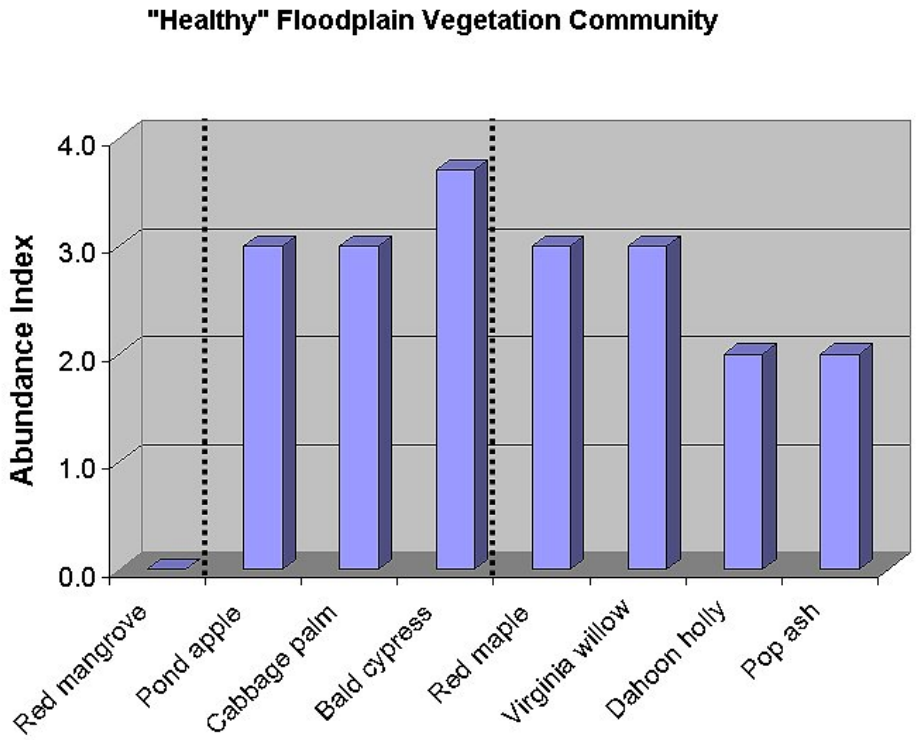

Figure 7-6. Reference "Healthy" Floodplain Swamp Community from the SAVELOX Model.

Four upstream sites that lie within Jonathan Dickinson State Park and along the "Wild and Scenic" River Corridor were included in this analysis: RM 9.12, KC at RM 8.13, VT9 at RM 7.06 and Boy Scout Dock at RM 5.92. For each of the restoration scenarios, the *Ds*/*Db* ratios at these four sites were calculated and the resulting salinity regimes in relationship to the vegetation abundance index were simulated with SAVELOX.

Results and Discussion

Table 7-13 presents the *Ds*/*Db* ratios for the base condition and the five alternative flow scenarios. Salinity-exposure events increased in magnitude and frequently from RM 9.12 to Boy Scout Dock (RM 5.92) for all flow conditions. A *Ds*/*Db* value over 0.3 indicates salinity stress for the salinity sensitive species.

Table 7-13. An Analysis of a **1 ppt Salinity Threshold** at 4 Sites Along the Northwest Fork of the Loxahatchee River: Ratio of Salinity Event Duration (*Ds*, days) and Time Between Events (*Db*, days).

Station	Flow Restoration Scenarios					
	BASE	LD65	LD65TB65	LD90TB110	LD200	LD200TB200
Boy Scout Dock (RM 5.92)	57.64	54.49	54.49	46.79	32.32	17.73
VT9 (RM 7.06)	5.92	5.40	5.11	3.76	0.85	0.00
KC (RM 8.13)	1.71	1.47	1.00	0.00	0.00	0.00
RM 9.12	0.62	0.02	0.00	0.00	0.00	0.00

The resulting vegetation community simulated with the SAVELOX site at RM 9.12 is shown in **Figure 7-7**. Examination of the **BASE** indicates that a mix of saltwater-tolerant and freshwater species is present at this site. The predicted vegetation composition shows a habitat that is fresher than what is observed under current conditions. This appears to be justified because the **BASE** assumes that G-92 operates under the current operation scheme throughout the entire 39-year POR. However, adverse impacts occurred in the floodplain prior to the construction of G-92. In conclusion, a flow of 65 cfs or higher provides sufficient freshwater to support a freshwater floodplain community at this site. The abundance index of bald cypress and other freshwater species are all above 2.

The SAVELOX Model analyses of site KC (RM 8.13) salinity time series are shown in **Figure 7-8**. The **BASE** floodplain community at this site is dominated by red mangrove with remnants of freshwater vegetation (pond apple, cabbage palm and bald cypress). The model results, however, predict little change at this site between the **LD65** and **LD65TB65** scenarios. Upon examination of the salinity time series, it was noted that the magnitude and duration of salinity events above 1 ppt had been significantly reduced in the LD65TB65 scenario as compared to the LD65 alternative (**Figure 7-9**). When calculating the *Ds/Db* ratio with the long-term salinity time series data, we rounded all values to whole numbers to be conservative. A close examination of the long-term salinity data for the LD65TB65 scenario indicates that the salinity during the dry season is mostly between 0.5 to 0.7 ppt (**Figure 7-9**). The method of rounding the salinity data up yielded a *Ds/Db* ratio close to 1.0 at site KC, which would otherwise be close to 0. To better understand tidal influence on salinity fluctuation on this site, a model run using the hydrodynamic and salinity model (RMA) was conducted to examine salinity during a lunar month (28 days) with a constant inflow of 130 cfs distributed accordingly in all tributaries of the Northwest Fork. The result is presented in **Figure 7-10** which indicates that the salinity was above 1 ppt only briefly at high tides during the spring tide (7 out of 28 days). The daily average salinity is still well below 1 ppt. This confirms that a *Ds/Db* ratio of 1.0 is not a true reflection of salinity regimen at this site, but an artifact of rounding up the salinity data. Thus, recovery of the freshwater vegetation at the Kitching Creek site is likely to occur with the LD65TB65 scenario. In this case, the SAVELOX Model produced an output that is more conservative on the side of restoration than was expected to occur.

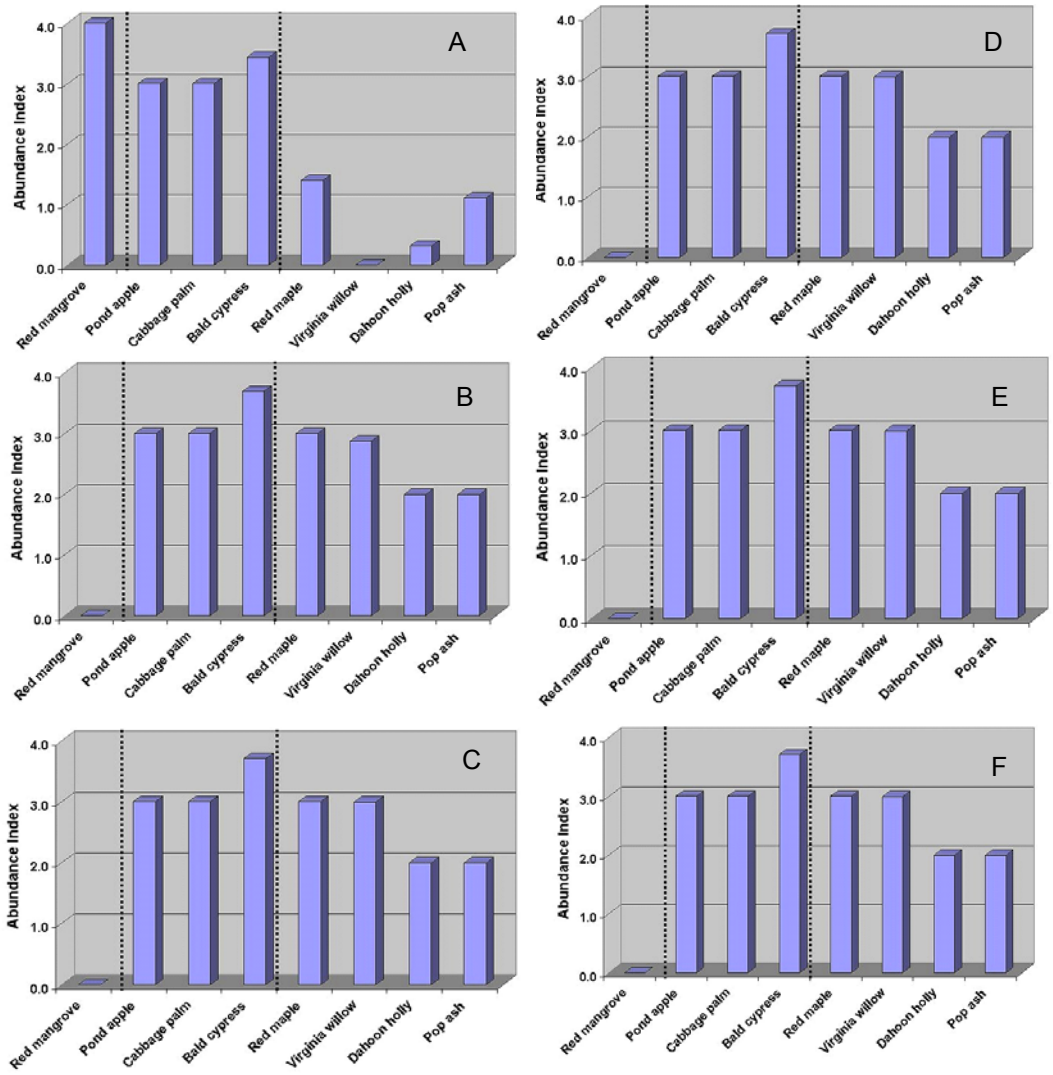

Figure 7-7. SAVELOX Model Analysis of Site RM 9.12: A. BASE, B. LD65, C. LD65TB65, D. LD90TB110, E. LD200, and F. LD200TB200.

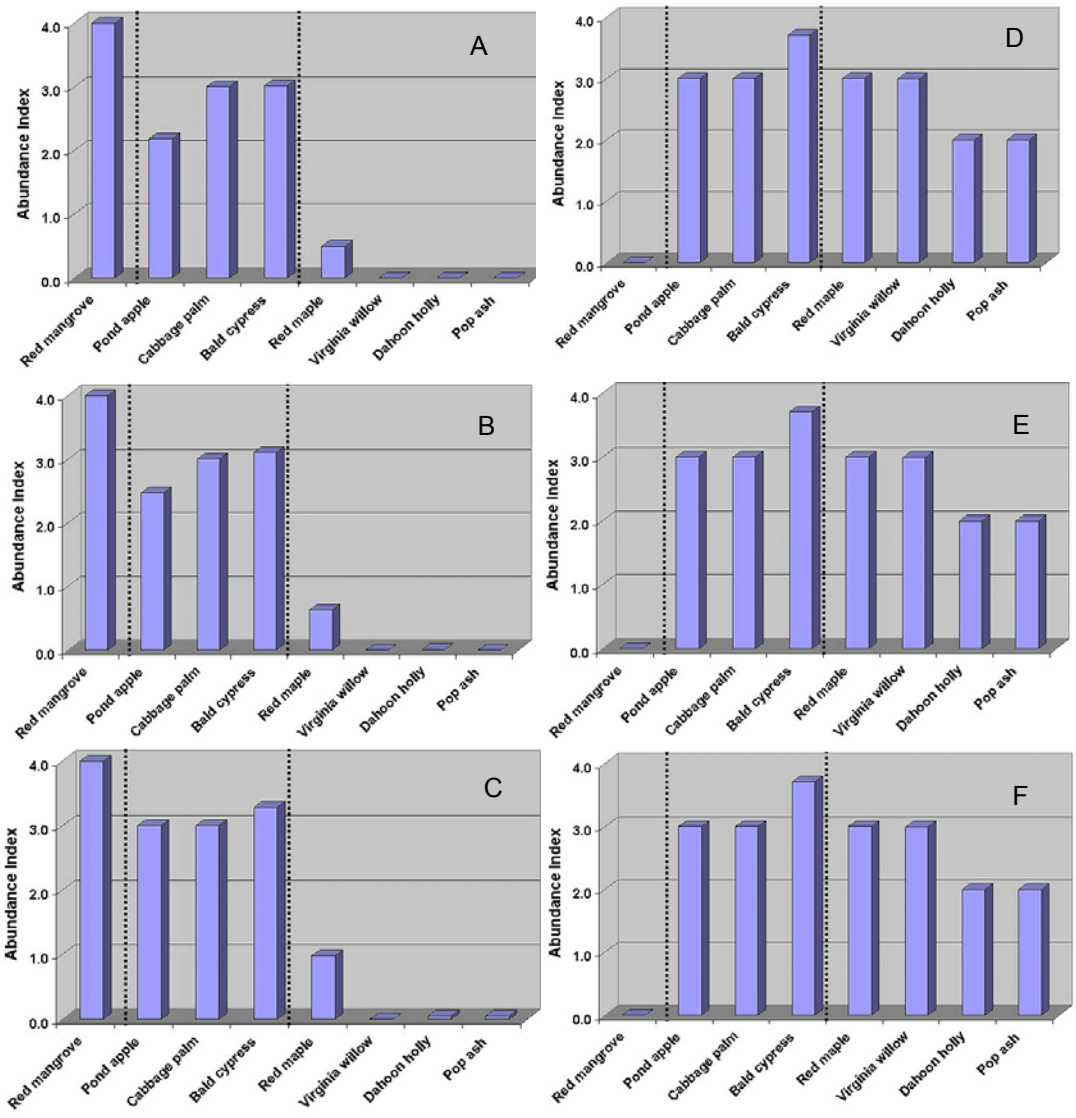

Figure 7-8. SAVELOX Model analysis of Kitching Creek Site: A. BASE, B. LD65, C. LD65TB65, D. LD90TB110, E. LD200, and F. LD200TB200.

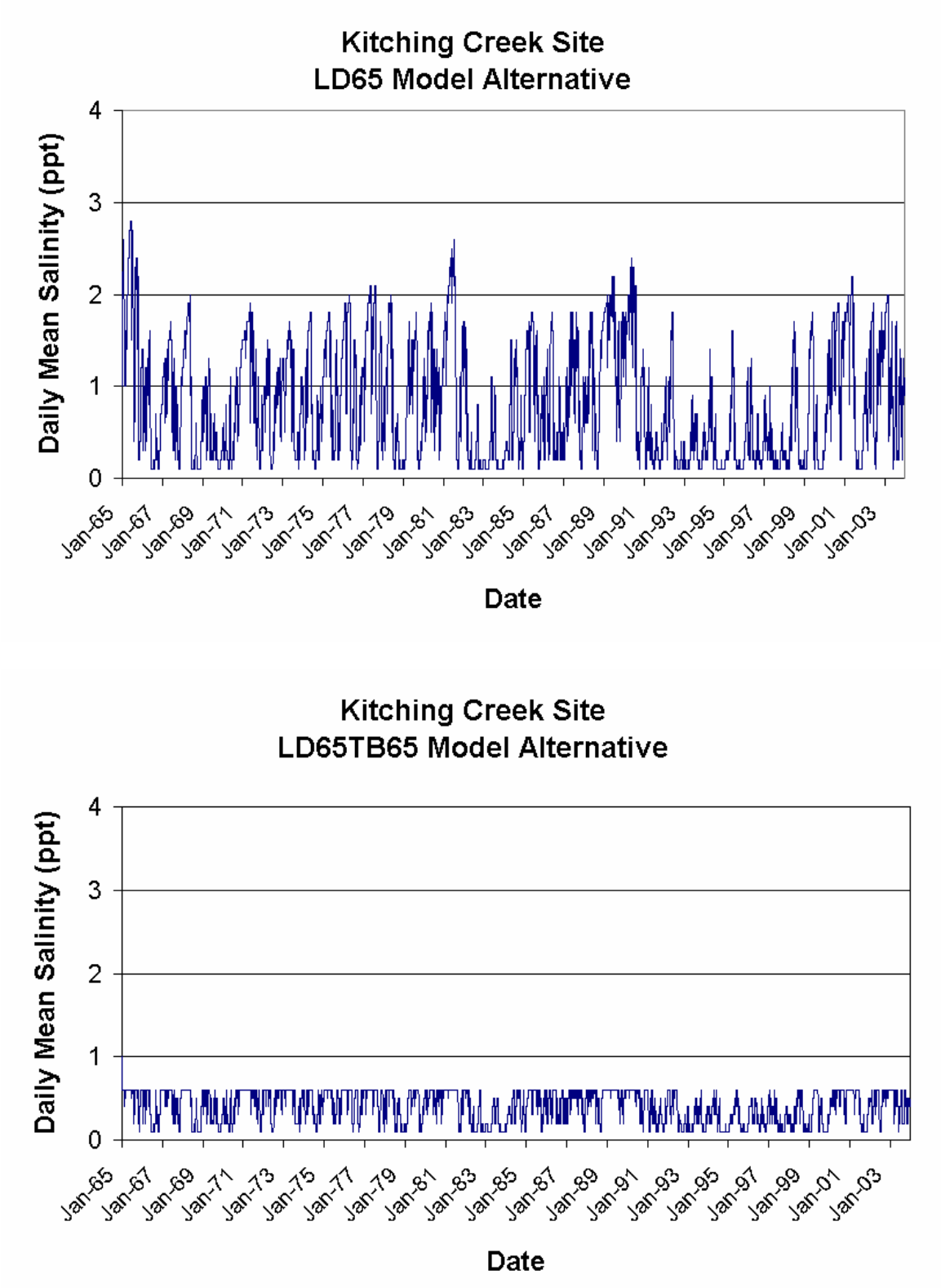

Figure 7-9. Modeled Salinity Time Series at the Kitching Creek Site for Scenarios LD65 and LD65TB65**.**

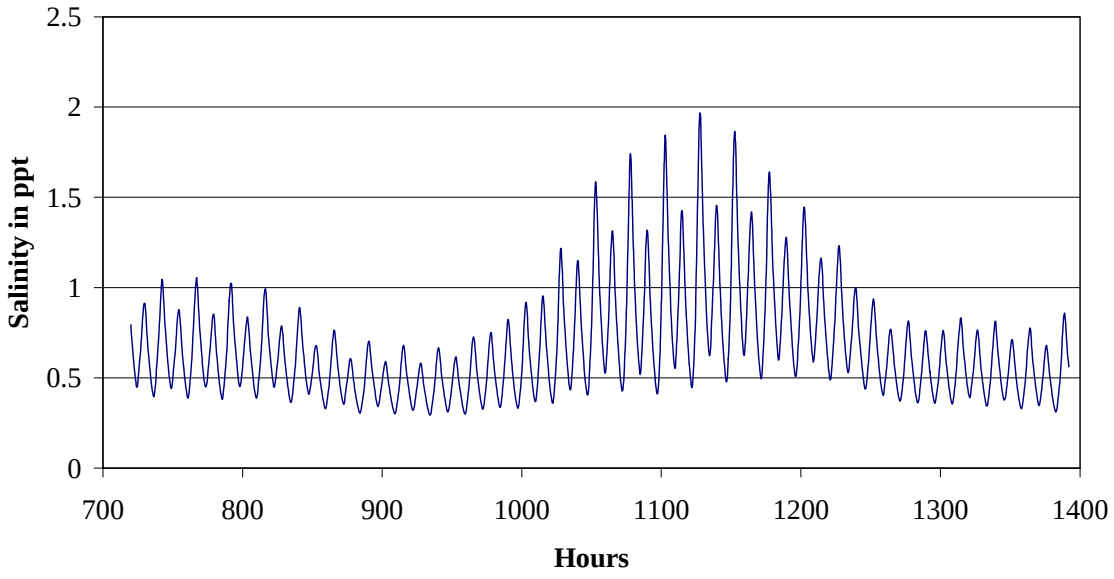

Figure 7-10. RMA Model Output of Salinity at Kitching Creek Station (KC) Over a Lunar Month with Total Freshwater Flow to the Northwest Fork of 130 cfs (LD65TB65).

In the tidal reaches, additional freshwater flows should assist in the flushing of salt from surface, groundwater and soils and in delivering more nutrients across the floodplains during the growing season. Additional nutrients may improve the production of target species seeds or sapling production. Furthermore, the additional freshwater flows should discourage the further spread of upland and transitional species, assist in the control of some exotics, and encourage the growth of freshwater deciduous tree and understory species within the floodplains. Our evaluation shows that a minimum flow in the range of 130 and 200 cfs (Lainhart Dam plus other tributaries) is required to provide sufficient freshwater to support freshwater floodplain vegetation down to the mouth of Kitching Creek. A combined flow of greater than 400 cfs would be required to provide freshwater conditions to the edge of Jonathan Dickinson State Park. It is recognized that the occasional very dry season will provide good conditions for freshwater tree seedling and sapling production and germination to rebuild the forest communities as they age.

Sustaining a flow of 400 cfs would result in a significant change to the present river flow patterns. Large increases in flows have the potential to: 1) increase the elevation of surface water across the floodplain; 2) produce large increases in hydroperiods within the floodplain; 3) increase the potential for scouring and deepening of the river channel; 4) increase the potential for bank erosion and shifts in the course of the river channel; 5) transport of sediment and silt to the downstream estuary and 6) substantially reduce or eliminate low water (dry down) events in the floodplain swamp. All of these factors can have significant adverse impacts to existing floodplain vegetation. These additional issues (besides salinity) need to be considered when examining the desirability of a restoration scenario for enhancing freshwater floodplain vegetation. An example of these concerns is that high flows during the dry season would impede germination of bald cypress and hinder seedling/sapling growth due to flooding. Operational modifications will be required for the selected scenario to create an occasional dry season exclusively for bald cypress germination, and seedling/sapling production, to increase new

recruits into the floodplain swamp community, rather than restoring flows that maximize protection of existing freshwater communities and restoration of impacted areas downstream.

In the restored floodplain communities, once the salinity issue is reduced or eliminated, freshwater plant species would be expected to return to the desired distribution over time. Again, elevation appears to be the major factor in the distribution of forest types. In the upper tidal reach, the restored freshwater floodplain swamp communities would be represented predominantly by bald cypress and pond apple communities. The few mangroves in the upper tidal section should revert to sub-canopy level within the vegetative swamp communities with the growth of freshwater canopy trees over time. Hydric hammocks would be dominated by cabbage palm in both reaches. However, due to the dominance of swamp communities and the narrow transitional area between uplands and swamp communities in the tidal floodplain, true hydric hammock communities would be rare. A mixed forest type of swamp and hydric hammock species would probably prevail. Other freshwater plant species (pop ash, red maple, Carolina willow, etc.) would be present in lower numbers. Additionally, increases in light availability (due to historic logging activities, hurricane impacts, or exotic removal or treatment) in the riverine and upper tidal reaches should improve recruitment of other freshwater target species and keep species diversity high.

In the lower tidal reach where mangrove swamps are the dominant feature, the recruitment of freshwater seedlings and saplings would be hindered by the thickness of the mangrove root systems, persistent tidal flooding due to low elevations, and low levels of light reaching the forest floor. Thus, in spite of the anticipated change of floodplain vegetation community, the canopy and shrub-size mangroves are expected to remain in areas where mangroves are the predominant species (such as at VT9 and JDSP boundary). The presence of mangroves in this limited segment can be viewed as beneficial since it is a buffer between the saline and fresh water environment and it provides essential habitat for tidal wetland and estuarine ecosystems for benthic organisms, juvenile fish, and wading birds.

EVALUATION OF LOW SALINITY ZONE: FISH LARVAE

Evaluation Methods

The Loxahatchee River and Estuary contain one of the more unique tropical peripheral ichthyofaunas within the United States. Jupiter Inlet lies only 7 km (4.6 mi) from the western edge of the Florida Current making the Loxahatchee River the only river on the east coast of the United States so close to a major tropical oceanic current. Thus, its biota is greatly influenced by adjacent tropical marine ecosystems, including those in the Antilles and Central America (Christensen, 1965; Gilmore, 1977, 1993, 1995; Gilmore et al., 1981; Snyder, 1989; Swain et al., 1995). As a result, the most species rich estuarine communities within the continental United States are found in the Loxahatchee River and Indian River Lagoon (Swain et al., 1995).

Major recruitment of larvae into the Loxahatchee River occurs from riverine, estuarine or ocean spawning grounds during different estuarine inflows and times of the year. Most temperate and warm temperate estuaries have major freshwater flows during the winter and spring (Peterson and VanderKooy, 1995; Blaber, 2000). Tropical systems differ significantly, however, since most inflows occur during the summer and fall, typically peaking in the fall (Yanez-Arancibia, 1985; Lowe-McConnell, 1985; Blaber, 2000). Many tropical estuarine and euryhaline freshwater species recruit during the winter and spring dry season when freshwater flow rates are minimal (Gilbert and Kelso, 1971; Nordlie, 1979, 1981; Gilmore 1993) which is the time period of interest for this evaluation. Since the Loxahatchee River Estuary contains a major tropical biota component it is likely that a high proportion of the biota have a life history strategy requiring tropical flow regime. A major, well-documented zooplankton event that predictably occurs

throughout the world tropics during the dry season is an invasion of coastal tributaries to the lower salinity zone (LSZ) by large numbers of fish and invertebrate larvae (Gilbert and Kelso, 1971; Nordlie, 1979, 1981). Our study was undertaken during the dry season to determine the influence the LSZ in the Northwest Fork has on larvae recruitment and abundance as well as species composition (Shenker, 1983; Houde, 1994; Blaber, 2000; Dege and Brown, 2004). The results of this study will be used to determine the flow at which the influx of larvae utilizing the Loxahatchee LSZ may be stressed.

Four regions between River Miles 6 and 10 were chosen for the initial collections in this portion of the Loxahatchee River (**Figure 7-11**). Each region centered on/around RM 7, 8, 9, and 10 with a single replicate tandem plankton tow within 20-50 m of the previous tow. This allowed eight paired stations: Stations 1 and 2 (RM 10), Stations 3 and 4 (RM 9), Stations 5 and 6 (RM 8) and Stations 7 and 8 (RM 7). During late June (25th) and early July (6th) Stations 1 and 2 had to be abandoned due to extremely low water levels.

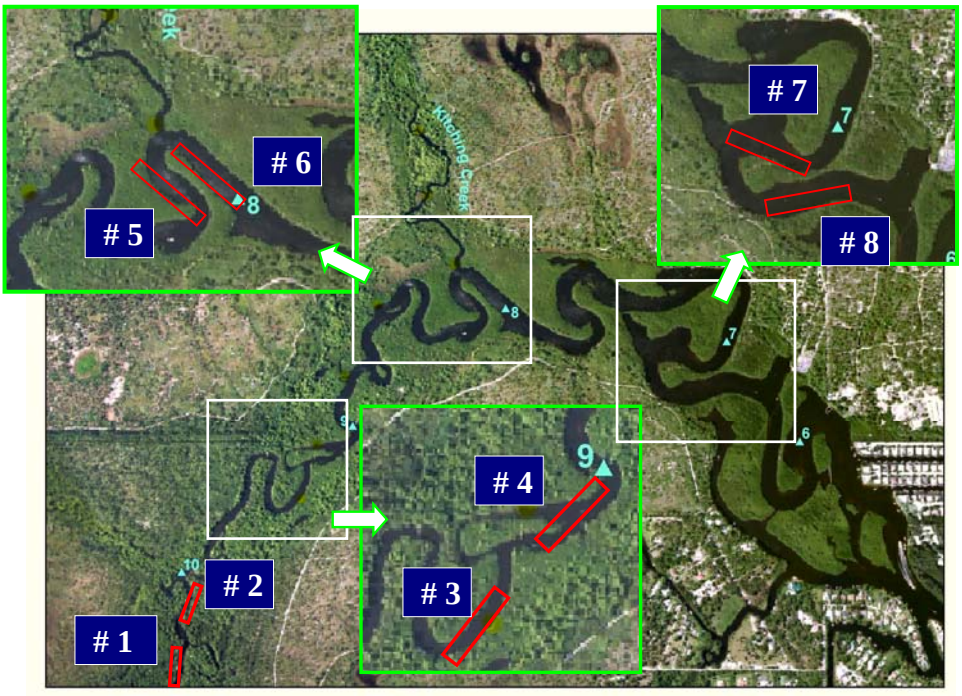

Figure 7-11. Location of Zooplankton Transects. Blue Numbers Indicate River Mile, White Numbers on Blue are Station Numbers. East, Downstream is to the Right.

The mid to late dry season was chosen for study to determine the extent of saline intrusion into the Loxahatchee River relative to zooplankton, particularly fish larvae. Previous work in tropical American estuaries had indicated that major migrations of fish larvae occur from the ocean or estuary into riverine ecosystems during the dry season each spring, just before the wet season begins. Initial experimental collections were made on 17 May 2004 to determine practical limitations in sampling frequency, location and gear behavior. The first routine samples were made during a flooding tide on 17 June. All samples were taken between 1912 and 0030 hours 17 June through 6 July. Nocturnal plankton tows were made using a 0.5-m diameter, 500 micron mesh plankton net pulled 50 m behind a the boat. A 1.0 to 2.0 minute tow was made at each site at standard boat rpm rate of 1,500 rpms, which translated to 0.832 - 1.13 m/sec, or 49 to 136 m per tow. Samples were fixed in 10% buffered formalin for 1 week then rinsed in freshwater and

placed in 35% isopropyl alcohol for preservation. All specimens were sorted and identified using a Wild M5 stereo-microscope and placed in species specific containers for permanent storage in 35% isopropyl alcohol.

Water quality information was taken when samples were collected, however, the most robust data were obtained from continuously recording USGS water quality monitoring sites located within 0 – 200 m of the tow site. The primary data of interest was salinity and water level information as these were most likely to reveal salinity frontal boundaries and water flow/level conditions, factors which have great influence on biota distribution in the water column and river channel.

From January 1986 to January 1988 monthly zooplankton samples were taken with 5 minute standard tows of a 0.5 m, 505 micron mesh net set from a boom off the side of a boat. These samples were all taken at night on a flooding tide. The two stations whose data we used were located below Loxahatchee RM 8. Station 28 was located at the same general location as our Stations 7 (RM 7.0) and 8 (RM 6.8) taken in 2004. Station 25 was located at RM 5.3. All fish larvae captured during 1986-1988 were identified to species whenever possible. However, these data were used in this study at the family level only. One of the major reasons for this is that the majority of larval gobioid fishes which dominate the Loxahatchee River ichthyoplankton, have not been described as larvae. The potential for a variety of tropical species to occur in the collections is great.

Temporal and spatial variations in fish larval and planktonic invertebrate communities were examined statistically using non-parametric statistics due to a variety of data limitations, most notably temporal and sample intensity constraints. Non-parametric statistics were used to determine spatial, temporal and physical parameter relationships with the zooplanktonic community. The PRIMER (Plymouth Routines In Multivariate Ecological Research) statistical program was used for data analyses.

Results

2004 Zooplankton Collections

Total Zooplankton Community Definition*:* Nineteen 1-2 minute plankton tows captured 124,436 zooplankters on June 17, 25 and July 6, 2004. These samples were sorted and identified with emphasis on larval fish, however, every invertebrate was kept for documentation. Larval fish were often identifiable to species except for eleotrids and gobies. There are at least thirteen larval gobioid fishes (Gobiidae and Eleotridae) that occur within the Loxahatchee River. The larval stages of a number of these have not been described, most notably the tropical *Ctenogobius* species (*C. pseudofasciatus* and *C. fasciatus*), *Awaous banana, Gobiomorus dormitor* and *Gobioides brousonettii*. Complete developmental series of *Gobiosoma bosc* were captured and the eleotrid, *Dormitator maculatus* was well represented. However, for these analyses familial and superfamily level classifications were most practical. The only larval pipefish captured were opossum pipefish, *Microphis brachyurus lineatus*. This is the first time larval opossum pipefish were captured as they migrated seaward from their release in freshwater tributaries.

A total of 27 different taxonomic groups were separated for this analysis. Crustaceans dominated the samples accounting for 80% to 96% of the number of individuals captured **Figure 7-12**. Larval fish abundance increased from >1% of the catch to 4%. No eggs were collected on June 17, but 1,092 of at least three types were collected at Stations 7 and 8 on June 25; on July 6, 20 eggs were collected at Station 3 and 27 eggs were collected at Station 8. This indicated spawning activity in late June and upstream and downstream in early July. Circular eggs with oil droplets were attributed to fish spawning activity.

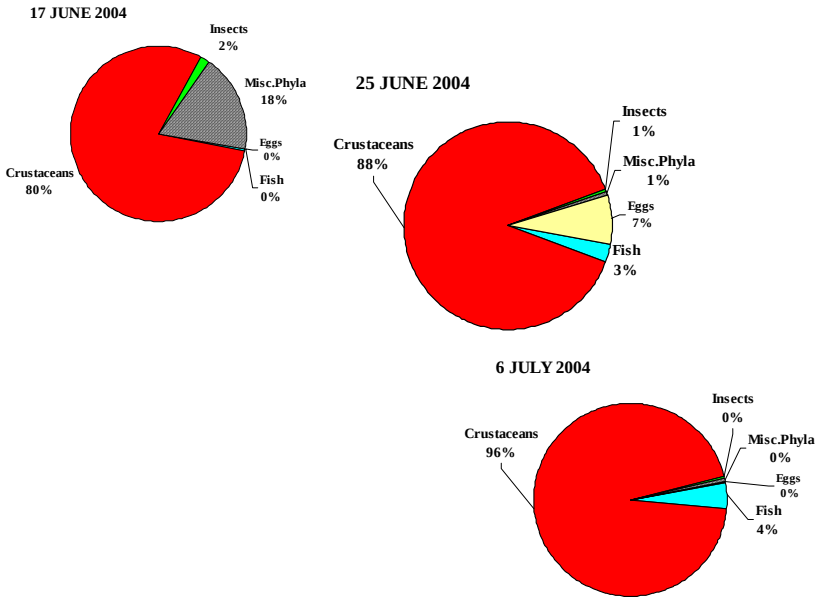

Figure 7-12. Composition of Entire Zooplankton Collection Based on Number of Individuals Captured.

The "meroplankton," which are temporary zooplankton consisting primarily of the larval stages of various non-planktonic aquatic or aerial/terrestrial organisms, were separated from the "holoplankton," which are those planktonic groups that spend their entire life history in a planktonic environment. Several mysid morphologies were observed and placed in the holoplankton category.

The holoplankton consisted primarily of mysids (at least two species), cumaceans and copepods (**Figure 7-13**). Relative numbers of mysids increased significantly, an order of magnitude from 17 June, 45% (111 individuals), to 25 June, 91% (1,899 individuals), then decreased to 77% (1,594 individuals) by 6 July (**Figure 7-13**). Mysids were consistently most abundant at Station 6, at the mouth of Kitching Creek. Cumaceans declined in relative abundance, contribution to the entire sample, but total numbers remained about the same or increased as well as an increase in the number of sites they were captured, one to four of six stations from 17 June to 6 July. Cumacean populations were most abundant at the higher salinity locations, Stations 5, 6, 7, and 8. Copepods were not most effectively captured with a 505 micron mesh plankton net, so accurate numbers were not obtained. However, nearly all copepods were captured at the highest salinities at Stations 7 and 8, increasing numbers from 17 June, 69 individuals to 322 individuals on 6 July.

Temporal analysis of the meroplankton was divided between crustacean and teleostean taxa. Crustacean meroplankton consisted of brachyuran crab larvae, zoea, megalopa and palaemonid shrimp, as well as cypriid, barnacle parts (**Figure 7-14**). Also included were peracardean crustaceans, amphipods (three species) and isopods (two species). Judging from the number of amphipod tubes and benthic isopods captured it is possible that these latter taxa were brought up from the bottom by turbulence from the boat passage or with net contact with the bottom, however, the majority of individuals were captured at the deeper higher salinity stations

downstream, Stations 7 and 8, where it was least likely that the net or boat motor turbulence came in contact with the bottom. Amphipods contributed 7% to 26% of the total crustacean meroplankton catch, increasing in numbers captured from 668 17 June to 2,911 on 6 July. Zoea larvae contributed the largest relative number of individuals to the meroplankton, 49% (1,264 individuals) 17 June increasing to 84% of the catch (9,307 individuals) on 25 June, then declining to 64% (7,337 individuals) by 6 July. The majority of zoea larvae were captured at Station 5 on 17 June, but at Station 6, 25 June and 6 July surrounding the mouth of Kitching Creek. The majority of megalopa larvae were captured at Stations 5 and 6 around the mouth of Kitching Creek, particularly at Station 6; 25 June and 6 July.

When comparing overall abundance of meroplankton versus holoplankton it is obvious that the temporary increase in larval forms of crustaceans and teleosts makes the greatest overall contribution to the zooplankton of the Loxahatchee River using a 505 micron mesh net.

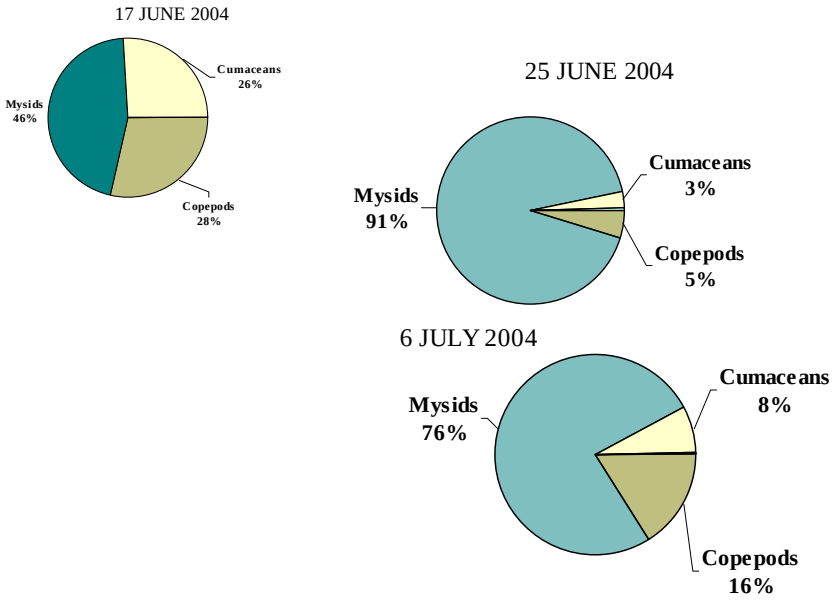

Figure 7-13. Crustacean Holoplankton Contribution Based on Densities (number/m^3).

Fish contributed a relatively small percentage of the meroplankton and total zooplankton, 0.01% to 4% in our collections (**Figure 7-13**). Station and monthly trends in ichthyoplankton abundance follows that of the meroplankton with increases in overall fish abundance from 10 individuals captured on 17 June to 423 and 461 on 25 June and 6 July. The majority of fish larvae captured on 25 June and 6 July were captured at Station 6, which is just downstream of Kitching Creek. The most numerous taxa were gobioid fishes (gobiidae and eleotridae). The most abundant identifiable species was the naked goby, *Gobiosoma bosc*, a benthic species that typically associates with benthic structures such as oyster reefs. At least five other species of gobies contributed to our gobioid larval collections, but these species have not been definitively identified. There are fifteen additional gobies known to occur in the Loxahatchee River. These gobies are the freshwater tolerant species. Gobies by far outnumber all other ichthyoplankton families in biomass, numbers and species. They represent the richest and most productive fish

larval component in the Loxahatchee River ecosystem. The Loxahatchee, St. Lucie and St. Sebastian Rivers contain the richest gobioid fish fauna within the continental United States (Hastings, 1979; Gilmore in prep.).

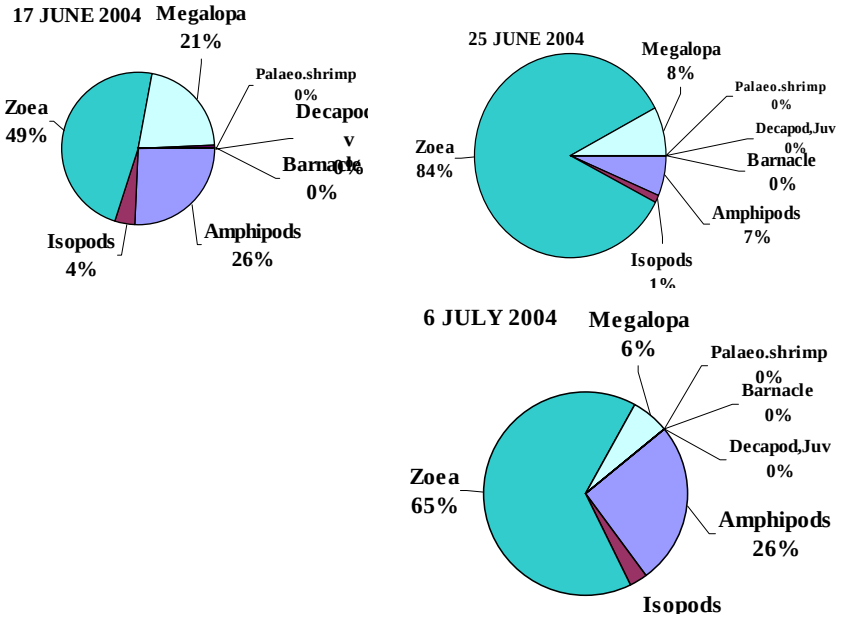

Figure 7-14. Crustacean Meroplankton Composition Based on Densities.

The next most abundant fish larvae were the anchovies (engraulidae) which also substantially increased in abundance from 17 June (1 individual) to 6 July (86 individuals), over 75% of these being taken at Station 6, near the mouth of Kitching Creek. *Anchoa mitchilli* was the only species for which a definitive identification was made. Other *Anchoa* species that have been recorded from the Loxahatchee River and adjacent estuary are *A. hepsetus, A. cubana*, and *A. lyolepis*.

Syngnathid larvae were also consistently captured each month increasing from 1 to 7 between 17 and 25 June, declining to 2 on 6 July. All syngnathid larvae were identified as the tropical opossum pipefish, *Microphis brachyurus lineatus*, which is the only catadromous fish species in the Loxahatchee River besides the American eel, *Anguilla rostrata* (not collected). Opossum pipefish juvenile metamorphose to adults in freshwater and spawn in freshwater. The larvae drift downstream to the ocean where they develop for an undetermined period before returning to freshwater to mature and mate. They were first described by Gilmore (1977).

Silversides, atherinidae, were fourth in relative abundance. Four atherinid species occur in the Loxahatchee River and adjacent estuary, *Membras martinica, Menidia beryllina, M. peninsulae* and *Labidesthes sicculus*.

Other notable fish larvae captured include larval tarpon, *Megalops atlantica*, (megalopidae) captured upstream at Station 3 on 6 July and mojarra larvae (gerreidae) captured downstream at Station 7 on 17 June. Though there are at least eleven gerreid species occurring in the Loxahatchee River and adjacent estuary, only four routinely enter freshwater, *Diapterus auratus, Eugerres plumieri, Eucinostomus harengulus* and *E. gula*. Larvae of these species cannot be identified as no descriptions have been published. A larval soleid, *Trinectes maculatus* was taken at Station 6, 25 June.

Notably absent from the Loxahatchee River collections were the larvae of the common snook, *Centropomus undecimalis*. Many larval snook were captured in a plankton tow made in the Jupiter Inlet on 2 July, 2004 where spawning adult snook were noted. However, since our riverine collections were made when local snook populations were spawning, it appears that snook larvae do not enter the Loxahatchee River. However, seine collections made during June and July in the Loxahatchee River not only captured small juveniles stages of the common snook, but also a new record to the continental United States, the smallscale fat snook, *Centropomus mexicanus*.

Also notably absent from these ichthyoplankton collections were any primary freshwater fish species, cyprinids, catastomids or centrarchids. They were totally absent even at the low salinity (<1.0 ppt) stations taken in mid June. They all are known to spawn at this time of year in warm temperate and temperate rivers further north and on Florida's Gulf coast. It appears the Loxahatchee river ichthyofauna is numerically dominated by fish species with marine affinities. Most are diadromus species and tropical.

Historical 1986-1988 Zooplankton Collections

Zooplankton collections were made within the Loxahatchee River and Estuary from January 1986 to January 1988 by Robert Chamberlain of SFWMD. The 1986-1988 study allowed a qualitative and quantitative comparison to be made with 2004 zooplankton collections. From this comparison the Loxahatchee River ichthyoplankton community is defined.

The only location that completely overlapped between the 2004 and the 1986-1988 studies was our Stations 7 and 8 with Chamberlain's Station 28. These sites were identical. For this reason all the monthly collections at Station 28 were used for most of the quantitative analyses in this study. The most complete monthly collection year was 1987. The relative composition of the various fish families to the collections at Station 28 are presented in **Figures 7-15 and 7-16.** It is obvious that the same families dominated in the same order of numerical abundance in 1987 as it did in our limited collections in 2004: gobioids first (30% - 93% of the April to July 86-87 fish fauna), engraulids second (5%-69%), syngnathids third (0.4%-52%). These three families were the only ones to have 100% occurrence in zooplankton samples in 2004 and April to July in 1986-1987.

Atherinids were common (0 - 5%) in the 25 June 1986 samples as they were in the 25 June 2004 samples (1%). However, clupeids (0-5%) and sciaenids (0-2%) were more abundant in the historical collections on a year round basis. This is undoubtedly due to their spawning activity in fall, winter and spring, periods we missed in our collections.

Chamberlain's Station 25 was examined, as it would give us some indication of potential change in zooplankton densities with salinity. Ichthyoplankton concentrations and species composition was considerably lower at Station 25 when compared to Station 28. This difference is a major factor under examination in the next section, where physical attributes of the water column are examined relative to fish larval abundance.

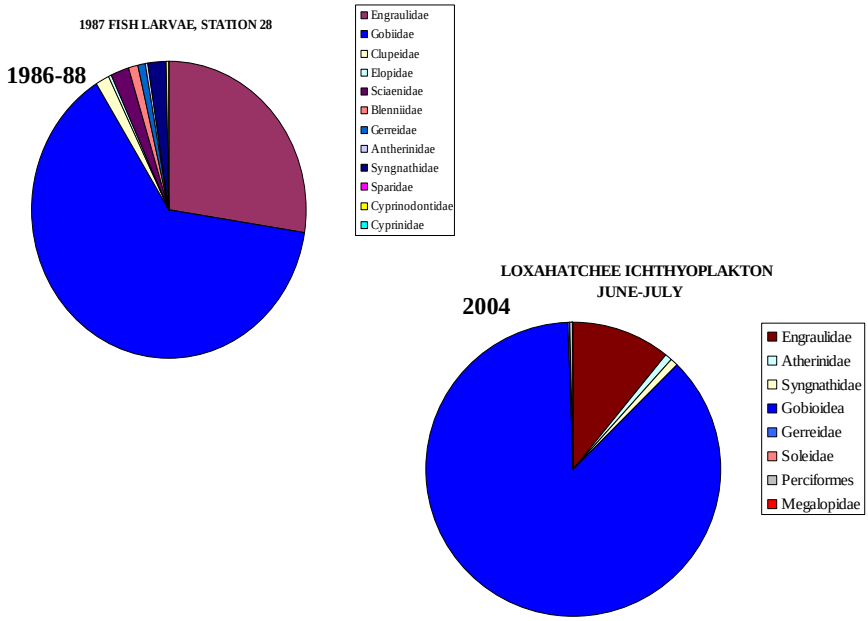

Figure 7-15. Ichthyoplankton Composition: All Collections Combined for 1986-1988 and 2004.

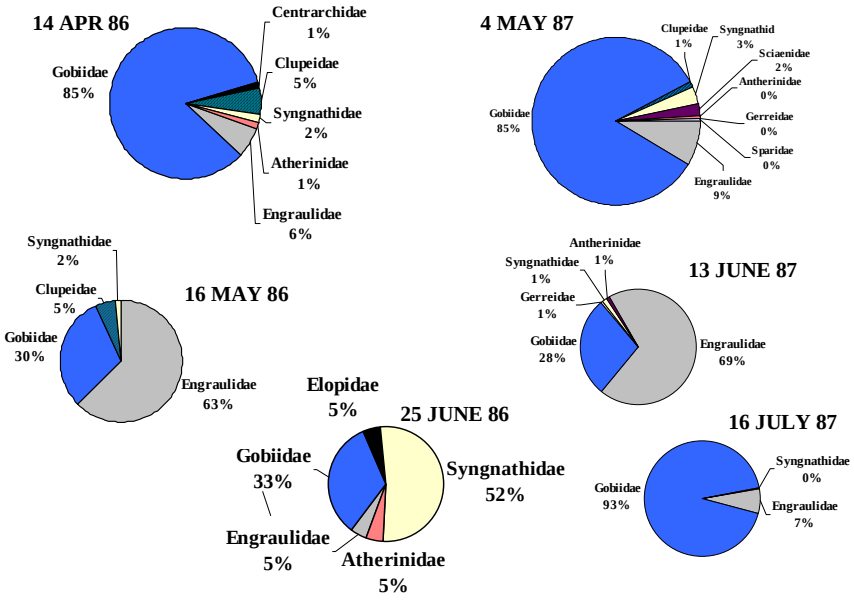

Figure 7-16. 1986-1988 Data Showing Seasonal Change in Relative Abundance of Ichthyoplankton During the Spring-Early Summer, Dry-Wet Season Transition.

Ichthyoplankton Dynamics: Differential Influence of Water Level and Salinity

Ichthyofaunal Spatial-Temporal Distribution: Differential Effect of Water Level, Location and Salinity: The major concern in this work was the influence of fresh water versus salt water on ichthyoplankton distribution. Flow rates and turbidity were significant factors. There are several physical parameters for which we had data to compare with our biological collections in the Loxahatchee River. These included dissolved oxygen, various nutrients, water turbidity, flow rates**,** water level, temperature, tides, lunar phase, pH and salinity. Dissolved oxygen remained relatively high through both 1986-1988 and 2004 collection periods with only a couple of instances of significantly low values. Temperature was more of a seasonal factor and not as much a factor at this latitude as water level and salinity. Since obvious water level effects were observed in this very shallow stream, even to the point of not allowing 0.5 m plankton tows to be made upstream of River Mile 9, this parameter had to be examined.

The three primary parameters to be analyzed for this report are water level, station location and salinity. Once water level factors are understood then salinity effects can be clearly defined. Although salinity was chosen as a primary parameter, there are other factors associated with salinity and freshwater flows can influence these data. Turbidity, nutrient levels, phytoplankton productivity and species composition can all show direct relationships to salinity levels. Thus salinity can act as a potential indicator of these other factors. Detailed physical parameter data were taken continuously within minutes at the USGS gauging stations; only the mean values were used.

2004 Water Level Effects: Figure 7-17 plots the water level variation during the day of zooplankton collections 17, 25 June, and 6 July 2004. The blue shaded box designates the period of actual sample collection, 1900 – 2400 hrs. Collections were made on an incoming flood tide on 17 June with a mean water level of 1.94 m during the sampling period. Collections made 25 June and 6 July were made on an ebbing tide with maximum water levels of 0.3 m on the 25th, possibly less on 6 July. This presented a significant difference in water levels between the 17 June and the later collections which could potentially influence the zooplankton collections.

Figure 7-18 represents a cluster from a similarity analysis using salinity and water level values from all stations. It reveals a closer similarity between stations upstream of RM 8, though the high water collections made on 17 June still show some differentiation. RM 7 shows the greatest distinction from upstream stations using these physical factors. Zooplankton clusters follow a similar pattern.

1986-1988 Water Level Effects: Historical 1986-1988 data from the Loxahatchee River was examined for water level effects. It was anticipated that water level influence would be identical at both Stations 25 and 28 while salinities would differ between the two. A comparison of ichthyoplankton collections reveals a much greater densities of fish larvae at Station 28, than at Station 25, particularly during the dry season, February to July 1987 (**Figure 7-19**). As water level fluctuations were not that dissimilar between the two locations it would appear that salinity would have a greater effect. However, at both locations the lowest fish larvae captures occurred during the highest water levels, fall both in 1986 and 1987. This reveals a seasonal water level effect. An unusual dry season peak in water level, March 1987, still revealed high fish larval abundance. This occurrence has implications on water level influence which may be different from that observed in the 2004 work. Reasons for this will be discussed with some comparative documentation in the "Discussion Section."

A PCA analysis of 1986-1988 fish larval data from Stations 25 and 28 relative to water levels and salinities at both stations reveals close overlap in water level values for both stations and a wide salinity separation with the Station 28 salinity revealing the greatest affinity to the fish

larval abundance pattern. The salinity at Station 25 was most divergent from all the other parameters. This implicates salinity as a major factor influencing fish larval abundance.

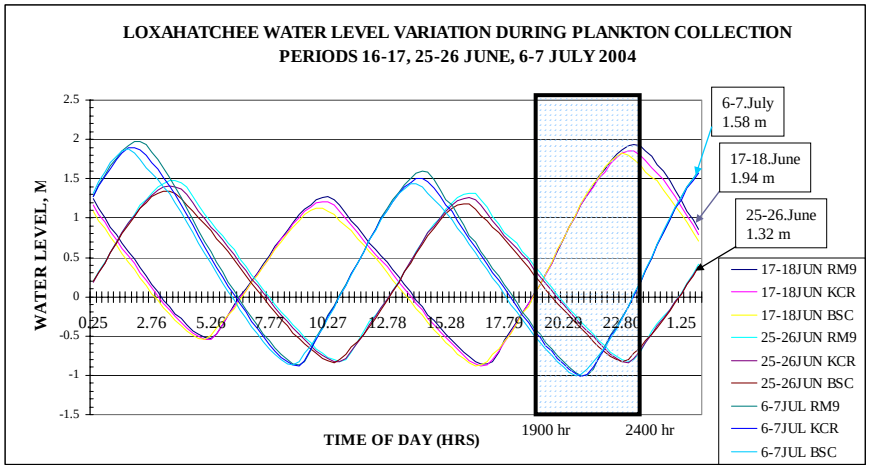

Figure 7-17. Water Level Fluctuation Before and During Zooplankton Sampling 17-25 June and 6 July 2004 Taken From All USGS Stations Between RM 6 and RM 9.

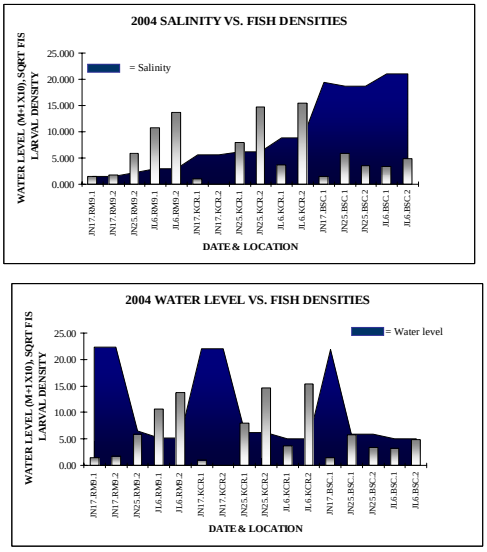

Figure 7-18. Mean Fish Density for All 2004 Stations Relative to Water Level (in Meters +1 ×10) and Salinity (ppt).

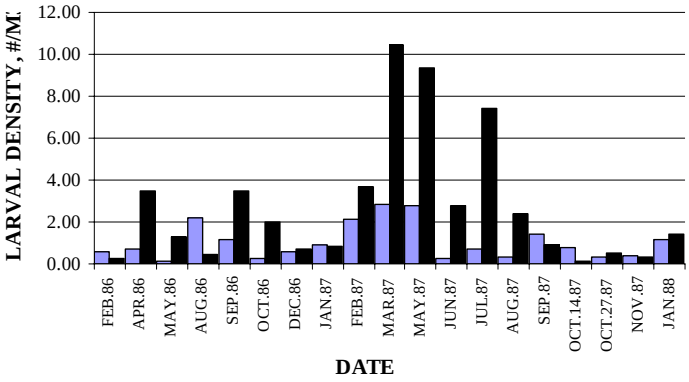

Figure 7-19. Comparison of Spatial Variation in Larval Densities from Station 25 (Blue) and Station 28 (Black), 1986-1988.

2004 Salinity Effects: USGS salinity data were analyzed for a 3-month period, 1 June to 31 August 2004 from gauging stations at RM 6, RM 8 and RM 9. The major change in salinity from greater than 15 ppt to less than 10 ppt occurs between RM 6 and RM 8; RM 8 is at the mouth of Kitching Creek. From RM 8 to RM 9 the salinity consistently stays below 5 ppt even during this drought period. The passage of Hurricane Charlie is apparent in August pushing RM 6 post-hurricane salinities to salinities similar to those at RM 8 observed during the drought period. This is significant in that most June and early July larval fish were captured at salinities between 2 ppt and 8 ppt between RM 8 and RM 9.

Figure 7-20 presents larval fish and crustacean abundance relative to salinity and collection station in 2004. Two patterns are apparent: 1) both crustacean and fish numbers decline between Stations 5/6 and Stations7/8; 2) larval fish and crustaceans are most abundant at Stations 5/6, fish from 3 to 6, where salinities ranged from 2 ppt to 8 ppt. **Figure 7-21** presents the fish and crustacean data converted as square root number of individuals, showing both fish and crustacean numbers decline considerably at RM 7, Stations 7/8 where salinities exceed 12 ppt.

1986-1988 Data: Spatial and Temporal Distribution: Differential Effect of Water Level and Salinity: The 1986-1988 data allows considerable perspective on temporal distribution of both physical and biological parameters. Multiannual, seasonal and monthly patterns in water level and salinity are apparent (**Figures 7-22** and **7-23**). The 2 ppt to 8 ppt salinity window that coincided with the greatest zooplankton abundance in the 2004 study is marked by a yellow line in **Figures 7-22** and **7-23**. At Station 28, (RM 7), the general periods when salinities are within the 2-8 ppt range are January-April both in 1986 and 1987 with June and August hovering around 2 ppt. When compared to Station 25 further toward the estuary (**Figure 7-23**), the only periods when salinities enter the 2-8 ppt window are in June, August and October. The remainder of the year they are above 8 ppt, typically between 10 and 20 ppt at this location. The typical regional highest water levels associated with high rainfall, river flow and annual sea level rise is observed in the fall in both Stations 25 and 28. However, 1987 appears to be a drier summer-fall year with

salinities remaining high in spite of a water level increase. This means during 1987 the freshwater flow component of annual sea level rise (of the three major components, rainfall and freshwater runoff, onshore easterly winds and North Atlantic Ocean basin expansion due to warming) was not very large. Low 1986 summer-fall and winter salinities and freshwater flows in the Loxahatchee River during this period reduced salinities from June 1986 to March 1987. The atypical rise in water level in March 1987 associated with a low salinity at Station 28 must be due either anomalous rainfall at this time or freshwater release from water control structures.

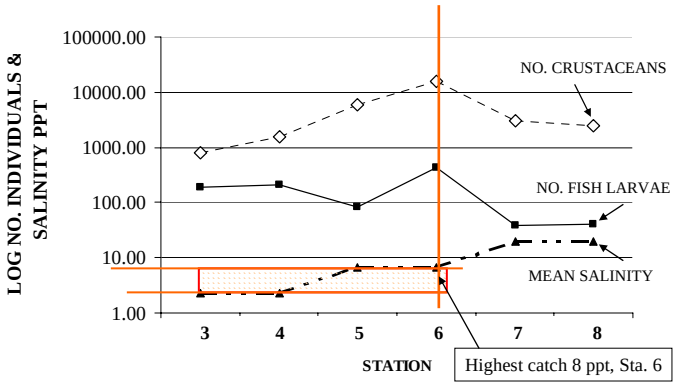

Figure 7-20. Larval Fish (sq. root number of individuals) and Salinity for All 2004 Collections Downstream of Stations 1 and 2. Orange Box Surrounds Salinity Region of Greatest Fish Larval Abundance.

Fish larval densities are plotted with the salinities in **Figure 7-24**, again with the 2-8 ppt salinity box depicted. Fish densities associated with salinities within the 2-8 ppt range are noted with orange boxes. These periods also mark the time of the highest concentration of fish larvae at Station 28 during the 2-year period. The third highest larval count was taken in July 1987 at salinities above 14 ppt. However, this is the period of the year with the lowest water levels, thus the potential to concentrate larvae, or move larvae downstream from exposed and reduced upstream habitats. Since the majority of the typical wet season in 1987 shows high salinities at Station 28, it is likely that drought conditions were occurring late spring to fall. This would produce low flows, low water levels and higher than average salinities. The result would be little optimum salinity occurrence, 2-8 ppt at Station 28 and few fish larvae. This was the case September 1987 through January 1988.

Fish larval collections were considerably lower at Station 25 than those at Station 28. The ambient salinity pattern at Station 25 is high relative to Station 28 and only showed the optimum 2-8 ppt window June through October 1986. This was the period when most fish larvae were captured in 1986. Numbers of larvae were also captured February through May in 1987 when salinities dropped from 20 ppt to between 10-15 ppt and water levels fell.

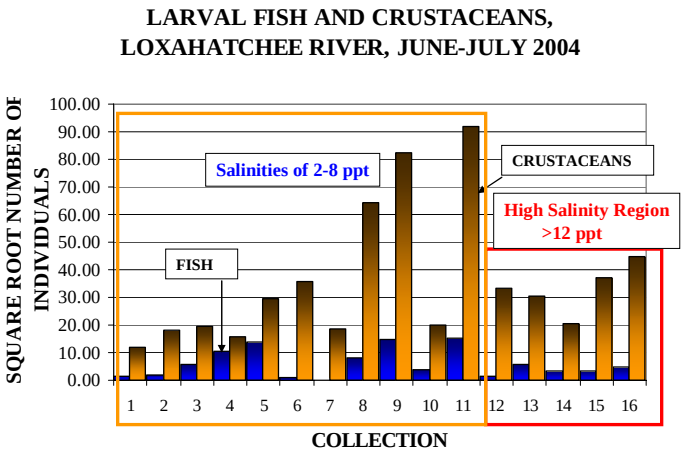

Figure 7-21. Larval Fish and Crustacean Abundance from Upstream Collections 1-5 to Downstream Collection 12-16 Revealing Differential Spatial Distribution June-July 2004.

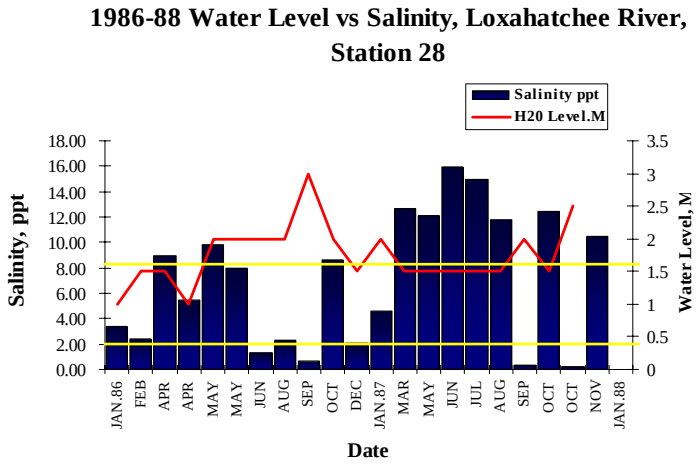

Figure 7-22. Water Level and Salinity, Station 28, 1986-1988. Yellow Lines Demark the 2-8 ppt Salinity Preference Observed for Goby Larvae in 2004 and 1986-1988 Data.

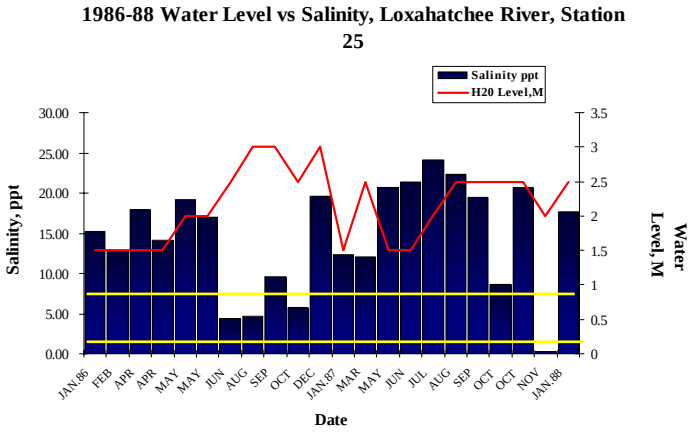

Figure 7-23. Water Level and Salinity, Station 25, 1986-1988. Yellow Lines Demark the 2-8 ppt Salinity Preference Observed for Goby Larvae in 2004 and 1986-1988 Data.

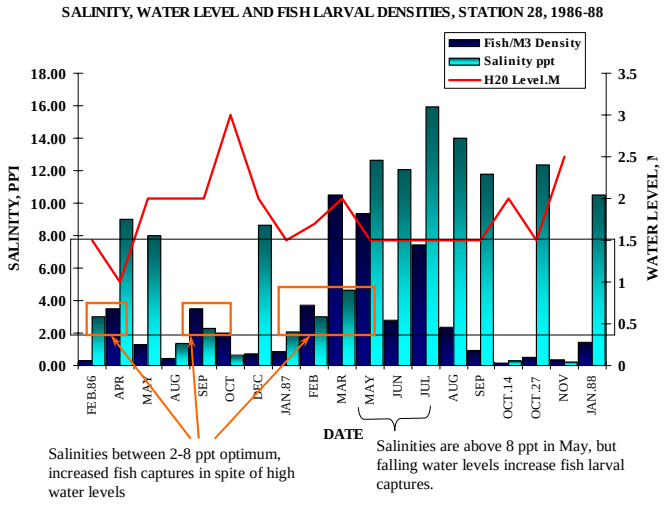

Figure 7-24. Plot of Fish Larval Densities from 1986-1988 with Water Level and Salinity for Station 28 Only. Salinity Larval Density Periods of Interest Are Noted.

When salinity for every month at Station 28 is used to produce a similarity matrix and clustered with Bray Curtis group average similarity analysis (**Figure 7-25**) the periods of salinity dry and wet seasons are apparent. The highest regional rainfall typically occurs in September to October, Group TW in **Figure 7-25** shows this pattern with salinities below 1.0 ppt. The TD group is a dry season group with salinities typically above 8 ppt. The optimum group for fish larvae is the AW group with salinities below 6 ppt, which did in fact have the largest fish larval captures. The same analysis using both Station 25 and Station 28 data reveals a similar cluster in **Figure 7-26.**

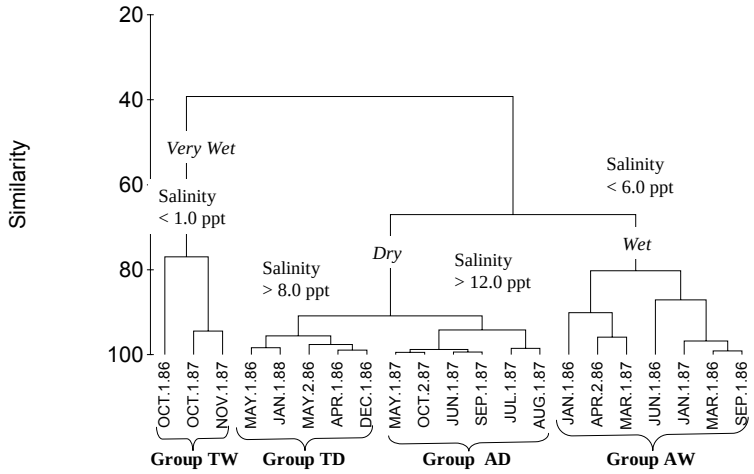

Figure 7-25. Cluster Based on a Group Average Similarity Analysis Using Mean Daily Salinity for Station 28, 1986-January 1988. Salinity for Date of Zooplankton Capture.

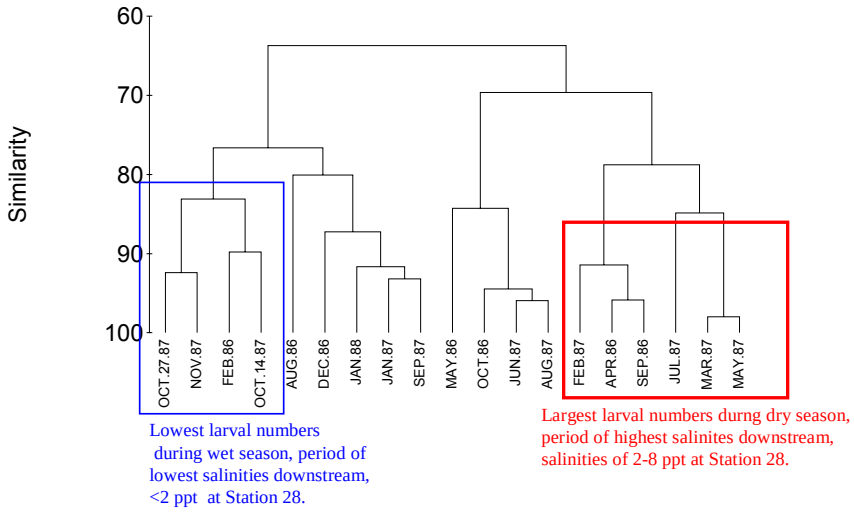

Figure 7-26. Similarity Analysis Bray-Curtis Group Average Cluster Plot Based on Fish Larval Density form Station 25 and Station 28, 1986-1988.

Results and Discussion

The optimum natural condition in which to examine the influence of freshwater flow on a riverine fauna is to examine the fauna at the lowest possible flow condition over a broad enough range of salinity within the shortest spatial and temporal (diel) range practical. This would insure temporal continuity between samples, therefore limiting potential impacts from factors that change rapidly during a sampling period, such as water levels and tidal action. Appropriate replication and adequate ancillary data should be acquired. We attempted to include all these considerations in this analysis of dry season larval fish recruitment, zooplankton abundance in the protected portion of the Loxahatchee River during the late spring and early summer 2004. We tested two null hypotheses: 1) "H^o_1 No particular taxon consistently numerically dominates the larval fish communities indigenous to the Loxahatchee River"; and 2) "H^o_2 Fish larval abundance is evenly distributed between RM 6 and RM 10 in the main course of the river during the "dry season" low rainfall, low flow periods, winter to late spring/early summer (December to July)."

"H^o_1" Loxahatchee River Larval Fish Community Defined: Our results demonstrated that a diverse yet predictable larval fish community occurs within the Loxahatchee River and is consistently numerically dominated by three to four fish families. This fauna consists primarily of gobies (gobioids), anchovies (engraulids), pipefishes (syngnathids) and silversides (atherinids) during the dry season. These same taxa numerically dominated samples taken at Station 28 in 1986 to 1988 and in 2004 revealing a long term consistency in fish larval community structure within the Loxahatchee River.

Station 25 collected from 1986 to 1988 was located below RM 6.0 at RM 5.3. Salinities at this location ranged between 1 ppt and 24 ppt, most often between 10 ppt and 20 ppt. The ichthyofauna was richer at Station 25 and revealed a higher diversity at the family level (**Figure 7-27**). Gobioids, the most abundant fish larvae in the Loxahatchee River, are known to occur in the freshwater tributaries to the Indian River Lagoon including the Loxahatchee River are listed in **Table 7-14**. The relative numerical abundance of various gobioid species is presented from data recently published by Paperno and Brodie (2004).

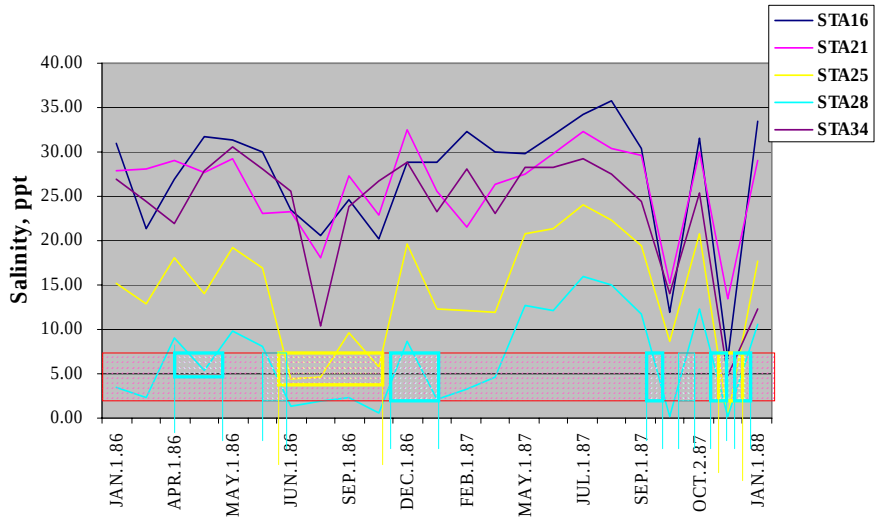

Figure 7-27. 1986-1988 Mean 24-Hour Salinity for Date of Zooplankton Capture, Stations 16 through 34 in the Loxahatchee River and Estuary. Periods of Optimum Salinity for Fish Larval Capture Is Indicated with the Red Band, Within Which Optimum Station Captures for Station 25 (Yellow) and Station 28 (Blue) are Boxed, Based on 2004 Capture Data.

Table 7-14. Gobioid Species of the Loxahatchee River.

	Taxa	Larval Capture	Abundance No. Individuals (% Occurrence)	Spawning Migration Tendency
Eleotridae				
1	*Gobiomorus dormitor*	?	114 (18)	Freshwater Semi-catadromous
2	*Dormitator maculatus*	X	374 (21.1)	Freshwater Semi-catadromous
3	*Eleotris amplyopsis*	?		Freshwater Semi-catadromous
Gobiidae				
4	*Awaous banana*	?		Freshwater Semi-catadromous
5	*Bathygobius soporator*	?		Estuarine, non migratory
6	*Ctenogobius pseudofasciatus*	?	14 (3.9)	Freshwater Semi-catadromous
7	*Ctenogobius fasciatus*	?		Freshwater Semi-catadromous
8	*Ctenogobius schufeldti*	?	11 (5.5)	Freshwater
9	*Gobioides brousonettii*	X		Freshwater Semi-catadromous
10	*Gobionellus oceanicus*	?		Estuarine, non migratory
11	*Gobiosoma bosc*	X	165 (15.6)	Estuarine, non migratory
12	*Gobiosoma robustum*	X		Estuarine, non migratory
13	*Gobiosoma macrodon*	?		Estuarine, non migratory
14	*Lophogobius cyprinoides*	?	134 (25.8)	Estuarine, non migratory
15	*Evorthodus lyricus*	X	464 (27.3)	Freshwater Semi-catadromous
16	*Microgobius gulosus*	X	123 (23.4)	Estuarine, non migratory

Data from Paperno and Brodie, 2004

Tropical marine invaders, the Diadromus Domination: The warm Florida Current flows along the lower east coast of the Florida producing a subtropical-tropical coastal oceanographic and climatic/hydrological setting for the Loxahatchee River. A typical tropical coastal climate pattern occurs in the region of the Loxahatchee River (Christensen, 1965; Gilmore, 1977, 1985; Gilmore and Hastings, 1983). A distinct wet season with natural high riverine flow rates occurs during the summer and fall, followed by a dry season low flow high salinity period starting in the late fall extending though the winter and spring (Gilmore, 1977; Gilmore and Hastings, 1983). This pattern differs significantly from the seasonal freshwater flow periodicity in other southeastern tributaries of the Piedmont coastal plane north of 28° 30' N (Rogers et al., 1984; Peterson and Meador, 1994). Climatic and biological conditions in these regions, as well as Gulf coastal Florida, are not representative of southeast Florida tributaries and coastal estuaries (Gilmore et al., 1978; Rakocinski et al., 1992; Gilmore, 2001; Streams of Florida). This is largely due to differences in the geomorphology of the Florida peninsula and proximity of warm tropical ocean currents. Most other Florida stream systems on the upper Gulf coast and north of Cape Canaveral, Florida show high stream flows during the fall through winter/spring, and often have drier summers (Rogers et al., 1984; Peterson and Meandor, 1994). These differences in seasonal flow patterns has some influence on aquatic organism spawning periodicity and larval recruitment as well as levels of primary and secondary productivity, with tropical systems differing significantly from warm temperate systems.

A local geological and geographic setting of the southern Indian River Lagoon and its freshwater tributaries has produced high biodiversity in local aquatic ecosystems. The climatic and ocean frontal boundaries between 26° and 29° N Longitude creates a biogeographic transition zone with significant overlap in tropical and temperate biological elements. Various portions of

each biological community are numerically dominated by either warm temperate, temperate or tropical species. Historical documentation of biotas within Jupiter Inlet, Hobe Sound and the Loxahatchee River region revealed a biota that is largely numerically dominated by tropical and warm temperate species (Christensen, 1965; Gilmore, 1977, 1995). Recent numerical studies of a neighboring small coastal stream system, the St. Sebastian River, produced similar results (Paperno and Brodie, 2004).

The dominance of gobioid larvae is typical of tropical estuaries throughout the world. Where gobies have adapted to temperate estuaries they numerically dominate the ichthyoplankton (Shenker et al., 1983). The gobioid fishes can also numerically dominate open ocean ichthyoplankton (Richards, 1984; Ahlstrom, 1971, 1972; Nellen, 1973). This fish family has the most species occurring to ocean depths of 1,500 feet (Gilmore, personal observation) as well as inhabiting freshwater streams and anoxic mangrove forest habitats. They are also the richest fish faunal element in the Loxahatchee River with at least 16 species occurring in this small coastal stream system.

The anchovies, engraulidae, are next in abundance possibly including both tropical and temperate species. They are typically the most numerically abundant marine and coastal estuarine fish as adults. This may be why engraulid larvae numerically dominated ichthyoplankton captures at Station 25, but not at Station 28 during 1986-1988.

Other marine and estuarine species that were common, or occurred, in both historical samples, 1986-1988, and in the 2004 samples, were larval mojarras (gerreidae), drums and croaker (sciaenidae), herrings/sardines/menhaden (clupeidae), silversides (atherinidae), and pipefishes (syngnathidae). The historical collections also included some larval blennies (blennidae), and various flatfishes (soleidae, bothidae and cynoglossidae). These are families which are commonly represented in the ichthyoplankton of tropical freshwater tributaries elsewhere in the world (Blaber, 2000).

Noticeably absent were larval snook (centropomids). There are five species of snook in the Loxahatchee River, the common snook, *Centropomus undecimalis*, largescale fat snook, *C parallelus*, smallscale fat snook, *C. mexicanus*, tarpon snook, *C. pectinatus* and the swordspine snook, *C. ensiferus*. All of these species have been captured as juveniles and adults in the Loxahatchee, St. Lucie and St. Sebastian Rivers. No other stream or river system in Florida has all of these species recorded from it. However, larvae of any species of centropomid were absent from all the historical samples and the 2004 samples. Nevertheless, snook eggs and larvae were abundant in a sample made within Jupiter Inlet on 2 July 2004 indicating that snook were spawning at that time. The eggs and larvae must be carried into habitats which were not sampled.

Larvae of primary freshwater fishes, centrarchids, cyprinids, percids, and catostomids, were also absent from in the 2004 samples. Centrarchids and cyprinids were listed as having been taken in the 1986-1988 samples at Station 28, but did not form a large portion of the larval collections. The primary freshwater fish fauna of the southern Florida peninsula is depauperate relative to northern Florida. Freshwater faunas of the southern peninsula are numerically dominated by euryhaline secondary freshwater families, anguillidae, cyprinodonts, poeciliids and atherinids and many marine invaders particularly in coastal streams. Euryhaline marine/estuarine invaders are present either as juveniles and adults, but not necessarily as larvae. These include bull sharks, ladyfish, tarpon, ariid catfishes, and mullets, snooks, centropomidae, mangrove snapper, burro grunt, sheepshead porgy, sciaenids, cichlids and various flatfishes, bothids, cynoglossids and soleids. Soleid larvae were represented in our 2004 samples. These families and the general invasion of freshwater by adults and juveniles of marine and estuarine phyla is a worldwide tropical phenomenon (Blaber, 2000). Spawning is another matter. Very few marine fishes in these families place their eggs and larvae into low salinity waters. Nearly all spawn in

the ocean and their larvae require higher salinities to survive. The marine fish families, gobiids, synganthids and engraulids are the top euryhaline spawners.

Tropical island and coastal continental freshwater stream faunas are often numerically dominated by marine and estuarine species that may enter freshwater for extended periods of time. They often depend on freshwater to complete vital developmental or reproductive periods. Diadromy is a common life history strategy for these species (McDowall, 1988). The numerical dominance of tropical marine and estuarine species in freshwater habitats is typical of many coastal settings in the tropical Americas and Caribbean islands (Blaber, 2000).

"H^0 $_2$" Fish Larval Dynamics Relative to Salinity and Water Depth: The dynamics of the Loxahatchee river ichthyoplankton community was examined relative to collection sites, salinity, and water level using the 2004 and in the historical 1986-1988 collections . Additional parameters evaluated for the 2004 collections included temperature, dissolved oxygen and water flow rates but since these parameters did not vary significantly between stations during the recent ichthyoplankton survey it appears that salinity is the major factor responsible in influencing densities. However, the major portion of the ichthyofauna was captured at the confluence of the Kitching Creek and the main course of the Loxahatchee River. This could also be a site of nutrient flow, organic materials and consequently, primary productivity which would then produce a microzooplankton bloom of copepods and ostracods that were not captured with the net we used. This microzooplankton bloom would then feed larger invertebrate plankton and fish larvae. Nutrients and organic material concentrations were not examined so the influence of these parameters on fish larval distribution could not be determined. It is also possible that the large low tide captures on an ebbing tide, 25 June and 6 July 2004 could be due to the fact that even though the fish and invertebrate larvae typically migrate to the surface at night, they might not do so on an ebbing tide as they may be carried out into the adjacent estuary. In order to maintain an upstream position they would migrate to the river bottom. The 0.5-m plankton net may have sampled this bottom habitat in upstream waters between RM 8 and RM 9 while the water depth was too great to sample the bottom habitat at Stations 7 and 8 at RM 7. This would produce higher larval densities upstream simply as a sampling artifact. However, the high tide collection made on 17 June also captured more invertebrates between RM 8 and RM 9 than at RM 7, indicating the 2-8 ppt salinity region and its high ichthyoplankton density was likely not a sampling artifact.

The 1986-1988 collections were always made on a flood or high tide yet revealed the same fish larvae species ranking based on numerical abundance with most larvae captured when salinities were between 2 and 8 ppt for both Stations 28 and 25 **(Figure 7-27)** with the greatest abundance at Station 28 at RM 7. Where this salinity range (2 to 8 ppt) occurred, the greatest concentration of fish larvae also occurred in 2004 between RM 8 and RM 9 (**Figure 7-28)**, with most larvae being captured in the vicinity of the mouth of Kitching Creek at RM 8. The highest density of fish larvae captured in the Pautuxent River (Shenker et al., 1984) were captured between salinities of 2-3 ppt. Similar salinity association patterns were observed in the San Francisco Estuary (Dege and Brown, 2004). Apparently, fish larvae concentrate in the Low Salinity Zone of estuarine systems, however, since each system has unique characteristics, field investigations need to document this important low salinity range for each estuary. Thus, the 2 to 8 ppt range, under low flow conditions in the Loxahatchee River, is unique to this estuary. The most downstream location of this salinity range we documented from the historical data is near RM 7. Hence, we cannot show the natural concentration of fish larvae will occur further downstream than RM 7 with increased base flows due to changes in hydrodynamics with increased flows. Increased base flows will reduce the particle residence time within the appropriate salinity range and may affect the formation of a turbidity maximum. Further, as this range progresses downstream the physical attributes of the estuary (i.e., bathymetry, water surface area) will change hydrodynamic conditions possibly needed to facilitate increased zooplankton

concentrations in the turbidity maximum. Significant physical changes occur downstream of RM 6. For example, the surface area of water and length of shoreline from RM 7 to RM 6 is 30.7 acres and 92,835 ft in contrast to one mile downstream (RM 6 to RM 5) has 88.8 acres and 152,045 ft of shoreline, respectively (**Chapter 3**;**Table 3-5**). Additionally, the impact of human influences such as lighting and hardening shorelines which cause the loss of shallow shoreline transitional habitat, increases significantly downstream of RM 6 and has unknown affects on fish larvae recruitment.

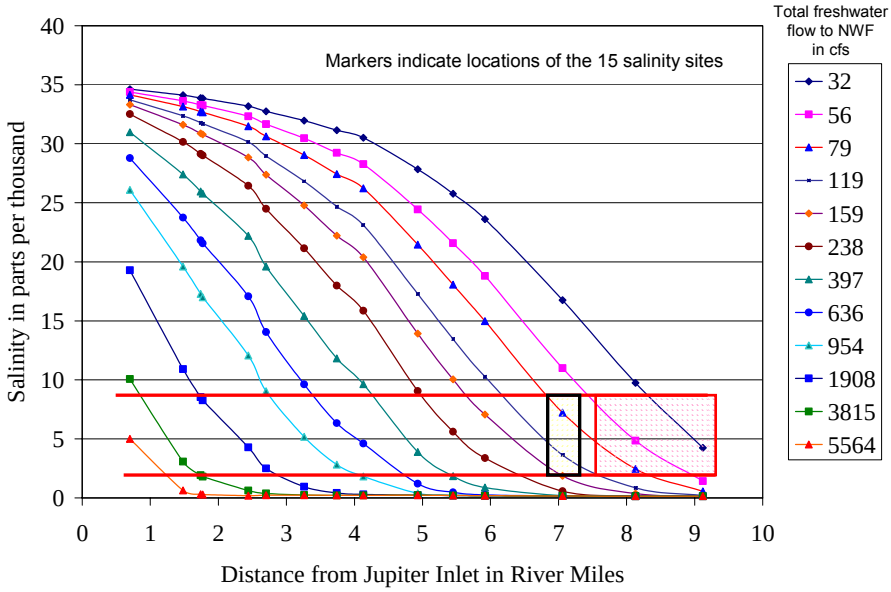

Figure 7-28. Red Rectangle Represents Location and Salinity at Which Largest Zooplankton Captures Were Made in June-July 2004, Yellow Rectangle, 1986-1988.

Since these important changes in the estuary occur downstream of RM 6, the preferred salinity range should not extend beyond this location during the dry season when it is most important to fish larvae. **Figure 7-28** shows a base flow near 140 cfs (Scenario **LD65TB65**) provides a salinity of 2 ppt at RM 7.2 and 8 ppt at RM 6. To corroborate these findings, daily salinities for all scenarios at RM 5.92 were examined and the same conclusion was established. Therefore, scenario **LD65TB65** is the maximum flow recommended to avoid significant alteration of conditions favorable to fish larvae in the estuarine area of the Northwest Fork of the Loxahatchee River.

EVALUATION OF MESOHALINE ZONE: OYSTERS

Evaluation Methods

Favorable estuarine habitat conditions for the eastern oyster are predominately determined by salinity, quality and quantity of food, available substrate (cultch), water flow, presence of disease organisms, and predation. Low densities (167 oysters/m^2 at RM 5.9) manifest poor oyster habitat conditions in the inner estuary of the Northwest Fork primarily due to frequent exposures to unfavorable low salinities while low densities in the outer estuary (downstream of RM 4.2) result presumably from disease (*Perkinsus marinus*), predation, limited food supply, and lack of appropriate substrate. Suitable oyster habitat is present in the middle portion of the Northwest

Fork from near RM 5.9 to RM 4.1 where yearly salinity averages between about 10 to 20 ppt. As yearly average salinity increases in this area, the density of oysters also increases to a maximum of 901 oysters/m^2 at RM 4.1 (**Chapter 4**). The increase in oyster density in this area is indicative of increasing favorable habitat conditions, with the existing hydrology, for reproduction, growth, and reduced influence of disease and predators. The evaluation for oysters is limited to this area where disease and predation are minimized. Oyster life history and salinity thresholds to address stress are used as the controlling factors of oyster presence, even though other factors are undoubtedly important, they are difficult to quantify and beyond the scope of this evaluation.

To describe the relative suitability of habitat within the area of interest, salinity tolerance thresholds for each life stage were established. Although overlapping life stages were observed throughout the year, major spring spawning occurs mostly in March and April when water temperatures are rising. Any protracted spawning during the year is considered insignificant even though other Florida estuaries appear to experience a minor fall spawn (Volety et al., 2003). Therefore, salinity concentrations and duration thresholds for oyster life stages (eggs, larvae, spat, and adult) that cause stress, harm, and mortality were introduced as the oyster Performance Measures where larval presence from March to May follows egg development from January to April (**Chapter 4, Table 4-3**). Spat and juvenile oysters are present from April through July while year class adults are present from June to December.

This salinity tolerance and life stage information were used to develop a Loxahatchee Oyster Stress Model (LOSM) that determines the number of days of "no salinity stress" (good conditions), stress (mixed conditions), and mortality (unhealthy conditions) for each life stage during the year throughout the oyster bars distributed in the middle of Northwest Fork (RM 4.1 to RM 5.9). The percent of time within one year for each level of stress is obtained from the LOSM model. To reduce the variability of salinity, a daily mean salinity value is used as input to the model. Long-term daily salinities (from 1965 to 2003) at four locations near oyster beds documented in a November 2003 survey (Bachman et al., 2004) were simulated using the LSMM. In addition to the base case and the five flow restoration scenarios, two addition alternatives were evaluated. These two alternatives are **LD60TB40** representing a minimum base flow of 60 cfs from Lainhart Dam and 40 cfs from the other tributaries into the Northwest Fork, and **LD80TB80** representing a minimum base flow of 80 cfs from Lainhhart Dam and 80 cfs from the other tributaries. All alternatives were compared and contrasted with the base case to determine the maximum quantity of base flow to the Northwest Fork without significantly harming oyster resources. To visualize how levels of oysters stress varied among years, an EXCEL stackable bar chart was utilized. Box and whisker plots (Sokal, 1965) generated with the statistical software SYSTAT 10.2 visually depicted the distribution of 39 years of oyster salinity stress levels for all salinity time series by revealing the median percent of days per year of stress and harm as well as death conditions, 95% confidence limits, and range of data.

Major assumptions of this assessment are: 1) most of the variability associated with the success of a year class of oysters can be explained by exposure to daily mean salinities (or salinity as a surrogate) during four life stages; 2) the life history of oysters in the Northwest Fork estuarine area emulates that in St. Lucie estuary oysters; and 3) a long-term evaluation of oyster habitat suitability can be determined by assessing salinity conditions for each year class.

Results and Discussion

The LOSM model used the 39-year POR to predicted average daily salinities at four locations in the Northwest Fork (**Chapter 6, Figure 6-10**) to determine levels of stress for up to eight inflow scenarios. These four stations are BD (Boy Scout Dock at RM 5.92), Oyster Station 6 (RM 5.45), Oyster Station 5 (RM 4.93), and Oyster Station 4 (RM 4.13) as shown in **Figure 7-29**.

Figure 7-29. Oyster Evaluation Stations in the Northwest Fork of the Loxahatchee River. The Oyster Beds Surveyed in 2003 Are Shown in Yellow. Red Dots Are Monitoring Sites.

For each scenario, the level of stress on the oyster year class (four life stages) was determined by comparing these salinities with salinity stress thresholds. **Figures 7-30, 7-31,** and **7-32** provide an example of how the output from the model was used to visualize affects of all scenarios inflows on the year class life stages. These figures show the percent of time each year class experienced one of three levels of stress for the base case and two scenarios. The base case (**Figure 7-30**) reveals that good conditions existed for egg development at RM 4.93 (Station 5) during most years. As inflows increased with successive alternatives and were compared to the base case, more oyster stress was observed. **Figure 7-31** shows that scenario **LD90TB110**, (total base inflow of about 200 cfs) is the maximum inflow that oysters at this particular location could accept before dramatic increases in harm (mixed conditions) were evident for scenario **LD200** (total base inflow of about 230 cfs; **Figure 7-32**). A total of 128 plots were visually inspected to select the maximum base inflow scenario for all life stages as demonstrated with these figures for the egg development stage. All of these results were compiled for comparison and validation with the results from the following analysis. Note that there is a critical base flow which resulted in a significant increase in the percent of the mixed condition from **LD90TB110** to **LD200**. The current distribution of oysters manifests the present salinity regimen. If additional flows are introduced to the system, it is expected that the oysters that are experiencing low density and stressed conditions upstream (RM 5.9) will be lost. However, oysters have the ability to shift populations within the estuary to meet their salinity requirements. As stated in **Chapter 4**, healthy oyster beds existed much further downstream (near the railroad bridge) when salinities were

lower before the oysters were dredged and the amount of sea water exchange to the Northwest Fork was limited.

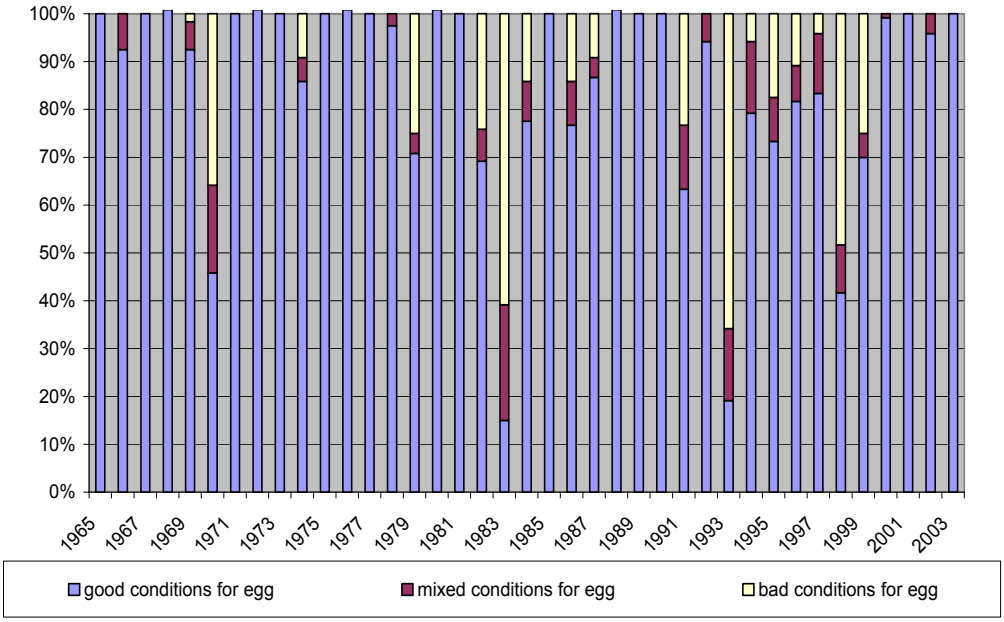

Figure 7-30. Percent of Time for Three Levels of Salinity Stress on Oyster Eggs at Station 5 (RM 4.93) for the BASE Case.

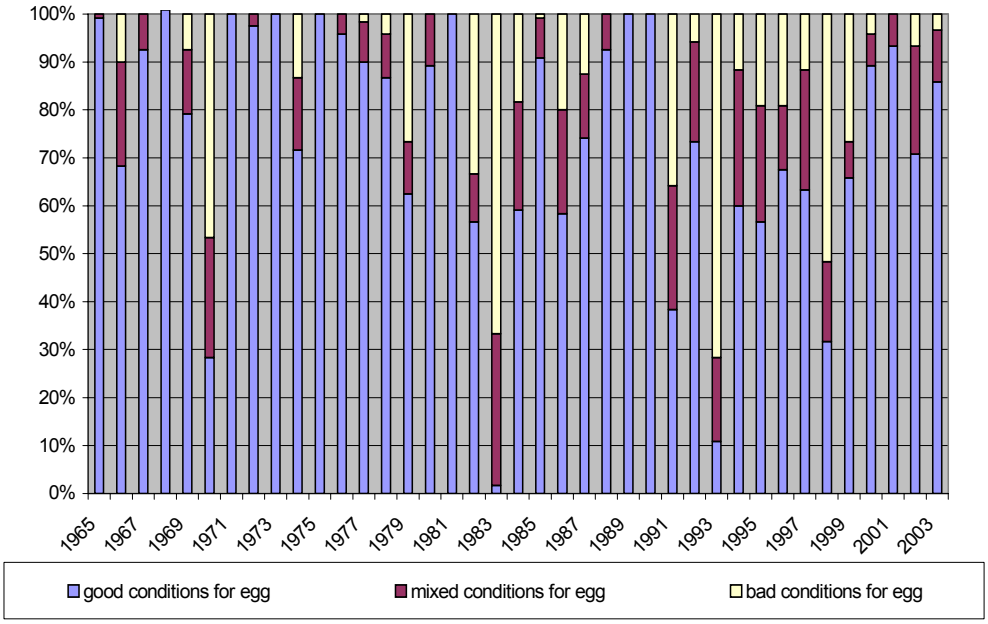

Figure 7-31. Percent of Time for Three Levels of Salinity Stress on Oyster Eggs at Station 5 (RM 4.93) for the LD90TB110 Scenario.

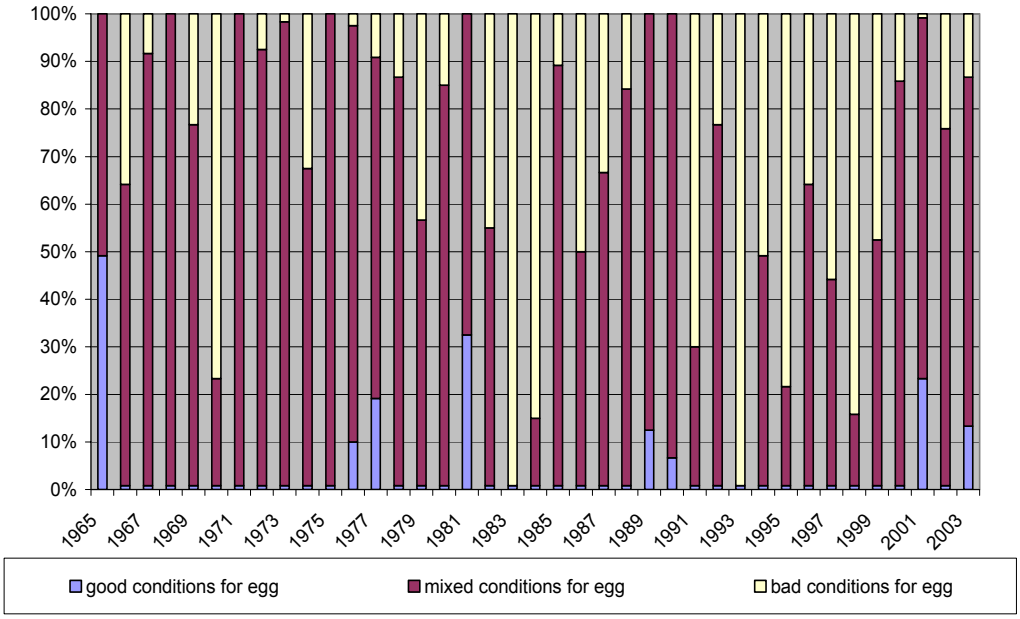

Figure 7-32. Percent of Time for Three Levels of Salinity Stress on Oyster Eggs at Station 5 (RM 4.93) for the LD200 Scenario.

In addition to the visual, individual year class evaluation for each life stage, the median, 95% confidence limits and range of the 39-year distribution of percent of time for death and harm/stress conditions were depicted with box and whisker plots (BWP) for all life stages at four stations in **Figures 7-33** through **7-40**. As an example of the linkage between the visual analysis **(Figures 7-30, 7-31,** and **7-32)** and the BWP (**Figures 7-37** and **7-38)** for Station 5, depicts information in which the visual analysis concluded significant harm condition for eggs occurring with base inflows greater than scenario **LD90TB110**. It is apparent that the 39-year distribution data for alternatives validate the visual analysis.

As a performance measure, the existing oyster resources, and the flow alternatives for each station are those that avoid stress to the most salinity sensitive life stage; oyster larvae. These larvae are present in the system during the late dry season (March, April, and May, see **Chapter 4**, **Table 4-3**) which is the time period the evaluation was conducted for this life stage and when problems with salt water intrusion historically occur. Oyster larvae at the most upstream station (Boy Scout Dock or RM 5.92) are the most sensitive to increased base flows. Base flows greater than scenario **LD65** (about 90 cfs) will result in a significant increase in stress (**Figure 7-33**) and a significant increase in unhealthy conditions in this area may occur with scenario **LD60TB40** (about 100 cfs, **Figure 7-34**).

Additional results for downstream station, Station 6, are shown in **Figures 7-35** and **7-36** and indicate that the flows in scenario **LD65TB65** (about 130 cfs) causes stress to the larvae. Using the same logic for larvae at Station 5, **Figures 7-37** and **7-38** reveal that scenario **LD80TB80** (about 160 cfs) is the flow which causes stress and scenario **LD90TB110** (about 200 cfs) for death. A dramatic increase in stress occurs from scenario **LD80TB80** to **LD90TB110** (**Figure 7-37**). However, it dramatically decreases from scenario **LD90TB110** to **LD200** due to the increase in death occurring with scenario **LD200**. This decrease in stress/harm with increasing base flows can be observed at other stations. The least impact on oyster larvae by increases in base flows is the most downstream Station 4. **Figures 7-39** and **7-40** show that Station 4 can tolerate scenario **LD 200** (about 230 cfs) before significant stress/harm occurs with **LD200TB200** (about 400 cfs). Therefore, any scenario that increases the flow greater than 90 to 100 cfs should be avoided to maintain the existing upstream oyster bars. However, if flows greater than 90 to

100 cfs are needed to restore other important habitats, the loss of the most upstream highly stressed oysters can be mitigated by providing additional substrate (cultch) in downstream areas (near RM 4.5) that would be experiencing favorable salinities.

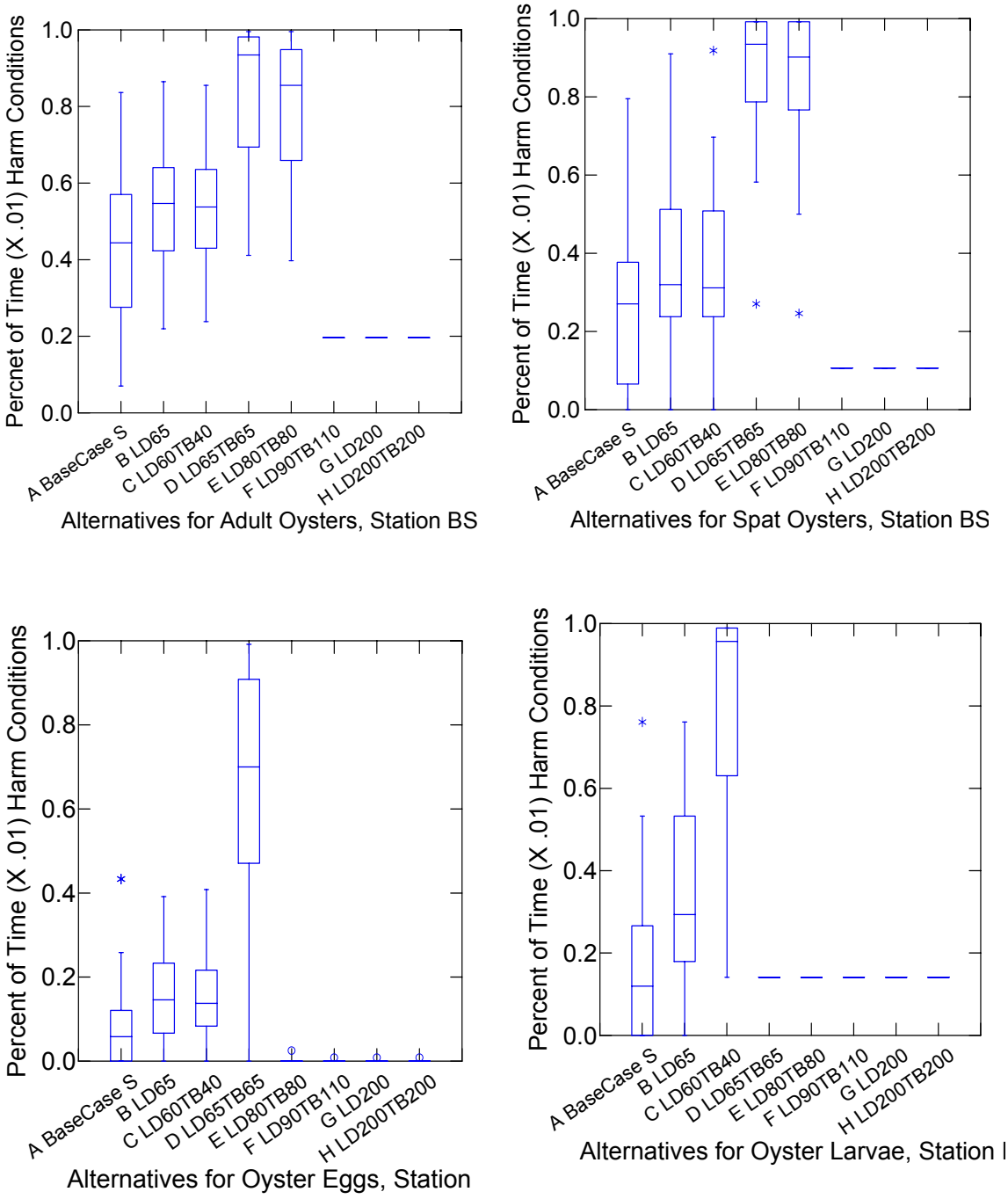

Figure 7-33. Box and Whisker Distribution Plots of the Predicted Percent of Time Harm Conditions Existed for Adults, Spat, Larvae, and Eggs in the BASE Case and Seven Alternative Base Inflow Scenarios at Boy Scout Dock.

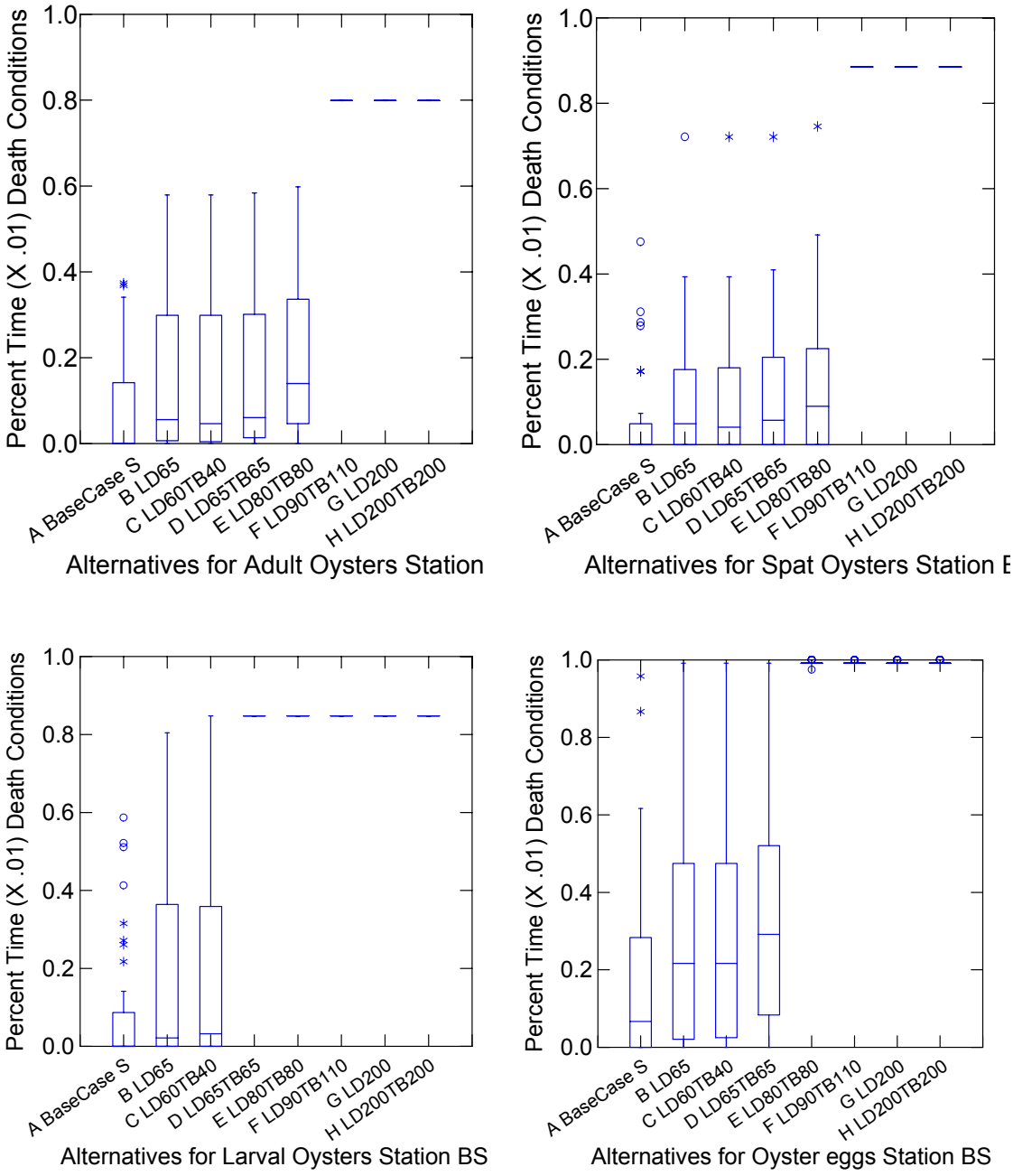

Figure 7-34. Box and Whisker Distribution Plots of the Predicted Percent of Time Death Conditions Existed for Adults, Spat, Larvae, and Eggs in the BASE Case and Seven Alternative Base Inflow Scenarios at Boy Scout Dock.

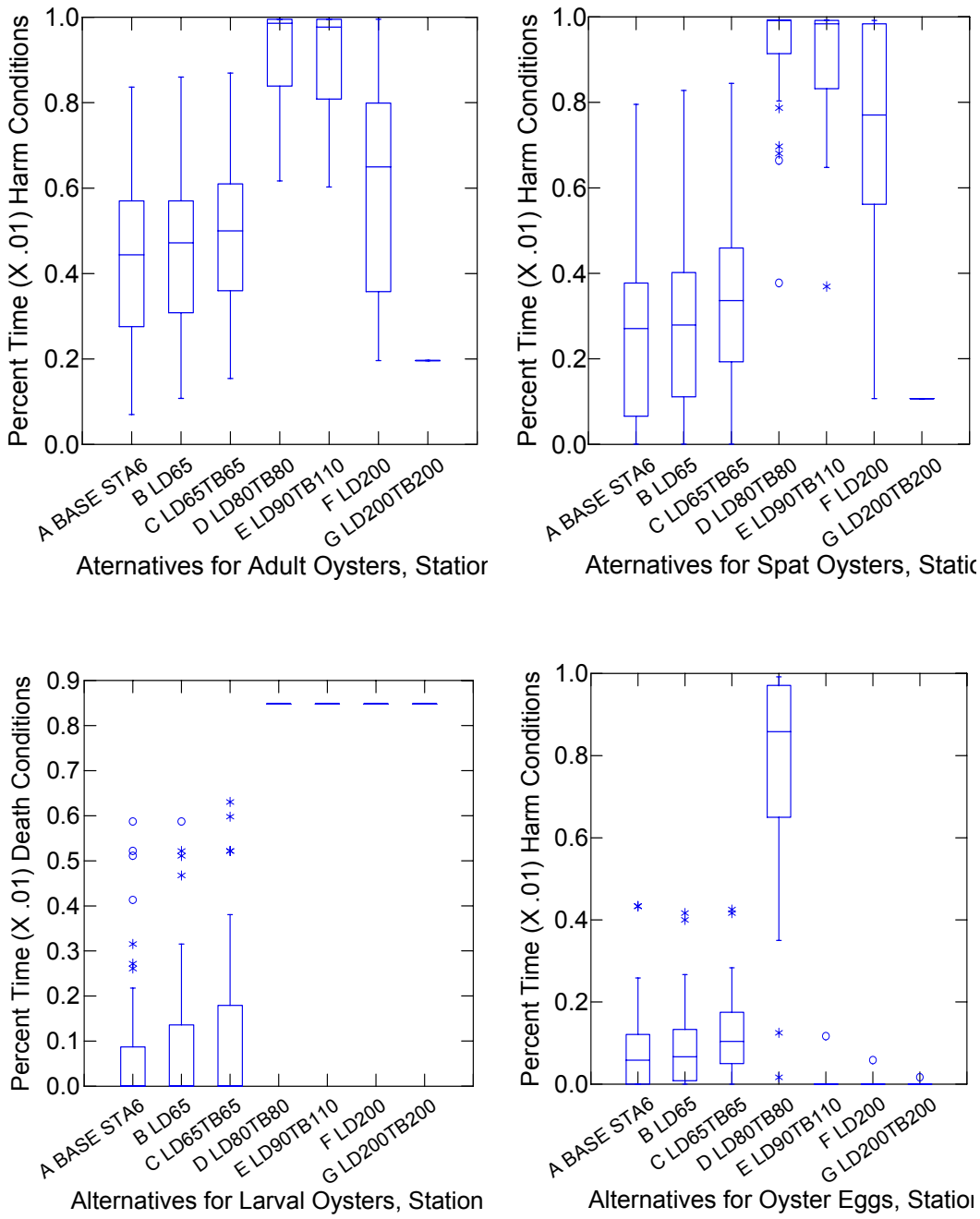

Figure 7-35. Box and Whisker Distribution Plots of the Predicted Percent of Time Harm Conditions Existed for Adults, Spat, Larvae, and Eggs in the BASE Case and Six Alternative Base Inflow Scenarios at Station 6.

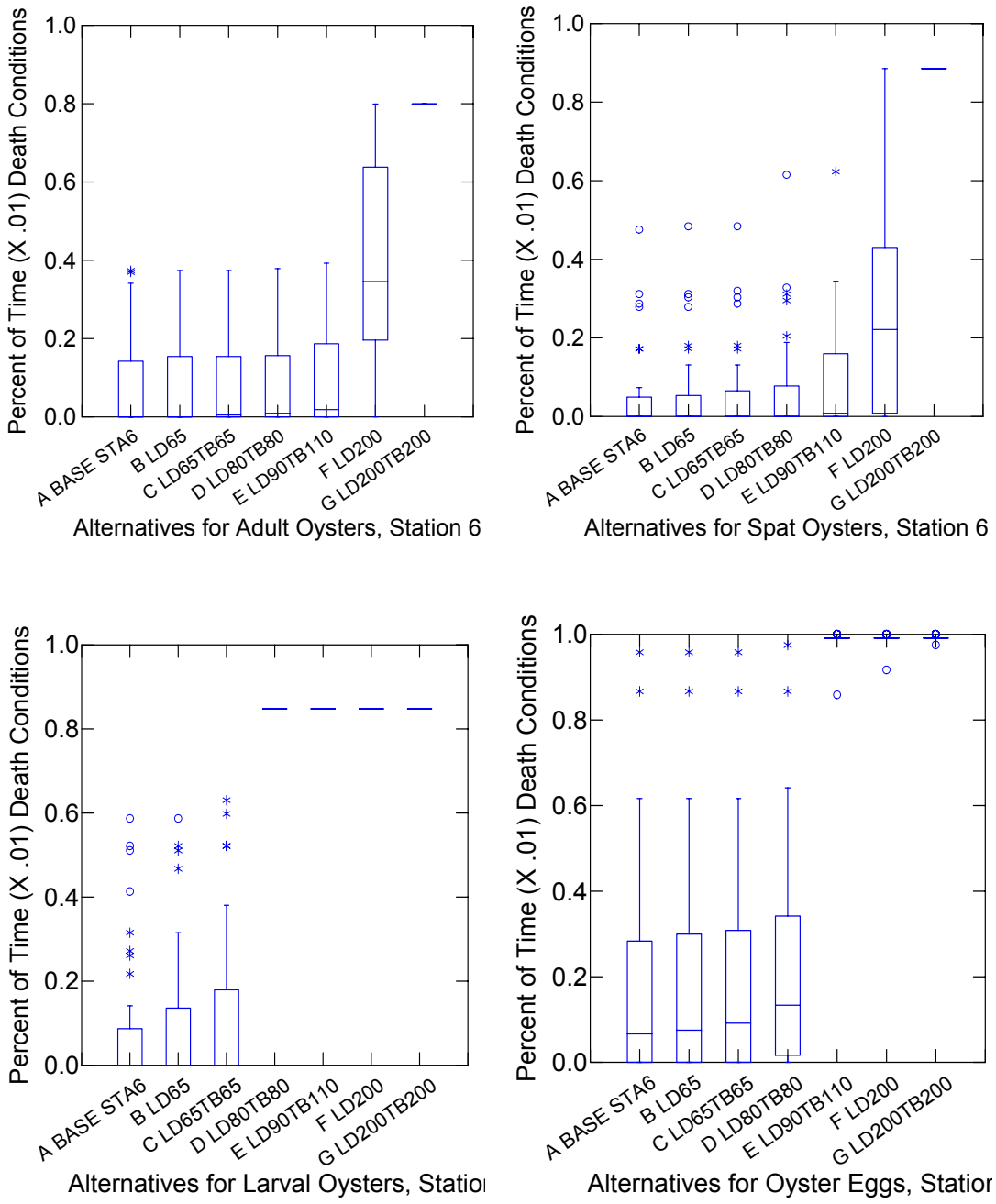

Figure 7-36. Box and Whisker Distribution Plots of the Predicted Percent of Time Death Conditions Existed for Adults, Spat, Larvae, and Eggs in the BASE Case and Six Alternative Base Inflow Scenarios at Station 6.

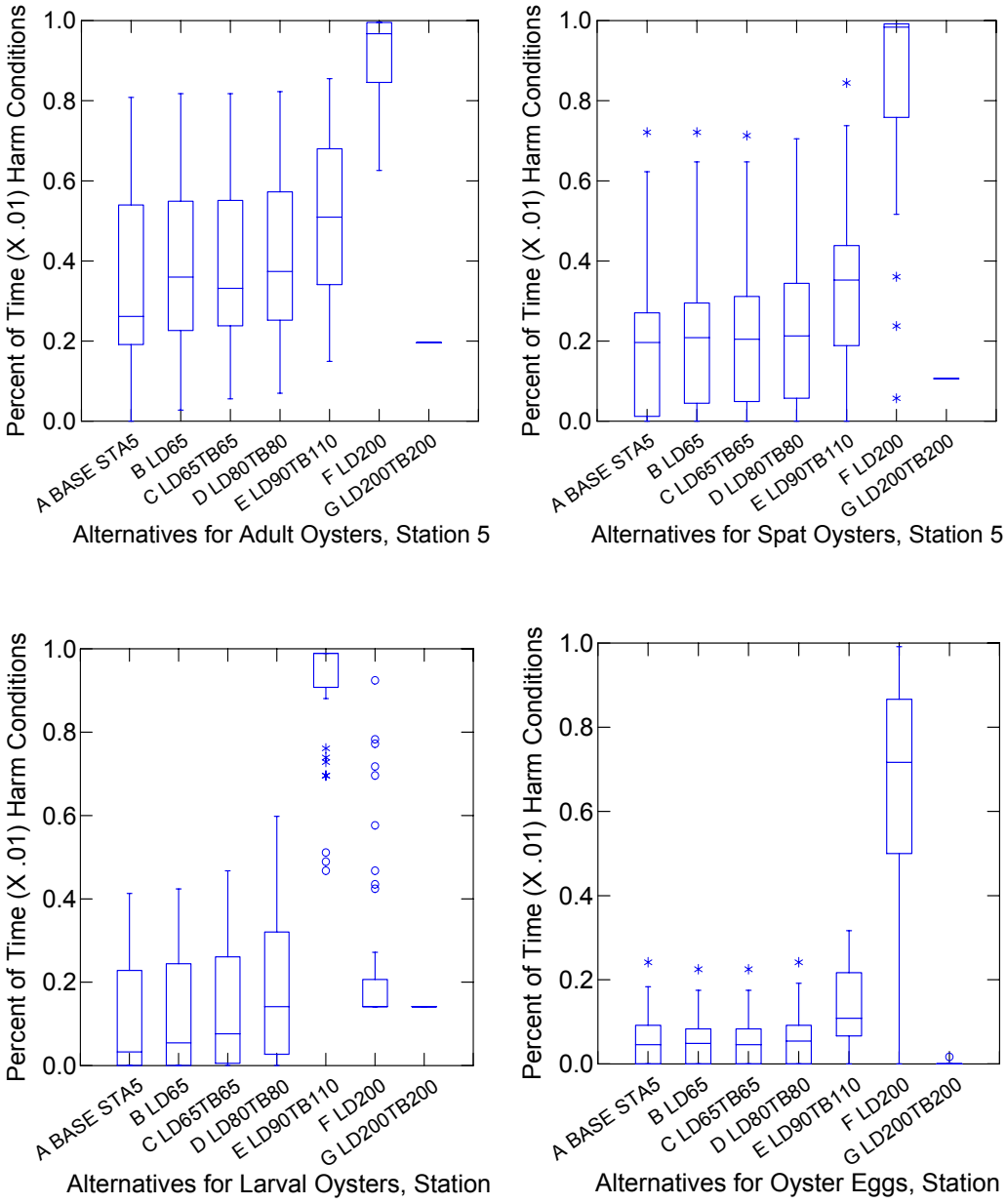

Figure 7-37. Box and Whisker Distribution Plots of the Predicted Percent of Time Harm Conditions Existed for Adults, Spat, Larvae, and Eggs in the BASE Case and Six Alternative Base Inflow Scenarios at Station 5.

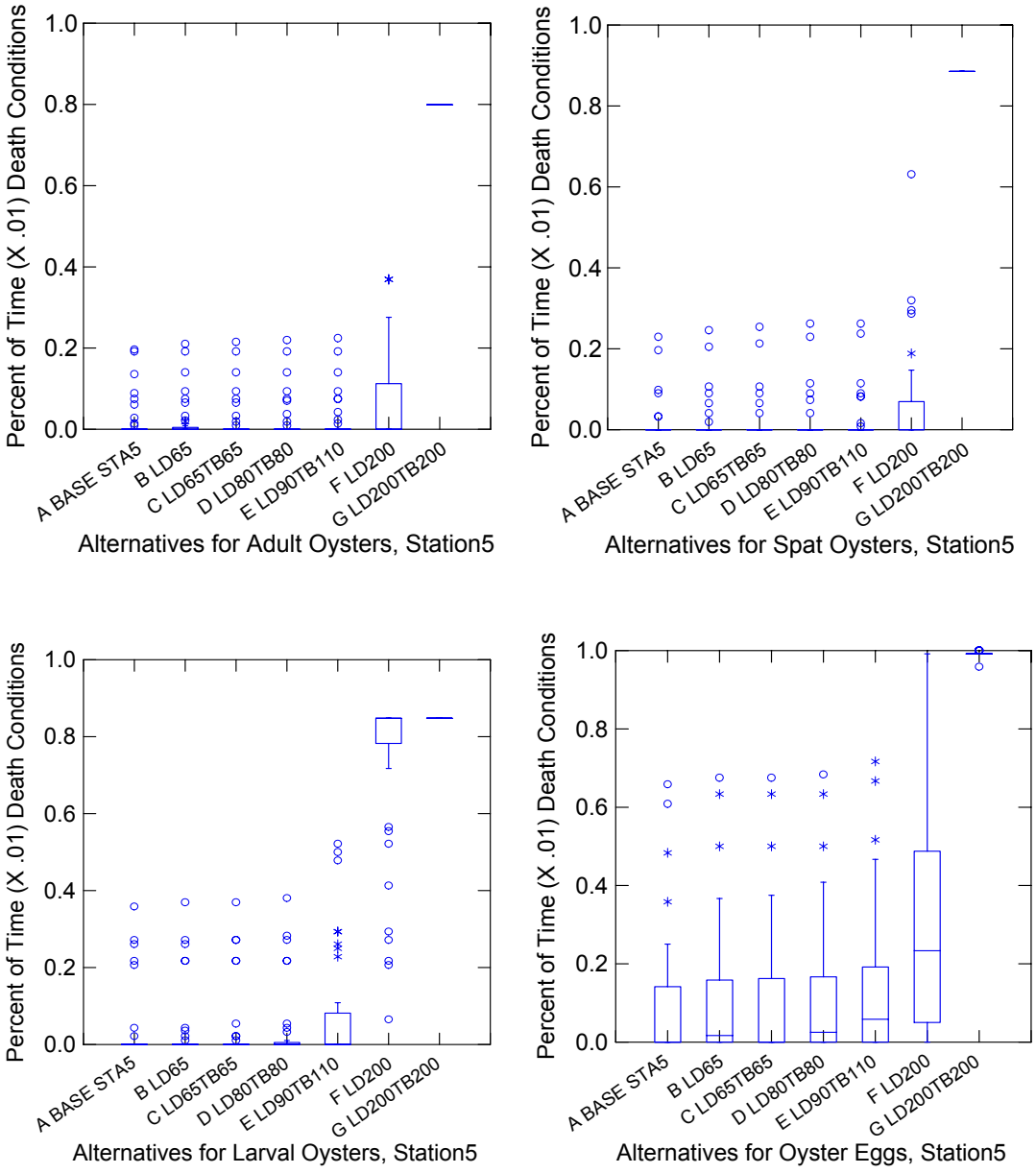

Figure 7-38. Box and Whisker Distribution Plots of the Predicted Percent of Time Death Conditions Existed for Adults, Spat, Larvae, and Eggs in the BASE Case and Six Alternative Base Inflow Scenarios at Station 5.

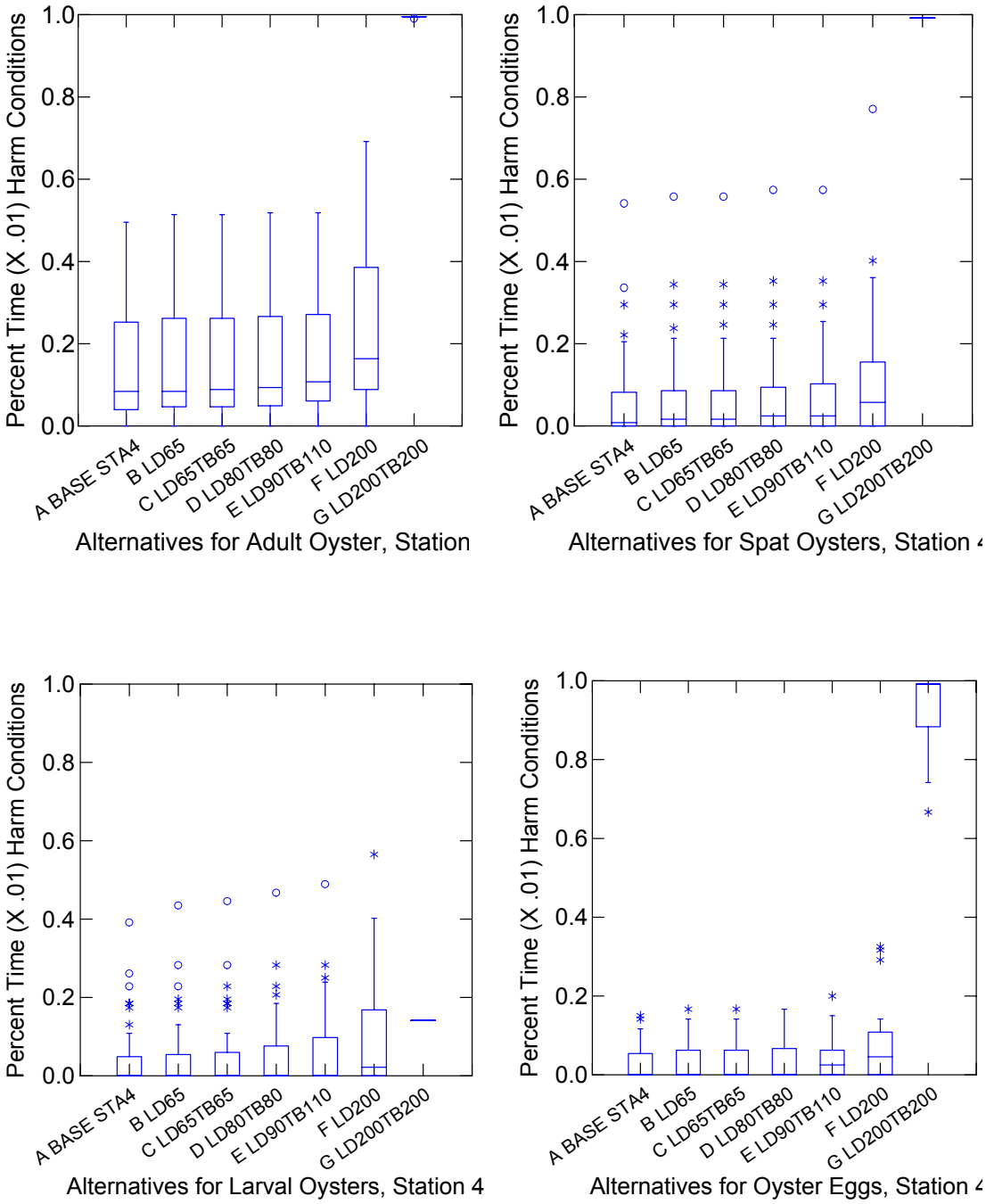

Figure 7-39. Box and Whisker Distribution Plots of the Predicted Percent of Time Harm Conditions Existed for Adults, Spat, Larvae, and Eggs in the BASE Case and Six Alternative Base Inflow Scenarios at Station 4.

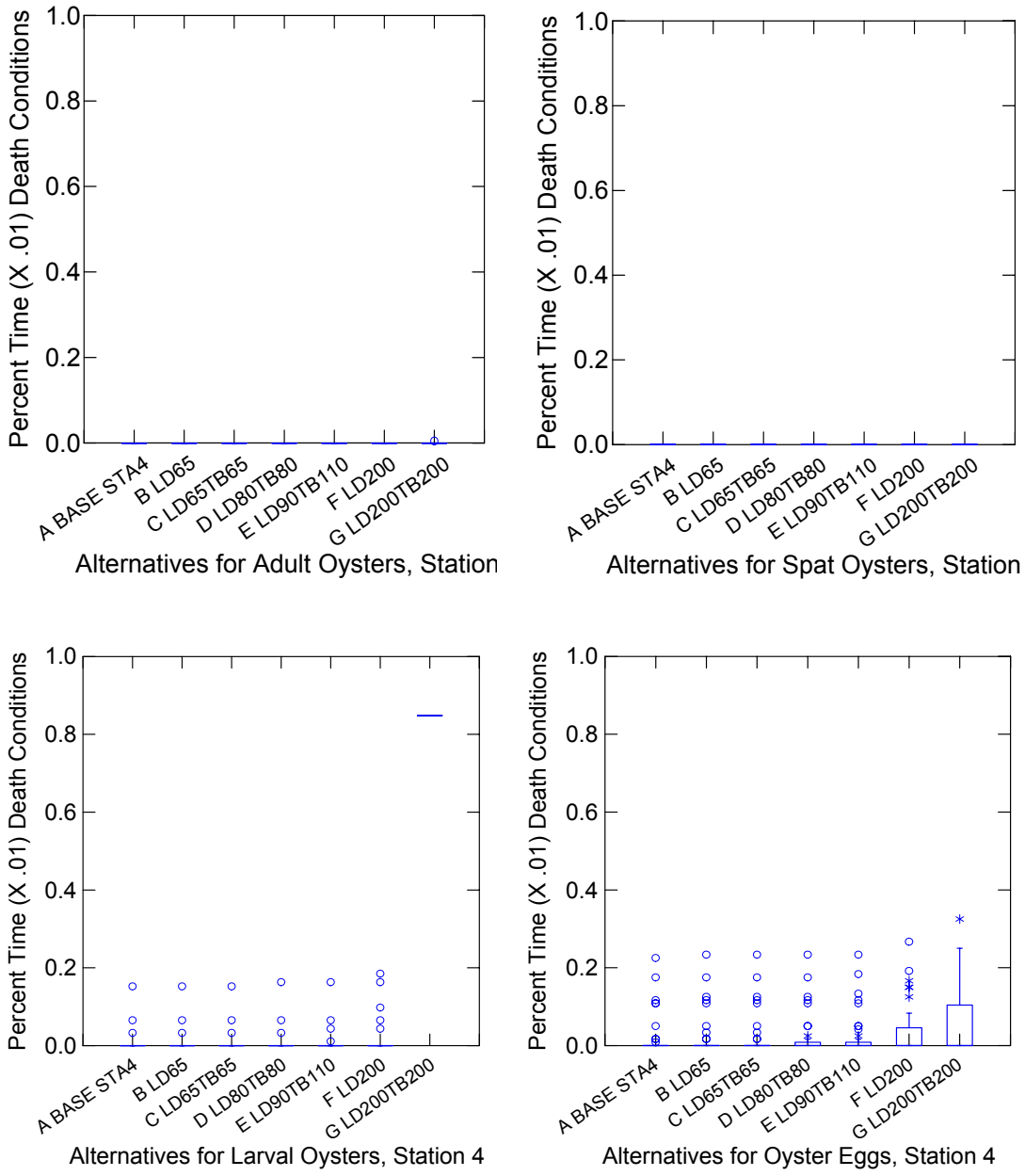

Figure 7-40. Box and Whisker Distribution Plots of the Predicted Percent of Time Death Conditions Existed for Adults, Spat, Larvae, and Eggs in the BASE Case and Six Alternative Base Inflow Scenarios at Station 4.

The overall results of both the visual and BWP analyses of the four oyster growth stages in terms of "Death" and "Harm" stress categories are summarized in **Table 7-15.** The "Harm" category in the table is "bolded" to highlight the critical flow or scenarios. The critical flow (total flows from Lainhart Dam and other tributaries) is 90 cfs for the Boy Scout station, 130 cfs for Station 6, 160 cfs for Station 5, and 230 cfs for Station 4.

Table 7-15. Maximum Flow Scenario (bolded) at Each Station and Oyster Life Stage to Avoid Significant Stress and Harm to Oyster Resources.

Station (River Mile)	Adult Death	Spat Death	Larvae Death	Egg Death	Recommended Scenario (Maximum Flow)
BS (RM 5.92)	LD65LD65	LD65LD65	LD60TB40	LD60TB40	LD60TB40 (~100 cfs)
Station 6 (RM 5.45)	LD90TB110	LD80TB80	LD65TB65	LD80TB80	LD65TB65 (~130 cfs)
Station 5 (RM 4.93)	LD90TB110	LD90TB110	LD90TB110	LD90TB110	LD90TB110 (~200 cfs)
Station 4 (RM 4.25)	LD200TB200	LD200TB200	LD200	LD200	LD200 (~230 cfs)
	Adult Stress/Harm	**Spat Harm**	**Larvae Harm**	**Egg Harm**	
BS (RM 5.92)	**LD60TB40**	**LD60TB40**	**LD65**	**LD60TB40**	**LD65 (~90CFS)**
Station 6 (RM 5.45)	**LD65TB65**	**LD65TB65**	**LD65TB65**	**LD65TB65**	**LD65TB65 (~130CFS)**
Station 5 (RM 4.93)	**LD80TB80**	**LD80TB80**	**LD80TB80**	**LD80TB80**	**LD80TB80 (~160CFS)**
Station 4 (RM 4.25)	**LD200**	**LD200**	**LD200**	**LD200**	**LD200 (~230 cfs)**

EVALUATION OF POLYHALINE ZONE: SEAGRASSES

Evaluation Methods

The purpose of this section is to describe methods used to evaluate whether increases in upstream inflows could impact downstream seagrass resources. This evaluation is based on the results of salinity model runs and the seagrass salinity performance measures presented in **Chapter 4**. This evaluation focuses only on potential impacts on seagrasses from changes in salinity. However, other factors (particularly water quality parameters which impact light availability) are clearly important in understanding potential impacts to seagrasses. As restoration efforts move from the planning stage to more specific design phases it may be necessary to develop more comprehensive methods for evaluating potential impacts to seagrasses.

The first step in this preliminary evaluation of potential impacts to seagrasses was to identify areas of the estuary where seagrasses occur and should be protected. Based on the data presented in **Chapter 4**, seagrass beds extend upstream to approximately RM 3.4. Accordingly, the "seagrass protection zone" for this plan includes all areas of the estuary downstream of approximately RM 3.4. The next step in the evaluation was to identify modeled salinity sites that would represent the range of salinity within the "seagrass protection zone." Five modeled salinity sites were identified: 1) Coast Guard Station (RM 0.70); 2) North Bay (RM 1.48); 3) Sand Bar (RM 1.74); 4) Pennock Point (RM 2.44); and 5) Site O2 (RM 3.26, nearest station to RM 3.4).

At each of the five sites, results of six model runs (BASE, LD65, LD65TB65, LD90TB110, LD200, and LD200TB200) were compared by determining the total number of days within the 39-year modeling period (January 1, 1965 – December 30, 2003) that fell within each of the seagrass performance measure "stress" categories presented in **Table 4-5**, **Chapter 4**. Model runs that simulated the "base" conditions indicated no impacts to seagrass resources beyond those experienced under existing salinity conditions. Model runs that had more days that fell within the "potential stress" and "stress" categories than existing conditions were considered less desirable than existing conditions and potentially detrimental to the seagrass resources.

To determine appropriate performance measures to use for each site, the seagrass species map (**Figure 4-10, Chapter 4**) was used to identify one key seagrass species for each modeled salinity site. Since turtle grass (*Thallasia testudinum*) is found upstream to the North Bay site, salinity performance measures for this species were used for the Coast Guard and North Bay sites. The upstream limit of manatee grass (*Syringodium filiforme*) is currently the Sand Bar location, so manatee grass salinity performance measures were used for this site. For the remaining two locations, shoal grass (*Halodule wrightii*), the dominant species at these sites, was used as the key species. Because Johnson's seagrass (*Halophila johnsonii*), a threatened species, was found at all five locations during the summer of 2004, a second evaluation of the data was conducted using the salinity performance measures for Johnson's seagrass at all five locations.

Another analysis was conducted using the performance measures presented in **Table 4-6**. These performance measures were based on literature salinity tolerance values that included duration of a salinity threshold associated with a severe stress event (such as blade mortality). The data were evaluated for each site and each model run to determine how many "stress" events occurred over the 39-year period of record. If a stress event occurred then it was assumed that the seagrass did not recover until the next growing season (March of the following year). Model runs with more stress events than existing conditions were considered less desirable than existing conditions and potentially detrimental to the seagrass resources. The same key species used for the above evaluations were used for this evaluation. The "stress" performance measures for Johnson's seagrass were also evaluated at all five sites.

These frequency evaluations were also conducted on data sets for a recent wet year (1995) and a recent dry year (2000). This evaluation was geared to understand the shorter term impacts associated with wet or dry conditions. The same key species used for the 39-year evaluation were also used for this analysis. As for the 39-year evaluation, the performance measures for Johnson's seagrass were also evaluated at all five sites.

The results of these evaluations were compared to identify which model runs produced salinity conditions similar to existing conditions and which runs resulted in more seagrass "potential stress" and "stress" than existing conditions.

Results and Discussion

Long-Term (39-Year) Data Evaluation:

Predicted salinities for six model runs, for a 39-year period, were compared to the salinity tolerances of key seagrass species (**Table 4-5**) at five locations along a salinity gradient in the Loxahatchee Estuary. The results are summarized in **Figure 7-41**. At the three downstream locations (Coast Guard, North Bay, and Sand Bar), model results were similar per site; conditions were optimal for the key seagrass species all or most of the time for all model runs. When conditions were not optimal, these less desirable conditions were experienced similarly across model runs.

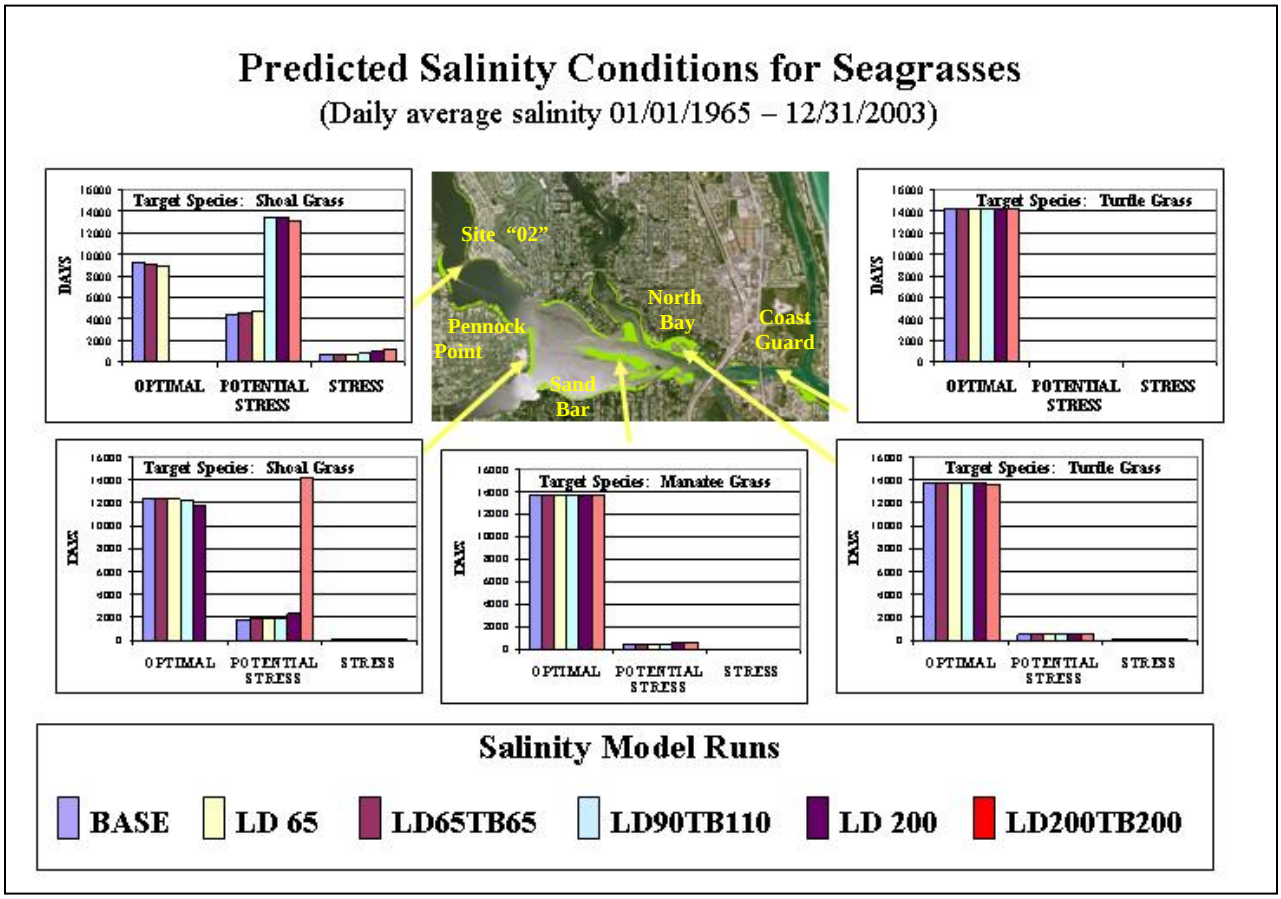

Figure 7-41. Predicted Salinity Conditions for Key Seagrasses at Five Locations Within the Polyhaline Ecozone.

At the Pennock Point location, results of the highest discharge model run (LD200TB200) differed from all other model runs. There were no "optimal" days for shoal grass and the number of "potential stress" days was substantially higher than for all other model runs. At the most upstream seagrass location (Site O2), results of the three highest discharge model runs (LD90TB110, LD200, and LD200TB200) had considerably more "potential stress" days for shoal grass than all other model results. Additionally, no "optimal" days occurred for these three model runs. Model runs LD65 and LD65TB65 were similar to base conditions at all five locations.

Since Johnson's seagrass was found throughout the estuary in 2004, the same evaluation was done for this threatened species at all five locations. Results (**Figure 7-42**) were similar to those observed in **Figure 7-41**. The base, LD65, and LD65TB65 model results were similar at all five locations. The highest discharge model run (LD200TB200) was different from all other model runs at the Pennock Point location; with no "optimal days" for Johnson's seagrass and substantially more "potential stress" days than all other model runs. Additionally, the LD90TB110, LD200, and LD200TB200 had considerably more "potential stress" days at Site O2 than all other model runs.

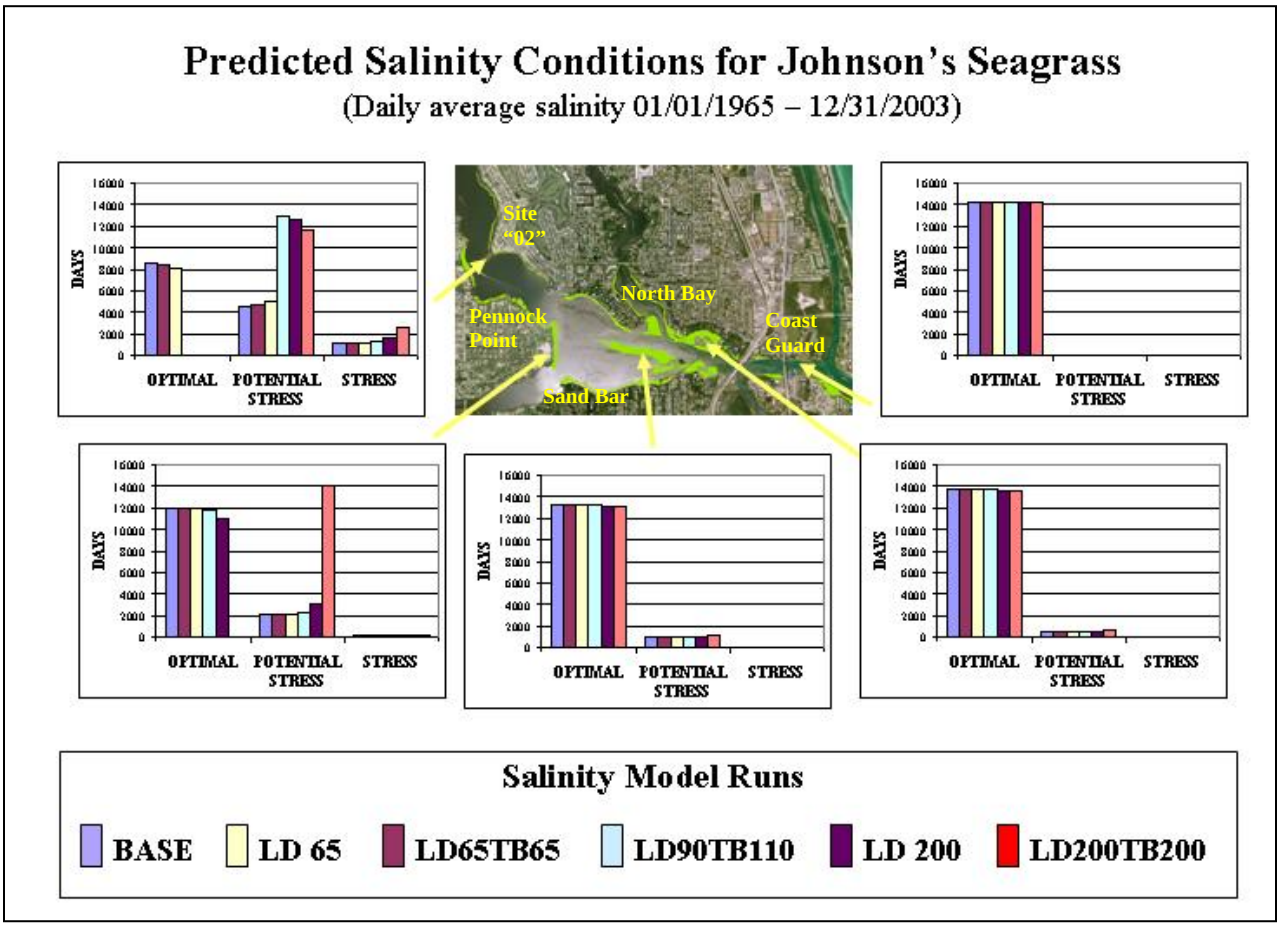

Figure 7-42. Predicted Salinity Conditions for Johnson's Seagrass at Five Locations Within the Polyhaline Ecozone.

Despite clear differences in model runs at the upstream locations, the number of "stress" days for all model runs at all sites were similar, with a small increase above the base run for model runs LD200 and LD200TB200 at Site O2. These differences were more pronounced for Johnson's seagrass than for shoal grass, but were still relatively small.

The 39-year data set was further evaluated for each location and each model run using the performance measures presented in **Table 4-6** for the "Stress" category. These performance measures were based on limited literature salinity tolerance values that included duration of a salinity threshold associated with a stress event (such as blade mortality). The total number of stress events per model run per location are summarized in **Table 7-16**. There were no differences between the number of "stress events" for any of the model runs at any of the sites. Only one stress event was noted and it occurred at Site O2 for Johnson's seagrass for all model runs in October 1995. This result is consistent with **Figures 7-41** and **7-42** which indicate that significant stress is unlikely for that model runs.

Table 7-16. Number of Stress Events per Model Run Based on Daily Average Salinity from 1/1/1965 – 12/30/2003.

Location	Target Seagrass Species	Stress Event (Salinity/Duration[a] Threshold)*	Number of Stress Events Per Model Run					
			BASE	LD 65	LD65TB65	LD90TB110	LD 200	LD200TB200
Coast Guard	Turtle grass	≤ 4 ppt for 7 days	0	0	0	0	0	0
	Johnson's seagrass	≤ 5 ppt for 3 days	0	0	0	0	0	0
North Bay	Turtle grass	≤ 3.5 ppt for 21 days	0	0	0	0	0	0
	Johnson's seagrass	≤ 5 ppt for 3 days	0	0	0	0	0	0
Sand Bar	Manatee grass	≤ 15 ppt for 26 days	0	0	0	0	0	0
	Johnson's seagrass	≤ 5 ppt for 3 days	0	0	0	0	0	0
Pennock Point	Shoal grass	≤ 5 ppt for 30 days	0	0	0	0	0	0
	Shoal grass	≤ 3.5 ppt for 21 days	0	0	0	0	0	0
Site O2	Shoal grass	≤ 5 ppt for 30 days	0	0	0	0	0	0
	Shoal grass	≤ 3.5 ppt for 21 days	0	0	0	0	0	0
	Johnson's seagrass	≤ 5 ppt for 3 days	1	1	1	1	1	1

[a] The duration in this evaluation is in consecutive days.

Short-Term (Wet vs. Dry Year) Data Evaluation:

Shorter term data sets were also evaluated. One recent wet year and one recent dry year were selected for this evaluation. The wet year selected was 1995 (the year when all model results showed a "stress event" at Site O2) and the recent dry year selected was 2000 (**Figure 7-43**).

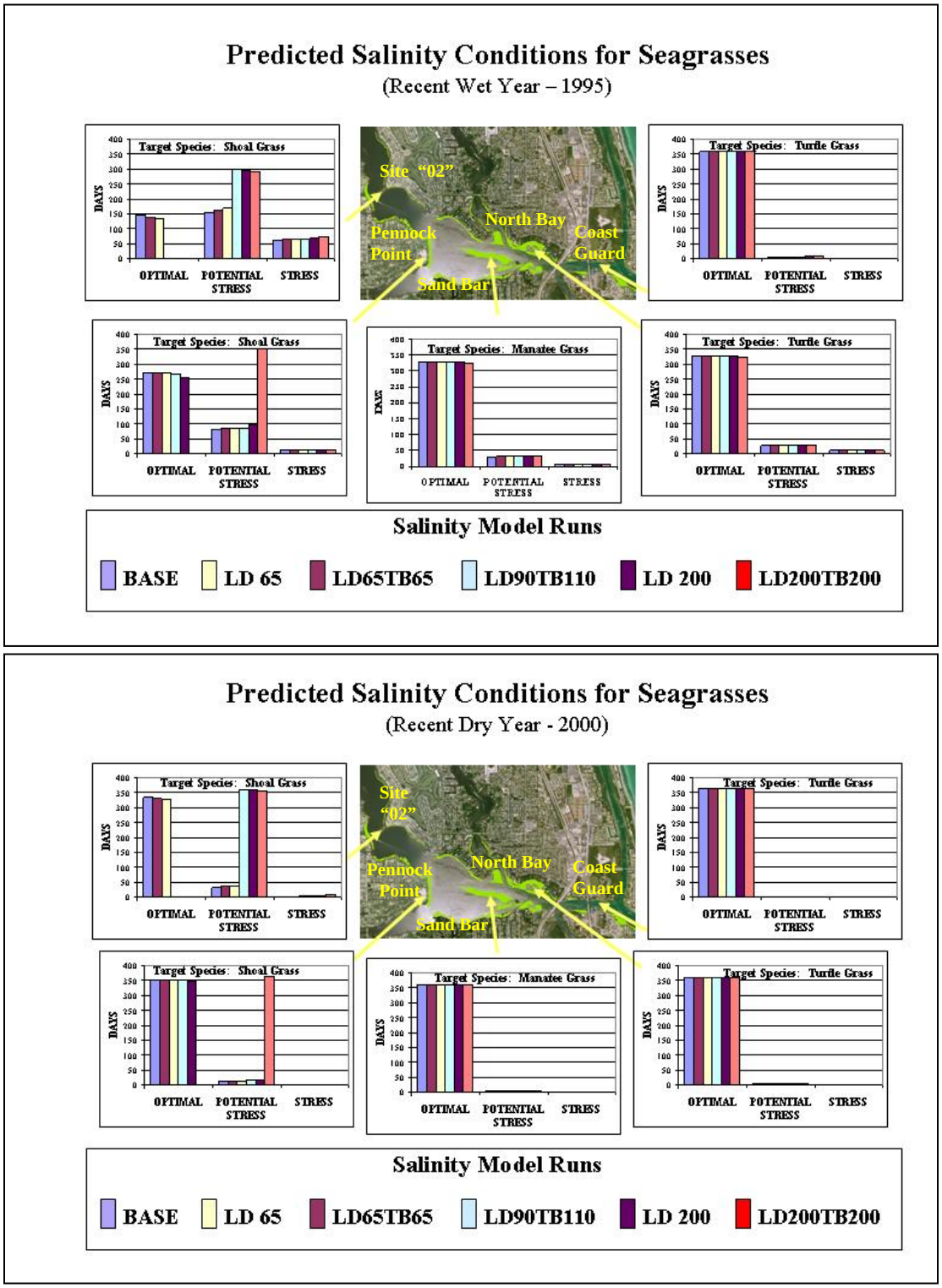

Figure 7-43. Predicted Salinity Conditions for Key Seagrasses at Five Locations Within the Polyhaline Ecozone During a Recent Wet (1995) and Dry Year (2000).

More "potential stress" and "stress" days were noted in the wet year than in the dry year (**Figure 7-43**). However, as observed for the 39-year data set, the number of "stress" days was similar across model runs at all sites for both wet and dry years. The general trends discussed above, were also observed in both wet and dry years. Model runs at the three downstream stations were similar per site in both the wet and dry year. At Pennock Point the highest discharge model run became distinctly different from all other model runs in both the wet and dry years. No "optimal" days occurred and the number of "potential stress" days was greater than for all other model runs. At Site O2, the three highest discharge model results were distinctly different from the base, LD 65, and LD65TB65 model results for both the wet and dry year (just as observed for the 39-year data set). Similar results were observed when the wet/dry year evaluation was conducted for Johnson's seagrass (**Figure 7-44**).

To further evaluate the wet/dry year data, daily average salinities were plotted for three of the seagrass stations (Coast Guard, Sand Bar, and Site O2; **Figure 7-45**). In general, greater differences between model run results at a given location occurred during the dry year than during the wet year. As expected, there were more days of salinities below "optimal" conditions for seagrasses in the wet year than during the dry year. Additionally, periods of lowest salinities were similar for all model runs in both the wet and dry years.

At the Coast Guard Station, salinities were optimal for seagrasses the entire dry year and much of the wet year (salinities never fell below 20 ppt in the wet year for any model run). This supports above results that indicate salinity conditions are good for seagrasses under all model scenarios at the Coast Guard Station. This area includes the "critical habitat" for Johnson's seagrass.

At the Sand Bar location, all model runs were similar during the wet year. During the dry year, LD200TB200 results were different (lower salinities) than all other model runs, but the results remained within optimal conditions for approximately the same number of days as all other runs. These results indicate that existing seagrass resources at the Sand Bar location would not be adversely impacted by any of the proposed discharges.

At Site O2, model run LD200TB200 results were distinctly different from all other model runs. In both the wet and dry years salinities produced by this model run were near or within stressful salinity ranges for seagrass most of the time. This supports previous results that this discharge level would be unlikely to support healthy seagrass beds at Site O2. Results of model runs LD90TB110 and LD200 were more similar to the base run in the wet year than in the dry year. Although these two runs produce "potential stress" day counts similar to LD200TB200 (**Figures 7-43** and **7-44**), salinities were often 8 ppt or higher than LD200TB200 results. Due to the higher salinities associated with model runs LD90TB110 and LD200, seagrass impacts should not be as great under these scenarios as they would be for the LD200TB200 discharges.

In summary, inflows associated with LD200TB200 are substantially different from the base case conditions at Pennock Point. This difference is even greater at Site O2. Model runs LD65 and LD65TB65 produce results similar to base conditions at all seagrass locations and are not expected to impact seagrasses beyond impacts currently experienced. Model runs LD90TB110 and LD200 are similar to base conditions at the four downstream locations, but begin to diverge from base conditions at Site O2. These differences could potentially impact seagrass resources.

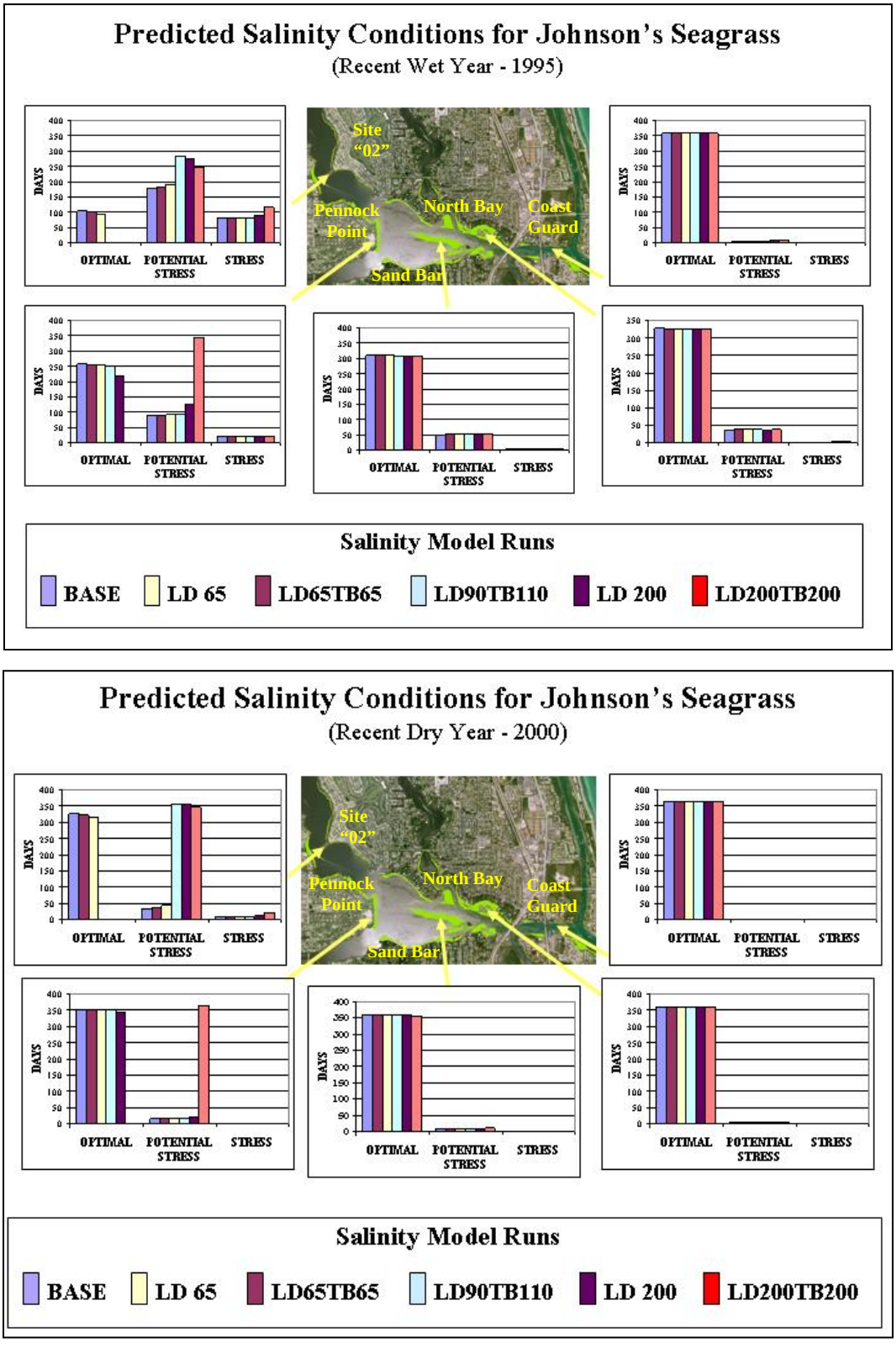

Figure 7-44. Predicted Salinity Conditions for Johnson's seagrass at Five Locations Within the Polyhaline Ecozone During a Recent Wet (1995) and Dry Year (2000).

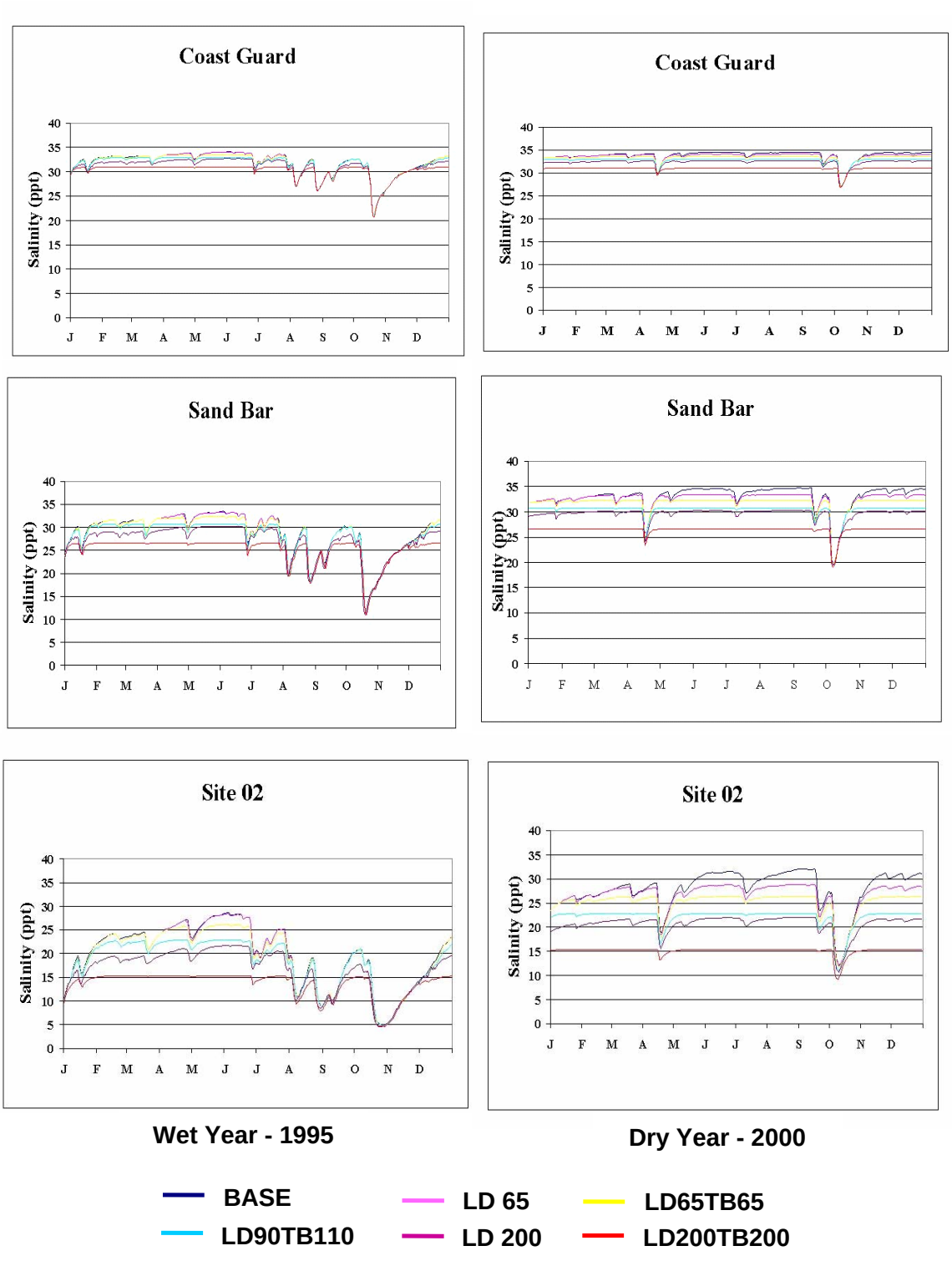

Figure 7-45. Comparison of Daily Average Salinity Conditions at Three Seagrass Locations for a Recent Wet Year (1995) and a Recent Dry Year (2000).

SUMMARY AND CONCLUSIONS

The Loxahatchee Watershed Model (WaSh) and the Loxahatchee Long-Term Salinity Management Model (LSMM) were used to simulate a 39-year (from 1965 through 2003) flow and salinity for the base condition and five flow scenarios, representing different flow augmentations for restoration. For each segment of the ecosystem including riverine floodplain, tidal floodplain, low salinity zone, mesohaline zone, and polyhaline zone, the ecological benefit or impact is evaluated according to the VECs and PMs established in **Chapter 4**. An overall summary of the evaluation is presented in **Table 7-17** which considers all the VEC components in the Northwest Fork and the Loxahatchee Estuary. A semi-quantitative score system consisting of "+, -, and 0" signs is assigned. A "+" sign represents a positive habitat benefit while the "-" sign indicates that the alternative will result in a negative impact for a particular VEC. The base case is represented with the "0" sign. The relative significance of an impact or benefit within an eco-zone is represented by the number of "- or +" signs. Note that such comparisons are valid only within a component of VECs, and one should not equate a benefit or impact of a VEC with that of another.

In the riverine floodplain, the relationship between flow from the Lainhart Dam and the stage in the river and floodplain were established through survey and field measurements. Transects 1 and 3 were selected for evaluation in this chapter. The elevation of swamp and hydric hammock in these transects were surveyed in the field, and their hydroperiod requirements were compared with each of the flow alternatives. The scenarios of LD65, LD65TB65, and LD90TB110 provide a flow significantly higher than for the base condition, particularly in the dry season. Improvement in the wet season inundation requirement of LD65 and LD65TB65 is not as significant as for LD90TB110. The hydroperiod of the hydric hammock areas is provided by severe storms with a flow from the Lainhart Dam ranging from about 190 cfs to over 300 cfs. Thus, none of the three scenarios influence the hydroperiod of the hydric hammock areas. However, the scenarios of LD200 and LD200TB200 would impose significant adverse impacts on the hydroperiod requirements for both the freshwater swamp and hydric hammock areas.

The characteristic salinity regime as defined by *Ds/Db* ratio using 1 ppt as the critical salinity standard is calculated using salinity data at four locations in the tidal floodplain of the Northwest Fork for all scenarios. Our evaluation shows that a restoration flow (Lainhart Dam plus other tributaries) in the range of 130 cfs (LD65TB65) to 200 cfs (LD90TB110) is required to provide sufficient freshwater to support freshwater floodplain vegetation down to the mouth of Kitching Creek. A combined base flow of greater than 400 cfs would be required to provide freshwater conditions to the edge of Jonathan Dickinson State Park. However, a flow at this high level may likely impose adverse impacts such as over-extended hydroperiod for the floodplain swamp and an erosion hazard in riverbed.

Evaluation of the LSZ employs a different methodology from the other VECs because we are using a mobile organism (zooplankton) as the indicator in contrast to all the other VECs that are sessile. A field study was conducted along with an examination of a family of salinity curves and the simulated salinity data at a fixed location close to the JDSP boundary to evaluate the scenarios. A salinity range from 2 to 8 ppt during the months between December and July when fish reproduction is active provides the highest density of fish larvae within the reach of the river upstream of the JDSP boundary (RM 6.0). An examination of the family of salinity curves and our long-term salinity data indicates that a base flow about 140 cfs (slightly higher than LD65TB65) provides a salinity of 2 ppt at RM 7.2 and 8 ppt at RM 6. Flows higher than 140 cfs may likely results in alteration of the conditions favorable to fish larvae in the Northwest Fork.

Table 7-17. Overall Summary of the Evaluation of Northwest Fork Ecosystem Restoration Scenarios.

Eco-Zone	VEC Component	Flow Restoration Scenario					
		BASE	LD 65	LD65TB65	LD90TB110	LD 200	LD200TB200
Riverine Floodplain	Swamp	0	+	+	++	- - -	- - -
	Hydric Hammock	0	0	0	0	- - -	- - -
Tidal Floodplain	Swamp upstream RM 9	0	++	++	++	-	- -
	Swamp upstream RM 8 (Kitching Creek Station)	0	0	++	++	++	- -
	Swamp upstream RM 6.14 (VT9 Station)	0	0	0	0	+	- -
	Swamp upstream RM 5.92 (Boy Scout Dock)	0	0	0	0	0	- -
Low Salinity Zone	Fish Larvae	0	0	0	-	-	- -
Mesohaline Zone	Oysters upstream RM 5.92 (Boy Scout Dock)	0	-	- -	- - -	- - -	- - -
	Oysters upstream RM 5.45 (Station 6)	0	0	-	- -	- - -	- - -
	Oysters upstream RM 4.93 (Station 5)	0	0	0	- -	- -	- - -
	Oysters upstream RM 4.13 (Station 4)	0	0	0	-	- -	- - -
Polyhaline Zone	Seagrasses upstream RM 3.26 (Site O2)	0	0	0	- -	- -	- - -
	Seagrasses upstream RM 2.44 (Pennock Point)	0	0	0	-	-	- -
	Seagrasses upstream RM 1.74 (Sand Bar)	0	0	0	0	0	0
	Seagrasses upstream RM 1.48 (North Bay)	0	0	0	0	0	0
	Seagrasses upstream RM 0.70 (Coast Guard)	0	0	0	0	0	0

0 = No change; +, ++ = Beneficial impact; -, - - , - - - = Negative impact.

An oyster stress model was used to evaluate how the restoration scenarios influence the existing oyster bed between RM 6.0 and RM 4.0. The analysis concluded that a critical flow exists for each of the four locations evaluated to protect the downstream oyster bed. The critical flow (total flows from Lainhart Dam and other tributaries) is 90 cfs (**LD65**) for the Boy Scout station, 130 cfs (**LD65TB65**) for Station 6, 160 cfs (**LD80TB80**) for Station 5, and 230 cfs (**LD200**) for Station 4. Since one of the governing principles for the Northwest Fork restoration is that restoring one component of the ecosystem should not damage or destroy any other component, it is necessary to consider "relocating" some of the existing oyster beds to a down stream location in selecting the final restoration scheme (refer to **Figure 4-6** for the acreage of oyster beds from RM 6.0 to RM 3.7).

Evaluation of seagrass involves five sites in the embayment area of Loxahatchee Estuary. None of the scenarios creates the impact of the "Stress" category for seagrasses at all the site. Scenarios **LD65** and **LD65TB65** produce results similar to the base condition at all seagrass locations and are not expected to impact seagrasses beyond what is currently experienced. Scenarios **LD90TB110** and **LD200** are similar to base conditions at the four downstream locations, but begin to diverge from the base conditions at the most upstream location, Site O2, along with an increase in the number of days with low salinity of "Potential Stress." These differences could potentially impact seagrass resources. The **LD200TB200** scenario is substantially different from the base case conditions at the Pennock Point site. This difference is even greater at Site O2.

In conclusion, our evaluation did not come up with one alternative that met all the requirements of the VECs in the ecosystem. Refinement of the flow scenarios will be conducted during the public review process. It needs to be noted that all of the scenarios tend to reduce the variability of flows, and this could favor certain species within the communities and reduce diversity of the ecosystem. A flow pattern capturing the natural dry and wet season variability needs to be considered to maximize the ecologic benefit. In addition, there are uncertainties involved with the evaluations. Our understanding of the ecosystem and the evaluation methods are not perfect. It is also unlikely that the future hydrological condition will follow exactly the same pattern, which is the case in model simulations. Both the watershed model and the salinity model involve uncertainties in predicting freshwater inflow and salinity. Therefore, it is likely that the day-to-day system operation decisions will be based on the actual salinity reading from the monitoring stations with the freshwater flow versus salinity relationship provided by the model as a guideline. It is also anticipated that the system operation and ecosystem response in the future will take an adaptive management approach based on consistent system monitoring. The ecosystem monitoring plan for Northwest Fork Ecosystem Restoration is described in **Chapter 9**. The salt water barrier as a restoration opportunity is analyzed in **Chapter 8**.

CHAPTER 8

TABLE OF CONTENTS

LIST OF FIGURES

LIST OF TABLES

Chapter 8:

The Saltwater Barrier as a Restoration Opportunity

INTRODUCTION

Managing freshwater inflow to the Loxahatchee River and Estuary is the most natural way to manage salinity levels within the Northwest Fork. However, too much freshwater during the dry season can reduce the establishment of riparian tree seedlings within the floodplain and reduce plant diversity. Using a saltwater barrier may provide a supplemental means to manage salinity when freshwater amounts are inadequate or are needed for best management practices for the health of the river.

This chapter summarizes two previous proposals to place saltwater barriers in the Northwest Fork of the Loxahatchee River. A preliminary modeling study was conducted to examine the effectiveness of using two types of saltwater barriers in different locations for salinity management in the Northwest Fork. Based on the modeling results and the evaluation of the potential ecological impacts of the barrier system on the floodplain forest and estuarine communities, evaluations are made based for the location and type of barrier. The model simulations described in this chapter were conducted under average dry season flow conditions.

SUMMARY OF PREVIOUS SALTWATER BARRIER PROPOSALS

THE 1975 PROPOSAL

In 1975, the Jupiter Inlet District and Florida Department of Natural Resources applied to the U.S. Army Corps of Engineers for a permit to construct a saltwater barrier weir in the Northwest Fork near River Mile 6.0. The project would have involved the construction of a weir at an elevation 4-feet below mean sea level within the south boundary of Jonathan Dickson State Park and near an existing power line crossing. The weir would prevent a wedge of saline water from extending up river during the dry season. This project was planned to occur in conjunction with another permit application for removal of oyster bars near and under the FEC railroad bridge and the A1A Bridge.

The U.S. Fish and Wildlife Service (FWS) expressed concern that there was no hydrologic study that could confirm the effectiveness of such a weir structure in preventing saltwater intrusion. They recommended that the permit be denied until a hydrological analysis was made by the U.S. Army Corps of Engineers to demonstrate the effectiveness of the proposed weir. The FWS also recommended the study include other salinity management alternatives such as increasing freshwater flows and adding an inflatable structure on top of the proposed weir.

The U.S. Environmental Protection Agency (EPA), Region IV, also objected to the proposal. The EPA was not convinced that the proposed structure would prevent saltwater from intruding upstream since the weir would be overtopped frequently by tidal action due to it's low height. They were also concerned that the structure would trap saltwater, allow organic material to be

deposited behind the weir, and degrade water quality due to reduced tidal flushing. The permit to construct the saltwater barrier was not granted pending further study.

THE 1986 FEASIBILITY STUDY

In 1986, the Jupiter Inlet District initiated a study on the feasibility of using a barrier to limit saltwater intrusion upstream. In anticipation of possible impact upstream of the Loxahatchee River associated with the proposed inlet dredging program. This study investigated the need for and feasibility of placing one or more submerged weir(s) to limit the salinity intrusion that might result from the proposed Jupiter Inlet dredging. The study included a literature search on various types of installations for salinity control and identified potential sites within the Loxahatchee River for barrier placement. The literature search found that "little published information exists on the use or performance of submerged weirs for salinity control." The feasibility report concluded that design of a submerged structure on the Loxahatchee River would require comprehensive study to verify its performance. Three sites were recommended as potential locations for the submerged weir salinity barrier: Island Way Bridges near River Mile 5.0; River Mile 5.5; and River Mile 6.0 (Cubit Engineering, 1986).

PRELIMINARY MODELING EVALUATION OF SALINITY MANAGEMENT WITH SALTWATER BARRIERS

DEVELOPMENT OF A 3-D MODEL FOR HYDRODYNAMIC AND SALINITY SIMULATIONS OF SALTWATER BARRIERS

Saltwater barriers include many types of structures designed to prevent saltwater intrusion ranging from tide gates that can block out tide entirely to more common weir-type barriers that can be submerged during high tide. The simulation of a saltwater barrier requires a hydrodynamic computer model with special capabilities. When the tide falls below the crest of a saltwater barrier, freshwater from upstream will pour down the barrier crest and form a water fall. Such a flow phenomenon is called "supercritical flow" in hydraulics. Most existing hydrodynamic models, such as the RMA (USACE, 1996), only simulate "subcritical flow" with a smooth water surface. To simulate supercritical flow over a saltwater barrier, a three-dimensional numerical model, CH3D, was modified to suit the task. The CH3D model is a non-orthogonal curvilinear grid hydrodynamic model that has been used in the Chesapeake Bay restoration study by U.S. Army Corps of Engineers and EPA. The boundary-fitted grid feature of CH3D is well suited for the Loxahatchee River where natural river channel patterns of bends and oxbows are preserved. The modified CH3D model covers the entire Loxahatchee River including the Southwest Fork, North Fork, and Northwest Fork. It also covers part of the Intracoastal Waterway north to St. Lucie Inlet and south to Lake Worth Inlet.

The modified CH3D model was verified using the most recent tide, flow, salinity and meteorological data collected by the South Florida Water Management District (SFWMD) and the U.S. Geological Survey (USGS). Then the model was used to study the relationship between freshwater inflow and tidally averaged salinity at selected sites as a double check on the relationships that were established by previous 2-D model simulations. The modified CH3D model was used to study the effectiveness of a proposed saltwater barrier to reduce the saltwater intrusion problem in the Loxahatchee River during the dry season. A number of design alternatives were modeled and results were evaluated to determine the effectiveness of each alternative.

Design of Salinity Barrier Alternatives

SALTWATER BARRIER TYPES

Two types of saltwater barriers were simulated. The Type 1 saltwater barrier has a single opening with barriers extending from each bank of the river. The opening was placed along the existing navigational channel. When the navigational channel is along the bank, only one barrier was needed. To model the Type 1 barrier, it has to be placed as one side of a grid cell that CH3D regards as an idealized thin barrier across which there is no flow.

The Type 2 saltwater barrier is inflatable and extends across the entire channel. Supercritical flow occurs over the Type 2 structure at low tide, the modified CH3D model is able to simulate this type of supercritical flow.

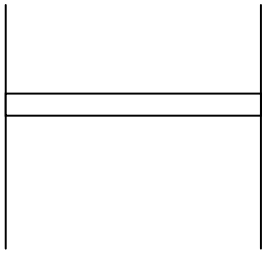

SALTWATER BARRIER LOCATIONS

Three barrier site locations were tested in the simulations (**Figure 8-1**). The first location (Location 1) is within the boundary of Jonathan Dickinson State Park at RM 6.0. and represents the downriver edge of the existing oligohaline or low salinity zone ecozone. The second site (Location 2) is at the Island Way bridges (RM 5.0) and is located in the midpoint of the mesohaline ecozone. The third location (Location 3) is near the sand bars at RM 4.0, and represents the upper edge of the polyhaline ecozone.

The locations of these simulation sites were chosen for modeling purpose only. The objective was to examine the difference of effectiveness of a barrier in each general area.

Figure 8-1. The Three Locations of the Saltwater Barriers Used for the Salinity Simulations Within the Northwest Fork of the Loxahatchee River.

SALINITY BARRIER ALTERNATIVES

A total of 14 salinity barrier alternatives were simulated as listed in **Table 8-1**. Alternative S0 represents the baseline condition with no salinity barrier. Alternatives S1 through S11 represent the use of one or more Type 1 barriers. For Type 1 barriers, the water depth at the opening was kept a minimum of 3.3 feet and the opening was kept at least 25 feet wide in order to meet the requirement for small craft navigation (State Organization for Boating Access, 1996). Alternatives S12.1, S12.2, and S12.3 represent the use of a Type 2 (inflatable) barrier at Location 1. The difference between these three alternatives is the crest elevation; for S12.1, S12.2 and S12.3 the crest elevations are –1.0, +0.1, and +1.0 feet NGVD29, respectively. For each of the 14 alternatives, the 2004 dry season was repeatedly simulated using the modified CH3D code developed by Coastal Tech. Each simulation run lasted 10 days.

Table 8-1. Description of the 14 Saltwater Barrier Alternatives Modeled in the CH3D Simulation for the Northwest Fork of the Loxahatchee River.

Alternative	Barrier Location	Barrier Type	Opening width (ft)	Depth at opening (ft, NGVD29)	Description
S0	--	--	--	--	No barrier
S1	1	1	100	Local depth	
S2	2	1	100	Local depth	
S3	3	1	100	Local depth	
S4	1	1	100	Local depth	Three barriers used (see **Figure 8-2**)
S5	1, 2 & 3	1	100	Local depths	Combination of S1, S2 & S3
S6	1	1	80	3.3	
S7	1	1	25	3.3	
S8	1	1	25	3.3	Three barriers used (Similar to S4, **Figure 8-2**)
S9	2	1	25	3.3	
S10	3	1	25	3.3	
S11	1, 2 & 3	1	25	3.3	Combination of S8, S9 & S10
S12.1	1	2	--	1.0	Crest elevation = –1.0 ft NGVD29
S12.2	1	2	--	0.1	Crest elevation = +0.1 ft NGVD29
S12.3	1	2	--	-1.0	Crest elevation = +1.0 ft NGVD29

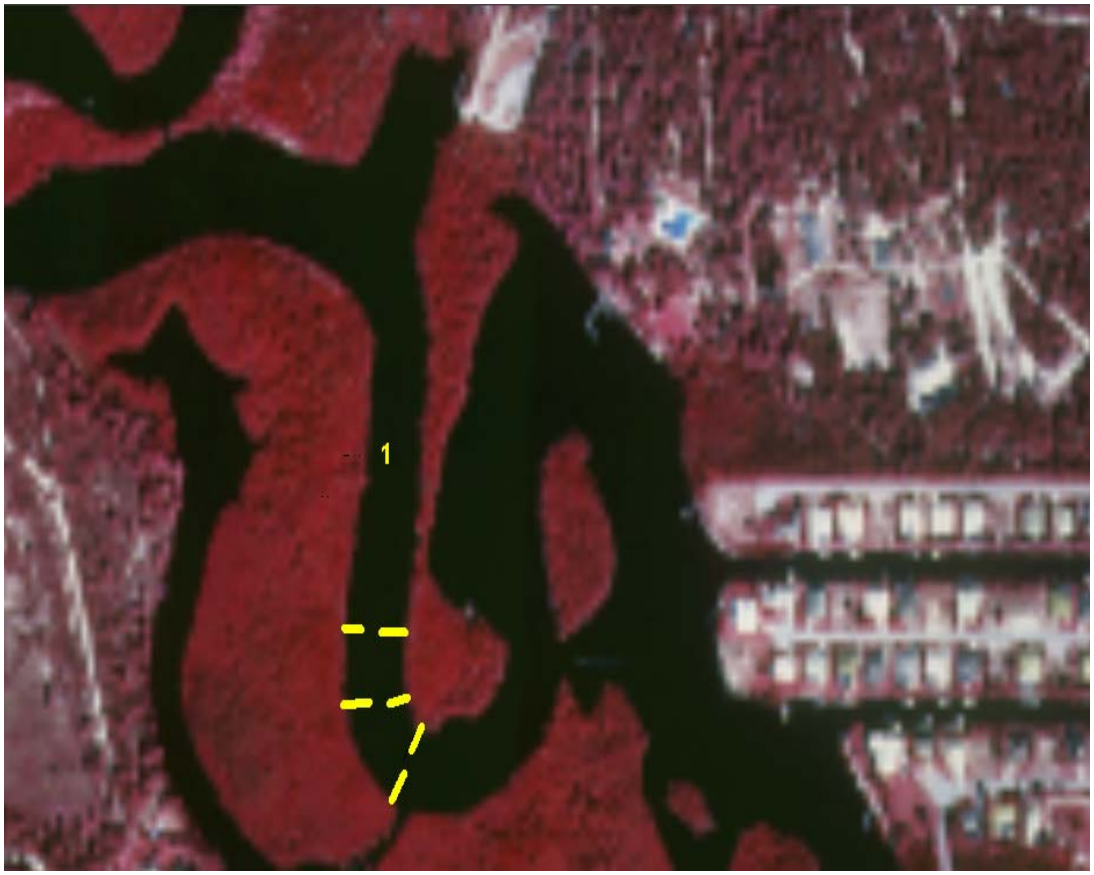

Figure 8-2. Placement of the Three Type 1 Saltwater Barriers at Location 1 for Alternatives S4 and S8. The Actual Placement Locations of the Three Barriers Were Selected for Modeling Purposes Only. The Objective Was to Examine the Effectiveness of a Series of Barriers vs. a Single Barrier. These Barriers May or May Not Be Allowed Within the Boundary of the Wild and Scenic River.

Salinity Model Applications

Figure 8-3 shows the freshwater inflows used as boundary conditions at S-46, Lainhart Dam, Cypress Creek, Hobe Grove Ditch and Kitching Creek for January 2004. To avoid tidal influences, the Kitching Creek USGS flow gauge was placed north of the mouth of Kitching Creek. Therefore it does not record all the runoff from the entire Kitching Creek watershed. **Figure 8-4** shows the tidal elevation used at the open ocean boundary. The ocean open boundary condition for salinity was kept 35.5 ppt as a constant when the flow is coming in (flood tide). During ebb tide, salinity at the open ocean boundary was computed by the model.

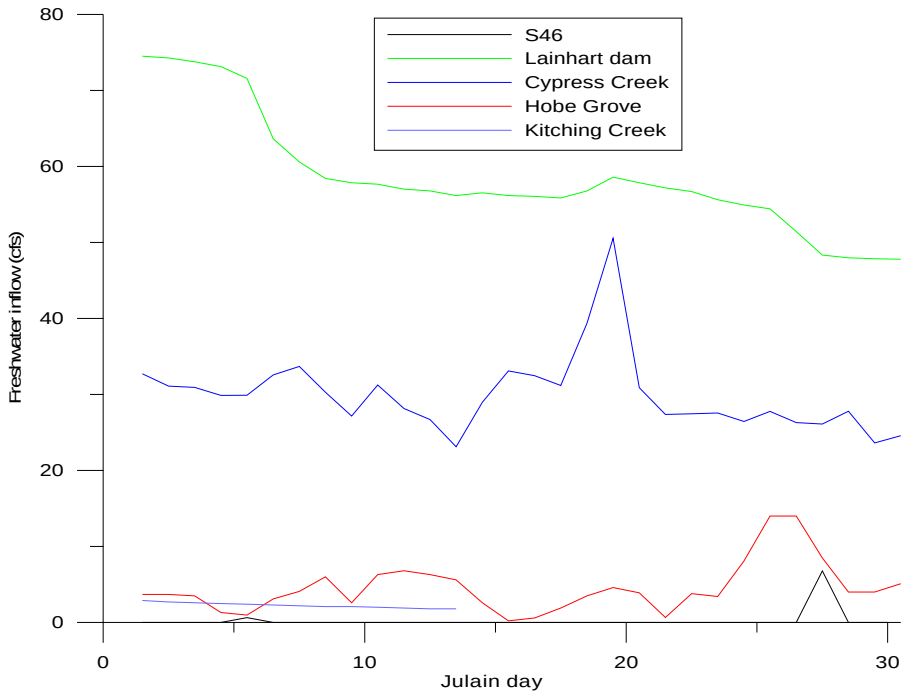

Figure 8-3. Freshwater Inflows at S-46, Lainhart Dam, Cypress Creek, Hobe Grove Ditch, and Kitching Creek for January 2004.

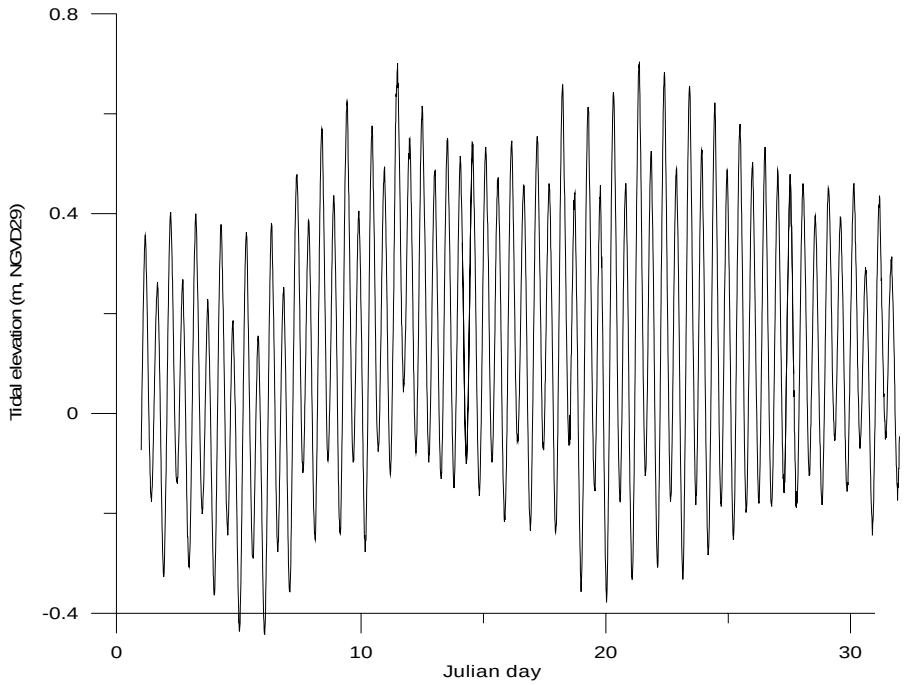

Figure 8-4. Tidal Elevation at the Coast Guard Station for January 2004.

The simulation of changes in salinity after introducing the 15 saltwater barriers alternatives was performed. The target range for the saltwater barrier performance simulation was to keep the salinity at River Mile 6.2 below 2 ppt.

TYPE 1 SALINITY BARRIER SIMULATIONS

Figure 8-5 shows the modeled salinity at RM 6.2 for Alternatives S0 through S5. For this group of alternatives, Type 1 barriers are used (except S0, which is the base condition for comparison). The central opening is 100 feet wide. In S1, S2 and S3, only one barrier is placed at each location. In S4, three Type 1 barriers are all placed at Location 1 (see **Figure 8-2**). And in S5, one Type 1 barrier is placed at each of the three locations. There is little reduction of salinity at River Mile 6.2 with any of these alternatives. Further upstream at Kitching Creek (RM 8.13; **Figure 8-6**), salinity reduction less than 1 ppt was seen for all the alternatives.

Figure 8-7 shows the modeled salinity at River Mile 6.2 for Alternatives S6, S7, and S8. For this group of alternatives, Type 1 barrier is used only at Location 1. For these three alternatives, the width of the central opening was decreased from 100 feet (as used in S1, S2, S3, S4, and S5) to 80 feet (S6) and 25 feet (S7 and S8). In S8, three barriers are placed at Location 1 (similar to S4, see **Figure 8-2**). Again, there is little reduction in salinity at River Mile 6.2. However, peak salinity at Kitching Creek (RM 8.13; **Figure 8-8**) is significantly reduced under Alternatives S7 and S8. This is because as the central opening at the barrier becomes increasingly smaller, the total salinity brought upstream by flood tide is significantly reduced leading to lower salinity at upstream locations after the initial 'jet' has dissipated.

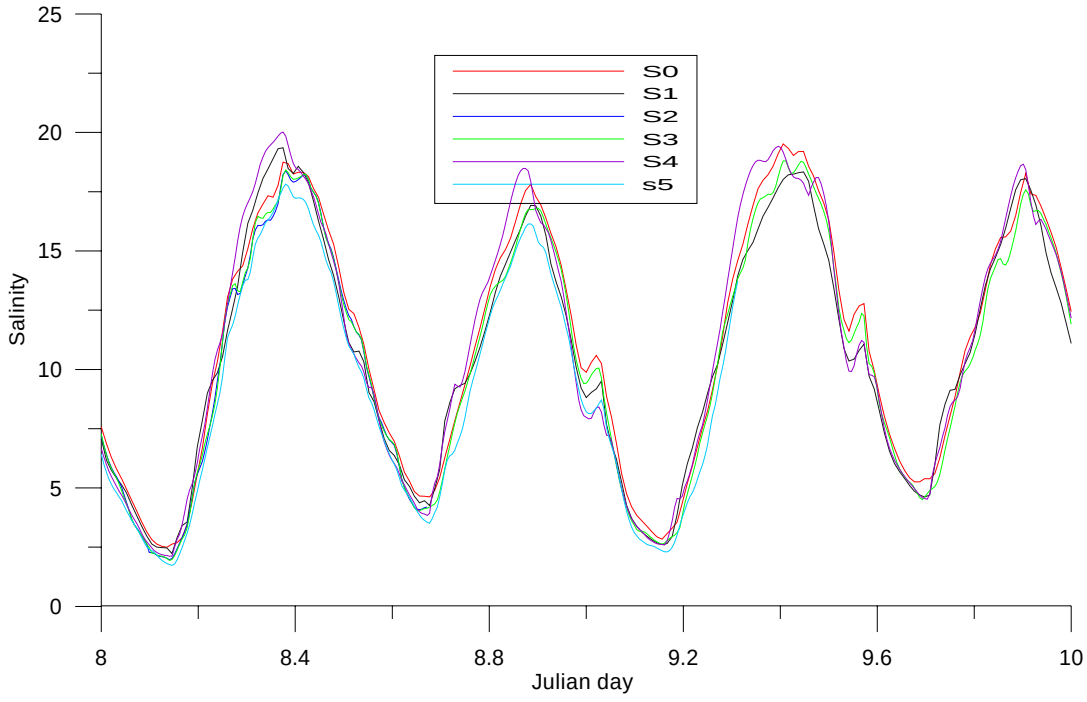

Figure 8-5. Simulated Upper Layer Salinity (in ppt) at River Mile 6.2 for Alternatives S0 to S5.

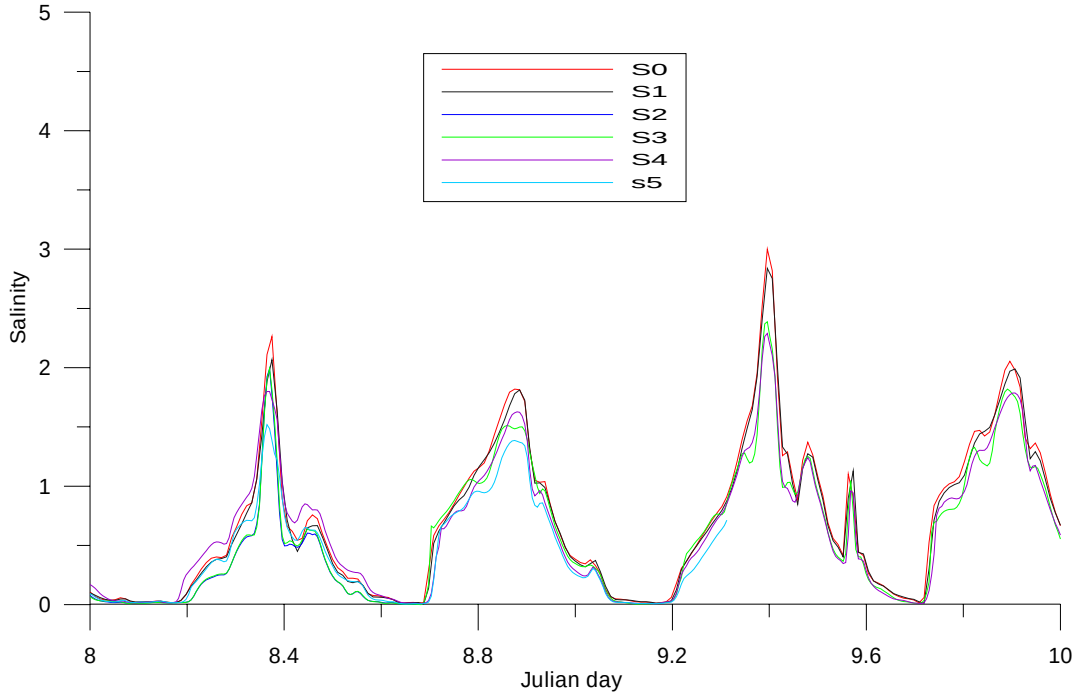

Figure 8-6. Simulated Upper Layer Salinity (in ppt) at Kitching Creek (RM 8.13) for Alternatives S0 to S5.

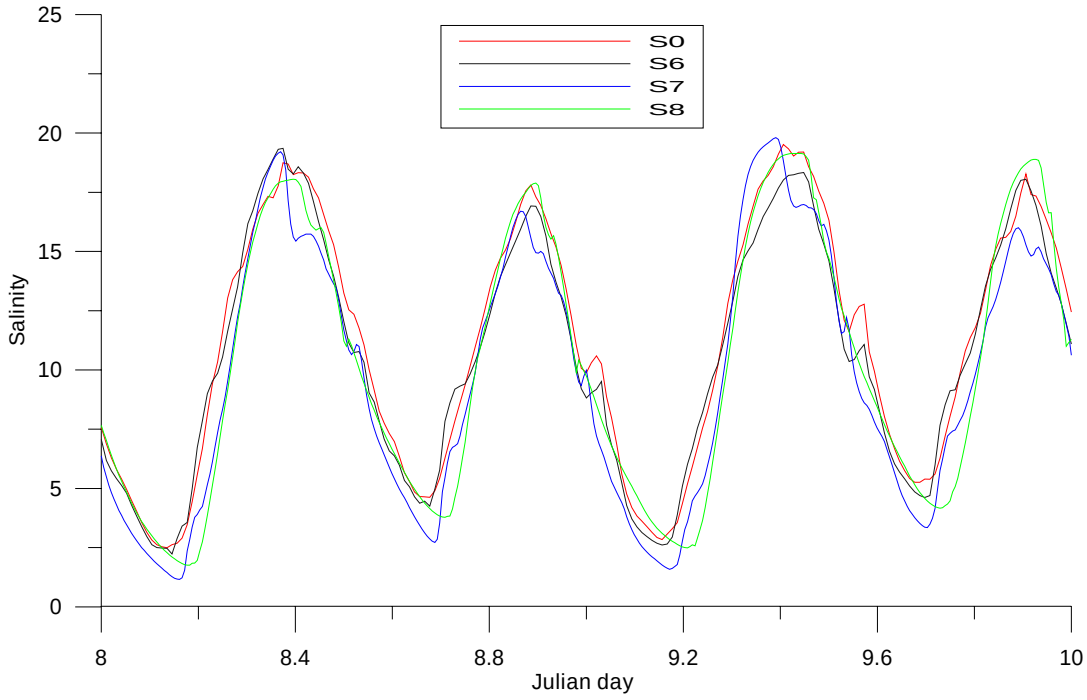

Figure 8-7. Simulated Upper Layer Salinity (in ppt) at River Mile 6.2 for Alternatives S6 to S8.

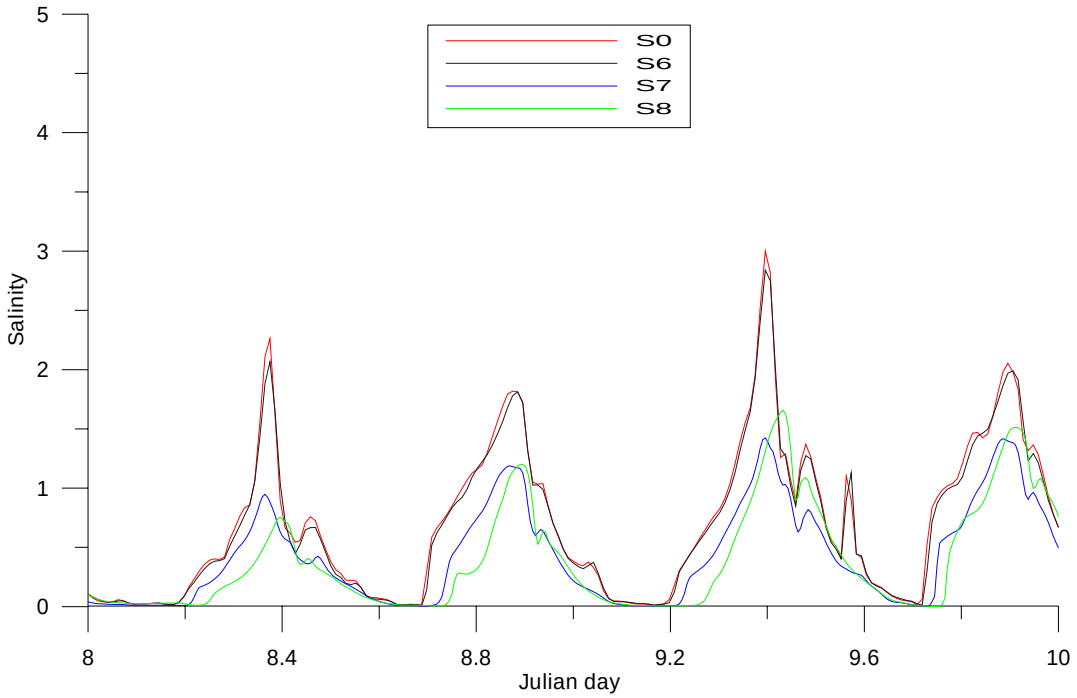

Figure 8-8. Simulated Upper Layer Salinity (in ppt) at Kitching Creek (RM 8.13) for Alternatives S6 to S8.

Figure 8-9 shows the modeled salinity at River Mile 6.2 for Alternatives S9 to S11. Alternatives S0 and S7 are also shown for comparison. For this group of alternatives, Type 1 barriers with 25-foot wide opening were used. In S7, S9 and S10, only one such barrier is used at each of the three selected sites. Alternative S11 is a combination of S7, S9, and S10 (i.e., three barriers are used, one at each site). Little or no salinity reduction at River Mile 6.2 is seen for Alternatives S7 and S10. However, significant salinity reduction is seen for Alternatives S9 and S11. Salinity reduction is more significant in terms of percentage at Kitching Creek (RM 8.13; **Figure 8-10**) for all the alternatives. For Alternative S11, the most effective alternative, peak salinity reduction is approximately 25% and 80% at River Mile 6.2 and Kitching Creek (RM 8.13), respectively. Alternative S9 seems to be the most effective alternative for a single barrier placed at a single site. For S9, peak salinity is reduced by approximately 20% at River Mile 6.2.

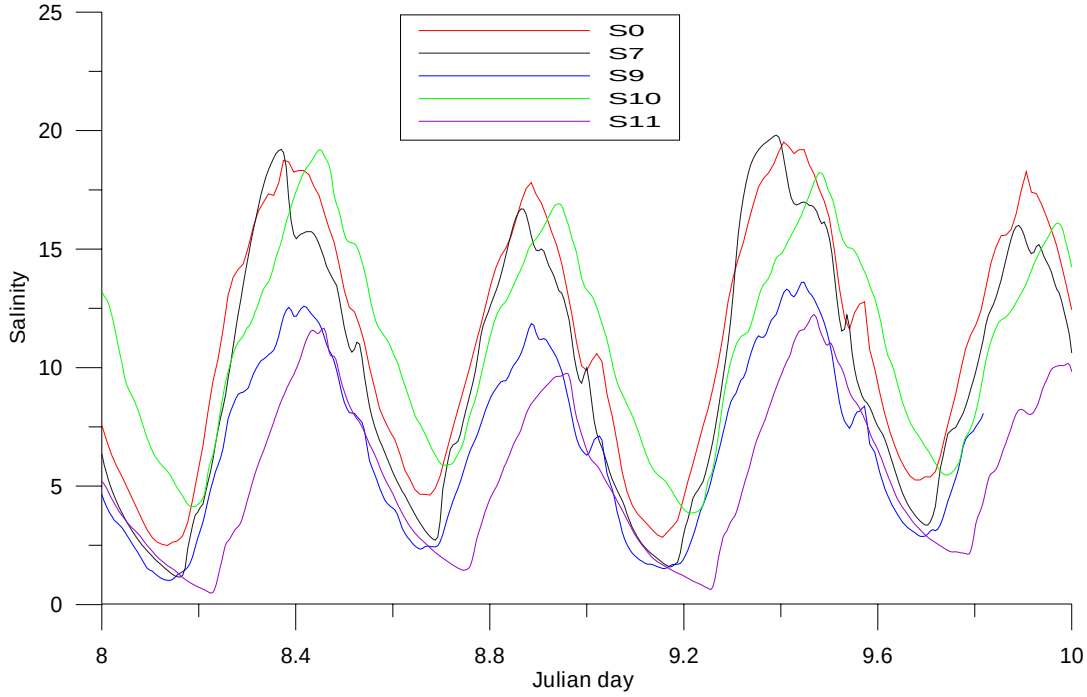

Figure 8-9. Simulated Upper Layer Salinity (in ppt) at River Mile 6.2 for Alternatives S7, S9, S10, and S11.

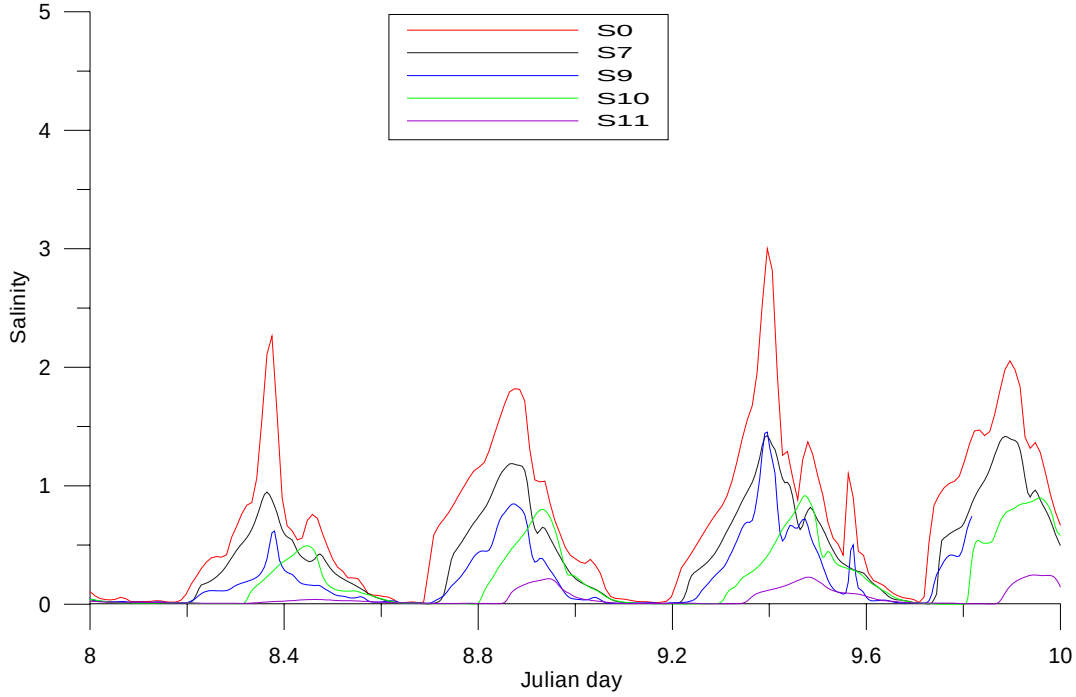

Figure 8-10. Simulated Upper Layer Salinity (in ppt) at Kitching Creek (RM 8.13) for Alternatives S7, S9, S10, and S11.

Summarizing the performance of Type 1 barriers, Alternatives S1 to S11, the simulation predicts significant salinity reduction when the width of the barrier opening was reduced to 25 feet. However, none of the simulations predict achieving the goal of keeping salinity at River Mile 6.2 lower than 2 ppt. By decreasing the width of the opening, the goal to achieve a salinity of less than 2 ppt at RM 6.2 should be possible, but there would be a likely negative impact to navigation for water craft. The minimum recommended navigable width requirement for small craft varies from state to state, but in most states, the minimum requirement is that the channel should be at least 20 feet wide and 3 feet deep at low tide. The simulation results suggests that using saltwater barriers in the Northwest Fork of the Loxahatchee River that meet this navigation requirement are not likely to achieve the specified goal for reducing salinity at River Mile 6.2 to less than 2 ppt.

TYPE 2 SALINITY BARRIER SIMULATIONS

Because Type 2 barriers extend across the width of the channel, navigation inevitably will be disrupted during the operation period. Using inflatable Type 2 barriers may alleviate some of the navigational disruption because they can be removed during the wet season when there is no need for saltwater barriers.

Figure 8-11 shows the modeled salinity at River Mile 6.2 for Alternatives S12.1, S12.2, and S12.3. As the crest elevation rises, the salinity at River Mile 6.2 decreases. Alternative S12.3 seems to nearly achieve the goal of salinity less than 2 ppt. At River Mile 6.2 it is less than 2 ppt throughout most of the tidal cycle except at high tide. Upstream at River Mile 7.0, the peak salinity is less than 2 ppt (**Figure 8-12**). Further upstream at Kitching Creek (RM 8.13), the water becomes almost fresh (**Figure 8-13**).

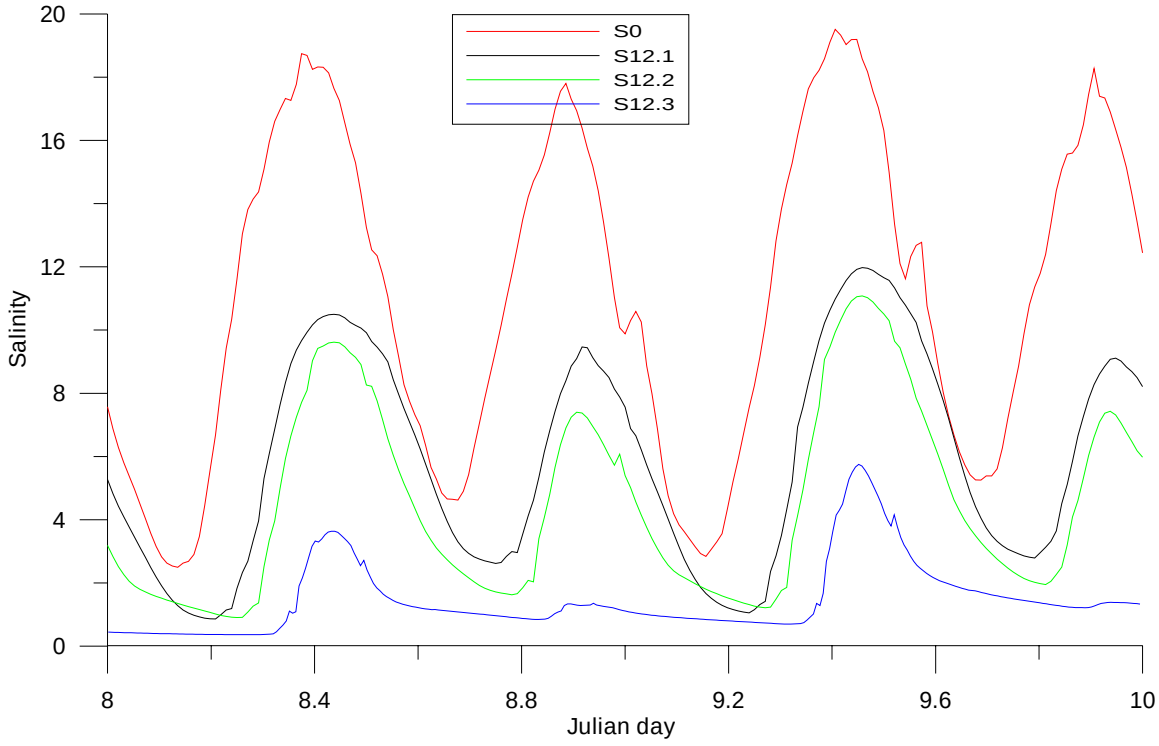

Figure 8-11. Simulated Upper Layer Salinity (in ppt) at River Mile 6.2 for Alternatives S12.1, S12.2, and S12.3.

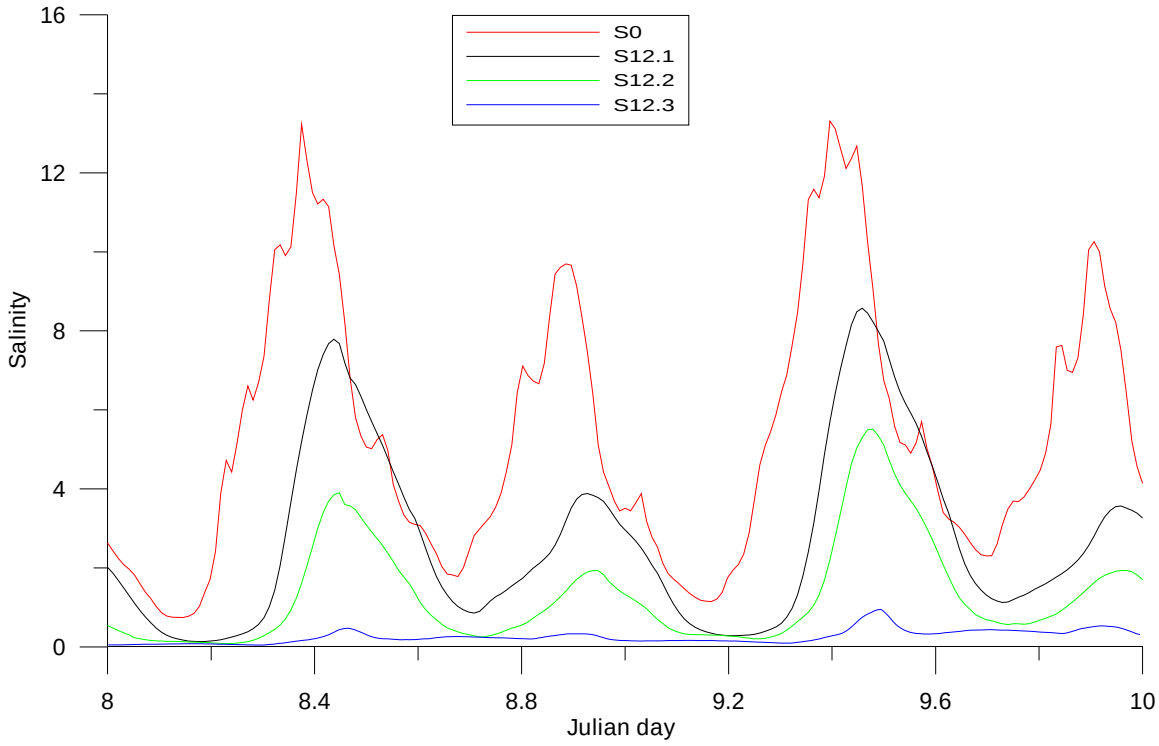

Figure 8-12. Simulated Upper Layer Salinity (in ppt) at River Mile 7.0 for Alternatives S12.1, S12.2, and S12.3.

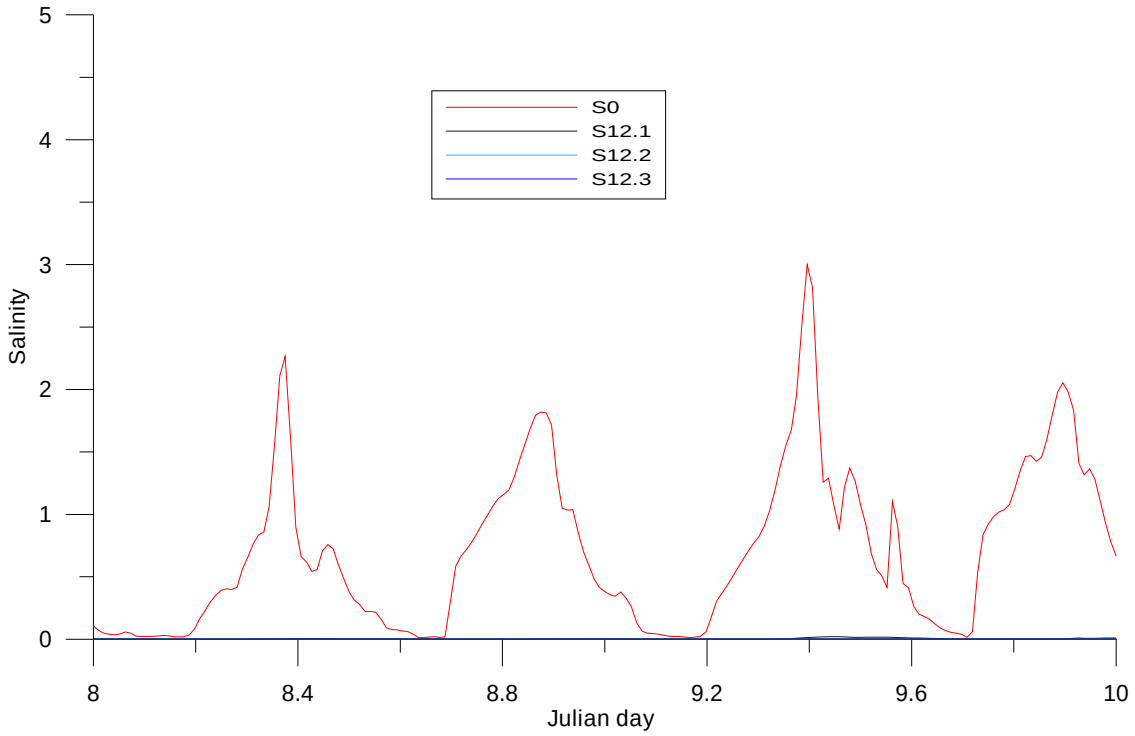

Figure 8-13. Simulated Upper Layer Salinity at Kitching Creek (RM 8.13) for Alternatives S12.1, S12.2, and S12.3.

Because of the relative effectiveness of the Type 2 barriers in reducing saltwater intrusion, their impact on water level (**Figure 8-14**) and flow rate (**Figure 8-15**) was compared with the base condition S0. Tidal range is greatly reduced with the presence of the saltwater barrier (**Figure 8-14**). Tidal range is less than 0.5 feet for Alternative S12.3 compared with tidal range of nearly 3 feet for the existing condition (S0). Flow rate is also greatly reduced as it is blocked by the barrier.

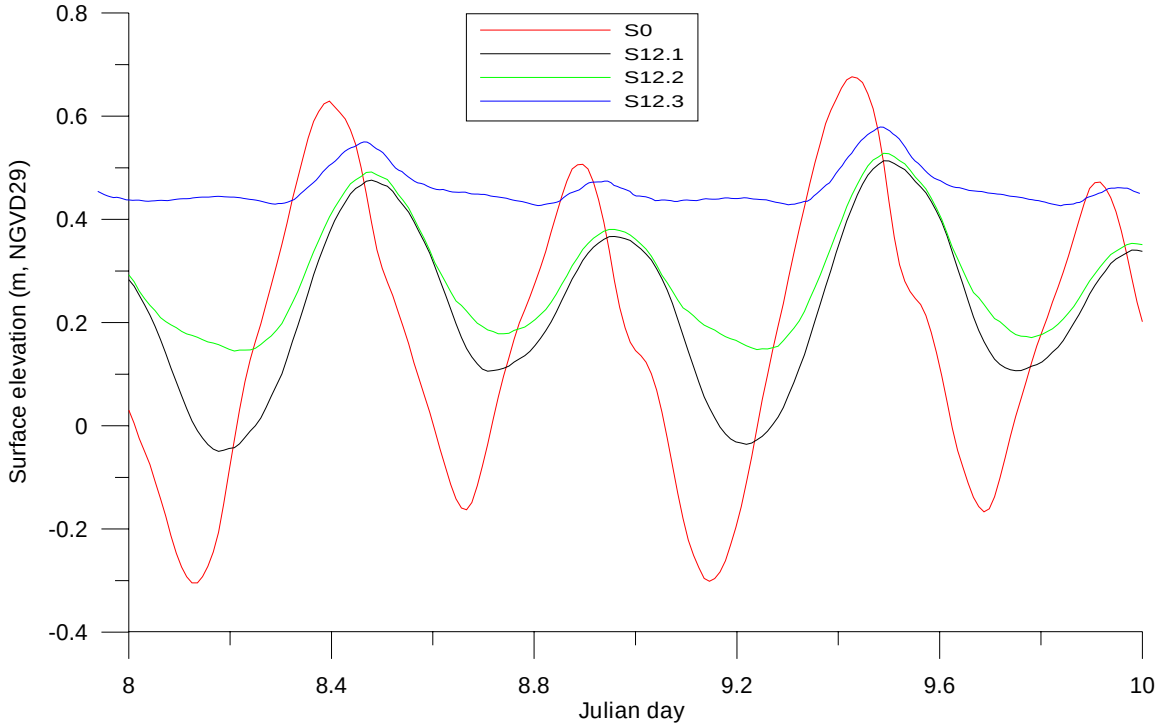

Figure 8-14. Simulated Water Surface Elevation at River Mile 6.2 for Alternatives S12.1, S12.2, and S12.3.

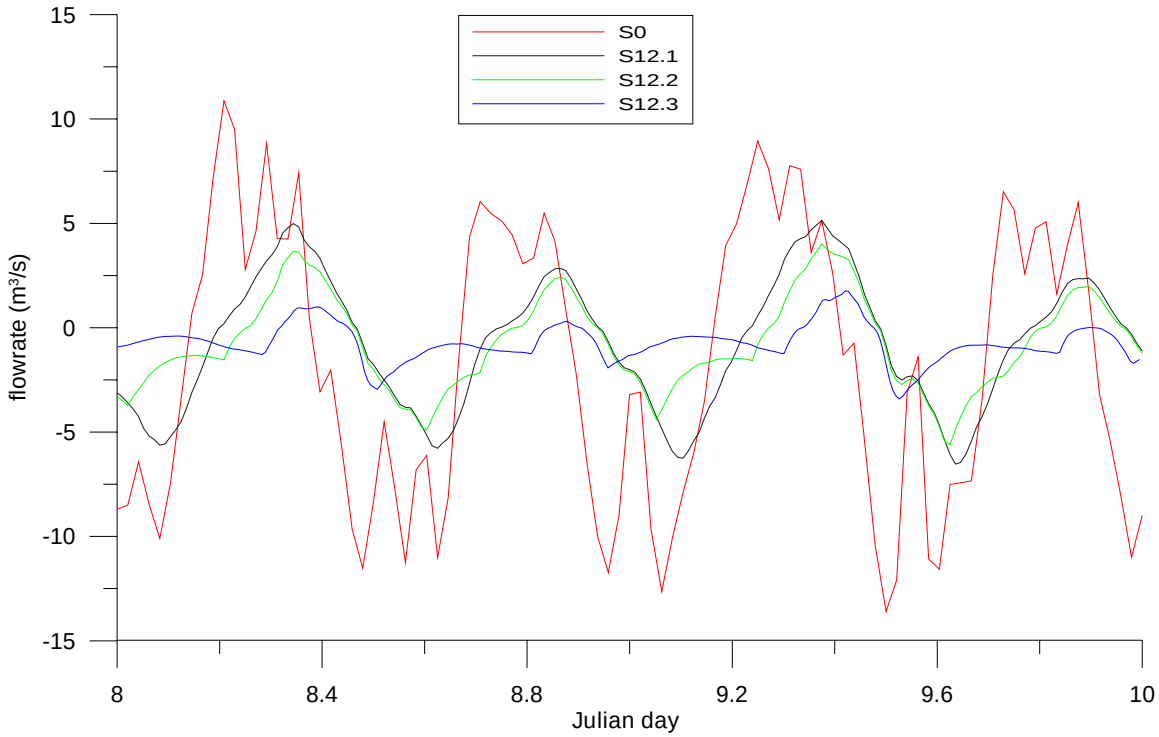

Figure 8-15. Simulated Flow Rate at River Mile 6.2 for Alternatives S12.1, S12.2, and S12.3. Flood tide +; Ebb tide -.

EVALUATION OF SALINITY BARRIER ALTERNATIVE MODELS

In summary of the performances of all the alternatives, **Table 8-2** lists the peak salinities at Boy Scout Dock (RM 5.92) and Kitching Creek (RM 8.13) during the period from Julian day 8 to 10 as predicted by the model. The lower the peak salinity, the more effective the alternative is. Another measure of the overall performance is the total salinity transported upstream of Boy Scout Dock. The better performing salinity reduction alternatives will transport less salinity upstream. The 6th column of **Table 8-2** shows the total salinity transported upstream at Boy Scout Dock during flood tide for the period from Julian day 8 to 10, 2004. All of the alternatives offer some degree of salinity reduction relative to the existing condition (S0). However, alternatives using the Type 2 barrier are significantly more effective in reducing salinity than are the alternatives using a Type 1 barrier.

Table 8-2. Comparison of the Performance of the Salinity Barrier Alternatives.

Alternative	Barrier		Peak Salinity (ppt)		Total salinity transport (kg)
	Location	Type	BSD	KC	
S0	--	--	19.51	3.00	2,100,836
S1	1	1	19.61	2.29	2,067,592
S2	2	1	15.55	0.92	1,541,236
S3	3	1	18.40	1.99	1,928,816
S4	1	1	20.01	2.26	1,997,935
S5	1, 2 & 3	1	14.88	1.57	1,557,198
S6	1	1	18.83	1.98	2,045,861
S7	1	1	19.81	1.42	1,786,714
S8	1	1	19.14	1.66	1,640,093
S9	2	1	13.60	1.45	1,295,635
S10	3	1	14.17	0.30	998,579
S11	1, 2 & 3	1	10.75	0.17	661,928
S12.1	1	2	11.97	0.03	630,869
S12.2	1	2	11.08	0.00	465,165
S12.3	1	2	5.80	0.00	102,148

Based on this modeling evaluation, we conclude that a weir raised to an elevation one foot above the mean tide is the most effective barrier type for salinity reduction in the Northwest Fork. This barrier can be effective at the immediate upstream if the crest elevation was higher than high tide.

For saltwater barriers with an opening to be effective, the width of the opening needs to be small. Barriers with 25-foot wide openings (the minimum allowable channel size for small watercraft) performed better than barriers with larger openings. Based on model simulations using barriers with an opening, salinity is not significantly reduced until approximately 1 mile upstream of the barrier.

ECOLOGICAL CONSIDERATIONS OF THE TYPE 2 SALINITY BARRIER

Using a salinity barrier that spans the full width of the Northwest Fork of the Loxahatchee River downstream from RM 6.0 offers significant salinity reduction. However, there are significant ecological concerns that also need to be addressed regarding the use of a saltwater barrier as a possible restoration alternative. Several questions have been raised though District staff's communications with the Park Service of FDEP (Roberts, 2004):

1. In the process of feasibility study, water quality needs to be considered, especially the location of the structure in relationship to stormwater run-off areas.
2. Should we be worried about nutrient concentrations and possible algal problems occurring behind the structure?
3. A saltwater barrier can cause both a temperature and dissolved oxygen imbalance in and around its vicinity.
4. The barrier structure will have an effect on the spawning and nursery areas for fish. Some type of "fish ladder" device will certainly be required by U.S. Fish and Wildlife Services.
5. There will also be concern about localized flooding when a weir type structure is built on the river.
6. Recreational boat traffic will need to be minimally impacted if the project is to succeed.

Discussions of some of these questions as they relate the Type 2 barrier are presented in the following sections.

ECOLOGICAL FRAGMENTATION

A paramount concern of using the Type 2 barrier is that, although this barrier is most effective for saltwater intrusion control, it would cause fragmentation of the estuary ecosystem by seriously reducing the area of essential, low salinity nursery habitat available to juvenile estuarine and marine fish and shellfish, and causing significant declines in fish abundance and diversity above the barrier (Mallen-Cooper, 1999). This loss of essential habitat could have a negative impact on the success of the year class of those species dependant on this estuarine nursery function during the dry season (North and Houde, 2001). These species include fishes popular with anglers, such as snook and redfish; those used commercially, such as eels and blue crabs; those species important in the estuarine food chain such as bay anchovies, mullet, gobies and mojarras; and threatened species such as the opossum pipefish. Furthermore, many tropical species that frequent the Loxahatchee estuary, such as five species of snook, seek the warm groundwater temperatures in the inner estuary during cold events. The Type 2 barrier would prevent these tropical species from migrating upstream to this warm water refuge during the winter.

Once the barrier is in place, the normal inner estuary tidal flushing, about 2 feet of amplitude, will be minimized. This tidal flushing normally transports runoff and inundates and drains a portion of the vegetated flood plain which consistently exports particulate organics and dissolved nutrients to the estuary. These substances are required for successful, healthy phytoplankton and zooplankton populations to nourish juvenile and adult fish and shellfish (oysters), the anticipated reduction of these substances from the inner estuary may reduce overall estuarine productivity and nursery function. Additionally, the retention of these substances upstream of the structure may provide suitable water quality conditions for harmful algal blooms.

WATER QUALITY

Because the Type 2 saltwater barrier only allows flows out of the inner estuary, the water quality and hydrology upstream and downstream of the saltwater barrier may be affected. Extensive surface water quality monitoring is being conducted on the Northwest Fork of the Loxahatchee by the Loxahatchee River Environmental Control District (LRD). In consultation with LRD staff, the most significant water quality issues that would be encountered with a saltwater barrier would be the lack of surface water circulation and deposition of muck and other sediment immediately behind the structure. This would affect several water quality parameters including water temperature, dissolved oxygen, total suspended solids, water clarity, turbidity, tannins, total organic carbons, chlorophyll, fecal coliform bacteria, pesticides, and herbicides. The stagnant water conditions created by the barrier would lower dissolved oxygen and water clarity, and raise the water temperature.

Dams serve as settling basins for pollutants. Of concern with a temporary inflatable structure would be the effect on water quality immediately after the deployment period ends. When the structure is removed, sediment plus the pollutants that fall out into that sediment immediately behind the structure would be carried downstream into the estuary and eventually offshore to the reef systems over a short period of time.

Thermal stratification would occur behind the structure and negatively impact dissolved oxygen concentrations by preventing the mixing of the two water layers. The bottom water layer becomes trapped and has no contact with the air. The oxygen in the lower layer would be gradually depleted as organic material that has been washed downstream settles to the bottom and decays (Tennessee Valley Authority, 2004). The depletion of dissolved oxygen and increase in Biological Oxygen Demand (BOD) are harmful to aquatic plants and animals.

Water temperatures can have significant effects on health, distribution, and abundance of fish, amphibians, aquatic insects, benthic organisms, and aquatic plants (Washington State Department of Ecology, 2004). Water impounded behind a dam has higher water temperatures than water in a free flowing river; the dam exposes more surface water area to solar and air temperature influences. Higher water temperatures can trigger algal blooms, excessive growth of aquatic macrophytes, and fish diseases.

Elevated levels of turbidity and total suspended solids can reduce water clarity. Increased turbidity can also clog gills; stimulate organism avoidance behavior; reduce the ability to find food; reduce the rate of photosynthesis and primary production; and smother benthic organisms, spawning areas, and habitat (Washington State Department of Ecology, 2004).

Nutrients are important for the growth of plants and algae in the river and estuary system. The effect of a salinity barrier on the amount of nutrients available for the estuary ecosystem during the periods of deployment is unknown. However, the rate of nutrient loading into the estuary may be temporarily increased when the salinity barrier is removed. This short-term nutrient enrichment can have an adverse impact on aquatic ecosystems. By adding chemical sealants to the sediments, this may help promote a slower, steady release of nutrients when the barrier is removed.

Fecal coliform bacteria are used as indicators of the presence of bird and mammal (including human) feces. The Northwest Fork of the Loxahatchee River has experienced high levels of fecal coliform bacteria in the past; this has resulted in closures of the Jonathan Dickinson State Park Public Swimming Area. Adding a dam structure to the river may increase the levels of fecal coliform bacteria as a result of reduced tidal flushing. Fecal coliform bacteria levels are generally lower in saline waters and are eventually destroyed by saline waters within the lower estuary and Atlantic Ocean.

The Washington State Department of Ecology (2004) recommended that as part of a formal compliance schedule for a dam that a water quality attainment plan be established to ensure the highest attainable water quality conditions at a structure. The water quality attainment plan should address current water quality standards, possible causes of impairment, monitoring considerations, and protection and improvement actions. Chapter 3 of the Guidance Manual provides a technical overview of many water quality parameters of concern, monitoring considerations, and some possible solutions to correct water quality problems.

FLOODPLAIN VEGETATION COMMUNITIES

As discussed in **Chapters 3** and **4**, the tidal floodplains of the Northwest Fork of the Loxahatchee River consist primarily of mangrove and pond apple swamp and sabal palm hammock communities. One concern with using the Type 2 saltwater barrier would be our ability to produce an occasional dry-dry season for freshwater deciduous seed germination and seedling/sapling growth. Because of the reservoir effect produced by the barrier and the low elevations of the floodplain in the tidal reaches, the floodplain areas with elevations lower than mean high tide would possibly remain flooded throughout the dry season. The critical periods for germination and seedling sapling growth (November-April) correspond to the dry season, which is the same time period that the saltwater barrier would be used to effectively control saltwater intrusion. Also, the higher water levels would change the short-term character of the groundcover and shrub communities to the advantage of plant species that are better adapted to flooding conditions. Those species that are not tolerant of flooding could become stressed or die. A major focus of the restoration plan for the Northwest Fork of the Loxahatchee River is to promote the return of freshwater canopy, shrub and groundcover species to the areas that have been invaded by red and white mangroves.

Although placing a Type 2 barrier across the entire river provides the most significant reduction in salt water intrusion, the potential ecological impacts are an obvious concern. However, using a Type 1 barrier that allows for some flow through the barrier provides significantly less reduction of salt water intrusion. Additional reductions in salt water intrusion might be achieved with improvements in the configurations, numbers, and locations of Type 1 barriers. Concerns about ecological fragmentation, water quality, and floodplain vegetation could be reduced as optimization of Type 1 barriers is achieved.

CONCLUSIONS

Based on the preliminary modeling evaluations, it is concluded that a weir raised to an elevation one foot above the mean tide is the most effective barrier for salinity reduction in the Northwest Fork of the Loxahatchee River. Because all of the simulations were conducted under the same hydrological conditions, comparisons between weir type and weir location are appropriate. As other restoration projects are implemented and dry season freshwater flows increase, it is possible that a weir alternative that was considered less effective in this assessment scenario may be sufficient under alternate freshwater flow conditions. Therefore additional modeling studies may be necessary when considering a saltwater barrier, combined with other restoration measures.

However, extreme caution must be used before a saltwater barrier is considered as a restoration option; the potential adverse impacts on the ecosystem, boat navigation, and recreational activities in the Northwest Fork may outweigh the benefits. Additionally, the saltwater barrier should only be considered if additional sources of water supply will not be available for restoration flows in the dry season. In addition, the selection of barrier types should

be carefully considered to allow for salinity management, flood control, navigation, and recreational use of the Loxahatchee River. Also, flexibility in operation is required so that if the water quality above the barrier decreases due to the impeded tidal circulation, the barrier can be quickly removed and the water quality restored. An inflatable weir seems to offer the flexibility to preserve the conveyance of the existing river channel and reduce negative impacts on flood control during the wet season. However, this has to be exercised with a precise operational schedule, taking into account the possibility of ecological segmentation and increases in salinity when the barrier is partially deflated.